UNIVERSIDADE FEDERAL DO RIO GRANDE DO SUL

ESCOLA DE ENGENHARIA

DEPARTAMENTO DE ENGENHARIA QUÍMICA

PROGRAMA DE PÓS-GRADUAÇÃO EM ENGENHARIA QUÍMICA

AUDITORIA E DIAGNÓSTICO DE MODELOS PARA CONTROLADORES PREDITIVOS INDUSTRIAIS

TESE DE DOUTORADO

Viviane Rodrigues Botelho

Porto Alegre

2015

UNIVERSIDADE FEDERAL DO RIO GRANDE DO SUL

ESCOLA DE ENGENHARIA

DEPARTAMENTO DE ENGENHARIA QUÍMICA

PROGRAMA DE PÓS-GRADUAÇÃO EM ENGENHARIA QUÍMICA

AUDITORIA E DIAGNÓSTICO DE MODELOS PARA CONTROLADORES PREDITIVOS INDUSTRIAIS

Viviane Rodrigues Botelho

Tese de doutorado apresentada como requisito parcial para obtenção do título de Doutor em Engenharia

Área de concentração: Pesquisa e Desenvolvimento de Processos

Linha de Pesquisa: Projeto, Simulação, Modelagem, Controle e Otimização de Processo Químicos.

Orientadores:

Prof. Dr. Jorge Otávio Trierweiler

Prof. Dr. Marcelo Farenzena

Porto Alegre

2015

UNIVERSIDADE FEDERAL DO RIO GRANDE DO SUL

ESCOLA DE ENGENHARIA

DEPARTAMENTO DE ENGENHARIA QUÍMICA

PROGRAMA DE PÓS-GRADUAÇÃO EM ENGENHARIA QUÍMICA

A Comissão Examinadora, abaixo assinada, aprova a Tese *Auditoria e Diagnóstico de Modelos para Controladores Preditivos Industriais*, elaborada por *Viviane Rodrigues Botelho*, como requisito parcial para obtenção do Grau de Doutor em Engenharia.

Comissão Examinadora:

Prof. Dr. Julio Elias Normey Rico

Dr. Antonio Carlos Zanin

Prof. Dr. Pedro Rafael Bolognese Fernandes

Resumo

A crescente demanda pela melhoria operacional dos processos aliada ao desenvolvimento da tecnologia da informação tornam a utilização de controladores preditivos baseados em modelos (MPC) uma prática comum na indústria. Estes controladores estimam, a partir dos dados de planta e de um modelo do processo, uma sequência de ações de controle que levam as variáveis ao valor desejado de forma otimizada. Dessa forma, dentre os parâmetros de configuração de um MPC, a baixa qualidade do modelo é, indiscutivelmente, a mais importante fonte de degradação de seu desempenho. Este trabalho propõe uma série de metodologias para a avaliação da qualidade do modelo do controlador preditivo, as quais consideram sua velocidade em malha fechada. Tais metodologias são baseadas na filtragem dos erros de simulação a partir função nominal de sensibilidade, e possuem a capacidade de informar o impacto dos problemas de modelagem no desempenho do sistema, além de localizar as variáveis controladas que estão com tais problemas e se os mesmos são provenientes de uma discrepância no modelo ou de um distúrbio não medido. As técnicas ainda possuem a vantagem de serem independentes do setpoint, o que as torna flexível de também serem utilizadas em controladores nos quais as variáveis são controladas por faixas. A abordagem proposta foi testada em dois estudos de caso simulados, sendo eles: a Fracionadora de Óleo Pesado da Shell e a Planta de Quatro tanques Cilíndricos. As técnicas também foram avaliadas em dados de processo da Unidade de Coqueamento Retardado de uma refinaria. Os resultados indicam que as mesmas apresentam resultados coerentes, corroborando seu elevado potencial de aplicação industrial.

Palavras-chave: Controle preditivo baseado em modelo, monitoramento, diagnóstico, função de sensibilidade, discrepância de modelo, distúrbio não medido.

Abstract

The growing demand for operational improvement and the development of information technology make the use of model predictive controllers (MPCs) a common practice in industry. This kind of controller uses past plant data and a process model to estimate a sequence of control actions to lead the variables to a desired value following an optimal policy. Thus, the model quality is the most important source of MPC performance degradation. This work proposes a series of methods to investigate the controller model quality taking into account its closed loop performance. The methods are based on filtering the simulation errors using the nominal sensitivity function. They are capable detect the impact of modeling problems in the controller performance, and also to locate the controlled variables that have such problems and if it is caused by a model-plant mismatch or unmeasured disturbance. The techniques have the advantage to be setpoint independent, making them flexible to be also used in MPCs with controlled variables working by range. The proposed approach was tested in two simulated case studies The Shell Heavy Oil Fractionator Process and The Quadruple-tanks Process. The methods are also evaluated in process data of the Delayed Coking Unit of a Brazilian refinery. Results indicate that the method is technically coherent and has high potential of industrial application.

Keywords: model predictive control, monitoring, diagnosis, sensitivity function, model-plant mismatch, unmeasured disturbance

“Sem sonhos, a vida não tem brilho.
Sem metas, os sonhos não têm alicerces.
Sem prioridades, os sonhos não se tornam reais.”
(Augusto Cury)

Agradecimentos

Agradeço a todos que, de alguma forma, contribuíram para que esta realização fosse possível, especialmente:

À Deus, que me deu capacidade e força para concluir esta etapa;

Aos meus pais, Tania e Gilberto por estarem sempre ao meu lado e confiarem nas minhas escolhas;

Ao meu marido, Anderson, pelo amor, companheirismo e incentivo para encarar as adversidades com fé e otimismo;

Aos meus irmãos, Luciana e Victor, pelo carinho, amizade e por todos os momentos de alegria.

Aos meus orientadores, prof. Jorge Trierweiler e prof. Marcelo Farenzena por me direcionarem nesta trajetória, sempre com muita competência. Obrigada pelo apoio técnico, pelas ideias e pela paciência!

À equipe da Trisolutions, pelo incentivo na idealização deste trabalho sob uma perspectiva prática.

Ao Engenheiro Luís Gustavo Longhi da REFAP, pela oportunidade de avaliar este trabalho em um caso real.

À Universidade Federal do Rio Grande do Sul e ao Programa de Pós-Graduação em Engenharia Química pela oportunidade de realização deste trabalho.

À FAPERGS e à Petrobras pelo apoio financeiro.

SUMÁRIO

LISTA DE FIGURAS

LISTA DE TABELAS

NOTAÇÃO E SIMBOLOGIA

ACF: Função de autocorrelação

AO: Coeficientes do modelo ARX

A_i: Área da secção transversal do tanque

ARX: modelo autoregressivo com entradas exógenas

BO: Coeficientes do modelo ARX

C: Modelo do controlador

cov: Covariância

CV: Variável controlada

det: Determinante

$dominance_{MPM}$: Dominância de MPM

cd_i: Coeficiente de descarga de tanque

ce_Z: Indicador de dispersão entre as distribuições estatística

co_Z: Indicador de correlação entre as distribuições estatística

cde_Z: Indicador de dispersão entre as derivadas das distribuições estatística

co_{dZ}: Indicador de correlação entre as derivadas das distribuições estatística

$\overline{DR}$: Razão de diâmetro da elipse de confiança

e^d: Erro proveniente dos distúrbios estocásticos

e_0: Erro nominal

$e_{0_{diag}}$: Erro nominal diagonal

e^p: Erro de predição

$expi$: Expoente do modelo do tanque cilíndrico

ev: Subespaço das saídas individuais

G: Modelo real do processo

G_d: Modelo real do distúrbio

G_0: Modelo nominal do processo

G_{d0}: Modelo nominal do distúrbio

GEVP*:* Problema de autovalor generalizado

f_d: Coeficiente de estatística quadrática assintótica

h_i: Nível do tanque

I: Matriz identidade

I_v: Índice de variabilidade global

I_{MPM}: Índicador de discrepância de modelo

$iMQI$:índice individual de qualidade do modelo

IP: Indicador de desempenho genérico

$Ivar$: Índice de variância

$Ivar_{basis}$: Índice de variância em relação ao caso base

$Ivar_{diag}$: Índice de variância diagonal

K: Modelo do controlador IMC

$k_i v_i$: Vazão da bomba

kts: Coeficiente de curtose

LL: Limite inferior de confiança nos autovalores

LQG: Linear quadratic Gaussian

mh: horizonte de controle

m_l: momento central de ordem l

$MO1$ and $MO2$: Ordens dos modelos ARX

MPC: Controlador preditivo baseado em modelo

MPM: Discrepância entre modelo e planta

MI: Inconsistência de modelo

MQI: Índice de qualidade do modelo

MS: Supressão de movimento

MV: Variável manipulada

MVC: Controlador de variância mínima

MW: Janela móvel

n_{MW}: número de janelas móveis

ns: número de amostras

nu: número de entradas

ny: número de saídas

OE: Modelo *output-error*

ph: horizonte de predição

P_w : Subespaço de degradação de desempenho

P_b: Subespaço de melhora de desempenho

PCA: Análise de componetes principais

PLS: *Partial Least Square*

$Q_{\Delta u}$: Supressão de movimento

Q_u: Peso das entradas

Q_y: Peso das saídas

R^2: Coeficiente de determinação

S: Função de sensibilidade

S_0: Função de sensibilidade nominal

$S_{0_{diag}}$: Função de sensibilidade nominal diagonal

S_d: Sensibilidade de projeto

SQR : Indicador de erro

skn: Coeficiente de assimetria

T: Função complementar de sensibilidade

T_0: Função complementar de sensibilidade nominal

$T_{0_{diag}}$: Função complementar de sensibilidade nominal diagonal

$TSSE$: Erro total de simulação

u: Entradas medidas

UL: Limite superior de confiança dos autovalores

u_{LL}: Limite inferior das entradas

u_{UL}: Limite superior das entradas

u_{hard}^{max} and u_{hard}^{min} : Restrições rígidas das entradas

u_{tgt}: Targets das entradas

v: Sinal aleatório

v_s: Distúrbios estacionários no controlador IMC

$V1_i$ and $V2_{i,j}$: Parâmetros dos modelos OE

W_y: Peso das saídas

X_i: Conjunto de dados analisado

$\bar{X}$: Média do conjunto de dados analisados

y: Saídas medidas

$\hat{y}$: Saídas preditas

y_0: Saídas nominais

$y_{0_{BADWE}}$: Saídas nominas segundo o método de Badwe *et al.* (2010)

$y_{0_{diag}}$: Saídas nominais diagonais

y_d: Sinal de distúrbio

y_{hard}^{max}: Limites superiores rígidos das saídas

y_{hard}^{min}: Limites inferiores rígidos das saídas

y_{set}: Setpoints

y_{sim}: Saídas simuladas

y_{soft}^{max} and y_{soft}^{min}: *Soft constraints* das saídas

y_{ss}: Saídas preditas no estado estacionário

y_{LL}: Limite inferior das saídas

y_{UL}: Limite superior das saídas

$\bar{\alpha}_Z$ *:* Ângulo da elipse de confiança reduzido ao primeiro quadrante

$\propto$: Coeficiente angular da aproximação linear

β: Intervalo de confiança de ${\theta_k}^b$ e ${\theta_k}^W$

γ: Inclinação da elipse de confiança

δ_y: Variável de folga para as *soft constraints*

ΔG: Discrepância entre modelo e planta

Δu: Ações de controle

ε : Componentes independentes dos modelos OE

ϵ: Entradas do controlador IMC

${\theta_k}^W$: Ângulo entre as saídas e os subespaços de degradação de desempenho

${\theta_k}^b$: Ângulo entre as saídas e os subespaços de melhora de desempenho

μ: Autovalores

ρ_d : Coeficiente de autocorrelação ao longo da direção do autovetor

τ_y: Penalização para violação da *soft constraint*

φ_u: Custo das variáveis manipuladas

$\%\ Fit$: Indicador da qualidade do ajuste

Capítulo 1 – **Introdução**

1.1 Motivação

De uma forma geral, a operação de plantas industriais envolve a utilização de estratégias capazes de controlar as variáveis de processo. As únicas estruturas disponiveis até poucas décadas eram baseadas no PID. Contudo, os avanços tecnológicos, ao mesmo tempo em que promoveram a elevação da complexidade destes processos, permitiram que novas técnicas de controle fossem desenvolvidas, surgindo o controle avançado de processos. Dentre as técnicas de controle avançado existentes, os controladores preditivos baseados em modelos (MPCs) são os mais utilizados atualmente em termos industriais. Os primeiros conceitos referente ao tema surgiram na década de 60. Porém o interesse pelo assunto só se intensificou ao final da década de 70, com o surgimento dos algoritmos IDCOM (Identification and Comand) e DMC (Dynamic Matrix Control) . Esses algoritmos impactaram de forma significativa no âmbito industrial e acadêmico, sendo utilizados até os dias atuais e servindo como base para muitos dos algoritmos existentes (Holkar & Waghmare,2010; Morari & Lee, 1999).

A Figura 1.1 ilustra o funcionamento de um MPC típico. A cada ciclo de execução este sistema executa as seguintes ações: a partir das medições dos valores passados, o controlador estima o comportamento inercial das variáveis controladas, i.e., o comportamento que teriam caso nenhuma ação de controle fosse tomada ao longo de um horizonte de controle. Em seguida um algoritmo de otimização determina uma sequência de ações de controle que levam as variáveis controladas ao seu setpoint de forma otimizada.

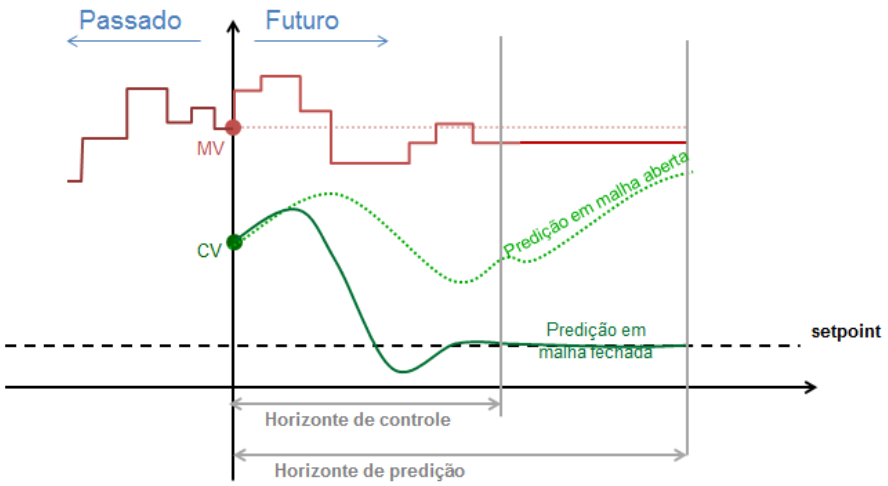

Figura 1.1: Diagrama Representativo de um MPC Típico

A capacidade preditiva destes controladores é uma de suas maiores virtudes, já que viabiliza a definição de ações de controle que respeitem as várias restrições do processo. Sua aplicação permite a otimização operacional, pois impacta na redução da variabilidade do sistema, levando o mesmo a operar próximo destas restrições, o que significa maximizar rentabilidade, minimizar custos, melhorar qualidade dos produtos, operar de forma mais segura e reduzir a geração de resíduos. Campos *et al.* (2013) estima que ganhos da ordem de 2% a 10% possam ser alcançados com a implementação de um MPC, através da maximização da recuperação de produtos nobres, aumento da capacidade de processamento da planta e minimização do consumo de energia no processo.

Após a correta e eficiente implantação de um MPC, os ganhos mencionados são evidentes. Porém, com o passar do tempo as condições de operação da unidade se alteram, o que reflete diretamente no desempenho do controlador. Com isso, estes sistemas passam a operar de forma limitada e muitas vezes acabam sendo desativados pela equipe de operação, caso não seja realizada a sua manutenção. A Figura 1.2 ilustra a um ciclo de vida típico de um MPC com e sem suporte.

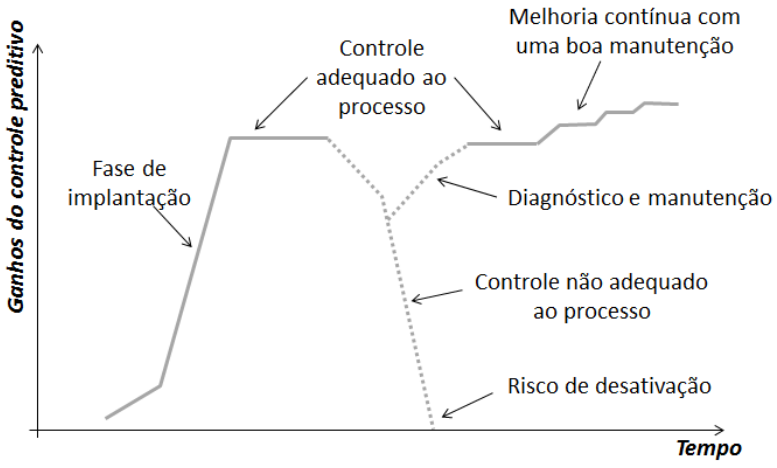

Figura 1.2: Ciclo de vida de um sistema de controle avançado.
Fonte: Campos *et al.*,2013

Embora sejam de fundamental importância, o monitoramento e diagnóstico de controladores preditivos ainda não é um tópico com uma solução completamente eficiente. Atualmente, o monitoramento é realizado, em sua maioria, com base em indicadores gerenciais, que fonecem um panorama da utilização do sistema de controle, indicando, por exemplo o número de variáveis controladas e manipuladas que estão em seus limites (PCAT e PMAT), percentual de tempo em que o controlador permanece ligado (FATOP), percentual de tempo em que as variáveis manipuladas permanecem em malha fechada (GUT), benefício econômico, dentro outros (Zanin *et al.*, 2014). Embora muito úteis para fornecer um panorama geral do controlador, estes indicadores são insuficientes, pois são incapazes de fornecer qualquer tipo de informação técnica a respeito do seu real comportamento bem como das fontes de sua degradação.

A avaliação dos MPCs sob um ponto de vista técnico ainda é um desafio, dada a sua natureza multicausal. A grande quantidade de parâmetros de sintonia, forte dependência com o modelo do processo, diversidade dos algoritmos de controle comerciais existentes são as principais dificuldades. Existe uma série de trabalhos acadêmicos propondo técnicas para o monitoramento e diagnóstico. Embora estas técnicas sejam diferentes, elas possuem aspectos em comum, não só relativos a sua finalidade, mas também em relação ao conteúdo de informações do processo necessário e as ferramenas matemáticas e estatísticas utilizadas para processar as informações. A Figura 1.3 resume tais aspectos.

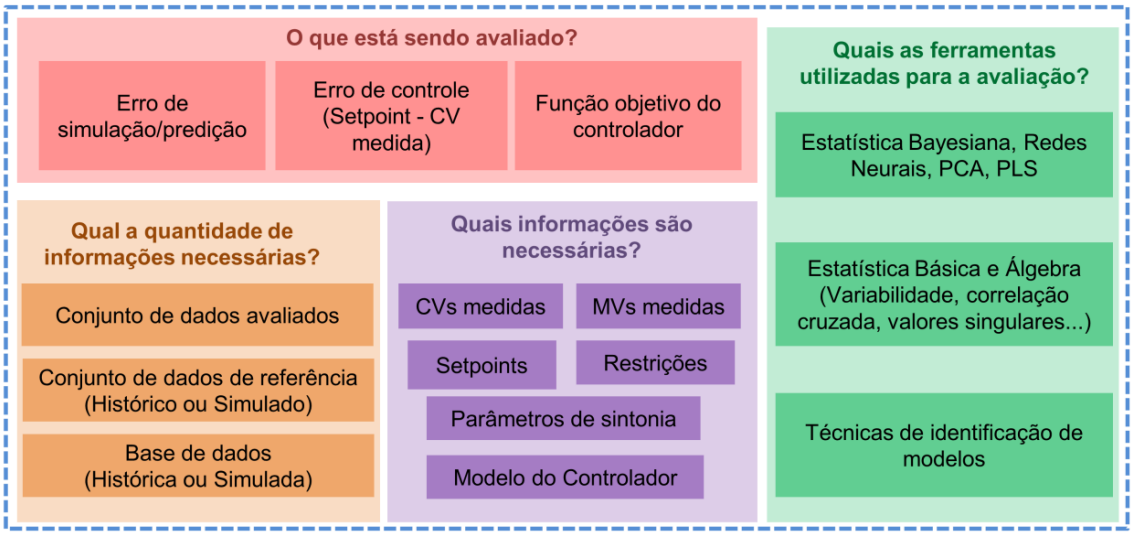

Figura 1.3: Aspectos em comum às técnicas de avaliaçao de MPCs

A partir da combinação dos diferentes aspectos ilustrados na Figura 1.3, cada metodologia é fundamentada, de modo que, o resultado final se resume a uma série de indicadores para avaliar a eficiência econômica do MPC, monitorar o seu desempenho global ou ainda detectar e quantificar as possíveis fontes de degradação de performance do controlador (sintonia, qualidade dos modelos, restrições do processo, falhas em equipamentos, etc).

Dentre as fontes de degradação mencionadas, a baixa qualidade dos modelos é a mais importante, visto que modelos ruins podem ocasionar ações de controles muito aquém daquelas que levam o processo a sua condição ótima, ou mesmo tornar o controlador instável. Sun *et al.* (2013) estima que mais de 80% do tempo de projeto de um controlador preditivo seja gasto na identificação deste modelo, dada a sua importância.

Levando em conta que o modelo é obtido em uma determinada condição de operação, qualquer alteração no processo pode ser suficiente para degradar a sua representatividade. Isso deixa evidente a necessidade de ser constantemente monitorado.

Muitas das técnicas disponíveis na literatura tem o objetivo de avaliar a qualidade dos modelos para o MPC (por exemplo Badwe *et. al*, 2009; Sun *et al.,* 2013; Kano *et al.*, 2010; Schäfer & Cinar, 2004; etc). Embora sejam eficientes, a maioria delas são pouco viáveis de serem aplicadas na indústria já que são embasada em estruturas de controle preditivo convencionais (i. e., que possuem setpoints fixos, conforme à apresentada na Figura 1.1), utilizando o setpoint das CVs como ferramenta para a avaliação. Na indústria, é comum a inexistência de graus de liberdade suficientes para manter todas as variáveis controladas em um único valor predefinido e por isso o MPC é configurado por faixas e tem o objetivo de manter as CVs dentro destes limites. Além disso, alguns controladores possuem uma camada de otimização em tempo real que estima o valor ótimo das variáveis manipuladas (*Targets*) sob o ponto de vista econômico, e estes *Targets* são variáveis da função objetivo do MPC. Dessa forma, o controlador não possui explicitamente setpoints para as variáveis controladas e por isso técnicas que utilizam o setpoint acabam sendo inadequadas para o seu diagnóstico. Com isso constatou-se a a necessidade do desenvolvimento de métricas para avaliar modelos de controladores preditivos para serem utilizadas em controladores industriais.

1.2 Objetivos

Com base no que foi descrito, a presente tese tem o objetivo de desenvolver uma ferramenta para a avaliação da qualidade dos modelos de controladores preditivos. O foco é que esta metodologia seja flexível à maioria das características inerentes aos controladores indústriais além de ser numericamente simples, de fácil aplicação e interpretação, utilizando apenas as perturbações normalmente empregadas durante a operação do controlador. Dessa forma, espera-se que a técnica seja capaz de:

- O1: Realizar o diagnóstico de modelos de MPCs que operem por faixas.

- O2: Quantificar o efeito dos problemas de modelagem no desempenho do MPC.

- O3: Localizar as variáveis cujos modelos possuem problemas relevantes.

- O4: Distinguir entre problemas oriundos de distúrbios não medidos e discrepância de modelos.

1.3 Estrutura do trabalho

Este trabalho está dividido em oito capítulos, nos quais seis deles estão estruturados na forma de artigos científicos, conforme a Resolução 093/2007 de 12/06/2007 da Câmara de Pós-Graduação da Universidade Federal do Rio Grande do Sul (UFRGS). No primeiro capítulo, é apresentada uma breve introdução e motivação a respeito do tema, bem como os principais objetivos deste trabalho e as contribuições resultantes da sua execução.

O Capítulo 2 apresenta uma revisão sobre avaliação de desempenho de controladores preditivos. Um overview sobre o tema é apresentado e as principais técnicas disponíveis na literatura são listadas e classificadas de acordo com seus objetivos e suas

características mais relevantes. Em seguida as premissas sugeridas por Hugo (2002) para a seleção de métricas ideais de avaliação de desempenho de controladores são discutidas. Algumas das técnicas são selecionadas de acordo com tais premissas para serem detalhadas e testadas. Dois estudos de caso simulados são utilizados nos teste comparativos das metodologias: A Fracionadora de Óleo Pesado da Shell (Prett & Morari, 1987) utilizando um controlador preditivo clássico e o Processo de Quatro Tanques Cilíndricos (Johanson, 2000) utilizando um MPC por faixas. Este capítulo também conta com uma breve apresentação das metodologias desenvolvidas neste trabalho, as quais são aprimoradas ao longo dos capítulos subsequentes. Ressalta-se que a demonstração matemática e o detalhamento das metodologias desenvolvidas nesta tese são apresentadas detalhadamente nos capítulos 3, 4 e 5. No capítulo 2, elas apenas foram parcialmente introduzidas de forma simplificada para permitir uma comparação com as metodologias mais promissoras encontradas na literatura.

No capítulo 3, uma técnica para a quantificação do impacto dos problemas de modelagem no desempenho do controlador é apresentada a qual é embasada no comportamento nominal do sistema em malha fechada. A dedução matemática da mesma é apresentada. O Processo de Quatro Tanques Cilíndricos (Johanson, 2000) é utilizado como estudo de caso a partir de diferentes configurações para o MPC e para a planta. Os resultados da técnica proposta são comparados com a metodologia proposta por Badwe *et al.* (2010).

No capítulo 4, uma extensão da metodologia apresentada no capítulo 3 é proposta com objetivo de localizar as variáveis controladas com os problemas de modelagem responsáveis pela degradação de desempenho do controlador. Esta técnica é útil especialmente em sistemas com elevado grau de acoplamento entre as variáveis, onde pequenos problemas de modelagem podem levar todo o sistema próximo a sua instabilidade. A metodologia é avaliada a parti de dois estudos de caso simulados: Uma coluna de destilação de alta pureza (Skogestad & Postlethwaite, 1996) e a Fracionadora de Óleo Pesado da Shell (Prett & Morari, 1987). Os resultados obtidos são comparados com a metodologia proposta por Sun *et al.* (2013).

No capítulo 5, uma metodologia que visa identificar se a degradação do modelo é proveniente de uma discrepância no mesmo ou de um distúrbio não medido é apresentada. Esta metodologia utiliza alguns dos conceitos apresentados nos capítulos 3 e 4 e tem o objetivo de comparar estatisticamente os erros de modelagem com o comportamento nominal do sistema. Um MPC SISO é utilizado para ilustrar os resultados gerados para avaliar qual o melhor indicador dentre uma série de hipóteses sugeridas. Em seguida, a metodologia é avaliada a partir de dois estudos de caso: A Fracionadora de Óleo Pesado da Shell (Prett & Morari, 1987) e o Processo de Quatro Tanques Cilíndricos (Johanson, 2000).

No capítulo 6 todas as metodologias desenvolvidas neste trabalho são testadas em um controlador preditivo por faixas, configurado na Fracionadora de Óleo Pesado da Shell (Prett & Morari, 1987). Testes exaustivos são gerados aleatoriamente a fim de quantificar o percentual de falha das técnicas. Além disso, um estudo é realizado para se avaliar o grau de incerteza admitido na função representativa do comportamento nominal do sistema.

No capítulo 7, as metodologias desenvolvidas são aplicadas a um controlador preditivo real da Unidade de Coqueamento Retardado da REFAP. O capítulo 8 apresenta as principais conclusões, bem como os aspectos a serem abordados em trabalhos futuros.

Nos apêndices A1, A2 e A3 são apresentados os principais detalhes relativos ás implementações das metodologias discutidas ao longo do trabalho.

1.4 Produção científica

Este trabalho resultou em uma série de artigos já aceitos ou submetidos para publicação em revistas científicas, os quais correspondem aos capítulos de conteúdo técnico. Além disso, as metodologias desenvolvidas fizeram parte de publicações em congressos e contribuíram para a realização de outros trabalhos desenvolvidos pelo grupo de pesquisa. A seguir são listadas as principais produções resultantes deste estudo.

1.4.1 Artigos Científicos

Capítulo 2: BOTELHO, V., TRIERWEILER, J., FARENZENA, M., DURAISKI, R. Perspectives and Challenges in Performance Assessment of Model Predictive Control. *The Canadian Journal of Chemical Engineering*. Status: Aceito para publicação.

Capítulo 3: BOTELHO, V., TRIERWEILER, J., FARENZENA, M., DURAISKI, R. A methodology for detecting model-plant mismatches affecting MPC performance. *Industrial & Engineering Chemistry Research.* Status: Aceito para publicação.

Capítulo 4: BOTELHO, V., TRIERWEILER, J., FARENZENA, M., DURAISKI, R. A. MPC model assessment of highly coupled systems. *Industrial & Engineering Chemistry Research*. Status: Submetido para publicação.

Capítulo 5: BOTELHO, V., TRIERWEILER, J., FARENZENA, M., DURAISKI, R. A. MPC Diagnosis of poor performance in model predictive controllers: Unmeasured Disturbance versus Model-Plant Mismatch. *Industrial & Engineering Chemistry Research*. Status: Submetido para publicação.

Capítulo 6: BOTELHO, V., TRIERWEILER, J., FARENZENA, M., DURAISKI, R. A. MPC Performance Assessment and Diagnosis of MPCs with Control Ranges. *Control Engineering Practice*. Status: Submetido para publicação.

Capítulo 7: BOTELHO, V., TRIERWEILER, J., FARENZENA, M., LONGHI, L., DURAISKI, R. A. MPC Model Assessment of an Industrial MPC. *Control Engineering Practice*. Status: Submetido para publicação.

1.4.2 Trabalhos completos publicados em anais de congresso

BOTELHO, V., TRIERWEILER, J., FARENZENA, M., MULLER, G. Desafios e perspectivas na auditoria de MPCs. *Congresso Brasileiro de Engenharia Química – COBEQ*. Florianópolis, 2014.

[1]BOTELHO, V., TRIERWEILER, J., FARENZENA, M., DURAISKI, R. Assessment of Model-Plant Mismatch by the Nominal Sensitivity Function for Unconstrained MPC. *International Symposium on Advanced Control of Chemical Process – ADCHEM*. British Columbia, 2015.

CLARO, E., BOTELHO, V., TRIERWEILER, J., FARENZENA, M. Model performance assessment of a predictive controller for propylene/propane separation. *Symposium on Dynamics and Control of Process Systems –DYCOPS*. Trondheim, 2016. Submetido.

1.4.3 Co-orientações em trabalhos de conclusão de curso.

Caetano Bevilacqua Kichel (2015). *Auditoria e Diagnóstico de Malhas SISO a partir da Resposta Nominal Estimada*. Orientador: Prof. Jorge Trierweiler, Co-orientadora: MSc. Viviane Botelho. Trabalho de diplomação em Engenharia Química – UFRGS.

1.4.4 Apoio em dissertações de mestrado

Érica Claro (defesa prevista para 2016). Auditoria de Modelos de Controladores Preditivos Industriais: Estudo de caso para um sistema de fracionamento de propeno. rientador: Prof. Dr. Jorge Trierweiler, Co-orientador: Prof. Dr. Marcelo Farenzena. Mestrado em Engenharia Química – UFRGS.

1.5 Contribuições

Pode-se listar como principais contribuições deste trabalho os seguintes pontos:

C1: Levantamento das metodologias disponíveis na literatura e avaliação da sua potencilidade de aplicação em MPCs por faixa.

C2. Desenvolvimento de uma metodologia para a estimação do comportamento do sistema isento de problemas de modelagem.

C3: Avaliação de métricas para avaliar impacto dos erros de modelagem com base no comportamento nominal do sistema.

C4. Desenvolvimento de metodologia para localizar as variáveis controladas com problemas de modelagem.

C5: Desenvolvimento de metodologia para avaliar estatisticamente a fonte dos problemas de modelagem (discrepância no modelo ou distúrbio não medido)

C6. Avaliação das metodologias propostas em MPCs por faixa.

C7. Aplicação das técnicas desenvolvidas em um sistema real.

1.6 Resumo gráfico

A Figura 1.4 apresenta um resumo gráfico desta Tese de Doutorado, relacionando os objetivos e contribuições descritos nas seções 1.2 e 1.5 com os capítulos da tese. A partir

[1] Trabalho reconhecido como melhor apresentação oral da sessão

desta figura é possivel se ter uma visão geral de como este trabalho está estruturado, e de como as etapas do desenvolvimento se interligam, levando a conclusão do estudo.

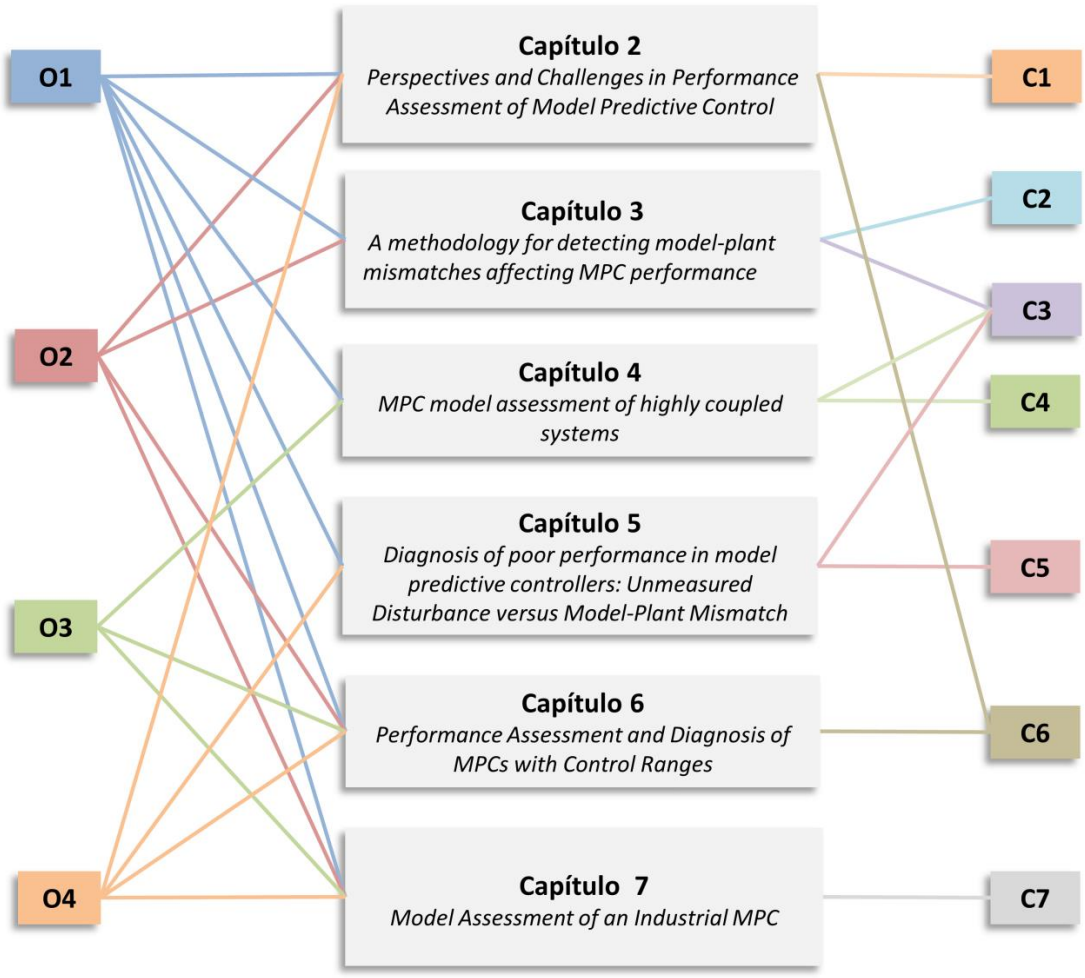

Figura 1.4: Resumo gráfico da tese

Capítulo 2 – **Perspectives and Challenges in Performance Assessment of Model Predictive Control**

Abstract[2]**:** The longevity of each MPC application is strongly related to its performance maintenance. This work provides an overview of the methodologies available to fulfill this task including a discussion about some special requirements of performance assessment methodologies for typical industrial MPC applications. The available methodologies were compared using these requirements. The best approaches were selected and compared to a new method proposed by the authors. These techniques have been applied in two case studies: the Shell benchmark process and The Quadruple-tank process. The results show that the control policy (setpoint, soft constraints, targets) followed in the MPC application should be the determining factor in the selection of the methodology for performance assessment.

Keywords: Model Predictive Control, Model Plant Mismatch, Model Quality, Control Performance Assessment

---

[2] *Aceito para publicação no periódico "The Canadian Journal of Chemical Engineering".*

2.1 Introduction

The increasing demand for operational improvement and the fast development of information technology are turning the use of model-based predictive control (MPC) into common practice in the industry. The use of these controllers allows operational optimization, which leads to maximized profit, safer operations and reduced waste generation. These benefits become evident after proper implementation of an MPC; however, the process conditions inevitably change over time, directly influencing controller performance. Thus, the longevity of a MPC application is strongly dependent of it maintenance and, given its importance, several methods are available in literature for monitoring and diagnosing a model predictive control.

Despite the wide diversity of techniques for MPC assessment, most of them can be grouped according to some common features, which relate to the information provided, as well as to the required input information. For example, a group of methods is based in comparisons of current data with a historical benchmark (e.g., Schäfer & Cinar, 2004; AlGhazzawi & Lennox, 2009; Agarwal & Huang, 2007), some methods rely on Minimal Variance Controller (MVC) as a benchmark (e.g. Huang & Thornhill, 2006; Zhao *et al.*, 2010). Others are focused on investigating the quality of the process model using the prediction error (e.g., Jiang *et al.,* 2012; Pannocchia & Luca, 2012), etc. Depending on these characteristics, a method can be adapted for industrial applications. Section 2 presents a "big picture" of the available techniques in literature, guiding the selection of an advisable method for a given application. This section also discusses desirable characteristics of a method for controller assessment in industrial applications, according to the criteria defined by Hugo (2010). Based on this analysis, three methods were deemed the most promising: the Sun *et al.* (2013) method, the Badwe *et. al.* (2009) method and the Yu & Qin (2008a and b) method. These three methods are then further compared against our approach, which can detect any modeling inconsistencies and whether these are due to a model-plant mismatch or unmeasured disturbance.

Even though model-based predictive controllers have core theoretical fundamentals, each industrial application of commercial MPCs has its particularities. For example a MPC can have hard and/or soft constraints, it may or not include an economic cost function, it can based in different kinds of models. An effective method for MPC assessment must have the ability to manage all these diferent policies. Section 3 discusses these policies and the challenges for a flexible method for MPC assessment.

Through the case study presented in Section 4, we assess the potential as well as the limitations of each selected technique in Section 2 and of the proposed one as well. Using two case studies: the Shell benchmark process (Prett & Morari, 1987) and the quadruple-tank process (Johanson, 2000), we set an MPC considering some control policies common to industrial processes, such as the existence of soft constraints and economic optimization.

Since 2001, our research group, GIMSCOP / UFRGS, has been developing research in control loop performance assessment and diagnosis to meet a demand from the most important refining industry of Brazil. The results of our work culminated in the development of an industrial tool, which is nowadays the default solution adopted by any companies for control loop performance assessment and diagnosis. Currently, there are over 12,000 control loops being monitored.

2.2 Assessment, monitoring, and diagnosis methodologies for MPCs

2.2.1 A brief overview of the literature

There is no clear consensus which is the best solution for performance assessment of predictive controllers. The difficulty associated with monitoring and diagnosing MPC is a direct consequence of the algorithm´s complexity. The dynamic process model lies at the heart of a MPC. Based on this model, outputs are predicted considering a set of control actions that are optimized along the control horizon. The optimization problem is restarted at each sample interval, according to a moving horizon approach. To set the optimization problems, constraints and weighting matrices are added to the control and prediction horizon. All these can be considered tuning parameters. Due to the spread of possible causes for poor MPC performances, finding the source of degradation in the controller is not a simple task. The existence of unmeasured disturbances further complicates this effort.

Industrial and academic interest in MPC assessment has grown significantly in the last decades, and several techniques have emerged. Some of these rely on Minimal Variance Controller (MVC) as a benchmark despite the fact that many authors consider the MVC an extremely unattainable benchmark for most MPCs applications. An extension of MVC is the linear quadratic Gaussian (LQG) curve, which displays the minimal achievable variance of the controlled variable versus the variance of the manipulated variable (MV). The LQG curve is a more suitable reference than MVC when applied in predictive controllers because it considers the variance of MVs. Nevertheless, for most real applications, the LQG curve is still not a practical reference, due to its complexity and computational demand for estimating states and for the solution of the Ricatti algebraic equations, in addition to the requirement of a complete state space process model. (Jelali, 2006; Zhang & Shaoyunan, 2006)

Despite the adversities associated with the use of the MVC or LQG as a benchmark, several works have been developed considering these approaches. Lee *et al.* (2008) suggested a method based on MVC, which consists of evaluating the sensitivity of the process variables in order to determine which one has a greater economic impact. Harrison & Qin (2009) proposed a minimum variance map based on LQG to verify the effects of constraints in the controller's operational quality. Zhao *et al.* (2009) developed an economic benchmark based on LQG controller, solving an optimization problem to determine the economic potential of the controller and compare it with the current performance. Zhang *et al.* (2013) proposed an improvement of LQG for multivariable systems, in which the multivariable system is deconstructed into multiple MISO (multiple-input single-output) subsystems. Then, the LQG is obtained for each subsystem. Huang & Thornhill (2006) suggested assessing the potential for reducing the variability by comparing different prediction levels using a moving average model identified from plant data. Zhao *et al.* (2010) expanded on this concept, but considering multi-steps ahead prediction in order to avoid problems arising from underestimated minimum variance.

As an alternative to MVC and LQG performance benchmarks, many authors proposed using as historical references periods in which good performance of the controller is known beforehand. Schäfer & Cinar (2004) proposed a methodology for MPC monitoring and evaluation based on a comparison of the current objective function with a reference value and with the achievable performance for the controller designed. The authors

suggest that the reference value can be calculated using LQG or historical data. Yu & Qin (2008a and b) proposed a methodology based on the investigation of the covariance of the reference periods and current data in order to determine whether the variability increased or not, which is verified with statistical tests. For detecting MPC irregularities in real time, AlGhazzawi & Lennox (2009) suggest using a comparison with a PCA (Principal Component analysis) or PLS (Partial Least Square) model obtained previously from a set of reference data. Tian *et al.* (2011) proposed a methodology based on dynamic PCA similarity measure, where the actual operating data is decomposed and compared with a historical benchmark. The Zhang & Shaoyuan (2006) method proposed a similar framework, where the actual PCA model is compared with a historical benchmark. If a decline in performance is detected, the Baseville (1998) criterion is used for diagnosis. Alcala & Qin (2009, 2011) use PCA and PLS as a diagnostic tool, suggesting new indicators for monitoring performance. Qi & Huang (2011) have introduced a class of methods based on building a Bayesian network to recognize patterns.

Many methods focus on investigating the quality of the process model used by the MPC, since this is one of the most important and critical points for the predictive controller operation. Sun *et al*. (2013) estimated that 80% of time spent on the design of an MPC is dedicated to obtaining a model. Among the methods available, Conner & Seborg (2005) proposed using the Akaike information criterion to assess the need for re-identification of the model. Badwe *et al* (2009) presented the evaluation of the partial correlation between inputs and residuals to identify the channels with significant model-plant mismatch. Sun *et al.* (2013) introduced a model quality index where the impact of stochastic disturbance is estimated and compared with the measured data.

Table 2.1 shows the most cited methods available in the literature following general attributes found in different approaches. These attributes relate to: each method´s applicability (i.e., whether the method is useful to evaluate system variability, model quality, controller tuning or detect problems based on pre-defined patterns), to the need for MPC information (such as controller model and tuning parameters), to whether the method is specific for MPC and to the need of intrusive tests and data-based model identification.

Table 2.1: Classification of Methods for MPC Assessment

Utility	Ref.	Specific Objective	*(a)	*(b)	*(c)	*(d)	*(e)	*(f)
Evaluate System Variability	Huang & Thornhill (2006)	Monitor and diagnose CV with increased variability	No	No	Yes	No	MVC	Yes
	Yu & Qin (2008a and b)	Monitor and diagnose CV with increased variability	No	No	No	No	HIST	No
	Zhao *et al.* (2009)	Evaluate Economical Potential considering a variability reduction	Yes	No	Yes	No	LQG	No
	Zhao *et al.* (2010)	Investigate potential of variability reduction	No	No	Yes	No	MVC	Yes
	Zhang *et al.* (2013)	Monitor and diagnose CV with increased variability	Yes	No	No	No	LQG	No
Evaluate Model Quality	Huang *et al.* (2003)	Model validation	Yes	No	Yes	No	No	Yes
	Conner & Seborg (2005)	Evaluate the need for model re-identification	Yes	No	No	Yes	No	Yes
	Badwe *et al.* (2009)	Identify MV *versus* CV model-plant mismatch	Yes	No	Yes	No	No	Yes
	Jiang & Huang (2009)	Validation and global model-plant mismatch detection	Yes	No	No	No	No	Yes
	Badwe *et al.* (2010)	Evaluate the impact of model-plant mismatch on MPC performance	Yes	Yes	Yes	No	No	Yes
	Kano *et al.* (2010)	Identify MV *versus* CV model-plant mismatch	Yes	No	Yes	No	No	Yes
	Whang *et al.* (2012)	Identify MV *versus* CV model-plant mismatch	Yes	No	Yes	No	No	Yes
	Ji *et al.* (2012)	Identify MV *versus* CV model-plant mismatch	No	Yes	Yes	Yes	No	No
	Jiang *et al.* (2012)	Prediction quality under several levels	Yes	No	Yes	No	No	No
	Pannocchia & Luca (2012)	Evaluate deterministic portion of prediction error	Yes	No	Yes	No	No	Yes
	Sun *et al.* (2013)	Identify CV with model-plant mismatch	Yes	No	Yes	No	No	Yes
Pattern Classification	Loquasto & Seborg (2003)	Identify MPC problems by comparing data with a simulated database	Yes	Yes	Yes	No	No	No
	Huang & Qi (2011)	Probability of failure causes using Bayesian criteria	No	No	Yes	No	HIST	Yes
	Tian *et al.* (2011)	Identify MPC problems comparing data with a historical database	No	No	No	No	HIST	No
	He *et al.* (2012)	Identify MPC problems comparing data with a simulated database	Yes	No	Yes	No	No	No
	AlGhazzawi & Lennox (2009)	Detect irregularities from comparison of a PCS/PLS model	Yes	No	Yes	No	HIST	No
MPC Tuning	Schäfer & Cinar (2004)	Monitor and diagnosis of Model *X* Tuning problem	Yes	Yes	Yes	No	HIST	No
	Argawal & Huang (2007a and b)	Evaluate variable constraints	No	No	Yes	No	HIST	Yes
	Harrison & Qin (2009)	Evaluate variable constraints	Yes	Yes	Yes	No	LQG	No

**(a) Use controller model? *(b) Use controller tuning parameters? *(c) Specific for MPC? *(d) Intrusive? * (e) Based in a Benchmark? (minimum variance controller: MVC, linear quadratic Gaussian: LQG and historical data: HIST) * (f) Needs any data-model identification?*

2.2.2 Guidelines for method selection

Despite the significant number of methods available to evaluate multivariable controllers, their industrial applicability is limited due to several constraints. Hugo (2002) recommends the following requirements for a universal metric:

- Sensitivity to tuning, model mismatch or equipment failures;
- Impact of disturbances or setpoint changes should be minimal;
- Non-intrusive;
- Ability to assess performance automatically, with minimal intervention;
- Should use an absolute benchmark;
- Should not require the actual process dynamics;
- Diagnose the cause of the bad performance;
- Quantify the economic impact of poor performance;

Additionally, an ideal method should be able to handle large datasets with strong correlation between variables without requiring much pretreatment. Finally, we feel confident that the ideal method ensures a simple and intuitive interpretation of controller problems. We selected some methodologies that meet most of these requirements, which are presented below for further evaluation.

Sun *et al.* (2013) method

This technique focuses on evaluating MPC model quality. It is based on residual assessment and feedback invariant principle, whereby disturbance innovations are not affected by the feedback controller. It allows the estimation of stochastic disturbance error $e^d(k)$ from the identification of a stable High Order Autoregressive Exogenous Model (HOARX) using the setpoints $y_{set}(k)$ and the measured outputs $y(k)$, according to

$$y(k) = \sum_{i=1}^{\infty} AO_i y(k-i) + \sum_{i=1}^{\infty} BO_i y_{set}(k-i) + e^0(k) \approx \sum_{i=1}^{MO1} AO_i y(k-i) + \sum_{i=1}^{MO2} BO_i y_{set}(k-i) + e^d(k) \quad (2.1)$$

where AO and BO are the parameters of ARX model and MO1 and MO2 are the model orders.

The prediction error $e^p(k)$ is obtained based on the one-step-ahead prediction (Ljung, 1999) which is the optimal prediction of the output given the past output measurement. For a process with identified disturbance model G_{d0}, $e^p(k)$is calculated according to:

$$\hat{y}(k) = {G_{d0}}^{-1}(q)G_0(q)u(k-1) + \left[1 - {G_{d0}}^{-1}(q)\right]y(k-1) \quad (2.2)$$

$$e^p(k) = \hat{y}(k) - y(k) \quad (2.3)$$

where G_0 is the process model. In cases where the disturbance model is not available, Ljung (1999) suggested projecting a filter (predictor) to capture the disturbance effect (i.e, $G_{d0}(q)e^d(k)$). The author suggests a performance indicator for model quality (MQI), defined by:

$$MQI = \frac{\sum_{i=1}^{ns} e^d(k)^T Q_y e^d(k)}{\sum_{i=1}^{ns} e^p\,(k)^T Q_y e^p\,(k)} \tag{2.4}$$

where Q_y are controlled variables weights in MPC controller and ns is the number of sampled data. The MQI varies between 0 and 1, such that $MQI = 1$ means that all error is due to stochastic disturbance and the model is perfect.

Badwe *et al.* (2009) method

This method aims to identify channels, i.e., sub-models involving controlled variable (CV) *versus* manipulated variable (MV) with significant model-plant mismatch. It is based on the investigation of partial correlation between the manipulated variables and residual of model output prediction. The use of partial correlation is necessary to avoid false detection of model mismatches given by the causal relation between the variables.

Considering that the input and output are noise filtered, the first step is to isolate the effect of each MV. This is accomplished by the identification of an Output-Error model (OE) between each MV over the others, according to:

$$u_i(k) = V1_i U^i(k) + \varepsilon 1_i \tag{2.5}$$

where $u_i(k)$ is the evaluated MV, $V1_i$ are the OE model parameters, $U^i(k)$ is the matrix of remaining MVs and $\varepsilon 1_i$ is the component of the evaluated MV uncorrelated with the others. Similarly, it is necessary to isolate the effect of each CV from all MVs, except the one being evaluated. This is done by identifying an OE model between the prediction error of evaluated CV and the remaining MVs, expressed as:

$$e_j(k) = V2_{i,j} U^i(k) + \varepsilon 2_{i,j} \tag{2.6}$$

where $e_j(k)$ is the prediction error of evaluated CV, $V2_{i,j}$ are the OE model parameters, $U^i(k)$ is the matrix of remaining MVs and $\varepsilon 2_{i,j}$ is the evaluated CV prediction error under the sole effect of the evaluated MV. Model mismatch is detected through the regular correlation of $\varepsilon 1_i$ and $\varepsilon 2_{i,j}$. A strong correlation between these variables is an indicator of a mismatch in the MPC model $u_i X\ y_j$.

Yu & Qin (2008a and b) method

This methodology is useful to monitor multivariable controllers based on the inspection of CV variability. This evaluation is done by comparing the actual operational data with a historical benchmark data, in which the controller performs in an acceptable or in the desired manner. The global variability I_v is computed as follows:

$$I_{v=} \frac{\det\{cov[y_{II} - y_{set_{II}}]\}}{\det\{cov[y_I - y_{set_I}]\}} \tag{2.7}$$

where II refers to monitored data and I to benchmark. I_v value greater than one means an increase in variability and probably decline in performance, while I_v less than one means a variability decrease. Covariance (cov) investigation is also an auxiliary tool for process diagnosis. Considering the generalized eigenvalue problem (*GEVP*):

$$cov(y_{II} - y_{set_{II}})p = \mu cov(y_I - y_{set_I})p \tag{2.8}$$

where μ are the eigenvalues and p the corresponding eigenvector. High eigenvalues (μ) mean that there is a difference in the variability (when compared with the benchmark) in that corresponding eigenvector direction (p). In order to produce reliable results, a statistical inference is constructed. Considering the quadratic asymptotic statistics proposed by Desborough and Harris (1992):

$$f_d^{(i)} = 1 + 2\sum_{j=1}^{ns_d}\left(1 - \frac{j}{ns_d}\right)\rho_{d(i),j}^2 \tag{2.9}$$

Where sub-index d refers to dataset (I for benchmark and II to monitored), $\rho_{d(i),j}$ represent the autocorrelation coefficients of data along the eigenvector direction i at lag j and ns is the number of sampled data. From $f_d^{(i)}$ the confidence interval of each eigenvalue are calculated:

$$UL(\mu_i) = \mu_i\left[1 - z_{\propto/2}\sqrt{2\left(\frac{f_I^{(i)}}{ns_I - 1} + \frac{f_{II}^{(i)}}{ns_{II} - 1}\right)}\right]^{-1} \tag{2.10}$$

$$LL(\mu_i) = \mu_i\left[1 + z_{\propto/2}\sqrt{2\left(\frac{f_I^{(i)}}{ns_I - 1} + \frac{f_{II}^{(i)}}{ns_{II} - 1}\right)}\right]^{-1} \tag{2.11}$$

where $z_{\propto/2}$ is the critical value of a standard normal distribution at $(1-\propto)100\%$ confidence level. In practice, $UL(\mu_i)$ and $LL(\mu_i)$ greater than one means a performance deterioration in the corresponding eigenvector direction, $UL(\mu_i)$ and $LL(\mu_i)$ smaller the one represent a performance improvement. Finally $UL(\mu_i) > 1$ and $LL(\mu_i) < 1$ means no significant difference between the evaluated data and benchmark.

Based on the direction of performance decline/improvement, it is possible to identify the associated controlled variable. First, the subspaces of deterioration/improvement are constructed (P_w and P_b), grouping the correspondent eigenvector. θ_k is the angle between these subspaces and each individual controlled variable (represented by the unit vector ev_k) and is an indicator of the canonical correlation between the controlled variable and the subspace. It is calculated as follows:

$$cos(\theta_k{}^W) = \left\|P_w({P_w}^T P_w)^{-1}{P_w}^T ev_k\right\| \tag{2.12}$$

$$cos(\theta_k{}^b) = \left\|P_b({P_b}^T P_b)^{-1}{P_b}^T ev_k\right\| \tag{2.13}$$

Since P and θ_k are calculated from sample covariance, the confidence limit for $cos(\theta_k)$ helps to determine the statistic significance of each controlled variable contribution. Considering a cutting factor of 45º, it is defined according to:

$$\beta = \sqrt{\frac{1}{2} + \frac{z_{\propto/2}}{\sqrt{2n_g}}} \tag{2.14}$$

where n_g is the geometric mean between sample size of benchmark and monitored dataset. In practice, $cos(\theta_k{}^W)$ and $cos(\theta_k{}^b)$ larger than β means that the corresponding controlled variable contributes significantly to the subspaces P_w and P_b, contributing to performance decline/improvement.

2.2.3 Proposed methods for MPC model assessment

This section presents our contributions towards the assessment of model-plant mismatch for MPC models. We are focused on developing a tool for industrial applications in accordance with the guidelines described in Section 2.2.2.

A process under MPC control shown in Figure 2.1 is initially considered, where C is the controller, G_0 is the identified process model (nominal model), G is the real process model, ΔG is the model-plant mismatch, G_d is the unknown disturbance model, y_{set} correspond to the setpoints, u are the manipulated variables, y are the measured outputs, y_0 are the nominal outputs, y_{sim} are the simulated outputs of the nominal model perturbed by the actual control action u, v are sequences of independent random variables and y_d are the unmeasured disturbance signals. Based on this information, the methods are discussed below. T is the closed-loop model, called complementary sensitivity function of the real system and , T_0 is the nominal complementary sensitivity function.

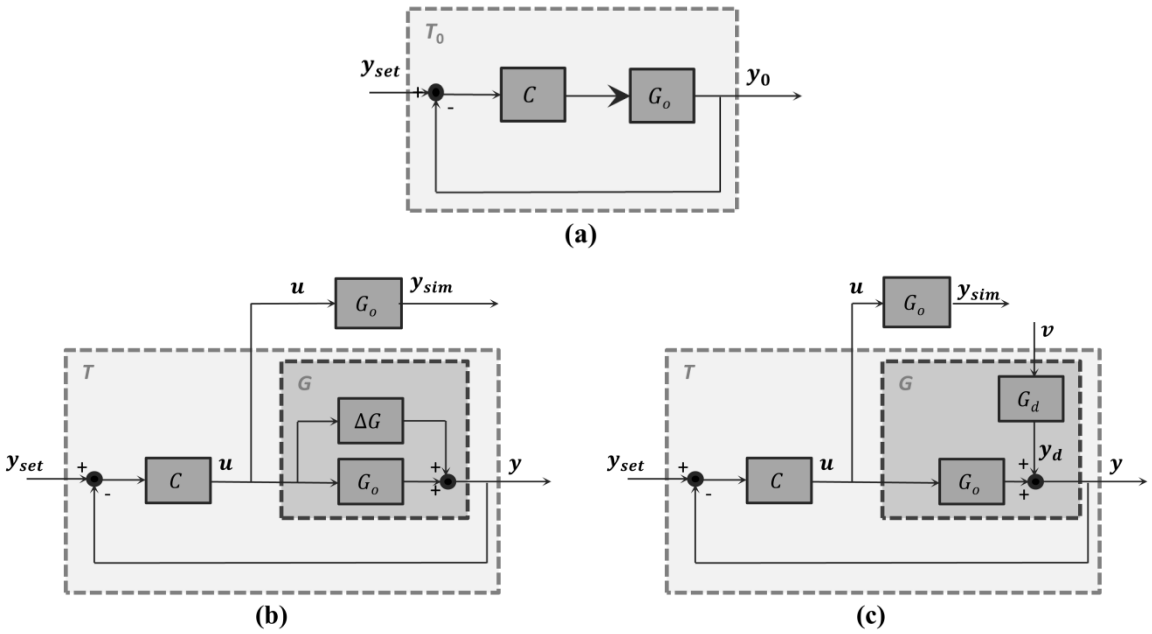

Figure 2.1: Schematic diagram of closed-loop (a) nominal system, (b) with model-plant mismatch and (c) with unmeasured disturbance.

Model quality evaluation for MPC using the nominal output sensitivity function

The method is based on the premise that an effective model should represent the real system at the frequency where the MPC works. Thus, to assess the real impact of model-plant mismatch, the closed-loop performance must be considered. The following

definitions for the closed loop behavior can be found in many control textbooks (e.g., Skogestad & Postlethwaite,1996):

$$y_0 = T_0 y_{set} \tag{2.15}$$

$$T_0 = G_0 C (I + G_0 C)^{-1} = (I + G_0 C)^{-1} G_0 C \tag{2.16}$$

$$S_0 + T_0 = I \tag{2.17}$$

$$y_{sim} \quad = G_0 u \tag{2.18}$$

Where S_0 is the nominal sensitivity funcion and I is the identity matrix. The nominal output y_0 (i.e., the output of the system in the absence of model-plant mismatch and unmeasured disturbance) could be estimated according to:

$$(\boldsymbol{y_0} - \boldsymbol{y}) = \boldsymbol{S_0}\ (\boldsymbol{y_{sim}} - \boldsymbol{y}) \tag{2.19}$$

The complete mathematical description as well as the theorem proof can be found in Botelho *et al. (*2015a/cap. 3)[3]. The expression (2.19) shows that it is possible to estimate the nominal closed-loop output from the controller model as well as plant input and output data. Since y_0 is an estimate of the output process in the absence of a model-plant mismatch or unmeasured disturbance, it could be considered a benchmark for controller-model output response. The main advantage is that, unlike of MVC/LQG, it is a realistic reference of the process model. It is important to emphasize that the diagnosis using y_0 relates merely to the process model quality or presence of unmeasured disturbance, being unaffected by poor tuning. Based on this reference, any output dependent on performance indicator could be applied. For example, a useful indicator is the comparison of output variances, called variance index (I_{var}), based in the indicator presented by Badwe *et al.* (2010) and expressed as :

$$Ivar = \frac{var(y - \bar{y})}{var(y_0 - \bar{y}_0)} \tag{2.20}$$

where $\bar{y}$ and $\bar{y}_0$ are the mean value of y and y_0, respectively. An $I_{var} \cong 1$ means that there is no modeling problem affecting the corresponding CV, since the variance of y and y_0 are similar. The output sensitivity function (S_0) can be obtained analytically from the nominal process model (G_0) and controller model (C), as shown in (2.16) and (2.17). However, given the complexity of MPC formulation, it is simpler and more straightforward to obtain S_0 from a simulation of the controller considering no model-plant mismatch and a sufficiently excited closed loop data. Then, the closed-loop model is identified based on the simulated data. Note that it is only necessary to apply this procedure again if the MPC tuning or nominal model is changed.

[3] Botelho *et al. (*2015a/cap. 3) refere-se ao artigo correspondente ao capítulos 3 desta tese.

Diagnosis of poor MPC model: Unmeasured Disturbance *vs.* Model-Plant Mismatch

Once the modeling problem in MPC is detected, it is desirable to identify its cause. A key issue is to determine whether the decline in performance is due to MPM or unmeasured disturbance. The former occurs when the process model cannot adequately describe the relations between model input and output variables and a re-identification is required. An unmeasured disturbance occurs when there is a deterministic unknown signal affecting output behavior. The effects of a MPM and unmeasured disturbance (UD) in the process outputs are very similar, thus, they are not easily distinguished. Botelho *et al*. (2015c/cap. 5)[4] proposed an alternative route to this diagnosis. The main idea is to compare the nominal outputs y_0 with the nominal error $e_0(k)$, defined as:

$$e_0(k) = y_0(k) - y(k) \tag{2.21}$$

Considering that $y_0(k)$ is the estimated output free from model-plant mismatches and unmeasured disturbances, $e_0(k)$ can be interpreted as the effect of the modeling problems in the loop. When the process output is under a MPM, $e_0(k)$ will be dependent on the references changes (setpoint or soft constraint), as well as $y_0(k)$, causing their variation to be similar. However, when the process output is under an unmeasured disturbance $e_0(k)$ will be independent of references changes, since the disturbances come from an external source. Nonetheless, $y_0(k)$ continues to be dependent from them. This means that the variation of $y_0(k)$ and $e_0(k)$ are uncorrelated. Therefore, the comparison between $y_0(k)$ and $e_0(k)$ patterns can be used to discriminate between model-plant mismatch and unmeasured disturbances.

The diagnosis procedure to distinguish between MPM and unmeasured disturbances consists of the statistical analysis of the distribution of $y_0(k)$ and $e_0(k)$ along a moving window (MW). The main advantage of this approach is its capability to better capture the dataset tendency. It means that the method capture how $y_0(k)$ and $e_0(k)$ are changing along the time. Botelho *et al*. (2015c/cap. 5)[4] show that this approach is more robust than the use of regular correlation because the regular correlation is a linear quantifier. Thus, when the process has some nonlinearity, the relation between $y_0(k)$ and $e_0(k)$ will also be nonlinear and the indicator will be misleading. The statistical distribution is evaluated by the skewness (skn) and kurtosis (kts) coefficients:

$$skn = \frac{m_3}{\left(\sqrt{m_3}\right)^3} \tag{2.22}$$

$$kts = \frac{m_4}{(\sqrt{m_2})^4} \tag{2.23}$$

where m_2, m_3 and m_4 are the second, third and fourth order central moment, defined as:

$$m_l = \frac{\sum_{i=1}^{MW}(X_i - \bar{X})^l}{MW}, l = 2,3,4 \tag{2.24}$$

[4] Botelho *et al. (*2015c/cap. 5) refere-se ao artigo correspondente ao capítulos 5 desta tese.

Where X_i is the evaluated dataset (y_0 or e_0) and $\bar{X}$ is it corresponding mean. A high value of kurtosis means that the data presents a large number of recordings away from the mean, when compared with a normal distribution. The sample skewness provides an indicator of how asymmetric is the distribution. A positive value of skewness means that there is a higher concentration of values below the mean. Figures Figure 2.2 and Figure 2.3 illustrate the skewness and kurtosis of a hypothetical case with MPM and unmeasured disturbance, respectively.

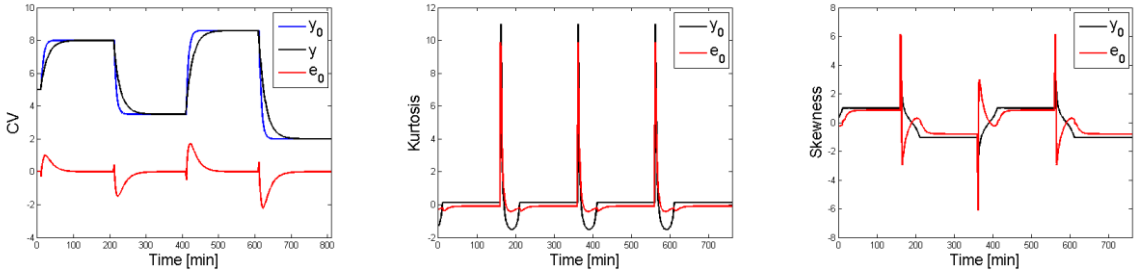

(a) **(b)** **(c)**

Figure 2.2: Hypothetical case with MPM: (a) measured $y(k)$ and estimation of $y_0(k)$ and $e_0(k)$, (b) kurtosis along a moving window and (c) skewness along a moving window.

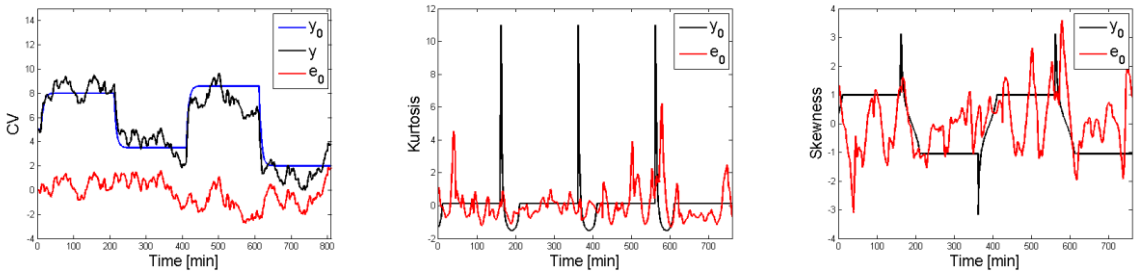

(a) **(b)** **(c)**

Figure 2.3: Hypothetical case with unmeasured disturbance: (a) measured $y(k)$ and estimation of $y_0(k)$ and $e_0(k)$, (b) kurtosis along a moving window and (c) skewness along a moving window.

The comparison of $y_0(k)$ and $e_0(k)$ are based on the kurtosis and skewness scatter. To quantify it, we have used a linear regression. The angular coefficient of the linear approximation $\cos(\propto)$ and its coefficient of determination R^2 provide an indicator of model-plant mismatch. The distribution of $y_0(k)$ and $e_0(k)$ become more similar closer to $\propto = 45°$ and when R^2=1. Thus, this is indicative of the presence of a model-plant mismatch, as shown in Figure 2.4.

A similar procedure is based on the confidence ellipse scatter. The ellipse is constructed considering the covariance matrix of $y_0(k)$ and $e_0(k)$ kurtosis and skewness. The angle of the largest eigenvalue corresponds to the ellipse inclination (γ). The ellipse diameters are given by the square root of the largest and the lowest eigenvalues multiplied by the critical chi-square value ($\chi_{\text{crit}}{}^2$) associated with a given probability level (Santos-Fernández, 2012). The confidence ellipse is less circular and more diagonal when the correlation between the statistical distributions of $y_0(k)$ and $e_0(k)$ is more significant, indicating the presence of a model-plant mismatch. Figure 2.4 shows the expected behavior of linear and elliptical approximation under MPM and unmeasured disturbance, respectively.

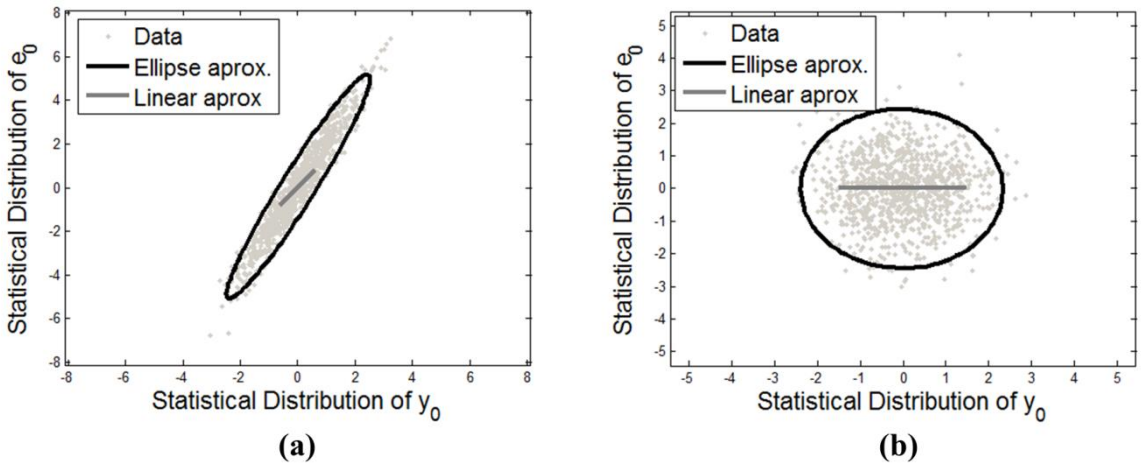

Figure 2.4: Expected response of linear and elliptical approximation (a) under MPM and (b) under unmeasured disturbance.

2.3 Industrial issues of MPC applications

Although predictive controllers rely on a solid theoretical foundation, most of the industrial application and commercial use MPCs use their own control policy (see Holkar & Waghmare, 2010; Qin & Badgwell, 2003). This means that they use different combinations of operational pratices, algorithms and variable considerations. MPC assessment techniques must be designed to manage this diversity of control policies. However, it is not simple because the mathematical formulation of the MPC is different for each case and most methods require adaptations in order to incorporate it into the assessment procedure.

The first adversity faced in MPC performance assessment is with regards to the process model. There are several model types used by the commercial controllers, which can be linear or non-linear, with empirical and phenomenological basis. Among the linear type, for example, it is common to formulate the model using transfer functions, step response, autoregressive models, impulse response, and state space. However, several MPC assessment techniques rely only on the analysis of transfer functions or state space models, so its application to other kinds of models will depend on some model conversion, which may corrupt the quality of analysis.

Another common industrial practice is the simplified real-time optimization layer. This structure has the objective of calculating the best operational region based in a steady state simulation, taking into consideration economic aspects and operational process constraints. Thus, the process model available should perform accordingly, both at controller frequency and in steady-state to complete the optimization layer (Campos *et al.*, 2013). Most of model evaluation techniques consider the modeling problems under a unified concept and do not take into account any aspect of the controller tuning, structure and objectives.

Another industrial practice that restricts the application of MPC assessment methods is the use of soft constraints, where the number of monitored variables is usually larger than the manipulated ones. Moreover, in some cases, the same controller has separate politics for different variables (setpoints and soft constraints). Thus, depending on the CVs prediction, the control problem can vary (change the set of controlled and manipulated

variable), in square or non-square scenarios. Most MPC assessment techniques use the setpoints as reference; however, for this kind of controller, there is no setpoint associated with the controller objective.

Additionally, there is a series of factors associated with plant operation, such as unmeasured disturbances (i.e., non-modeled deterministic variables), discontinuous disturbances and nonlinearities that hinder the development of a tool for monitoring and diagnosis.

2.4 Case Studies

2.4.1 Shell Benchmark Process

System Description

This Process was proposed by Prett & Morari (1987) and is composed by a heavy oil fractionator, as represented in Figure 2.5. The main feature of this process is the high interaction among the variables as well as large time delays.

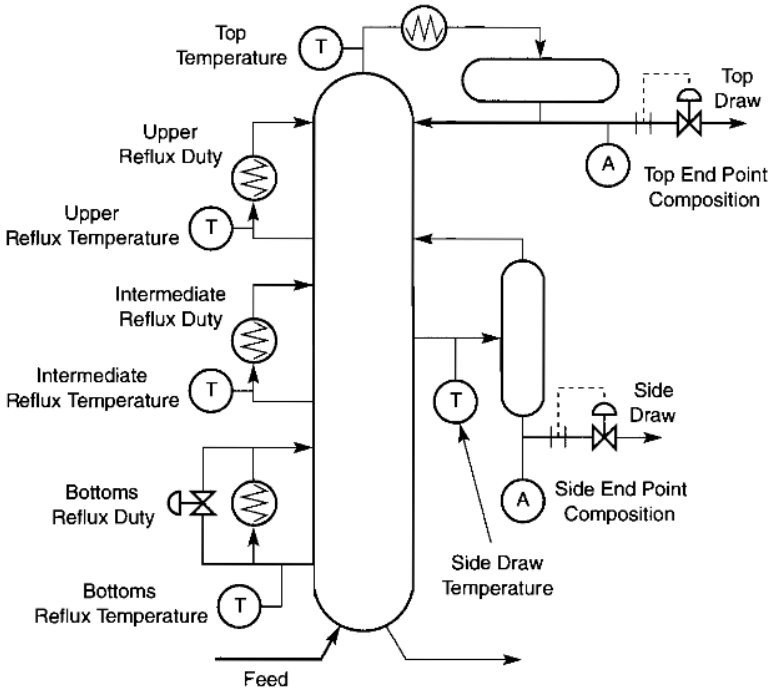

Figure 2.5: Schematic Representation of Shell Heavy Oil Fractionator (Maciejowski, 2002).

The control system is originally composed by 7 measured outputs, 4 manipulated inputs and 2 disturbances. In this case study the problem is reduced to a 3 X 3 structure and a linear MPC controller was configured in *Matlab*^{TM}*/Simulink*^{TM}. The objective is to control the top composition ($y1$), the side composition ($y2$) and the bottom reflux temperature ($y3$) by the manipulation of the top draw ($u1$), side draw ($u2$) and bottom reflux duty ($u3$). The process model (G_0) and the MPC cost function are:

$$G_0 = \begin{bmatrix} \frac{4.05}{50s+1}e^{-27s} & \frac{1.77}{60s+1}e^{-28s} & \frac{5.88}{50s+1}e^{-27s} \\ \frac{5.39}{50s+1}e^{-18s} & \frac{5.72}{60s+1}e^{-14s} & \frac{6.9}{40s+1}e^{-15s} \\ \frac{4.38}{33s+1}e^{-20s} & \frac{4.42}{44s+1}e^{-22s} & \frac{7.2}{19s+1}e^{-19s} \end{bmatrix} \quad (2.25)$$

$$\min_{\Delta u(k|k)\ldots\Delta u(mh-1+k|k)} \sum_{i=0}^{ph-1} \left\{ \sum_{j=1}^{nu} \left[|Q_u \Delta u(k+i|k)|^2_{i,j} \right] + \sum_{l=1}^{ny} \left[|Q_y (y(k+i|k) - y_{set}(k+i|k)|^2_{i,l} \right] \right\}$$
$$s.t. \quad u_{hard}^{max} \geq u \geq u_{hard}^{min}, \quad y_{hard}^{max} \geq y \geq y_{hard}^{min} \quad (2.26)$$

where mh is the horizon control, ph is the prediction horizon, nu is the number of available MVs, ny is the number of CVs, Q_y is the setpoint weighting of outputs, $Q_{\Delta u}$ is the move suppression, y_{hard}^{max}, y_{hard}^{min}, , u_{hard}^{max}, u_{hard}^{min} are the upper and lower constraint of CVs and MVs, respectively. The tuning parameters are presented in Table 2.2.

Table 2.2: MPC original tuning parameters: Shell Benchmark Problem

Sample Time	2min
Prediction Horizon (ph)	20
Control Horizon (mh)	4
Move Suppression ($Q_{\Delta u}$)	$Q_{\Delta u1} = Q_{\Delta u2} = Q_{\Delta u3} = 0.2$
CV Weight (Q_y)	$Q_{y1} = 1, Q_{y2} = 6, Q_{y3} = 2$
CV upper limit (y_{hard}^{max})	$y1_{hard}^{max} = y2_{hard}^{max}$=$y3_{hard}^{max}$=5
CV lower limit (y_{hard}^{min})	$y1_{hard}^{min} = y2_{hard}^{min}$=$y3_{hard}^{min}$=-5
MV upper limit (u_{hard}^{max})	$u1_{hard}^{max} = u2_{hard}^{max}$=$u3_{hard}^{max}$=20
MV lower limit (u_{hard}^{min})	$u1_{hard}^{min} = u2_{hard}^{min}$=$u3_{hard}^{min}$=-20

To compare the methods discussed in this paper, some inconsistencies were generated, including model-plant mismatch, unmeasured disturbance and changing tuning parameters (see Table 2.3). These inconsistencies were applied in the system and the simulations were performed, considering variations in the setpoints, according to Figure 2.7.

Table 2.3: Inconsistency Configuration: Shell Benchmark Problem

	Type	Value
M0	None	---
M1	Model-Plant Mismatch in $y1$ *versus* $u1$	$G_{1,1} = \frac{4.05}{80s+1} e^{-27s}$
M2	Unmeasured disturbance in $y2$	According to Figure 2.6
M3	Bad Tuning in $y3$	$Q_{y3} = 0.2$

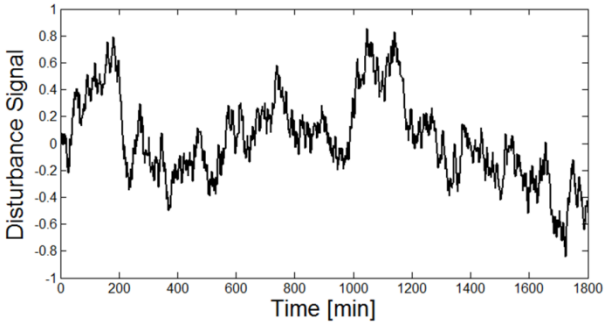

Figure 2.6: Unmeasured Disturbance in y2: Shell Benchmark Problem

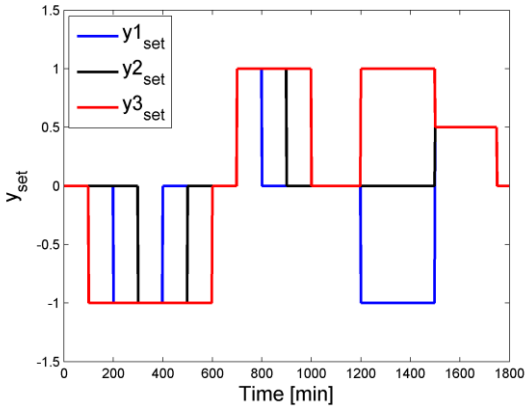

Figure 2.7: Step changes in each controlled variable setpoint: Shell Benchmark Problem

Results and discussions

The methods of Sun *et al.* (2013) Badwe et al. (2009) and Yu & Qin (2008a and b) as well the proposed method are applied in the generated data. Results are presented in Tables Table 2.4 and Table 2.5 and Figures Figure 2.8, Figure 2.9 and Figure 2.10.

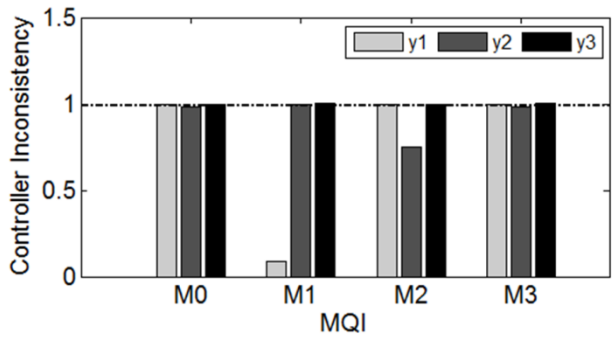

Figure 2.8: Results of Sun *et al.* (2013) method: Shell Benchmark Problem

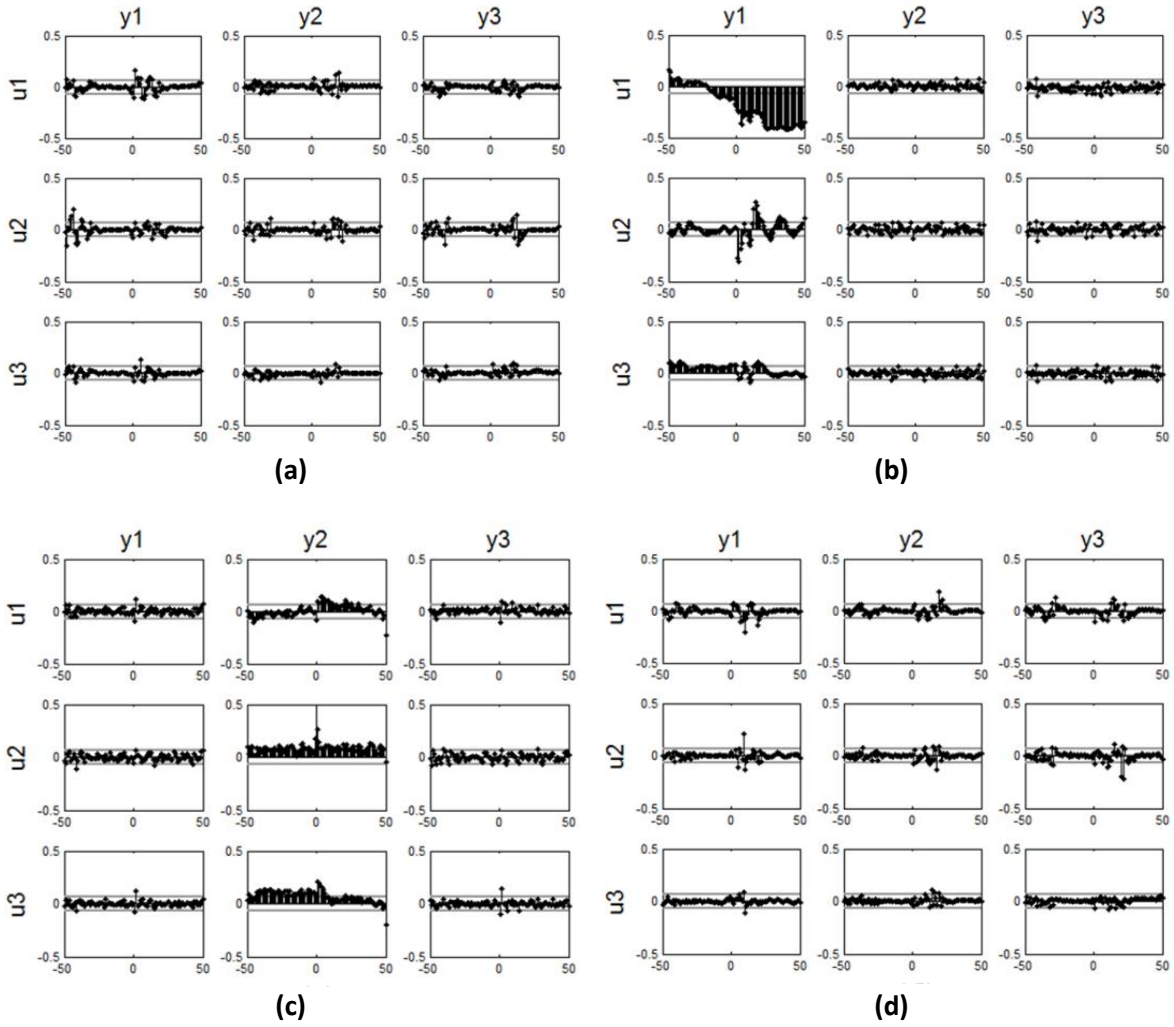

Figure 2.9: Results of Badwe *et al.* (2009) method: Partial correlation plots of Shell Benchmark Problem for $M0$(a), $M1$(b), $M2$(c) and $M3$(d)

Table 2.4: Results of Yu & Qin (2008a and b) method: Shell Benchmark Problem

	I_v	Worse Performance	Better Performance
M0	1.00	--	--
M1	4.76	$y1$	--
M2	2.14	$y2$	--
M3	2.83	$y3$	--

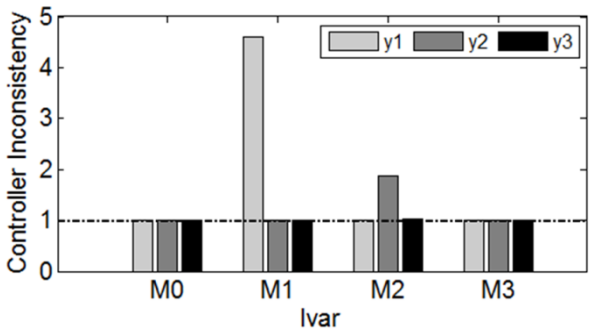

Figure 2.10: Results of proposed method: $Ivar$ for the Shell Benchmark Problem

Table 2.5: Results of proposed method: Kurtosis and Skewness indicators for Shell Benchmark Problem

	Ellipsoid Inclination (degrees)		**Ellipsoid Diameter Ratio**		**Linear Regression angle (degrees)**		$\|log(R^2)\|$	
	Kurtosis	***Skewness***	***Kurtosis***	***Skewness***	***Kurtosis***	***Skewness***	***Kurtosis***	***Skewness***
M1	27.17	64.00	2.22	1.55	20.14	11.99	3.42	0.26
M2	1.10	0.04	6.14	2.68	0.62	0.67	5.38	0.85

The Sun *et al.* (2013) method aims to detect modeling problems in the MPC. Figure 2.8 shows that the method is capable to ensure the correct diagnosis about the system, since it indicate MQI values smaller than one only when exist a model-plant mismatch or an unmeasured disturbance ($M1$ and $M2$).

The Yu & Qin (2008a and b) method detects changes in the general variability of the system and identify the CVs responsible for it. The diagnosis is independent of the source (disturbance, tuning or MPM). In this case study the evaluations were performed with a confidence level of 95% and using $M0$ as benchmark data. Table 2.4 shows that the method ensures the correct diagnosis in all cases, indicating an increase in I_v and associating with the correct variable responsible. For example, in $M3$ the method indicate $y3$ as responsible CV and the inconsistency in this case is performed in Q_{y3}.

The Badwe *et al.* (2009) method detects model-plant mismatch, as presented in Figure 2.9. The high partial correlation in $u1\ x\ y1$ indicates for case $M1$ indicates the presence of MPM in this model. For all other cases ($M0, M2$ and $M3$) the method indicates low partial correlation because they are not corrupted by a model-plant mismatch.

Results of Figure 2.10 show that the proposed method has correctly detected irregularities in the models and it has identified the variable affected by the mismatch in all cases. In $M1$ there is an indication of problems in $y1$ and for $M2$ there is an indication of problems in $y2$. The other cases ($M0$ and $M3$) have I_{var} near to one, because these cases do not have any modeling problem. For the cases with modeling problems ($M1$ and $M2$) the kurtosis and skewness indicators can be successfully applied to distinguish between model-plant mismatch and unmeasured disturbance, as presented in Table 2.5, since the angles (of linear approximation and ellipse) are smaller than 1.5^{o} presence of unmeasured disturbance and remains between 10º and 65º when a MPM is present. The ellipsoid diameter ratios are different from one, indicating the non-circle format of ellipse and validating the interpretation of the angles.

Thus, for this case study the methods of literature as well the proposed method, were adequate, generating results consistent with their assumptions.

2.4.2 The quadruple tank process

Process description

This system is composed of four cylindrical tanks that have been interconnected according to the diagram in Figure 2.11. Water is pumped into the tanks through the pumps with voltages $v1$ and $v2$. The flow of each pump is split using valves, whose openings are equal to $x1$ and $x2$, respectively. More details can be found in Johanson (2000).

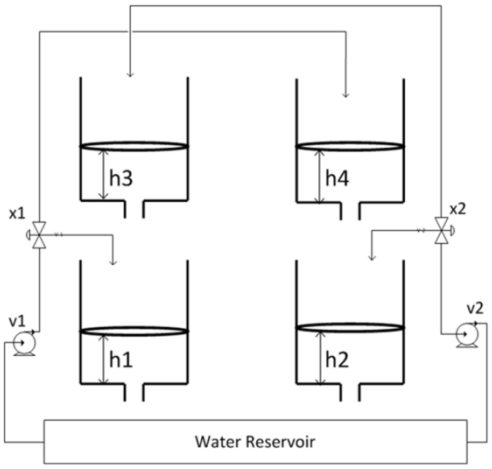

Figure 2.11: Schematic Representation of the Quadruple-Tank Process

The mass balances around each tank are:

$$\frac{dh_1}{dt} = -\frac{cd_1}{A_1}(h_1)^{exp1} + \frac{cd_3}{A_1}(h_3)^{exp3} + \frac{x_1 k_1}{A_1} v_1 \tag{2.27}$$

$$\frac{dh_2}{dt} = -\frac{cd_2}{A_2}(h_2)^{exp2} + \frac{cd_4}{A_2}(h_4)^{exp4} + \frac{x_2 k_2}{A_2} v_2 \quad (2.28)$$

$$\frac{dh_3}{dt} = -\frac{cd_3}{A_3}(h_3)^{exp3} + \frac{(1 - x_2)k_2}{A_3} v_2 \quad (2.29)$$

$$\frac{dh_4}{dt} = -\frac{cd_4}{A_4}(h_4)^{exp4} + \frac{(1 - x_1)k_1}{A_4} v_1 \quad (2.30)$$

where h_i is the level of each tank, $k_1 v_1$ and $k_2 v_2$ are the pumps´ output flow rate, A_i is the cross-section area of each tank, cd_i is the discharge coefficient of each tank and $expi$ is the discharge exponent. Table 2.6 provides the model parameter values.

Table 2.6: Original Parameter Values: The Quadruple-Tank Process

$\boldsymbol{A_1}$	$28\ cm^2$	$\boldsymbol{cd_4}$	$2.525\ cm^{2.5}/s$
$\boldsymbol{A_2}$	$32\ cm^2$	$\boldsymbol{k_1}$	$3.14\ cm^3/Vs$
$\boldsymbol{A_3}$	$28\ cm^2$	$\boldsymbol{k_2}$	$3.29\ cm^3/Vs$
$\boldsymbol{A_4}$	$32\ cm^2$	$\boldsymbol{exp1}$	0.5
$\boldsymbol{cd_1}$	$3.145\ cm^{2.5}/s$	$\boldsymbol{exp2}$	0.5
$\boldsymbol{cd_2}$	$2.525\ cm^{2.5}/s$	$\boldsymbol{exp3}$	0.5
$\boldsymbol{cd_3}$	$3.145\ cm^{2.5}/s$	$\boldsymbol{exp4}$	0.5

MPC configuration

For the process described above, we set a linear MPC controller in *Matlab™/Simulink™* with controlled variables being the four levels (h_1, h_2, h_3 and h_4) and manipulated variables being the pump voltages (v_1 and v_2) and valve openings (x_1 and x_2).

The linear plant model used by the MPC was obtained from the linearization of the nonlinear model at the operating point, defined by the manipulated variables $v1 = 3.2, v2 = 3.15, x1 = 0.43$, and $x2 = 0.34$ and is given by:

$$G(s) = \begin{bmatrix} \frac{0.048}{s+0.016} & \frac{0.0025}{s^2+0.028s+0.0002} & \frac{0.35}{s+0.015} & \frac{-0.0096}{s^2+0.41s+0.0004} \\ \frac{0.0009}{s+0.016} & \frac{0.035}{s+0.011} & \frac{-0.0055}{s^2+0.024s+0.0002} & \frac{0.323}{s+0.011} \\ 0 & \frac{0.078}{0.028s+0.25} & 0 & \frac{-0.37}{s+0.026} \\ \frac{0.045}{s+0.018} & 0 & \frac{-0.31}{s+0.018} & 0 \end{bmatrix} \quad (2.31)$$

The MPC used has a simple real-time optimization layer, which established the optimal operating point according to economic objectives. The scheme presented by Figure 2.12 illustrates its architecture.

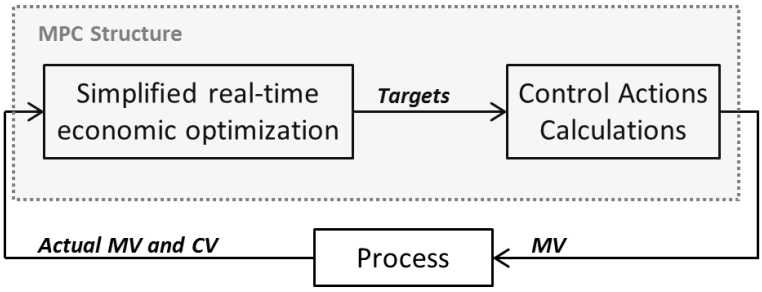

Figure 2.12: Architecture of MPC controller with optimizer (adapted from Campos *et al.*, 2013)

The cost function of the simple real-time optimization is defined by:

$$\begin{aligned} &\min_{u_{tgt}} \sum_{i=1}^{nu} (\varphi_u u_{tgt})_i \\ &s.t. \quad \begin{aligned} y_{soft}^{max} &\geq y_{set} \geq y_{soft}^{min} \\ u_{hard}^{max} &\geq u_{tgt} \geq u_{hard}^{min} \end{aligned} \end{aligned} \tag{2.32}$$

where φ_u are the manipulated variables costs, y_{set} are the setpoints (corresponding to the closed-loop steady-state prediction of CVs), y_{soft}^{max} and y_{soft}^{min} are the soft constraints of controlled variables, u_{hard}^{max} and u_{hard}^{min} are the constraints of MVs and u_{tgt} are the MVs targets.

The optimal values calculated from the optimizer (u_{tgt} and y_{set}) are transferred to the MPC optimization problem formulated as follows:

$$\begin{aligned} &\min_{\Delta u(k|k)\ldots\Delta u(mh-1+k|k),\delta} \sum_{i=0}^{ph-1} \left\{ \sum_{j=1}^{nu} \left[|Q_{\Delta u}\Delta u(k+i|k)|^2{}_{i,j} + |Q_u(u(k+i|k) - u_{target}(k+i|k)|^2{}_{i,j} \right] + \tau_y {\delta_y}^2 \right\} \\ &s.t. \quad \begin{aligned} u_{hard}^{max} &\geq u \geq u_{hard}^{min} \\ y_{hard}^{max} &\geq y \geq y_{hard}^{min} \\ y_{soft}^{max} + \delta_y &\geq y \geq y_{soft}^{min} - \delta_y \\ \delta_y &\geq 0 \end{aligned} \end{aligned} \tag{2.33}$$

where mh is the horizon control, ph is the prediction horizon, nu is the number of available MVs, Q_u is the target weighting of MVs, $Q_{\Delta u}$ is the move suppression, δ_y is the slack variable to soft the constraints of CV, τ_y is the penalization of CV soft constraint violation, y_{hard}^{max} and y_{hard}^{min} are the hard constraints of CVs.

It is important to emphasize that, as shown in (2.33), this MPC controller is configured in terms of manipulated variables, so that the CVs are penalized only in cases of soft constraint violations (given that, when there is no soft constraint violation, $\delta_y = 0$). This allows operation in a scenario where the number of controlled variables is greater than the number of manipulated variables, as discussed in Section 2.3. The tuning parameters for the controller are defined in Table 2.7.

Table 2.7: MPC original tuning parameters: The Quadruple-Tank Process

Sample Time	10s
Prediction Horizon	48
Control Horizon	12
MV Cost	$\varphi_{v1} = \varphi_{v2} = -350; \varphi_{x1} = \varphi_{x2} = +50$
MV Target Weight	$Q_{v1} = Q_{v2} = Q_{x1} = Q_{x2} = 10$
Move Suppression	$Q_{\Delta v1} = Q_{\Delta v2} = Q_{\Delta x1} = Q_{\Delta x2} = 50$
Penalization of the constraints violation	$\tau_{h1} = \tau_{h2} = \tau_{h3} = \tau_{h4} = 1.25E5$

Scenarios Configuration

Different scenarios are defined for simulating the system described above. They are configured by the manipulation of CVs and MVs constraints.

- Scenario 1: 4x4 System

This scenario illustrates a square system, i.e., the number of controlled variable and available manipulated variable is equal. In terms of control, this is the simplest situation, since there are enough degrees of freedom to keep all controlled variables in the optimal condition. The direction provided by the optimizer (equation 2.32) results in keeping the levels at their maximum limits. The behavior of this system is similar to a classical fixed setpoint case. Figure 2.13 shows the results when there is no modeling error.

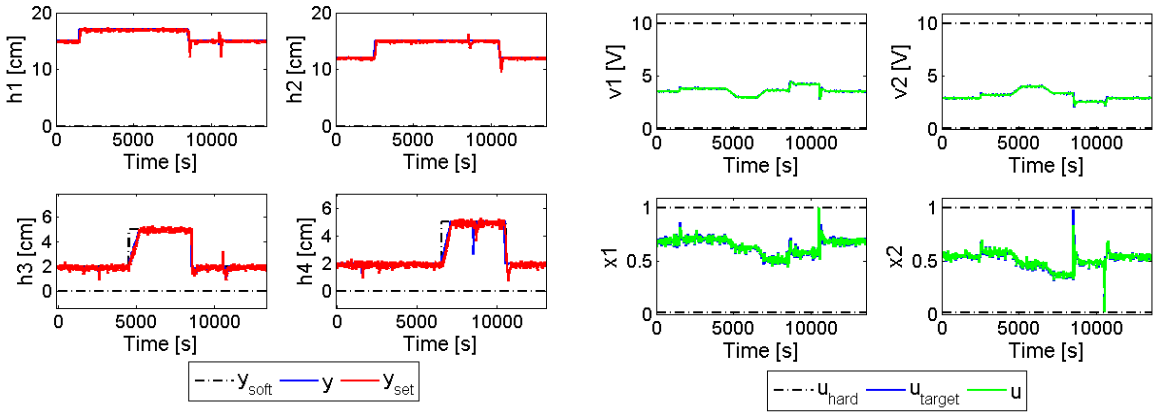

Figure 2.13: Expected behavior in Scenario 1: The Quadruple-Tank Process

- Scenario 2: $x1$ and $x2$ saturated at the upper limit

This scenario is created by reducing the upper limits of $x1$ and $x2$ and the soft constraint of $h3$ and $h4$ to a lower level, as shown in Figure 2.14. In this case, the valve openings remain saturated most of the time, which means that the system has only two manipulated variables (v_1 and v_2) available to control the four levels. The result is that two CVs are maintained at the optimal soft constraint and the others remain within the soft constraint.

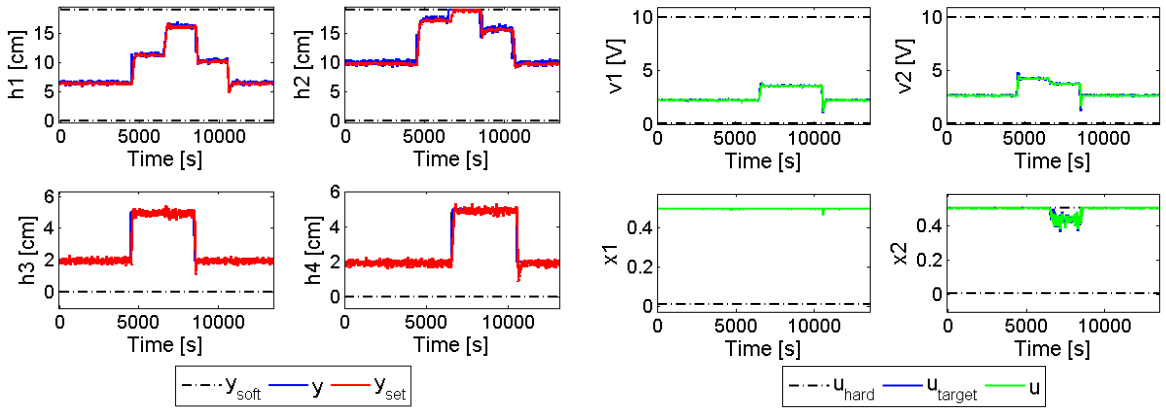

Figure 2.14: Expected behavior of Scenario 2: The Quadruple-Tank Process

Controller Inconsistencies Configuration

To compare the methods, several controller inconsistencies are performed, including model-plant mismatch, unmeasured disturbance and inappropriate tuning parameters, as presented in Table 2.8. These inconsistencies were applied in the system and the simulation was performed considering each scenario described above.

Table 2.8: Inconsistencies Configuration: The Quadruple-Tank Process

	Type	Value
M0	None	---
M1	Model-Plant Mismatch	$cd_2 = 6.47$
M2	Model-Plant Mismatch	$A_3 = 182$
M3	Model-Plant Mismatch	$cd_3 = 7.86$
M4	Unmeasured Disturbance	$Gd_{h4} = \frac{4}{70s+1}$
M5	Unmeasured Disturbance	$Gd_{h1} = \frac{5}{5s+1}$
M6	Model-Plant Mismatch	$exp3 = 0.1$
M7	Model-Plant Mismatch	$exp2 = 0.85$
M8	Tuning Modification	$Q_{v1} = Q_{v2} = Q_{x1} = Q_{x2} = 80$
M9	Tuning Modification	$Q_{\Delta v1} = Q_{\Delta v2} = Q_{\Delta x1} = Q_{\Delta x2} = 150$

Results and discussions

- Sun *et al.* (2013) method

The main objective of this method is to identify problems in the MPC model. The indicator proposed by the author is based in the weight of CVs (see equation 2.4). However, the MPC configured in this case study does not include a term for controlled variable penalization (considering that they are inside the range) in the cost function.

Therefore, in this case, the direct application of the indicator is not useful. An alternative is to evaluate the MQI for each CV, individually. Figure 2.15 and Figure 2.16 illustrate the results.

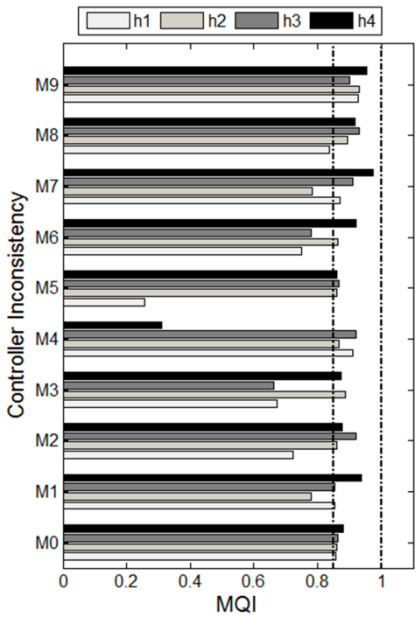

Figure 2.15: Results of Sun *et al.* (2013) method for Scenario 1 under model inconsistencies - MQI of controlled variables: The Quadruple-Tank Process

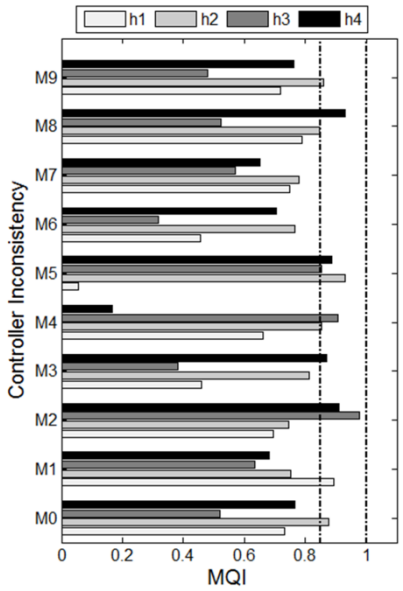

Figure 2.16: Resuls of Sun *et al.* (2013) method for Scenario 2 under model inconsistences - MQI of controlled variables: The Quadruple-Tank Process

According to the method, the model performs better when the MQI is near 1. An empirical tolerance limit of 0.85 was considered (dash line in figures), which means that MQI greater or equal to 0.85 does not indicate significant model-plant mismatch. Values below this tolerance are an indicator of poor model quality. Figure 2.15 shows that, for Scenario 1, the method correctly captures model mismatches or non-measured disturbance presence. For example, from phenomenological model (2.27) to (2.30) a mismatch on $cd2$ (M1) only affects $h2$, whereas a mismatch in $cd3$ (M3) will affect $h1$

and $h3$. This conclusion is correctly captured by the method for scenario 1. Similarly, a tuning mismatch does not lead to any indication, as shown in cases M8 and M9.

However, when the CVs are inside the range, the method does not perform as expected, according to Figure 2.16. This occurs because, in this case, the calculated setpoint (2.32) is just a result of the optimal control actions, not being strictly associated with the control objective (2.33). In practical terms, this means that the CV moves are not a direct consequence of setpoint changes, as estimated by the HOARX model suggested for the method (2.1).

- Yu & Qin (2008) method

The main objective of the method is to evaluate the general variability of the controlled variables and identify those responsible for changes in performance. The evaluations were performed using a confidence level of 95%. The benchmark data are from Scenario 1 without mismatch (M0), since it is the dataset closest to the design case, where the system has enough levels of freedom to optimize all CVs. Table 2.9 summarizes the results obtained.

Table 2.9: Results of Yu & Qin method: The Quadruple-Tank Process

	Scenario 1			**Scenario 2**		
	I_v	Worse Performance	Better Performance	I_v	Worse Performance	Better Performance
M0	1.00	--	--	0.08	$h2, h3, h4$	$h1$
M1	4.90	$h2, h3, h4$	--	0.042	$h2, h3$	--
M2	9.85	$h2$	--	2.74	$h2, h3, h4$	--
M3	4.3	$h2, h3$	$h1$	0.22	$h2, h3, h4$	--
M4	473.5	$h1, h2, h3, h4$	--	5.8e3	$h1, h2, h3$	--
M5	178.7	$h1, h3, h4$	--	0.83	$h2, h3, h4$	$h1$
M6	2.04	$h2, h3$	$h1$	0.16	$h2, h3$	$h1$
M7	1.4	--	--	0.037	$h2, h3$	$h1$
M8	4.12	$h2$	--	0.29	$h2, h3$	--
M9	1.52	$h2, h4$	$h1$	0.0068	$h2, h3, h4$	$h1$

Table 2.9 shows that, for Scenario 1 the model-plant mismatch or non-measured disturbance weaken the system´s performance in all cases, since I_v is bigger than 1. However, the variable associated with performance decline is not necessarily the same affected by the mismatch. This is to be expected given the mismatch impact on the MVs and the fact that this effect is captured for all CVs.

For Scenario 2, the method indicates improved performance of some CVs in all cases, except M4. This happens because, in the benchmark data, the setpoints are constant and remain in the optimal limit for the most part (Figure 2.13). However, when the CVs are inside the range ($h1$ and $h2$ in Figure 2.14), the setpoints (from the optimizer) capture the noise effect and the measured CV is closer to its value. In this case, the method provides an erroneous indication of improved performance. Thus, the MPC analysis using the Yu & Qin (2008a and b) method is inconclusive when the CVs are operating by range, since the method is setpoint dependent.

- Badwe *et al.* (2009) method

The main objective of this method is to identify the model channels (i.e. pair MV *versus* CV) that have significant model-plant mismatch. The method was applied in the generated data for each scenario and model inconsistences. It is important to emphasize that the saturated manipulated variables (Scenario 2) are removed of the evaluation procedure, to ensure the quality of OE models identification. This method is capable of identifying the model mismatches independent of the scenario evaluated. This result is consistent, since this method essentially evaluates the expected response of CVs given the MVs values, not relying on any aspect of controller objectives. Figure 2.17 exemplifies the results from Scenario 2. When a mismatch in $exp3$ occurs (M6), models directly associated with $h1$ and $h3$ indicate a problem. When a tuning mismatch occurs (M9), the model produces some indicative of high partial correlation, which means that there is no model-plant mismatch in this case.

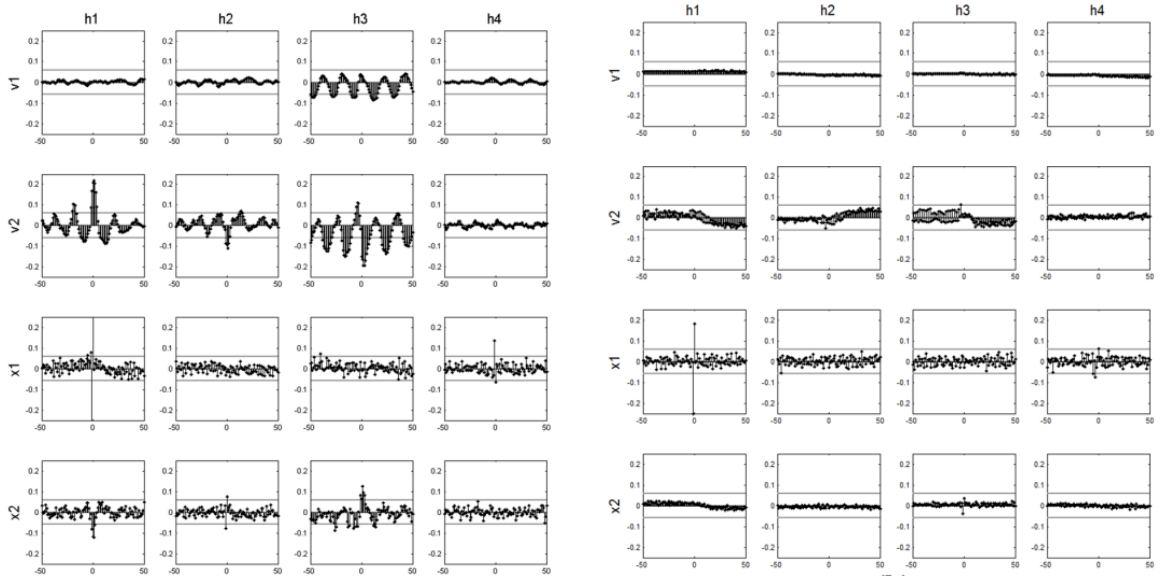

Figure 2.17: Results of Badwe *et al.* (2009) method: Partial correlation plot of (a) Scenario 2 – M6 and (b) Scenario 2 – M9: The Quadruple-Tank Process

Although the success of this method is independent of the control strategy used, the dynamic partial correlation analysis is not easily applied in practical terms. The first issue presented by the author is the need for enough MV and CV moves for the estimation of consistent OE models. This requires an extensive investigation of historical data to find operational conditions that satisfy this requirement. Another issue, presented by Carlsson (2010), is that many parameters need to be carefully chosen. For example, Figure 2.18

illustrates OE models estimated for Scenario 1 – M1, considering different orders. It is possible to see the poor OE model quality if a wrong order model is selected, which make automatic utilization of this method difficult.

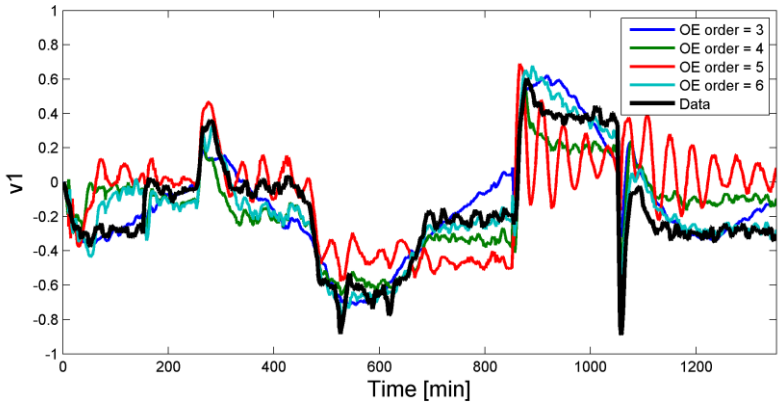

Figure 2.18: OE models estimated for Scenario 1 – M1 considering different orders: The Quadruple-Tank Process

- Proposed methods

The main objective of the method is to identify the controlled variables that have significant impact of modeling errors, using the nominal simulation as reference, and detect if the source is a model-plant mismatch or an unmeasured disturbance. The indicator used is the variance of outputs (2.20). The skewness and kurtosis indicator was performed for the CVs that suffered the greatest impact in each case. Figures Figure 2.19 and Figure 2.20 and Tables Table 2.10 and Table 2.11 summarize the results.

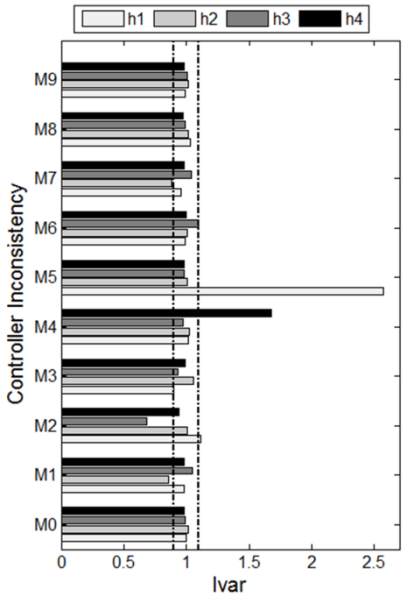

Figure 2.19: $Ivar$ for Scenario 1: The Quadruple-Tank Process

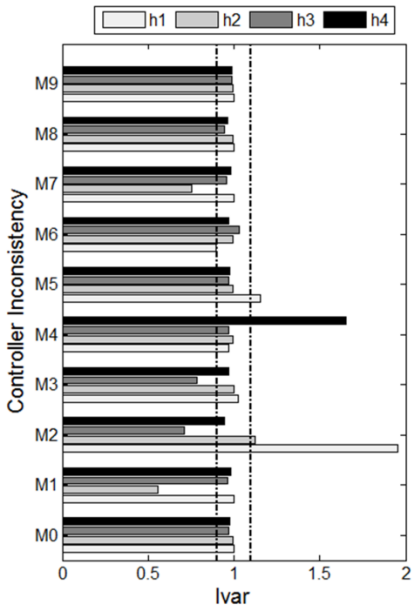

Figure 2.20: $Ivar$ for Scenario 2: The Quadruple-Tank Process

Table 2.10: Kurtosis and Skewness indicators for Scenario 1: The Quadruple-Tank Process

	Ellipsoid Inclination (degrees)		**Ellipsoid Diameter Ratio**		**Linear Regression angle (degrees)**		$\|log(R^2)\|$	
	Kurtosis	***Skewness***	***Kurtosis***	***Skewness***	***Kurtosis***	***Skewness***	***Kurtosis***	***Skewness***
M1	30.90	37.43	1.78	2.31	20.25	29.26	1.48	0.79
M2	32.45	37.72	1.47	1.87	16.16	25.36	2.16	1.20
M3	35.49	40.74	2.05	2.78	25.90	34.39	1.03	0.52
M4	12.59	15.33	2.37	2.99	10.32	13.58	1.91	1.15
M5	2.44	4.78	1.78	1.84	1.67	3.3768	5.91	4.45
M6	35.89	53.59	1.31	1.54	15.59	23.89	2.72	1.87
M7	38.72	37.56	1.65	1.65	22.38	21.95	1.57	1.57

Table 2.11: Kurtosis and Skewness indicators for Scenario 2: The Quadruple-Tank Process

	Ellipsoid Inclination (degrees)		**Ellipsoid Diameter Ratio**		**Linear Regression angle(degrees)**		$\|log(R^2)\|$	
	Kurtosis	***Skewness***	***Kurtosis***	***Skewness***	***Kurtosis***	***Skewness***	***Skewness***	***Kurtosis***
M1	38.42	37.48	2.55	2.27	31.45	28.99	0.65	0.83
M2	36.67	26.35	1.43	1.71	16.77	16.78	2.20	1.78
M3	34.82	38.19	2.02	3.01	25.15	33.21	1.08	0.47
M4	6.74	15.78	2.34	2.68	5.51	13.52	3.05	1.32
M5	6.54	1.55	1.57	2.30	3.87	1.26	4.51	5.97
M6	26.12	60.11	2.99	1.14	51.05	16.48	0.64	4.39
M7	40.29	38.13	2.32	2.66	31.36	31.80	0.77	0.59

Results of Figure 2.19 and Figure 2.20 show that, considering a $Ivar$ tolerance of ±0.1 (due to noise), the system nonlinearity does not interfere significantly in MPC performance, since $Ivar$ is close to one for all variables. The method has correctly detected irregularities in the models and it has identified the variable affected by the mismatch in all cases. For example, in both scenarios, for M1 there is an indication of problems in $h2$. This case corresponds to a mismatch in parameter $cd2$, which is associated to this level. In the presence of a tuning modification, the method does not indicate any variable affected, as expected.

Table 2.10 and Table 2.11 demonstrate that the kurtosis and skewness indicators can be successfully applied to distinguish between model-plant mismatch and unmeasured disturbance. The linear regression and ellipsoids approximation approaches provide similar results, so that, in general, the angles (of straight and ellipse) remain between 15^o and 55^o in presence of model-plant mismatch and exceed these limits when the process is under an unmeasured disturbance. It is not simple to define a relation between the ellipsoid diameter ratio and the source of discrepancy problem if this index is analyzed separately as well with as $|log(R^2)|$, however, combined with the angle investigation, a good estimation of data distribution is provided. Finally, to ensure reliable results, a good practice is also to investigate the skewness and kurtosis. They produce even better and conclusive results. Figure 2.21 and Figure 2.22 make evident the dependence relation of $y_0(k)$ and $e_0(k)$ in case of model-plant mismatch, since the peaks in the data occur at the same instant and have similar magnitude. However, this does not occur in presence of unmeasured disturbance. These figures also show the capacity of the proposed indicators to correctly indicate the kind of modeling problem considering the shape and inclination of ellipse and linear approximation.

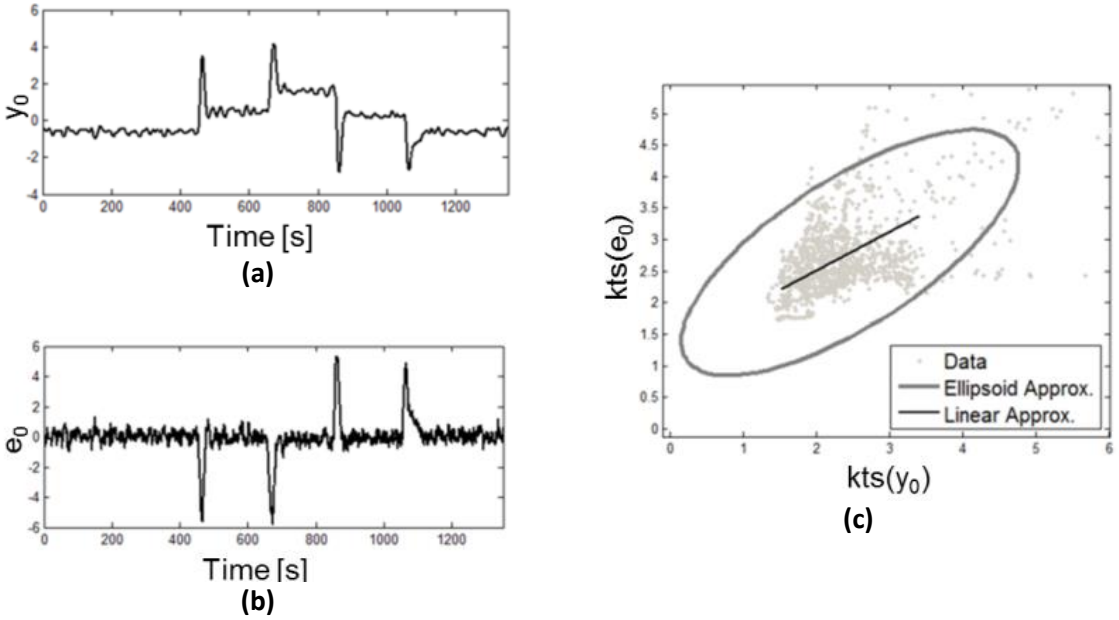

Figure 2.21: Scenario 2 – M1: (a) estimation of $y_0(k)$, (b) estimation of $e_0(k)$ and (c) scattering of $kts(\mathrm{y}_0)$ vs. $kts(e_0)$: The Quadruple-Tank Process

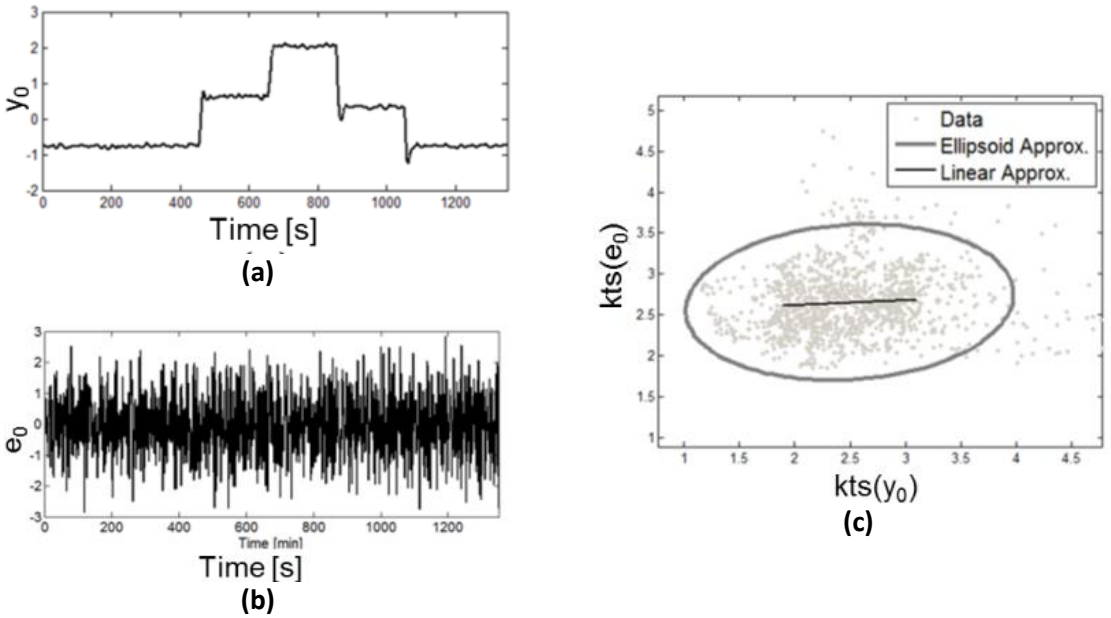

Figure 2.22: Scenario 2 – M5: (a) estimation of $y_0(k)$, (b) estimation of $e_0(k)$ and (c) scattering of $skn(\mathrm{y}_0)$ vs. $skn\ (e_0)$: The Quadruple-Tank Process

2.5 Conclusions

In this paper an overview concerning MPC performance assessment and diagnosis was accomplished. These techniques have been evaluated considering industrial premises, as proposed by Hugo (2002). Considering them, we selected the following methods: Sun *et al.* (2013) aim to point out the variables with strong impact of disturbances or model mismatch; Badwe *et al.* (2009) evaluate the model plant mismatch and isolate the channels that should be identified to improve the model quality; and the Yu & Qin (2008a

and b) method, that identifies the controlled variables that provide the major contributions to variability changes.

These techniques have been applied in two case studies: The Shell benchmark process and The Quadruple-tank process.

The Shell benchmark process is configured with a linear plant and MPC. The main objective of the controller is to maintain the controlled variables at their setpoints. A model-plant mismatch, an unmeasured disturbance and a bad tuning have been inserted to evaluate the methodologies. The results show that all methods presented in this paper were capable to ensure the correct diagnosis of the system in the evaluated cases.

In the quadruple-tank plant a linear MPC is applied in the (nonlinear) process. The controlled variables are supervised using soft constraints instead of setpoints, a common scenario in industrial applications. Several mismatches have been inserted to evaluate the methodologies. The Sun *et al.* (2013) and (2008a and b) methods provide reliable results when the controller has enough degrees of freedom to achieve all desired values. However, when the controlled variables remain inside the soft constraints, these methods failed, because of the absence of a specific setpoint. The method proposed by Badwe *et al.* (2009) is insensitive to the control strategy, because it requires only input and output data. The main limitation is that it requires a rich dataset to ensure correct identifications. This requirement can restrict the industrial application.

Since the MPC model is the most important source of controller degradation, we propose new a methodology for detecting modeling problems. This new approach allows evaluating the model-plant mismatch (MPM) impact specific to the actual controller performance, considering the output sensitivity function, which is a reasonable benchmark for MPC assessment. Moreover, its simplicity facilitates application in real plant data (online or offline), regardless of the control algorithm assumed. The proposed method was capable of indicating the impact of the modeling inconsistences in the system behavior, independent of the controller strategy used.

Another key issue for the modeling quality assessment is to determine whether the cause of poor performance comes from a model-plant mismatch or an unmeasured disturbance. This paper proposed an approach to distinguish between these two sources of degradation. The main idea was to compare the estimated behavior of the system in the absence of model-plant mismatch with the estimated modeling error. The comparison was made considering the statistical distribution (Kurtosis and Skewness coefficients) along a moving window. The diagnosis procedure is based on a linear approximation and the confidence ellipse of the statistical distributions. The proposed approach could detect the source of the discrepancy for all analyzed scenarios, independent of controller configuration.

Capítulo 3 – **A methodology for detecting model-plant mismatches affecting MPC performance**

Abstract[5]: The model quality for a model predictive control (MPC) is critical for the control loop performance. Thus, assessing the effect of model-plant mismatch (MPM) is fundamental for performance assessment and monitoring the MPC. This paper proposes a method for evaluating model quality based on the investigation of closed-loop data and the nominal output sensitivity function, which facilitates the assessment procedure for the actual closed-loop performances. The effectiveness of the proposed method is illustrated by a multivariable case study, considering linear and nonlinear plants.

Keywords: Model Predictive Control, Model-Plant Mismatch, Model Quality, Control Performance Assessment

[5] *Aceito para publicação no periódico "Industrial & Engineering Chemistry Research".*

3.1 Introduction

MPC is the consensual solution when an advanced controller is necessary. This status is based on more than 20 years of its successful application in many fields (Qin & Badgwell, 2003). The complex behavior and multivariable nature of chemical plants justify MPC proliferation. In each execution cycle, these controllers are capable of estimating a sequence of control actions that directs the process towards ideal operational conditions. Further details of MPC characteristics are provided in Camacho & Bordons (2004), Maciejowski (2002) and Rawlings & Mayne (2009). The "heart" of these controllers is the plant model, whose predictions are used to optimize control actions, which allows it to operate close to optimal conditions.

All processes are susceptible to external degradation factors that cause the plant to operate differently from that which is foreseen in the MPC design, such as sensors and equipment failure, variability of raw material, changes in product specifications and seasonal influence, reducing its profitability. As a consequence, assessing controller performance is essential to ensure controller longevity. Nonetheless, this remains a difficult task due to the processes' multi-factorial nature and complex structure. According to Sun *et al.*(2013), there are many sources of performance degradation, including tuning parameters (horizon length, weight parameters, time of control cycles, etc.), poor model quality, inappropriate constraint setup and the presence of unmeasured disturbances.

Industrial and academic interest in MPC assessment grew significantly in the last decades, giving rise to several techniques. Some of these are based on the concept of Minimal Variance Control (MVC) and/or its Linear Quadratic Gaussian (LQG) extension. For example, Lee *et al.*(2008) suggests a method based on MVC, which evaluates the sensitivity of variables in order to verify their contribution to the economic performance of the controller. Harrison & Qin (2009) suggest a minimal variance map to evaluate the effect of constraints. Zhao *et al.* (2010) propose an economic benchmark based on LQG. Zhang *et al.* (2013) suggested a deconstruction of a MIMO system in MISO subsystem to evaluate each controlled variable independently. Some authors, however, disagree on using LQG/MVC for MPC assessment, as they deem it an unattainable model for most real-life applications (Jelali, 2013). Alternatively, some authors proposed techniques that use historical benchmarks, such as Schäfer & Cinar (2004), who evaluated plant data based on MPC cost function. Other methods (e.g., Alcala & Qin, 2009 and 2011; AlGhazzawi & Lennox, 2009; Tian *et al*., 2011; Zhang & Shaoyuan, 2006) are based on the construction of PCA/PLS models to identify sources of controller degradation.

A significant number of methods focus exclusively on investigating the model's quality, given that it is the neuralgic component of MPC. Such is the case in Conner and Seborg (2005), who use the Akaike Information Criteria to asess the need for re-identification. Badwe *et al.* (2009) evaluated the partial correlation between input and output residuals to detect model discrepancies. Sun *et al.* (2013) measured model qualities based on the deconstruction of model residuals onto an orthogonal basis. Jiang *et al.* (2012) proposed an indicator, which compares residuals under different levels of prediction. Most of the available methods for model quality assessment focus on investigating the predictive capacity of the models in an open-loop approach. However, the model error effect on MPC performance is not only dependent on the mismatches, but also is function of the controller tuning and disturbances.

Badwe *et al.* (2010) incorporate this concept and propose the identification of the design plant behavior in closed-loop, also called design sensitivity (S_d) to quantify the impact of model-plant mismatch in MPC performance. A brief description of this method is presented below.

Consider the IMC structures presented in Figure 3.1, where K is the IMC controller, G is the real process model, G_0 is the identified process model, v_s are the stationary disturbances entering the loop, d are the model residual feedback and ϵ are the controller inputs. The designed sensitivity (S_d) supposes that the plant dynamics were exactly captured by the model (i.e., $G = G_0$) as illustrated in Figure 3.1, and is defined as:

$$S_d = \mathrm{I} - G_0 K \tag{3.1}$$

Badwe *et al.* (2010) suggest that the S_d should be identified by an Output-Error (OE) model using the measured plant outputs (y), the setpoints (y_{set}) and the predicted outputs ($\hat{y}$). Considering the achieved loop shown in Figure 3.1, the controller inputs (ϵ) are:

$$\epsilon = y_{set} - y + \hat{y} \tag{3.2}$$

So, the designed sensitivity model can be identified as follow:

$$(y_{set} - y) = S_d \epsilon \tag{3.3}$$

The outputs of the designed closed loop (Figure 3.1) are called designed outputs or nominal outputs ($y_{0_{BADWE}}$). They are defined as:

$$y_{0_{BADWE}} = y_{set} - S_d(y_{set} - v_s) \tag{3.4}$$

The authors suggest that $y_{0_{BADWE}}$ could be estimated through S_d and the process data. Therefore, it is necessary to identify another OE model to determine ΔGK, where ΔG is the model-plant mismatch (i.e., $G - G_0$), as following:

$$(y - \hat{y}) = \Delta GK\epsilon \tag{3.5}$$

The controller inputs (ϵ) presented in equation 3.2 can also be written as:

$$\epsilon = (I + \Delta GK)^{-1}(y_{set} - v_s) \tag{3.6}$$

Finally, solving for $(y_{set} - v_s)$ in (3.6) and substituting the result in (3.4) the designed output ($y_{0_{BADWE}}$) can be calculated by:

$$y_{0_{BADWE}} = y_{set} - S_d(I + \Delta GK)\epsilon \tag{3.7}$$

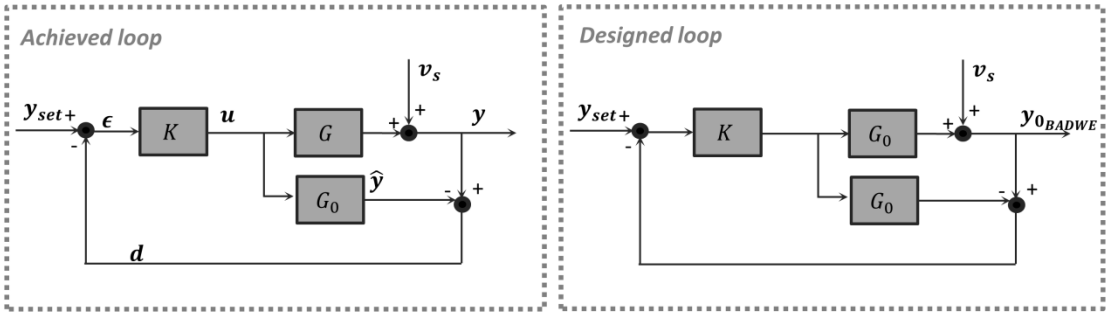

Figure 3.1**:** The IMC structure for the achieved and designed control loop (adapted from Badwe *et al.*, 2010)

Although the method proposed by Badwe *et al*.,2010 can produce good results, it has limited application, as it is setpoint dependent, being inappropriate for MPCs that work with soft constraints, for example. Furthermore the method requires two data-based model identifications. In order to avoid these drawbacks, we propose a new approach that is independent of setpoint perturbation and the data-based identification procedure. This method relies on the nominal output sensitivity function for MPM evaluation. The next section describes our approach.

3.2 The nominal sensitivity method for MPM

Initially, suppose a multivariable feedback control system, as shown in Figure 3.2, with a MPC controller C and nominal model G_0, which represents the real plant G. The mismatch magnitude is ΔG. The theoretical system without mismatch is shown in Figure 3.2a, for which nominal closed loop outputs are y_0. T_0 is the nominal complementary sensitivity function. The real system, in a scenario subject to mismatch, is shown in Figure 3.2b, where y_{set} corresponds to the setpoints, u are the manipulated variables, y are the measured outputs, y_{sim} are the simulated outputs of the nominal model perturbed by the actual control actions u, and T is the complementary sensitivity function.

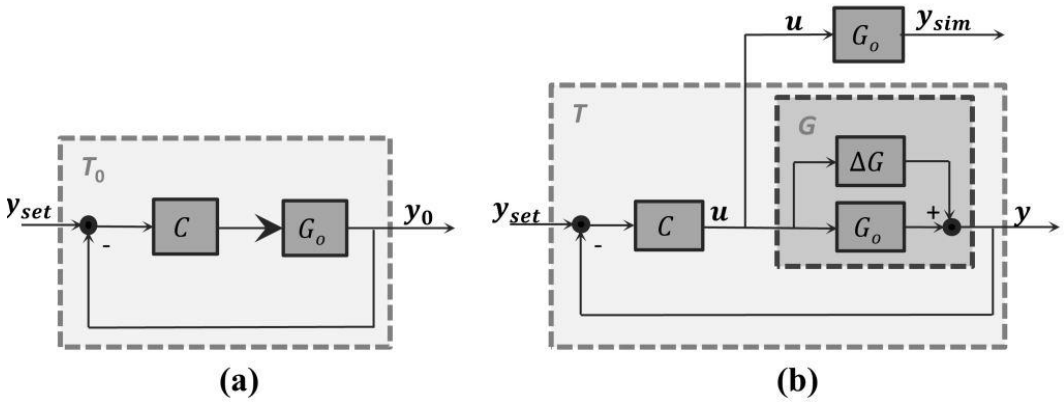

Figure 3.2**:** Schematic diagram of closed-loop system without model-plant mismatch (a) and with model-plant mismatch (b)

Merely investigating simulation residuals is not an appropriate metric to assess MPC model quality due to the feedback effect, in that large residuals are not necessarily an indicator of bad MPC model. A good model should represent the real system at the frequency in which the MPC works. For example, consider a typical unconstrained MPC cost function, given by:

$$\min_{\Delta u(k)\ldots\Delta u(k+mh)} \sum_{i=1}^{ph}\left[\sum_{j=1}^{ny} W_j\left[y_j(i+k) - y_{set\,j}(i+k)\right]^2 + \sum_{l=1}^{nu} MS_l[\Delta u_l(i+k)]^2\right] \quad (3.8)$$

Where nu is the number of controller inputs, ny is the number of controller outputs, ph is the prediction horizon, mh is the control horizon, Δu are the controller inputs changes, W_j is the weight of output j setpoint deviation and MS_l is the move suppression of input on the variable l. If a small MS_l and a large W_j are used MPC will work to lead the output variable to the setpoint with few but intense control actions. Similarly, if a large MS_l and a small W_j are used the MPC will work to lead the output variable to the setpoint with a large amount of small control actions. Thus, considering the corrective feedback effect and using the open loop dynamics as reference, two main different scenarios can be analyzed:

- The faster the tuning: The controller is less sensitive to stationary model-plant mismatch, but it is very sensitive to mismatches in the initial model dynamics.

- The slower the tuning: All dynamic models are relevant, but the sensitivity to mismatches is smaller, because the control actions are slower.

The previous considerations make evident the fact that a model-plant mismatch limits the attainable performance of a given system and its effect will be dependent on the current controller configuration (Trierweiler *et al.*, 1997). Thus, the nominal closed-loop performance must be considered in order to investigate the real effect of model-plant mismatch. Based on this idea, a method is proposed that uses closed-loop nominal sensitivity. The output sensitivity function concentrates information on controller tuning, providing the speed of response from each control loop. The following theorem is the kernel of the method.

Theorem: **The nominal closed loop output $\boldsymbol{y_0}$ (cf. Figure 3.2a) can be estimated by**

$$[\boldsymbol{y_0}(\boldsymbol{s}) - \boldsymbol{y}(\boldsymbol{s})] = \boldsymbol{S_0}\,(\boldsymbol{s})[\boldsymbol{y_{sim}}(\boldsymbol{s}) - \boldsymbol{y}(\boldsymbol{s})] \quad (3.9)$$

where $\boldsymbol{S_0}(\boldsymbol{s})$ is the nominal output sensitivity transfer matrix, $\boldsymbol{y}$ are the measured outputs, and $\boldsymbol{y_{sim}}$ are the simulated outputs of the nominal model perturbed by the actual control actions $\boldsymbol{u}$, as illustrated in Figure 3.2b.

Before proving the theorem, it is important to remember some simple and standard expressions between the different signals depicted in Figure 3.2, which can easily be found in process control textbooks (e.g., Skogestad and Postlethwaite,1996). To simplify the notation, the argument (s) associated with the transfer matrices and signals has been dropped.

The closed-loop transfer matrix (T), also referred to as complementary output sensitivity transfer matrix, is defined by:

$$y = Ty_{set} \quad (3.10)$$

$$T = GC(I + GC)^{-1} = (I + GC)^{-1}GC \quad (3.11)$$

The corresponding sensitivity transfer matrix is given by:

$$S = (I + GC)^{-1} \tag{3.12}$$

and the term “complementary” comes from the following expression:

$$S + T = I \tag{3.13}$$

Analogously, for the nominal case (i.e., free from model-plant mismatch, as shown in Figure 3.2a):

$$y_0 = T_0 y_{set} \tag{3.14}$$

$$T_0 = G_0 C(I + G_0 C)^{-1} = (I + G_0 C)^{-1} G_0 C \tag{3.15}$$

$$S_0 = (I + G_0 C)^{-1} \tag{3.16}$$

$$S_0 + T_0 = I \tag{3.17}$$

The manipulated variables (u) are:

$$u = CSy_{set} \tag{3.18}$$

whereby the open-loop simulated outputs are given by:

$$y_{sim} = G_0 u \tag{3.19}$$

Proving the Theorem:

To prove the theorem, we must substitute (3.10) and (3.19) in (3.9), which gives us:

$$y_0 - y = S_0(G_0 u - T y_{set}) \tag{3.20}$$

Substituting u in (3.20) with (3.18), we arrive at:

$$\begin{aligned} y_0 - y &= S_0(G_0 CS y_{set} - T y_{set}) \\ &= S_0(G_0 CS - T) y_{set} \\ &= (S_0 G_0 CS - S_0 T) y_{set} \end{aligned} \tag{3.21}$$

Based on the matrix property called push-through rule (Skogestad and Postlethwaite,1996), $(I + G_0 C)^{-1} G_0 C = G_0 C(I + G_0 C)^{-1}$ and combining with equation 3.15, the last equation can be rewritten as:

$$\begin{aligned} y_0 - y &= (G_0 CS_0 S - S_0 T) y_{set} \\ &= (T_0 S - S_0 T) y_{set} \end{aligned} \tag{3.22}$$

Now, replacing S and S_0 with (3.13) and (3.17), respectively, and using once more the definitions (3.10) and (3.14), finally, we arrive at:

$$\begin{aligned} y_0 - y &= [T_0(I - T) - (I - T_0)T] y_{set} \\ &= (T_0 - T) y_{set} \\ &= y_0 - y \end{aligned} \qquad \textbf{Q.E.D.} \tag{3.23}$$

The previous relation is derived from a loop free from disturbances. However, it can also apply to a more realistic case with external unknown perturbations. Figure 3.3 illustrates a system with unmeasured disturbance, where v are sequences of independent random variables, G_d is the unknown disturbance model and y_d are the disturbance signals. The effect of a disturbance on outputs is similar to that of a model-plant mismatch.

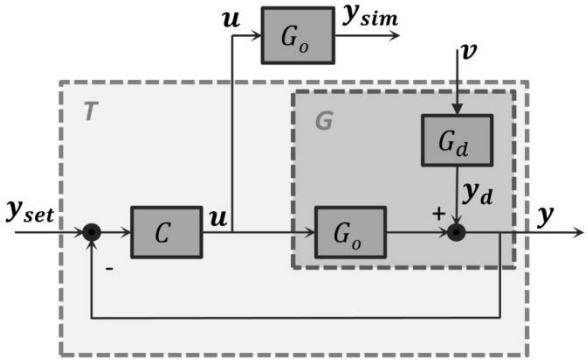

Figure 3.3: Schematic diagram of a closed-loop system with disturbance

To distinguish between them, the nominal error $e_0 = y - y_0$ can be compared with the nominal outputs (y_0). When a process output is under a MPM, e_0 will be dependent of the input movements, as well as y_0, resulting in a similar variation frequency. However, when the process output is under an unmeasured disturbance, e_0 will be independent because the disturbances come from an external source. Nonetheless, y_0 is still dependent of the input variables movements. This means that the frequency of variation of y_0 and e_0 are uncorrelated.

Considering that real processes often have unmeasured disturbances and MPM acting simultaneously, the simple investigation of the correlation between the signals is not satisfactory. Thus, we propose the comparison between the statistical distributions of y_0 and e_0 in order to capture the source of poor performance (MPM or disturbance). Then, the distributions are compared using a confidence ellipse scatter or a linear approximation. Figure 3.4 illustrates the expected result when a system is under MPM and unmeasured disturbance. More details of this approach will be explored in future work.

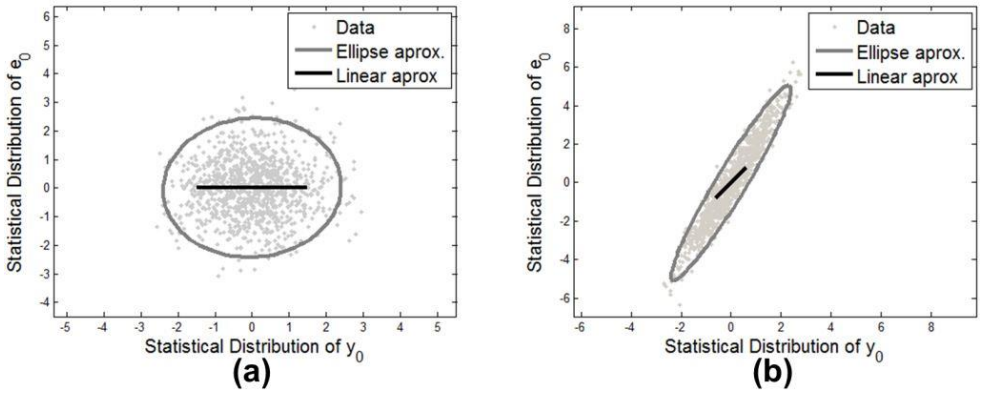

Figure 3.4: Expected response of linear and elliptical approximation (a) under unmeasured disturbance and (b) under MPM

The information that must be known to apply the method proposed in this study are: the nominal process model (G_0), which is the same as that which was configured in the controller, the input (y) and output (u) measured data and the sensitivity function (S_0). This function can be obtained analytically from the nominal process model (G_0) and controller model (C), as shown in equation (3.16). However, given the complexity of MPC formulation, knowing the controller model (C) is not a trivial task. In this case, it is simpler and more straightforward to obtain T_0 from a simulation of the controller, considering no model-plant mismatch and a sufficiently excited closed loop data. Then, the closed-loop model is identified based on the simulated data. It is important to note that this procedure should only be repeated if the MPC tuning or nominal model has changed (see appendix A3).

Given that y_0 is an estimation of the output process when there is no model-plant mismatch or unmeasured disturbance, it can be considered a benchmark for controller-model output response. The main advantage is that, unlike of the MVC/LQG, it is a more realistic reference of the process model. It is important to emphasize that the diagnosis using y_0 pertains only to model quality or the presence of unmeasured disturbance, remaining unaffected by poor tuning. Furthermore, this benchmark allows any output performance indicators to be applied. The diagnosis flowchart is represented by Figure 3.5, where IP is the performance indicator for the measured data and IP_0 is the performance indicator for the estimated nominal data.

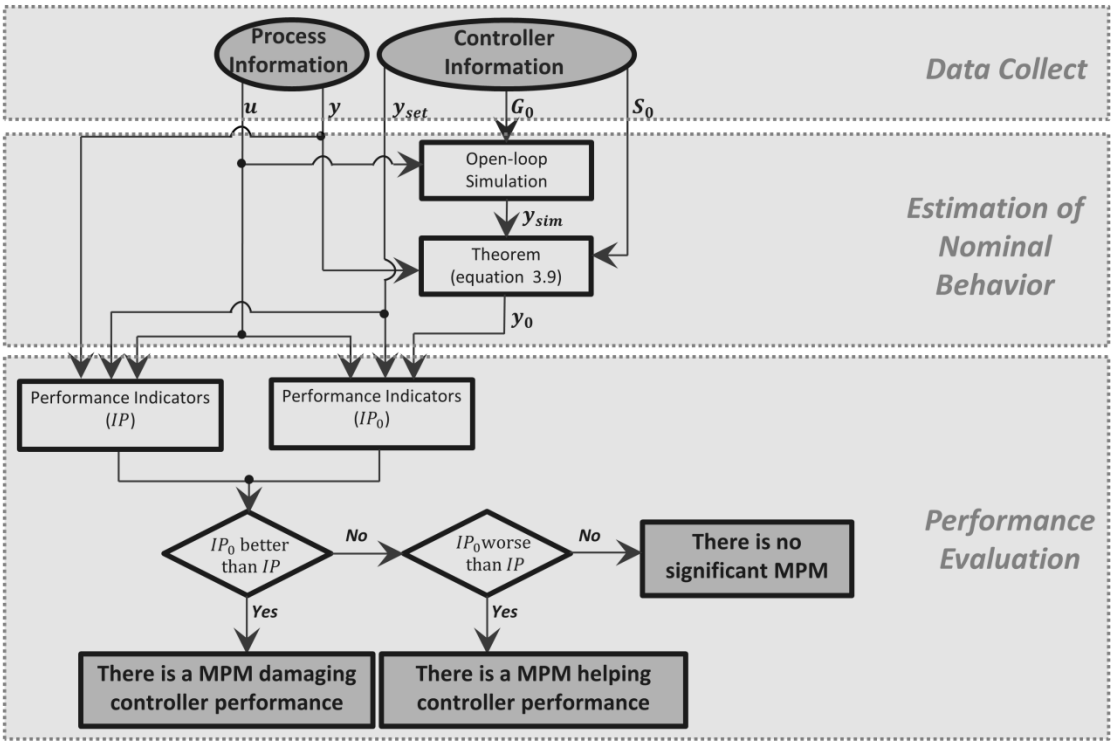

Figure 3.5: Diagnosis procedure according to the proposed methodology

As shown in Figure 3.5, the main idea of the procedure is to calculate the nominal output from the process information. Then, performance indicators for y and y_0 are calculated and compared. A situation where IP is worse than IP_0 means that the behavior of the real case is worse than the nominal case. Thus, there is a modeling problem impairing the controller. Similarly, if IP is better than IP_0 , this means that the behavior of the real case is better than the nominal case. In this case, there is a modeling problem

improving the controller. Case IP and IP_0 are similar, in that there is no modeling problem and the existence of undesirable behavior is a result of bad tuning. A useful indicator is the comparison of control error variances, as Badwe *et al.* (2010) suggested:

$$Ivar = \frac{var(y - y_{set})}{var(y_0 - y_{set})} \tag{3.24}$$

Another possibility is the analysis of autocorrelation function (ACF) of control errors (i.e., $y - y_{set}$ and $y_0 - y_{set}$). A high value of ACF means that the current control error is strongly correlated with past errors. The ACF curves are useful to analyze the effect of MPM in MPC performance indicating, for example, how these problems are affecting the MPC speed of response. In this case, the comparison of the decay rates of ACF(y) and ACF(y_0) indicates whether the MPC is slower or faster than was designed. The ACF also can be used to identify oscillatory behavior in control loops (Huang & Shah, 1999).

3.3 Case Study: The Quadruple-Tank Process

3.3.1 Process Description

The system (Johanson, 2000) is composed of four cylindrical tanks connected according to Figure 3.6. Water is pumped into the tanks through the pumps with voltages $v1$ and $v2$. The flow from each pump is split through valves, with openings equal to $x1$ and $x2$, respectively. The external flows $Fex1$ and $Fex2$ enter tanks 1 and 2, respectively. Mass balances around each tank are shown in the equations (3.25 to 3.28) and Table 3.1 provides the parameters used in this case study.

$$\frac{dh_1}{dt} = -\frac{cd_1}{A_1}(h_1)^{exp1} + \frac{cd_3}{A_1}(h_3)^{exp3} + \frac{x_1 k_1}{A_1}v_1 + \frac{Fex1}{A_1} \tag{3.25}$$

$$\frac{dh_2}{dt} = -\frac{cd_2}{A_2}(h_2)^{exp2} + \frac{cd_4}{A_2}(h_4)^{exp4} + \frac{x_2 k_2}{A_2}v_2 + \frac{Fex2}{A_2} \tag{3.26}$$

$$\frac{dh_3}{dt} = -\frac{cd_3}{A_3}(h_3)^{exp3} + \frac{(1 - x_2)k_2}{A_3}v_2 \tag{3.27}$$

$$\frac{dh_4}{dt} = -\frac{cd_4}{A_4}(h_4)^{exp4} + \frac{(1 - x_1)k_1}{A_4}v_1 \tag{3.28}$$

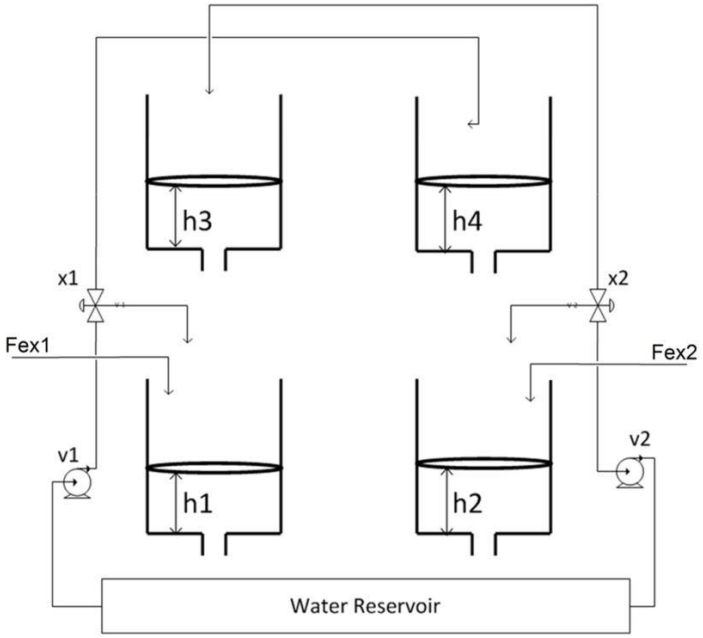

Figure 3.6: The Quadruple-Tank Process: Schematic diagram of the system

Where h_i is the level of each tank, $k_1 v_1$ and $k_2 v_2$ are the pumps' output flows, A_i is the cross-section area of each tank, cd_i is the discharge coefficient of each tank and $expi$ is the discharge exponent.

Table 3.1: The Quadruple-Tank Process: Original Parameters

$\boldsymbol{A_1}$	$28\ cm^2$	$\boldsymbol{cd_4}$	$2.525\ cm^{2.5}/s$
$\boldsymbol{A_2}$	$28\ cm^2$	$\boldsymbol{k_1}$	$3.33\ cm^3/Vs$
$\boldsymbol{A_3}$	$32\ cm^2$	$\boldsymbol{k_2}$	$3.35\ cm^3/Vs$
$\boldsymbol{A_4}$	$32\ cm^2$	$\boldsymbol{exp1}$	0.5
$\boldsymbol{cd_1}$	$3.145\ cm^{2.5}/s$	$\boldsymbol{exp2}$	0.5
$\boldsymbol{cd_2}$	$2.525\ cm^{2.5}/s$	$\boldsymbol{exp3}$	0.5
$\boldsymbol{cd_3}$	$3.145\ cm^{2.5}/s$	$\boldsymbol{exp4}$	0.5

To illustrate the proposed approach, we simulated a MPC in *Matlab/Simulink* using the four levels as controlled variables (h_1, h_2, h_3 and h_4), the pump voltages (v_1 and v_2) and valve openings (x_1 and x_2) as the manipulated variables.

The linear plant model used was obtained from the linearization of the nonlinear model at the operating point, defined by manipulated variables $v1 = 3.2, v2 = 3.15, x1 = 0.43$, and $x2 = 0.34$, given by:

$$G_0(s) = \begin{bmatrix} \frac{0.048}{s+0.016} & \frac{0.0025}{s^2+0.028s+0.0002} & \frac{0.35}{s+0.015} & \frac{-0.0096}{s^2+0.41s+0.0004} \\ \frac{0.0009}{s+0.016} & \frac{0.035}{s+0.011} & \frac{-0.0055}{s^2+0.024s+0.0002} & \frac{0.323}{s+0.011} \\ 0 & \frac{0.078}{0.028s+0.25} & 0 & \frac{-0.37}{s+0.026} \\ \frac{0.045}{s+0.018} & 0 & \frac{-0.31}{s+0.018} & 0 \end{bmatrix} \quad (3.29)$$

The controller was configured considering the cost function presented in equation 3.30, where y_{UL}, y_{LL} u_{UL} and u_{LL} are the upper and lower constraints of controlled and manipulated variable, respectively. The tuning values, computed according to RPN methodology (Trierweiler & Farina, 2003), and the controller constraints are shown in Table 3.2.

$$\min_{\Delta u(k)\ldots\Delta u(k+mh)} \sum_{i=1}^{ph} \left[\sum_{j=1}^{ny} W_j \left[y_j(i+k) - y_{set\,j}(i+k) \right]^2 + \sum_{l=1}^{nu} MS_l [\Delta u_l(i+k)]^2 \right]$$

$$s.t. \quad \begin{matrix} u_{UL} \geq u \geq u_{LL} \\ y_{UL} \geq y \geq y_{LL} \end{matrix} \quad (3.30)$$

Table 3.2: MPC controller tuning parameters and constraints

Sample Time (Ts)	10s
Prediction Horizon (ph)	48
Control Horizon (mh)	12
Controlled Variable Weight (W)	$W_{h1} = W_{h2} = W_{h3} = W_{h4} = 10$
MV Lower Limits (u_{LL})	$v1 > 0.01, v2 > 0.01, x1 > 0.01, x2 > 0.01$
MV Upper Limits (u_{UL})	$v1 < 10; v2 < 10; x1 < 1; x2 < 1$
CV Lower Limits (y_{LL})	$h1 > 0; h2 > 0; h3 > 0; h4 > 0$
CV Upper Limits (y_{UL})	$h1 < 20; h2 < 20; h3 < 20; h4 < 20$
Move Suppression (MS) of Tuning A (fast)	$MS_{v1} = MS_{v2} = MS_{x1} = MS_{x2} = 0$
Move Suppression (MS) of Tuning B (slow)	$MS_{v1} = MS_{v2} = MS_{x1} = MS_{x2} = 50$

The analysis is divided into three parts. In the first, both plant and controller use linear models. In the second, plant and controller use linear models but constraints activation is included. In the third, a linear controller is used to control a nonlinear plant.

3.3.2 Linear Plant Model without Constraint Activation

In this example, the controller and the plant are initially configured using the model presented in equation 3.29. There is no constraint activation of controlled and manipulated variables. Mismatches are added in the plant model $G(1,3)$, which is the response of the output h_1 to the input x_1. The first one (referred to as MPM 1) is a gain mismatch, but the initial dynamic behavior of the plant model is identical to the controller model; whereas the other (referred to as MPM 2) has a compatible steady state, but mismatches in dynamics. Figure 3.7 illustrates the responses for MPM1 and MPM2. For each mismatch, two MPC tuning modes were set (referred to as slow and fast), using the corresponding Move Suppression Parameters presented in Table 3.2. Figure 3.8 shows the complementary sensitivity function (T_0) for these tunings, and exposes the difference between the speed of response for each tuning.

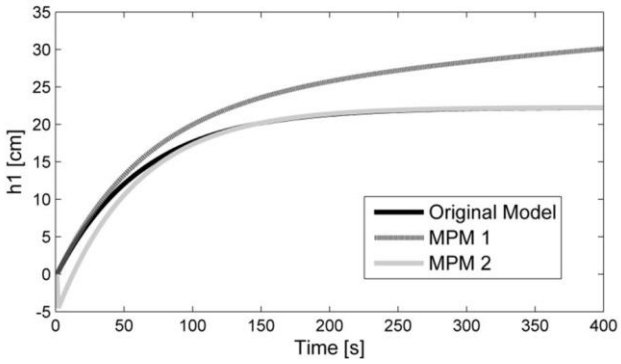

Figure 3.7**:** Step Response of plant model G for the x_1 vs. h_1 pair: Linear plant without constraint activation case

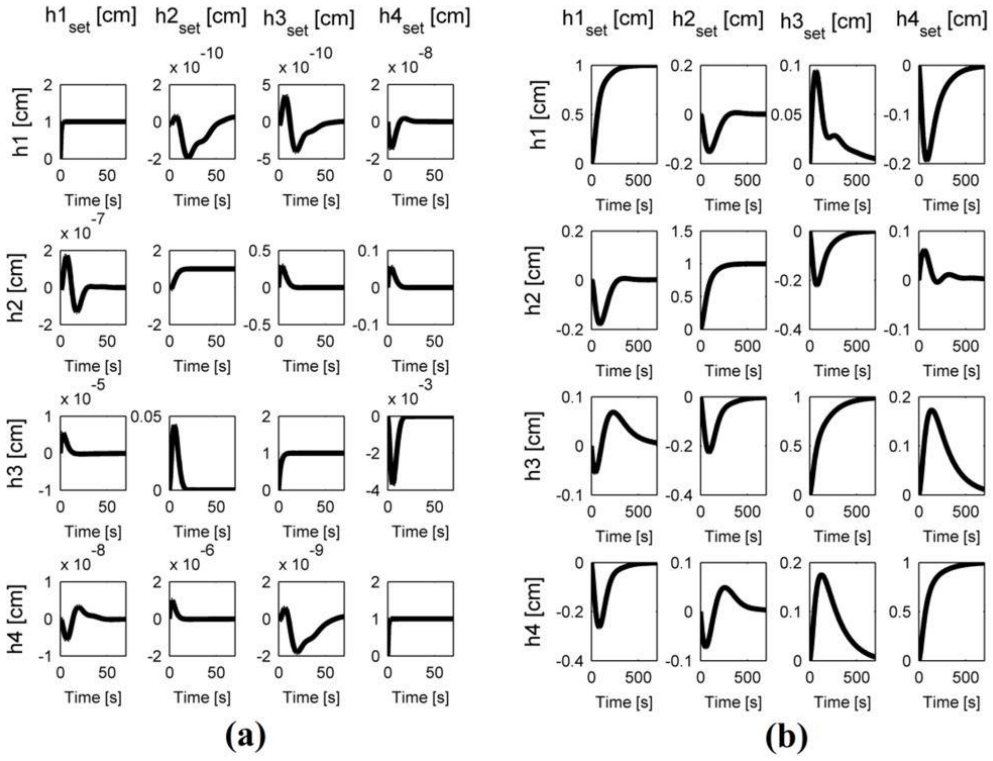

Figure 3.8**:** Step response of complementary output sensitivity function (T_0) for fast tuning (a) and slow tuning (b): Linear plant without constraint activation case

Combining the tunings and models, different scenarios are set according to Table 3.3. The controller is configured using the Original Model in all scenarios. Basis scenarios BF and BS correspond to situations without model-plant mismatches, with fast and slow tunings, respectively. Simulations are performed considering a series of step changes in the controlled variable setpoints, as illustrated in Figure 3.9. The external flows $Fex1$ and $Fex2$ are maintained equal to zero. No disturbance or noise was added. Figure 3.10 shows the simulation residuals (i.e., $y - y_{sim}$) for each scenario and Figure 3.11 compares the behavior of $h1$ with and without model-plant mismatch. The results are presented only for the variable $h1$ because this is the only output directly affected by the model-plant mismatches. The remaining outputs do not have MPM, meaning that the plant model is perfect and the simulation residuals are equal to zero.

Table 3.3: Scenarios Configuration: Linear plant without constraint activation case

Scenario Name	Controller Model	Controller Tuning	Plant Model
Basis Slow (BS)	Original Model	Tuning B (slow)	Original Model
Basis Fast (BF)	Original Model	Tuning A (fast)	Original Model
Model 2 Slow (M1S)	Original Model	Tuning B (slow)	MPM 1
Model 2 Fast (M1F)	Original Model	Tuning A (fast)	MPM 1
Model 3 Slow (M2S)	Original Model	Tuning B (slow)	MPM 2
Model 3 Fast (M2F)	Original Model	Tuning A (fast)	MPM 2

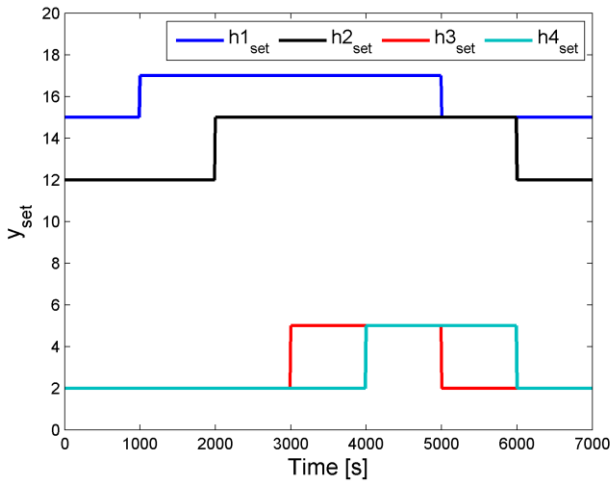

Figure 3.9: changes in each controlled variable setpoint

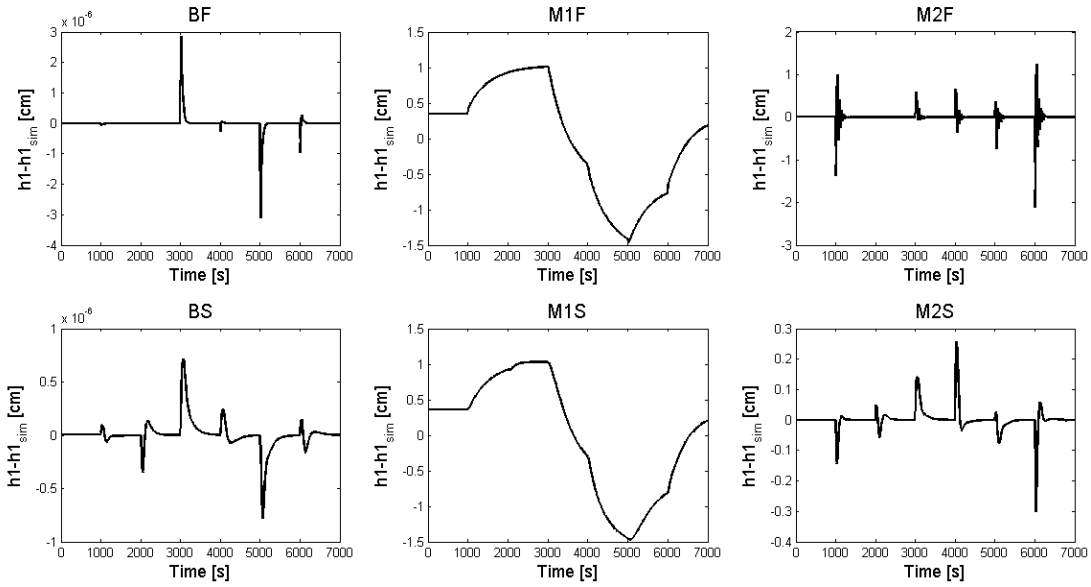

Figure 3.10 **:** Simulation residual ($y - y_{sim}$) of h_1 for the different scenarios: Linear plant without constraint activation case

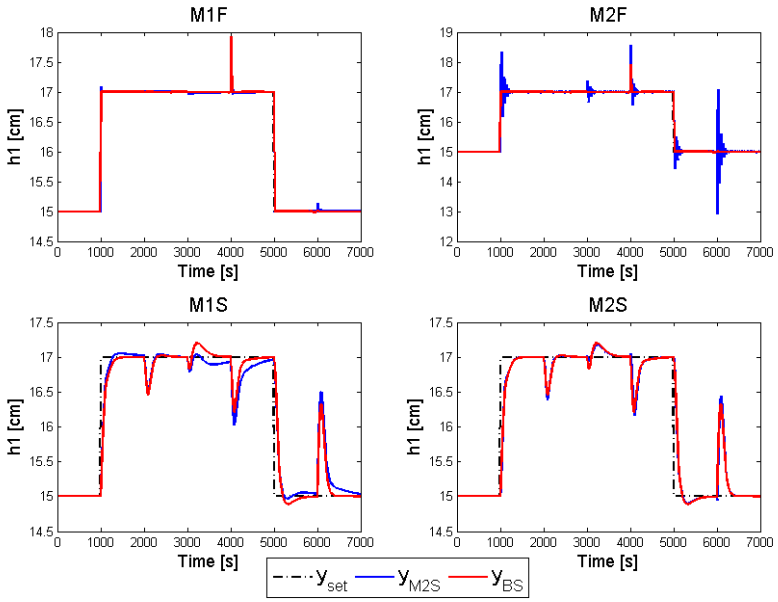

Figure 3.11: Comparative results of h_1 for the different scenarios: Linear plant without constraint activation case

The joint analysis of Figures 3.10 and 3.11 elucidates the expectation that model-plant mismatches cause different effects depending on the tuning of the system even if the simulation residual is significant. In Figure 3.11, there is no significant effect from model-plant mismatch in scenario M2S, because the controller tuning is slow and Model 2 has a steady behavior compatible with the Original Model, generating a result very similar to BS. Analogously, M1F and BF expectedly show similar results because Model 1 and the Original Model do not have dynamics mismatch. The model-plant mismatch in scenarios M2F causes an oscillatory behavior in $h1$. In the scenario M1S, the model-plant mismatch makes the $h1$ response slightly slower.

The nominal output (y_0) was estimated considering both Badwe *et al*.(2010) and our proposed approach. The models from the Badwe *et al*. (2010) method were identified using output-error (OE) parametric models and varying the orders between 3 and 7 and the best were used to generate y_0. The results are compared with the basis cases for each tuning, according to:

$$SQR_z = \sum_{i=1}^{nsample} \sqrt{\left(y_{Basis} - y_{0_z}\right)^2} \tag{3.31}$$

where z is the approach used for y_0 estimation and y_{Basis} is the data from the corresponding basis case. Table 3.4 summarizes the comparison.

Table 3.4: Comparison of SQR for the proposed and Badwe *et al.* (2010) methods: Linear plant without constraint activation case

Scenario	y_{0_z}	$h1$	$h2$	$h3$	$h4$
M1F	**Badwe *et al.* (2010)**	6.20	6.64	4.52	4.81
	Proposed Method	0.75	0.06	0.27	0.60
M1S	**Badwe *et al.* (2010)**	55.43	45.82	121.02	198.14
	Proposed Method	1.34	0.92	0.72	0.52
M2F	**Badwe *et al.* (2010)**	30.6	7.62	6.33	8.05
	Proposed Method	1.30	0.18	0.41	1.12
M2S	**Badwe *et al.* (2010)**	19.7	64.8	5.8	3.8
	Proposed Method	0.24	0.13	0.14	0.13

Table 3.4 shows that both approaches provide good approximations to y_0. However, the proposed method has superior results when compared with Badwe *et al.* (2010), since it produces results that are closer to the basis cases (i.e., small SQR error). This is a result of the two identification steps in Badwe *et al.* (2010), where model quality is strongly dependent on data quality and input excitation. Table 3.5 substantiates this statement, since there are cases where the best model fit is less than 50%. The best model fit index (% Fit) is the indicator used to evaluate the quality of identified model and is defined as:

$$\%\ \text{Fit} = 100\left(1 - \frac{\|y - y_{est}\|}{\|y - \bar{y}\|}\right) \tag{3.32}$$

where y_{est} is the output predicted by the OE model and $\bar{y}$ is the mean of the measured data. Furthermore, the best model order must be determined, which may be considered an additional drawback of the Badwe *et al.* (2010) method.

Table 3.5: Best OE models fit of Badwe *et al*. (2010) method: Linear plant without constraint activation case

	Scenario	$h1$	$h2$	$h3$	$h4$
$\%Fit$ of S_d estimation	**M1F**	80.94	77.42	84.5	83.3
	M2F	41.2	79.2	84.3	78.16
	M1S	99.9	99.8	99.9	99.5
	M2S	99.8	99.9	99.9	99.9
$\%Fit$ of ΔGC estimation	**M1F**	99.6	67.9	68.4	68.3
	M2F	77.1	82.0	64.9	58.1
	M1S	99.9	81.35	75.5	82.4
	M2S	99.8	59.6	36.7	46.1

The Variance Index (equation 3.24) and ACF curves are calculated considering the y_0 estimated by the proposed approach and for the Badwe *et al.* (2010) method. Results are shown in Table 3.6 and Figure 3.12.

Table 3.6: Relative Variance Index ($Ivar$) : Linear Plant without constraint activation case

	Proposed Method				**Badwe *et al.* (2010)**			
	$h1$	$h2$	$h3$	$h4$	$h1$	$h2$	$h3$	$h4$
M1F	0.99	1.00	1.00	1.00	1.03	0.95	1.03	1.04
M1S	1.14	1.00	1.00	1.02	1.29	0.99	0.89	1.08
M2F	3.26	1.00	1.00	1.00	0.13	0.82	0.41	0.85
M2S	1.04	0.99	0.99	1.00	0.98	0.93	1.00	0.98

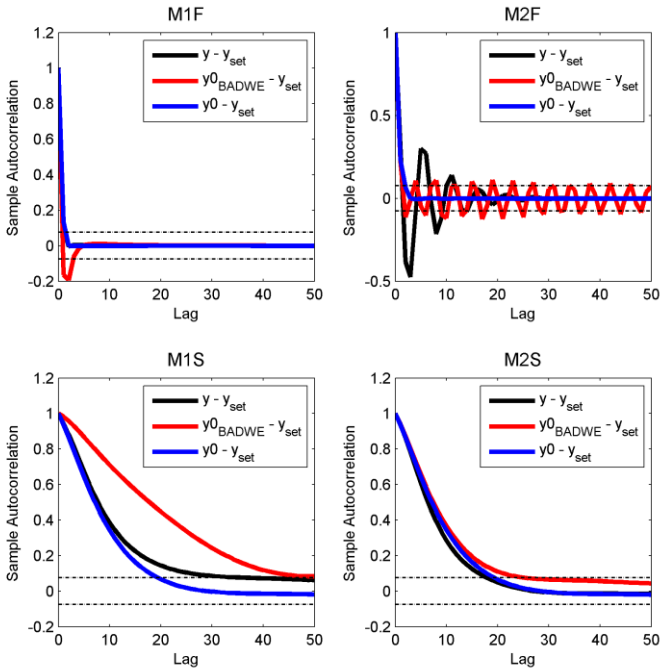

Figure 3.12: Comparative ACF of $(y - y_{set})$,$(y_0 - y_{set})$ estimated by the proposed method and $(y_0 - y_{set})$ estimated by the Badwe *et al.* (2010) method: Linear plant without constraint activation case

The result shows that the proposed method was capable of detecting the real effect of model-plant mismatch affecting in the system. According to Table 3.6, the $Ivar$ of $h1$ is equal to 1.14 and 3.26 in the M1S and M2F, respectively, indicating that there is MPM increasing the variance of this output. For all the others variables and scenarios, the $Ivar$ is close to 1. The ACF (Figure 3.12) of $h1$ in M2F have an oscillatory behavior for $(y - y_{set})$, which does not occur in $(y_0 - y_{set})$, denoting that $h1$ is oscillating due to MPM. Similarly, in M1S the decay of $(y - y_{set})$ is slower than the decay of $(y_0 - y_{set})$, indicating that the MPM is affecting the speed of MPC. These results are compatible with the comparison with the basis cases, presented in Figure 3.11. The proposed method has superior results when compared with Badwe *et al.*(2010), which provides some misleading results of $Ivar$ and ACF.

3.3.3 Linear Plant Model with Constraint Activation

In this scenario, the system is configured using the model shown in equation 3.29. The controller was tuned according to the slow tuning (Tuning B) of Table 3.2, except for $x1$ upper limit $(x1_{UL})$, which is set to 0.35, in this analysis. A model-plant mismatch (called MPM3) is added in the plant model x_1 vs. h_1, as illustrated in Figure 3.13. Simulations are performed considering the same step changes in setpoints used in the previous case study (Figure 3.9). Due to this MPM, the constraints of $x1$ remain active in some instances, as shown in Figure 3.14.

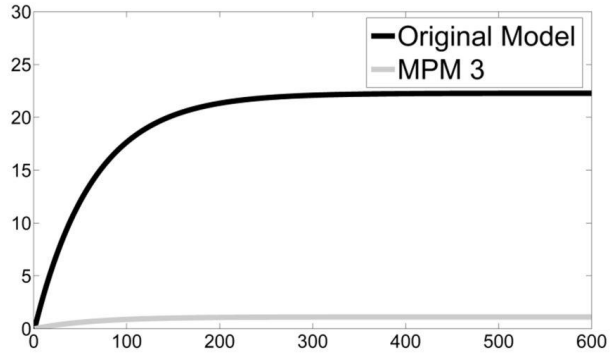

Figure 3.13**:** Step response of the plant model G for the pair x_1 vs. h_1 : Linear plant with constraint activation case

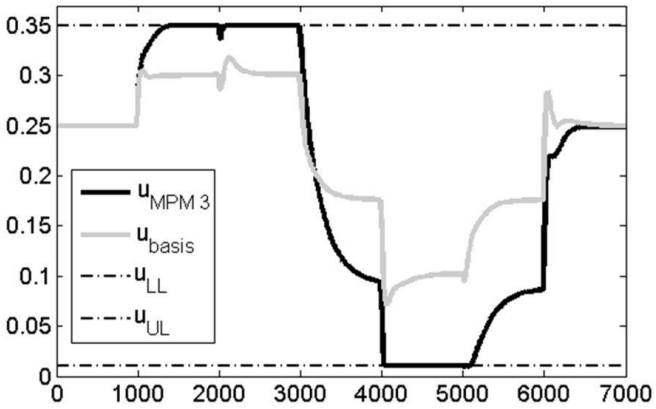

Figure 3.14: Behavior of x_1: Linear plant with constraint activation case

As shown in Figure 3.14, a saturation of $x1$ occurs over part of the time. Considering that the MPC is a linear time varying controller, when a variable becomes saturated the configuration of controller changes. In this case, the sensitivity function (S_0) compatible with the current local linearity must be used. Figure 3.15 presents the T_0 obtained with saturated $x1$.

The nominal output (y_0) was obtained through the proposed approach, considering the following:

- Assumption A: Using only the T_0 for inactive $x1$ constraint case (Figure 3.8b)

- Assumption B: Using only the T_0 for active $x1$ constraint case (Figure 3.15)

- Assumption C: Analyzing the inputs and using the compatible T_0 (Figure 3.8b or Figure 3.15, depending on $x1$ condition)

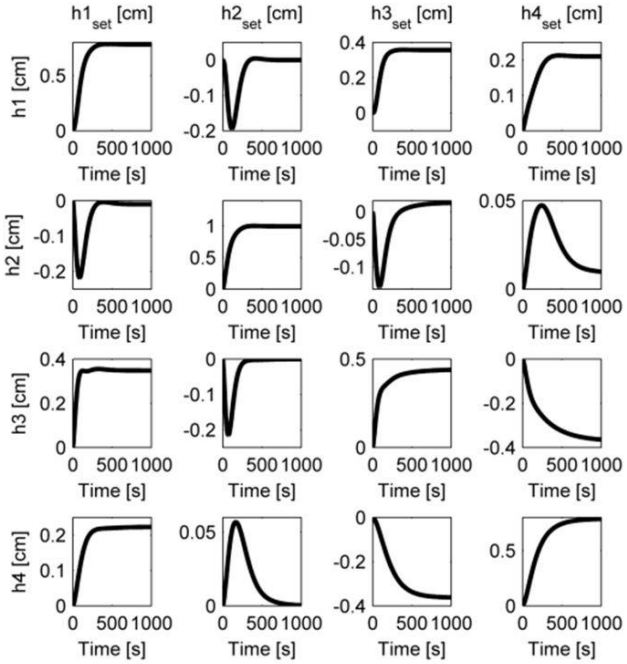

Figure 3.15: Step response of complementary output sensitivity function (T_0): Linear plant with constraint activation case.

The OE models of the Badwe *et al.* (2010) method were identified by varying the orders between 3 and 7 and the best were used to generate the y_0. The results were compared with the basis cases for each tuning, according to equation 3.31. Table 3.7 summarizes the comparison. The Variance Index (equation 3.24) is also calculated considering all approaches of y_0. The results are shown in Table 3.8. The ACF curves are performed for the Badwe *et al.* (2010) method and for the proposed approach considering the Assumption C, according to Figure 3.16.

Table 3.7: Comparison of SQR: Linear plant with constraint activation case.

y_{0_z}	$h1$	$h2$	$h3$	$h4$
Badwe *et al.* (2010)	69.05	8.88	96.27	353.09
Proposed Method: Assumption A	50.74	7.94	71.53	56.36
Proposed Method: Assumption B	17.11	4.72	21.17	17.58
Proposed Method: Assumption C	3.85	2.70	5.13	4.50

Table 3.8: Relative Variance Index ($Ivar$) : Linear plant with constraint activation case

y_{0_z}	$h1$	$h2$	$h3$	$h4$
Badwe *et al.* (2010)	1.89	0.98	1.12	0.31
Proposed Method: Assumption A	1.83	0.98	1.08	0.97
Proposed Method: Assumption B	0.80	0.99	0.16	0.54
Proposed Method: Assumption C	2.27	0.98	0.94	1.20
Basis Case	2.21	0.97	0.94	1.28

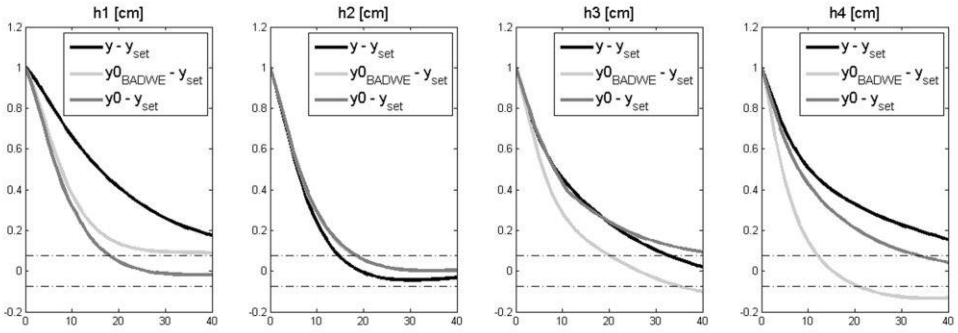

Figure 3.16: Comparative ACF of $(y - y_{set})$,$(y_0 - y_{set})$ estimated from Assumption C and $(y_0 - y_{set})$ estimated by the Badwe *et al.* (2010) method: Linear plant with constraint activation case

The similar results between Assumption C and the Basis Case presented in Tables 3.7 and 3.8 are evidence that the proposed method is capable of correctly detecting the effect of MPM even when a change in the control structure of MPC occurs (saturation of $x1$, in this case). The comparison between ACF$(y_0 - y_{set})$ and ACF$(y - y_{set})$ in Figure 3.16 makes evident the fact that the model-plant mismatch affects the speed of response of $h1$. The other outputs are also affected by the mismatch due to the interaction between the variables, but its effect is smaller. The method presents superior results when compared with that of Badwe *et al.* (2010), since in this case, the SQR and $Ivar$ are further from the basis case.

Results also show that, for this case study, the use of the compatible sensitivity function was fundamental for the success of the method (see Assumption A and B in Tables 3.7 and 3.8). However, it should be noted that the estimation of S_0 is quite a simple procedure, relying only on a closed-loop simulation.

3.3.4 Nonlinear Phenomenological Plant Model

In this case study, the plant model used was the dynamic phenomenological version, described in equations 3.25 to 3.28. Scenarios containing mismatches were generated by

the variation of model parameters in the plant model and the addition of unmeasured disturbance (Table 3.9). The datasets for model assessments were generated inserting step changes on the controlled variable setpoints. A white noise with magnitude 2% was added on measurements. The proposed and Badwe *et al.* (2010) methods were confronted using y_0 Variance Index (equation 3.24) and ACF curves. The results are summarized on Table 3.10 and Figure 3.17.

Table 3.9: Scenarios configuration: Non-linear plant case

Mistake in the plant (MP)	**Parameter**	**Value**	**Variables affected by the MP (according to equations 3.25 to 3.28)**
0	--	--	---
1	cd_1	$7.86\ cm^{2.5}/s$	$h1$
2	cd_3	$1.05\ cm^{2.5}/s$	$h1$ and $h3$
3	A_2	$256\ cm^2$	$h2$
4	A_4	$4\ cm^2$	$h2$ and $h4$
5	Unmeasured disturbance in $h4$	$\frac{8}{70s+1}$	$h2$ and $h4$
6	Unmeasured disturbance in $h2$	$\frac{5}{5s+1}$	$h2$
7	$exp3$	0.1	$h1$and $h3$
8	$exp2$	0.75	$h2$

Table 3.10: Relative Variance Index ($Ivar$) : Non-linear plant case

	Proposed Method				**Badwe *et al.* (2010)**			
MP	$h1$	$h2$	$h3$	$h4$	$h1$	$h2$	$h3$	$h4$
0	0.96	1.02	1.15	1.14	1.11	0.85	1.12	1.18
1	1.33	0.98	1.18	0.97	1.45	1.17	1.04	0.78
2	1.84	1.01	1.6	1.06	2.11	0.44	1.36	1.19
3	1.07	4.49	1.17	1.19	0.96	4.68	1.83	1.27
4	0.98	0.97	1.15	1.24	0.99	1.03	1.00	1.32
5	0.96	1.02	1.15	1.74	1.35	1.13	1.25	2.75
6	0.99	7.42	1.13	1.19	1.05	1.15	0.01	0.82
7	1.63	0.94	1.51	1.11	1.82	1.01	1.66	1.14
8	1.15	1.16	1.19	1.18	1.46	0.91	1.10	1.27

The results from Table 3.10 and Figure 3.17 show that, considering a $Ivar$ tolerance of ±0.2 (due to noise presence) the system nonlinearity does not interfere significantly in MPC performance, since $Ivar$ is close to one and the ACF of $y - y_{set}$ and $y_0 - y_{set}$ are similar in scenario MP0. The Badwe *et al.* (2010) method provided a misleading indication in over 60% of the cases. For example, in MP6, the $Ivar$ and ACF suggest a modeling problem in $h3$ despite the fact that this variable is not mismatched in these scenarios. The proposed method has correctly detected abnormalities in the models and has identified the variable affected by the mismatch in all scenarios. For example, in scenario MP2, there is an indication of problems in $h1$ and $h3$. This scenario corresponds to a mismatch in parameter $cd3$, which is associated to these levels. The method also detected the effect of unmeasured disturbance, although it could not be distinguished among the causes of the problem according to results from scenarios MP5 and MP6. It is important to emphasize that, in this case, the nonlinearity does not significantly affect controller performance. However, in cases when the plant is strongly nonlinear and linear MPC is used, the method will indicate the presence of a MPM.

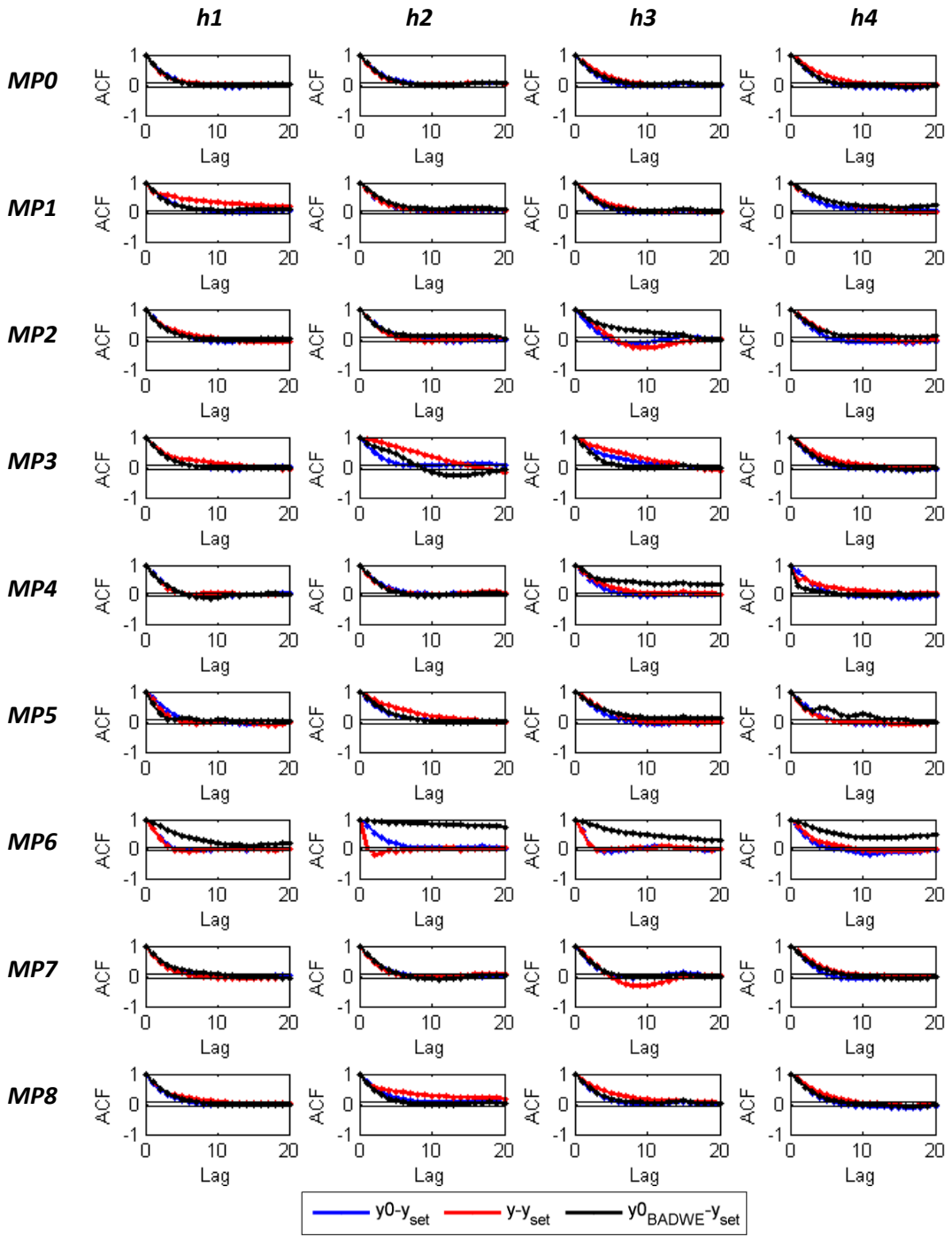

Figure 3.17: Comparative ACF of $(y - y_{set})$, ($y_0 - y_{set}$) estimated by the proposed method and $(y_0 - y_{set})$ estimated by Badwe *et al.* (2010) method: Non-linear plant case

3.3.5 Linear Plant Model with MPC using soft constraints

A significant part of industrial MPC applications does not have enough degrees of freedom to control all the outputs. It means that the number of manipulated variables is usually smaller than the number of controlled variables and it is not possible to maintain all of them in a fixed setpoint. The alternative is to control the outputs by range, were the MPC works to maintain all the controlled variables inside a band, called soft constraint (Campos *et al.,* 2013). This case study considers this kind of control structure. The controller was configured considering the cost function presented in equation 3.33, were

y_{UL}^{soft} and y_{LL}^{soft} are the upper and lower soft constraints of controlled variables, δ is the slack variable to soft the constraints of CV and τ is the penalization of soft constraint violation. The tuning parameters and the controller constraints are shown in Table 3.11.

$$\min_{\Delta u(k)\ldots\Delta u(k+mh)} \sum_{i=1}^{ph}\left[\sum_{l=1}^{nu} MS_l[\Delta u_l(i+k)]^2 + \sum_{j=1}^{ny} \tau_j {\delta_j}^2\right]$$

$$s.t. \quad \begin{matrix} u_{UL} \geq u \geq u_{LL} \\ y_{UL}^{soft} + \delta \geq y \geq y_{LL}^{soft} + \delta \\ \delta \geq 0 \\ y_{UL} \geq y \geq y_{LL} \end{matrix} \tag{3.33}$$

Table 3.11: MPC using soft constraints tuning parameters and constraints

Sample Time (Ts)	10s
Prediction Horizon (ph)	48
Control Horizon (mh)	12
Penalization of Soft Constraint Violation (τ)	$\tau_{h1} = \tau_{h2} = \tau_{h3} = \tau_{h4} = 120$
Move Suppression (MS)	$MS_{v1} = MS_{v2} = 50, MS_{x1} = MS_{x2} = 350$
MV Lower Limits (u_{LL})	$v1 > 0.01; v2 > 0.01; x1 > 0.01; x2 > 0.01$
MV Upper Limits (u_{UL})	$v1 < 10; v2 < 10; x1 < 1; x2 < 1$
CV Lower Limits (y_{LL})	$h1 > 0; h2 > 0; h3 > 0; h4 > 0$
CV Upper Limits (y_{UL})	$h1 < 20; h2 < 20; h3 < 20; h4 < 20$
Upper Soft Constraints (y_{UL}^{soft})	$h1 > 12; h2 > 12; h3 > 6.5; h4 > 6.5$
Upper Soft Constraints (y_{UL}^{soft})	$h1 < 14; h2 < 14; h3 < 7.5; h4 < 7.5$

Simulations are performed considering step changes in the external flows $Fex1$ and $Fex2$, according to Figure 3.18. These perturbations make the system violate the soft constraints and the MPC acts to bring the variable back to the desired range, as illustrated in Figure 3.19.

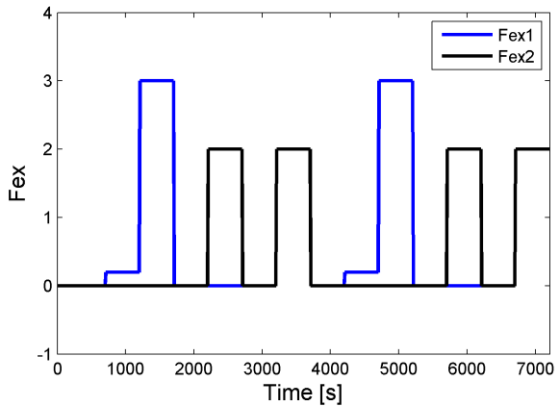

Figure 3.18: Step changes in the external flows: Linear plant model whit MPC with soft constraints

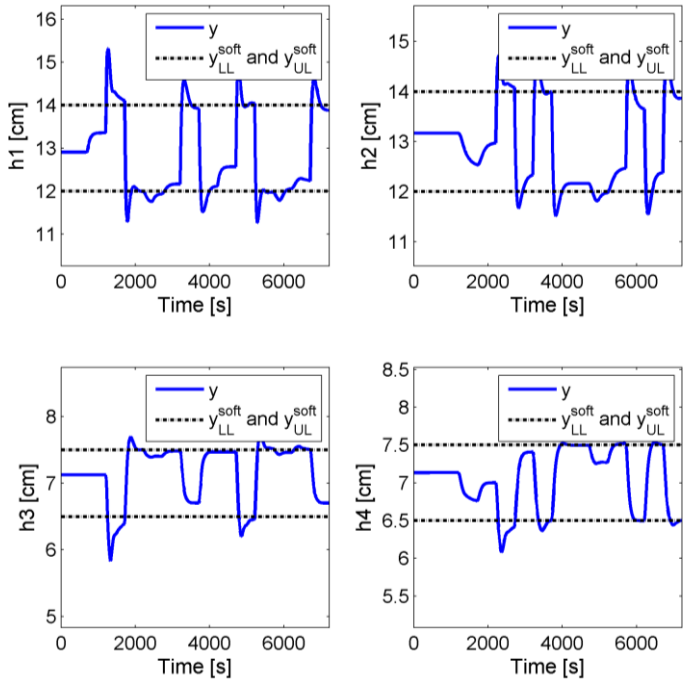

Figure 3.19: Expected behavior of outputs: Linear plant model whit MPC with soft constraints

Since this controller does not have setpoint, the complementary sensitivity function is defined in terms of the soft constraints violation. Figure 3.20 shows T_0 for this case. It is important to emphasize that T_0 is valid only when the variables are violating the soft constraints. When the variable is inside the range, there is no feedback effect of controller, so all the simulation error is conserved ($S_{0_{i,i}} = 1$) and the effect on the other outputs is null ($S_{0_{i,j}} = 0$).

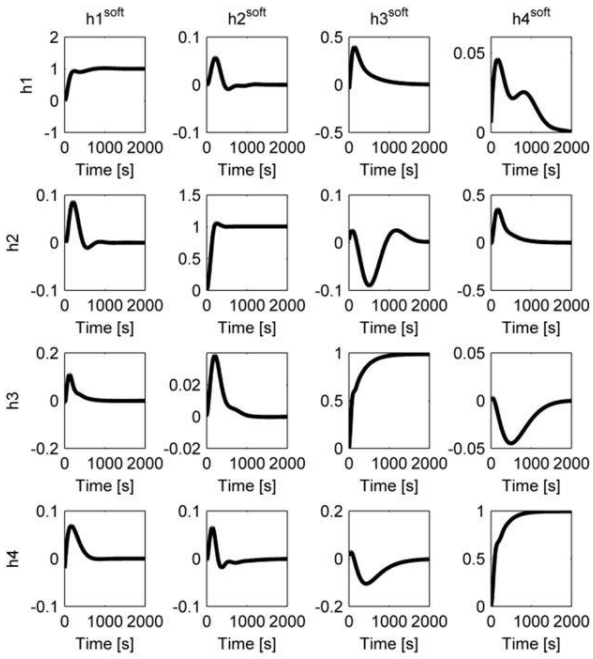

Figure 3.20: Step Response of Complementary Output Sensitivity Function (T_0): Linear plant model with MPC using soft constraints

Scenarios containing mismatches were generated by the variation of the linear models in the Figure 3.21. The datasets for model assessments were generated inserting step changes on controlled external flows $Fex1$ and $Fex2$, according to Figure 3.18. The estimation of y_0 was performed using the proposed method only, since Badwe *et al.* (2010) is dependent of setpoints (equations 3.1 to 3.7) which would not be viable in this case. The Variance Index (equation 3.24) and ACF curves are calculated and adapted for the steady state value (y_{ss}) of each output instead of y_{set}. Results are summarized in Table 3.12 and Figure 3.22.

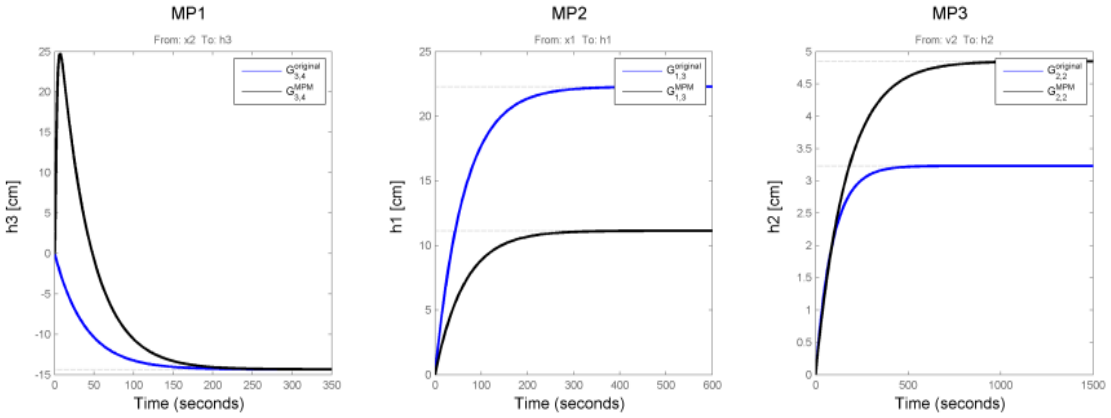

Figure 3.21: Scenarios Configuration: Linear plant model with MPC using soft constraints.

Table 3.12: Relative Variance Index ($Ivar$): Linear plant model with MPC using soft constraints

	Proposed Method				Basis case			
MP	$h1$	$h2$	$h3$	$h4$	$h1$	$h2$	$h3$	$h4$
1	0.87	1.04	**1.82**	1.01	1.01	1.05	**1.75**	0.99
2	**1.33**	1.02	1.07	0.96	**1.29**	1.01	1.15	1.04
3	0.96	**2.15**	0.98	094	1.12	**2.61**	1.02	0.97

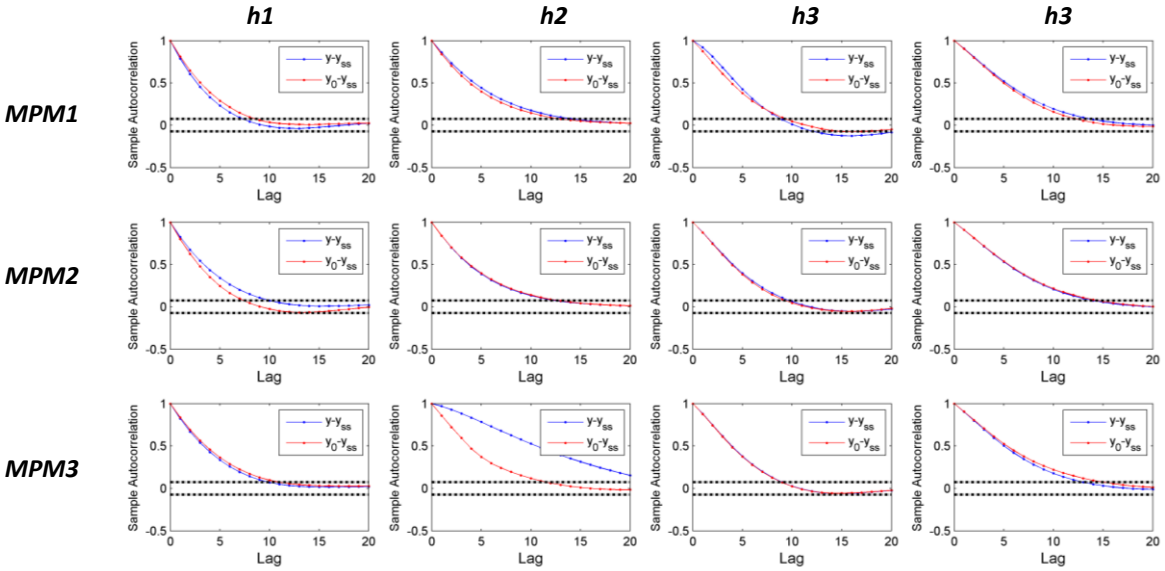

Figure 3.22: Comparative ACF of $(y - y_{ss})$ and $(y_0 - y_{ss})$ estimated by the proposed method: Linear Plant Model whit MPC using soft constraints

The results from Table 3.12 and Figure 3.22 show that the proposed method has correctly detected abnormalities in the models and has identified the variable affected by the mismatch in all scenarios, generating results very similar to the basis case. For example, in scenario MP3, there is an indication of problems in $h2$, because the $Ivar$ of this variable is far from one and the ACF indicate a difference between the settling times of y and y_0 curves. This scenario corresponds to a mismatch in the model $G_{h2,x2}$. These results make evident the capacity of the method to evaluate models of MPCs without a fixed setpoint.

3.4 Conclusions

This paper proposes a methodology for detecting model-plant mismatch affecting MPC performance. This new approach allows the evaluation of how the model-plant mismatch (MPM) affects the actual controller performance, considering the output sensitivity function, which is a more reasonable benchmark for MPC assessment. From this result, it is possible to detect and evaluate the need to re-identify the process

models. Moreover, its simplicity allows for easy application in real plant data (online or offline) regardless of the control algorithm used.

Two versions of the quadruple-tank system were evaluated as case studies. In the first, a linear plant was used and model-plant mismatches were added in a model channel. Simulations were performed considering a fast and a slow MPC tuning and constraint activation/deactivation. A MPC working by range (i.e, with soft constraints) was also configured. The second version considers a phenomenological plant model with modifications to original plant parameters and the addition of unmeasured disturbance signals to generate the scenarios. The results show that the effect of the model-plant mismatch is dependent on the controller tuning.

The proposed method is capable of correctly estimating y_0, since the results obtained are very similar to the cases where there are no model-plant mismatches. However, the use of a sensitivity function compatible with the current feedback controller is fundamental. Although the method has this constraint, the estimation of S_0 is quite a simple procedure, relying solely on a closed-loop simulation.

The quality of y_0 is superior to that in the Badwe *et al* (2010) approach, since it is independent of online closed-loop model identifications. Besides, the proposed method is independent of setpoint, which makes it flexible to different MPCs structures. The use of y_0 as a model benchmark is capable of indicating the effect of the model-plant mismatch in the system's behavior.

The results also show that the proposed method can detect the effect in closed-loop produced by unmeasured disturbances, due to its similarities with MPM.

Capítulo 4 – **MPC model assessment of highly coupled systems**

Abstract[6]**:** Systems with strong interactions among the variables are frequent in the chemical industry and the use of MPC is a standard control tool in these scenarios. However, model assessment in this case is more complex when compared with fairly coupled systems, because these interactions make all the system sensitive to uncertainties, which mask the detection of the model problem roots. This paper presents and extension for highly coupled systems of the method proposed by Botelho *et al.* (2015a/cap. 3) for model-plant mismatch evaluation in MPC applications, based on the use of the diagonal elements of the output sensitivity matrix. The effectiveness of the proposed method is illustrated by two cases studies: a high purity distillation column and the Shell Heavy Oil Fractionator.

Keywords: Model Predictive Control, Model-Plant Mismatch, Model quality, Unmeasured Disturbance, MPC performance assessment, highly coupled systems.

[6] *Submetido para publicação no periódico "Industrial & Engineering Chemistry Research".*

4.1 Introduction

Model predictive control is the most used advanced control solution in the industry, allowing the improvement of the operational performance, since the variability of the system can be reduced. According to Campos *et al.* (2013), the following gains are typically obtained with a MPC:

- Maximization of high valuable products recovery: 2-10%;
- Increase the plant capacity in presence of operational constraints: 5%;
- Minimize the energy consumption: 2-10%.

After the controller implantation, the improvements described above are evident, however, in the course of time the process change and the MPC performance is reduced. Thus, to ensure MPC efficiency, the application of techniques for controller monitoring and diagnosis are essential, although it is still not an easy task, due to the multi-cause nature and complex structure. There are many sources of MPC performance degradation, including tuning parameters (horizon length, weight parameters, sampling time, etc.), poor model quality, inappropriate constraint setup and presence of unmeasured disturbances.

Among the sources of performance degradation, the low quality of process model is one of the most frequent. Sun *et al.* (2013) attested the high cost of a good model in MPC configuration, where more than 80% of the time is spent in model identification. Thus, the precise model assessment is essential for MPC longevity. It is known that a model is an abstraction of the real system behavior, so that model-plant mismatch (MPM) will always be present. However, sometimes these MPMs are very strong that the closed loop cannot achieve good performance. Thus, it is necessary quantifying the MPM, which cannot be compensated by feedback controller, and, therefore, will deteriorate the corresponding closed loop behavior (Wang & Song, 2012). Many methods are available in literature to investigate the quality of the process model used by the MPC. For example, Huang *et al.* (2003) and Jiang *et al.* (2009) proposed techniques to assess the need for model re-identification. Others methods (e.g., Badwe *et al.*, 2009; Kano *et al.*, 2010; Ji *et al.*, 2012) have the objective to identify the pair (i.e., controlled *versus* manipulated variables) with model-plant mismatch. There are also methods that evaluate the predictive capacity of the model (e.g., Jiang *et al*., 2012).

Some industrial processes show strong interaction among process variables (e.g. high purity distillation columns). In this case, the use of MPC is advised, because of its strong multivariable nature. However, a small model-plant mismatch can lead the controller to a very poor performance, or even to instability, requiring an effective controller performance monitoring. Although this is a common problem in the industry, the methods of model assessment usually do no address this situation. Thus, their effectiveness when the processes are close to instability cannot be guaranteed.

This paper presents a method for MPC model assessment of highly coupled systems. It is an extention of the method proposed by Botelho *et. al.* (2015a/cap,. 3), which provides the estimation of the closed loop behavior in absence of model-plant mismatch (called nominal output), indicating the variable disrupted by modeling problems. The

proposed extension aims to indicate the controled variables (CVs) with poor model and their impact in the others process variables.

Sun *et al.* (2013) also proposed a method capable to detect the CVs with poor model. It is based on residual assessment and feedback invariant principle, whereby disturbance innovations are not affected by the feedback controller. It allows the estimation of stochastic disturbance error $e^d(k)$ from the identification of a stable High Order Autoregressive Exogenous Model (HOARX) using the setpoints $y_{set}(k)$ and the measured outputs $y(k)$, according to:

$$y(k) = \sum_{i=1}^{\infty} AO_i y(k-i) + \sum_{i=1}^{\infty} BO_i y_{set}(k-i) + e^0(k) \approx \sum_{i=1}^{MO1} AO_i y(k-i) + \sum_{i=1}^{MO2} BO_i y_{set}(k-i) + e^d(k) \quad (4.1)$$

where AO and BO are the parameters of ARX model and MO1 and MO2 are the model orders.

The disturbance errors (e^d) are compared with the one-step-ahead prediction errors (e^p) (Ljung, 1999). The author suggests a performance indicator for model quality (MQI), which provides the effect of modeling error as a whole, considering the variables costs in the controller, which is defined by:

$$MQI = \frac{\sum_{k=1}^{ns} e^d(k)^T Q_y e^d(k)}{\sum_{k=1}^{ns} e^p\,(k)^T Q_y e^p\,(k)} \quad (4.2)$$

where Q_y are controlled variables weights in MPC controller and ns is the length of the evaluated dataset. Alternatively, is possible to evaluate the modeling error of each CV as follow:

$$iMQI_{yi} = \frac{\sqrt{\sum_{k=1}^{N}\left[e_{yi}^d(k)\right]^2}}{\sqrt{\sum_{k=1}^{N}\left[e_{yi}^p(k)\right]^2}} \quad (4.3)$$

where yi is the evaluated CV. The $iMQI$ and MQI varies between 0 and 1, such that values near to one means that all the prediction errors are due to stochastic disturbance and the model is perfect.

4.2 Proposed method

4.2.1 Brief description of the original methodology

Botelho *et al.* (2015a/cap. 3) proposed a method for MPC model assessment based on the closed loop response, whose main idea is to compare the behavior of measured outputs with the nominal expected outputs, i.e., the outputs obtained in absence model-plant mismatch.

Consider the control loops illustrated in Figure 4.1, with a MPC controller C and nominal model G_0, which represents the real plant G. The model-plant mismatch (MPM) magnitude is ΔG. The theoretical system without mismatch is shown in Figure 4.1a, in which nominal closed loop outputs are y_0 and T_0 is the nominal complementary sensitivity function. The real system, in a scenario subject to MPM, is shown in

Figure 4.1b, where y_{set} corresponds to the setpoints, u are the manipulated variables, y are the measured outputs, y_{sim} are the simulated outputs of the nominal model perturbed by the actual control actions u, and T is the complementary sensitivity function.

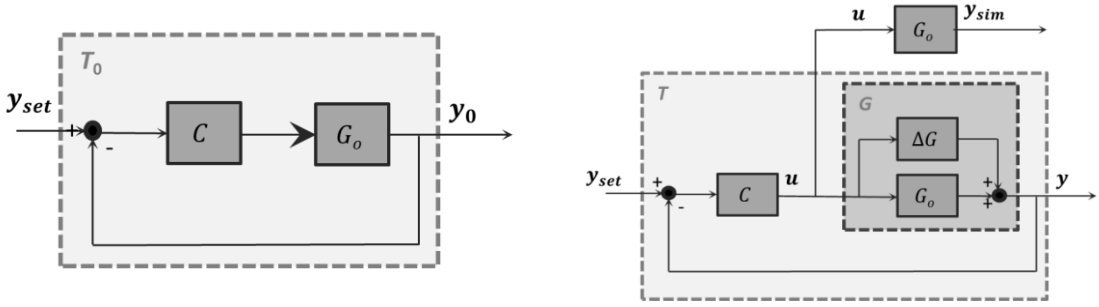

(a) **(b)**

Figure 4.1: Schematic diagram of closed-loop system: (a) nominal system (b) with model-plant mismatch.

An effective model should represent the real system at the frequency where the MPC works. Thus, to assess the real impact of model-plant mismatch, the closed-loop performance must be considered. The expression for these variables can be found in many classical control books (e.g., Skogestad and Postlethwaite,1996):

$$y_0 = T_0 y_{set} \tag{4.4}$$

$$T_0 = G_0 C(I + G_0 C)^{-1} = (I + G_0 C)^{-1} G_0 C \tag{4.5}$$

$$S_0 + T_0 = I \tag{4.6}$$

$$y_{sim} \quad = G_0 u \tag{4.7}$$

where S_0 is the nominal sensitivity funcion and I is the identity matrix. Botelho *et al.* (2015a/ cap. 3), proposed that the nominal output y_0 (i.e., the output of the system in the absence of modeling errors) could be estimated according to:

$$y_0 = S_0 \, (y_{sim} - y) + y \tag{4.8}$$

The authors suggest that, although the equations above are deduced for a MPC with model-plant mismatch (MPM), the same can be derived for cases where unmeasured disturbances (UD) are presented. The control loop of Figure 4.2 illustrates this scenario, where v are sequences of independent random variables, G_d is the unknown disturbance model and y_d are the disturbance signals. The effect of y_d on outputs is similar to that of a model-plant mismatch.

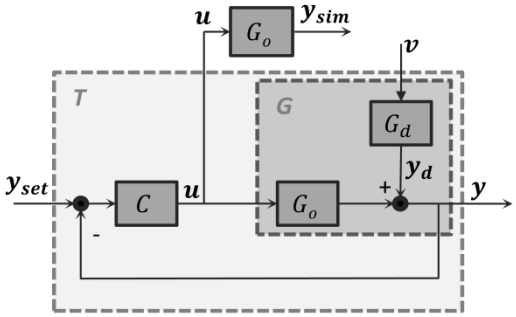

Figure 4.2: Schematic diagram of closed-loop system with unmeasured disturbance.

Since y_0 is an estimative of the output process considering inexistence of model-plant mismatch or unmeasured disturbance, it could be used as a benchmark for controller-model output response. From this benchmark, any output dependent performance indicator could be applied. For example, the comparison of control errors variances called variance index (I_{var}), as suggest by Badwe *et al.* (2010), can be used:

$$Ivar = \frac{var(y - y_{set})}{var(y_0 - y_{set})} \tag{4.9}$$

Variances index far from 1 mean that the measured data have a different behavior of the nominal case, meaning a model problem.

The autocorrelation function (ACF) of control errors (i.e., $y - y_{set}$ and $y_0 - y_{set}$) is also an indicator of MPC performance. A high value of ACF means that the current control error is strongly correlated with past errors. The ACF curves are also useful to analyze the effect of MPM in MPC performance evaluation. In this case, the comparison of the decay rates of ACF(y) and ACF(y_0) indicates whether the MPC is slower or faster than was designed. The ACF also can be used to identify oscillatory behavior (Huang & Shah, 1999).

4.2.2 Extension for Model Assessment of Coupled System

An important issue in industrial MPC applications is its behavior for coupled systems when the model has inconsistencies. First, let us consider the controlled variables $CV1$ and $CV2$ of a hypothetical highly coupled 2x2 system, whose output variables are shown in Figure 4.3. Note that both outputs have an oscillatory behavior with similar amplitude and frequency. The application of Botelho *et al.* (2015a/cap. 3) method (equation 4.8) indicates that the oscillatory behavior come from a model-plant mismatch (MPM) or unmeasured disturbance (UD) because the nominal outputs (y_0) are not oscillating (compare y and y_0 curves in Figure 4.3). However, it is not possible to know which controlled variable (or both) has the modeling problem.

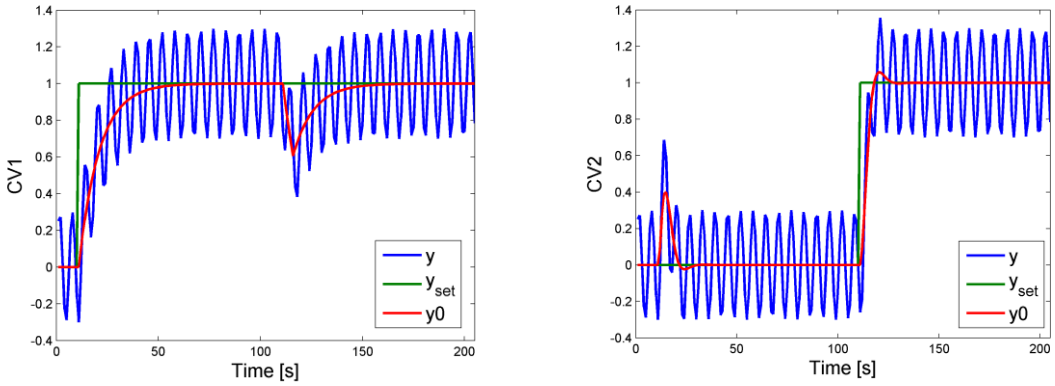

(a) **(b)**

Figure 4.3: Hypothetical coupled system with modeling problems.

To locate the modeling problems an extension of Botelho *et al.* (2015a/cap. 3) method is proposed. It aims to exclude the coupling effect and isolate the modeling errors of each CV. The method, as Botelho *et al.* (2015a/ cap. 3), is centered in the nominal sensitivity function (S_0). This function is a square matrix whose dimension is equal to the number of outputs. Its diagonal elements ($S_{0_{diag}}$) give the closed loop response of each output when its reference (setpoint or soft-constraints) is changed. The remaining elements provide the impact of this reference change in the others outputs. Thus, the off-diagonal elements of S_0 will be greater as coupled as the system is. Based on these concepts, we propose the estimation of the diagonal nominal outputs ($y_{0_{diag}}$) as an extension of equation 4.8 as follow:

$$y_{0_{diag}} = S_{0_{diag}} (y_{sim} - y) + y \tag{4.10}$$

The simulation error (e_{sim}), the nominal error (e_0) and the nominal diagonal error ($e_{0_{diag}}$) are defined respectively as:

$$e_{sim} = y_{sim} - y \tag{4.11}$$

$$e_0 = y_0 - y \tag{4.12}$$

$$e_{0_{diag}} = y_{0_{diag}} - y \tag{4.13}$$

The $S_{0_{diag}}$ works as a softening for the simulation error (e_{sim}), and retains only the part that is not removed by the controller feedback and is impacting in the performance of corresponding output. Thus, variables without significant MPM or UD will have $e_{0_{diag}} \cong 0$ (because $e_{sim} \cong 0$). The S_0 provides the complete diagnosis of the model, showing the effect of the MPMs or UDs in the corresponding output and how it is impacting in the others. Thus $e_0 \neq 0$ even for variables without significant MPM or UD. Considering the existence of MPM or UD, this difference will be amplified by the coupling between the variables.

Given that y_0 and $y_{0_{diag}}$ are related with the process outputs when there is no model-plant mismatch or unmeasured disturbances, they can be considered as benchmarks for controller-model output response. Furthermore, these benchmarks allow any output MPC performance indicators (IP) to be applied. The diagnosis procedure

starts with the comparison of the performance indicator of the real (IP) and the nominal (IP_0) outputs. The greater is the difference between IP and IP_0, higher is the incidence of performance deterioration due to modeling problems. To locate it, a comparison between IP_0 and $IP_{0_{diag}}$ is performed. A similar behavior between them means that the modeling problem is located in the own CV. Otherwise, the performance deterioration of the corresponding CV is due to an error in another CV model. Figure 4.4 summarizes the procedure.

Similarly with the Variance Index described in equation 4.9, the Diagonal Variance Index is useful for the model assessment and is defined as:

$$Ivar_{diag} = \frac{var(y - y_{set})}{var(y_{0_{diag}} - y_{set})} \tag{4.14}$$

The $Ivar$ and $Ivar_{diag}$ works as a ratio between IP versus IP_0 and IP_0 versus $IP_{0_{diag}}$, respectively. Thus, the closer to 1 they are, higher is the similarity between the related variances.

The autocorrelation function (ACF) of control errors may also be applied for the diagonal nominal output (i.e., $y_{0_{diag}} - y_{set}$) and compared with results of nominal and real cases.

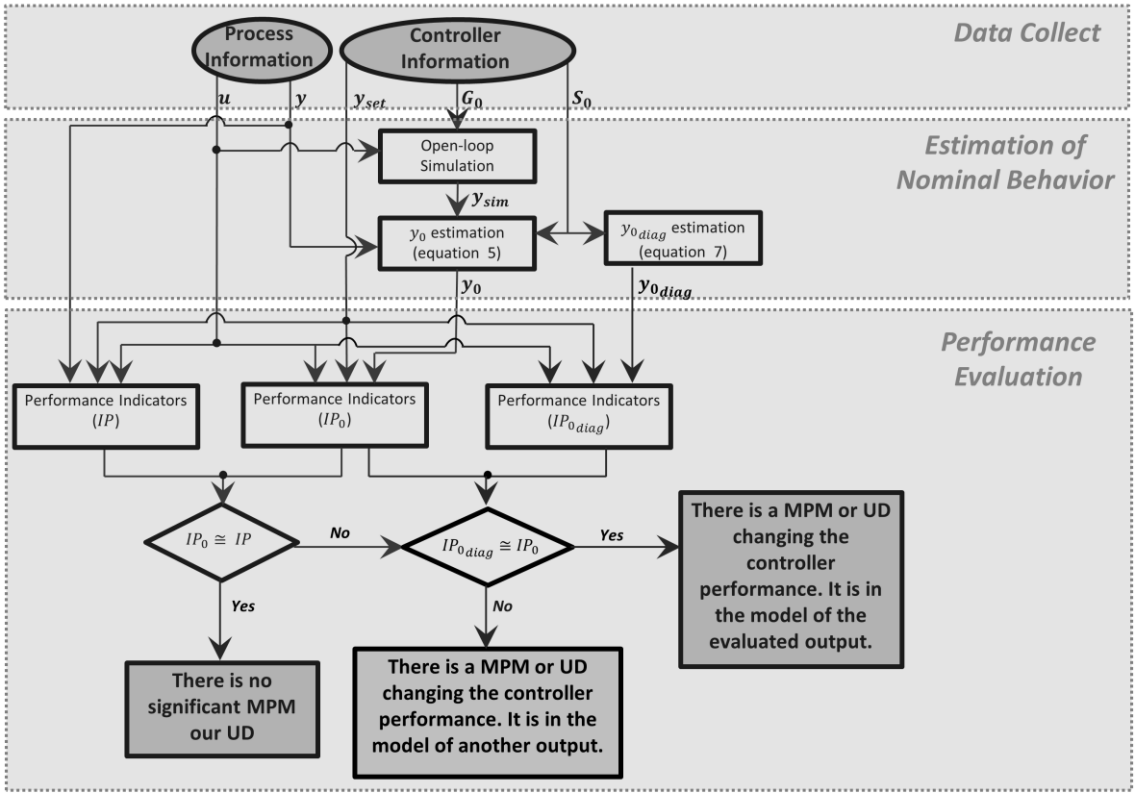

Figure 4.4: Diagnosis procedure for each output variable according to the proposed methodology.

4.3 Case Studies

4.3.1 High Purity Distillation Column

This process is originally presented by Skogestad & Postlethwaite (1996) and refers to a high purity binary distillation column. The feed (F) is an equimolar liquid mixture with relative volatility of 1.5. The pressure is assumed constant and the operating variables are such that we nominally have 99% purity for each product. This kind of distillation process is usually difficult to control because of strong interaction between its variables.

In this case study, a LV-control configuration was considered: i.e., the manipulated variables are the reflux (L) and the boilup (V). The controlled outputs are the top and the bottom product composition (yD and xB). The linear process model is:

$$G_0 = \frac{1}{75s+1}\begin{bmatrix} 87.8 & -86.4 \\ 108.2 & -109.6 \end{bmatrix} \tag{4.15}$$

This system was implemented in *Matlab/Simulink* and a MPC was configured. The controller was tuned according with the RPN methodology (Trierweiler & Farina, 2003) whose parameters are shown in Table 4.1:

Table 4.1: High purity distillation column case: Tuning Parameters of MPC

Sample Time	8 min
Prediction Horizon	30
Control Horizon	6
Controlled Variable Weight	$Q_{yD} = 0.5, Q_{xB} = 0.3$
Move Suppression	$Q_{\Delta L} = Q_{\Delta V} = 0.5$

The estimation of the output sensitivity function (S_0) was performed from a simulation of the system considering a perfect model ($G = G_0$) and the tuning of Table 4.1. From these results, the S_0 model was identified considering a Box-Jenkins model.

The coupling of a system could be measured through the diagonal elements of the dynamic *Relative Gain Array* (RGA) matrix. According to Luyben & Luyben (1997), when they are far from 1 there is an indicative of high interaction among the variables. The diagonal elements of the dynamic RGA in the frequency domain for this case study is shown in Figure 4.5. We compare the dynamic RGA with the RPN weight function (Trierweiler *et al.*, 1997), given by:

$$RPN(j\omega) = \bar{\sigma}[S_0(j\omega)T_0(j\omega)] \tag{4.16}$$

where $\bar{\sigma}$ is the maximum singular value. The maximum of RPN weight function occurs in the neighborhood of the controller frequency work. Figure 4.6 illustrates the RPN function for this case study.

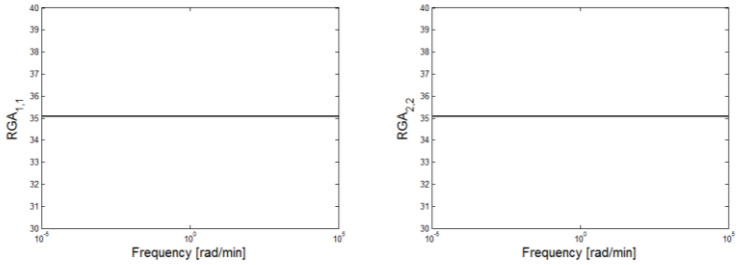

Figure 4.5: High purity distillation column case: dynamic RGA.

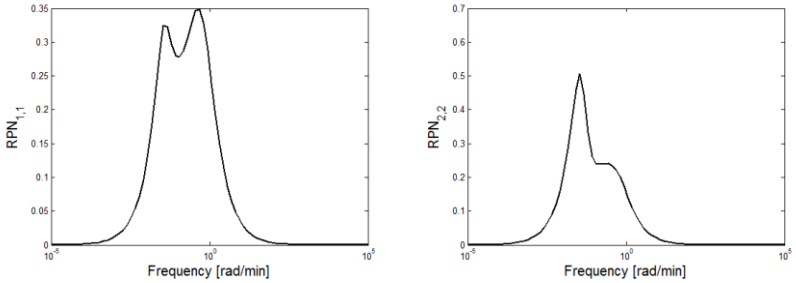

Figure 4.6: High purity distillation column case: RPN weight function.

From Figures 4.5 and 4.6 is possible to observe that in the frequency of the controller actuation ($\cong 10^{-2}\ rad/s$) the diagonal elements of the RGA are approximately equal to 35, which means that the coupling between the variables is very strong for the considered tuning.

For the described system, scenarios were generated considering step changes in the setpoints (y_{set}) and the addition of model-plant mismatches (MPM), unmeasured disturbances (UD), as described in Table 4.2. A white noise with zero mean and variance 10^{-3} was added in the measured outputs. Figure 4.7 show the generated outputs for the nominal case (i.e., in absence of MPM and UD) and Figure 4.8 the outputs of each scenario.

Table 4.2: High purity distillation column case: Scenarios configuration

Scenario	Type	Description
Scen1	MPM in $yd\ x\ L$	$G_{1,1} = \frac{151.9}{75s+1}$
Scen2	MPM in $yd\ x\ V$	$G_{1,2} = \frac{-86.4}{73s+1}$
Scen3	UD in xB	Sinusoidal signal with frequency 0.02/min and amplitude ±0.2
Scen4	MPM in $yd\ x\ L$ and UD xB	Scen1 + Scen3
Scen 5	MPM in $yd\ x\ L$ and UD xB	Scen1 + Integrator signal ($5e^{-5}t$)

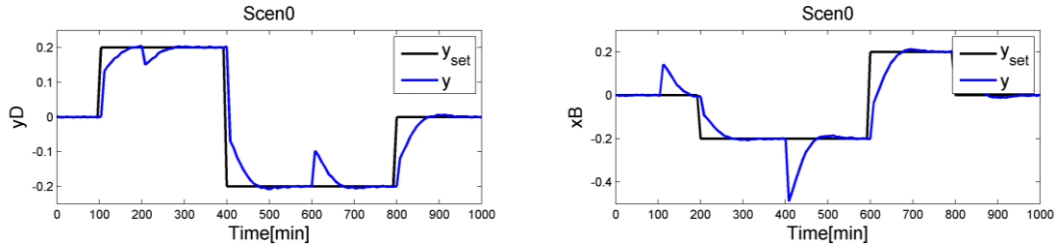

Figure 4.7: High purity distillation column case: System outputs of nominal case

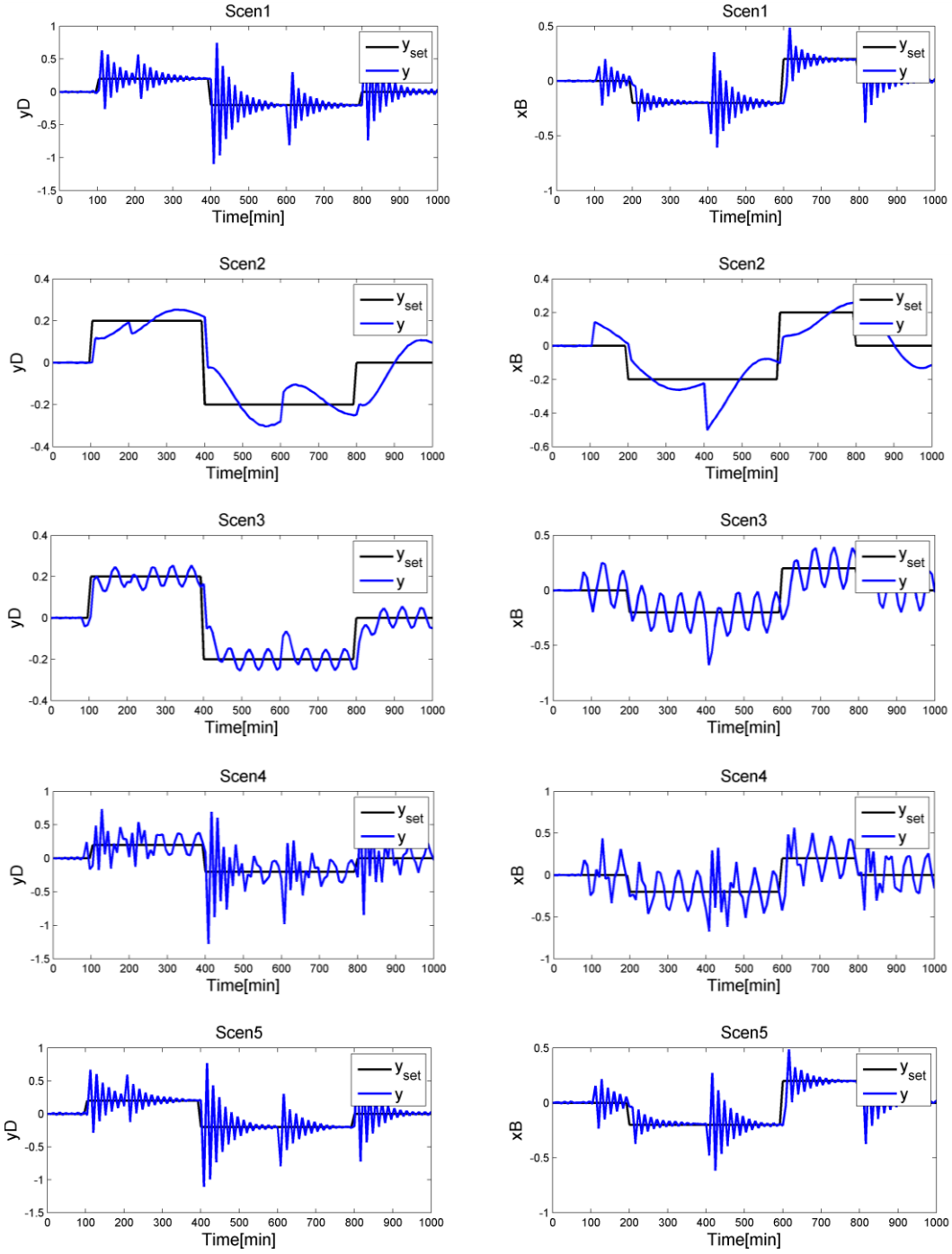

Figure 4.8: High purity distillation column case: System outputs of each scenario

Figure 4.8 shows that in all scenarios the outputs yD and xD have oscillatory behavior with similar magnitude. To check the existence of modeling problems, the methods presented in sections 4.2.1 and 4.2.2 were applied as well the Sun *et al.* (2013) method. The square sum of simulation errors (SSE) were also evaluated, according to:

$$SSE = \sqrt{\sum_{j=1}^{ns} [y(j) - y_{sim}(j)]^2} \tag{4.17}$$

The variances indexes (Ivar and $Ivar_{diag}$), SSE, $iMQI$ and MQI of each scenario are presented in Table 4.3. The corresponding ACF are presented in Figure 4.9.

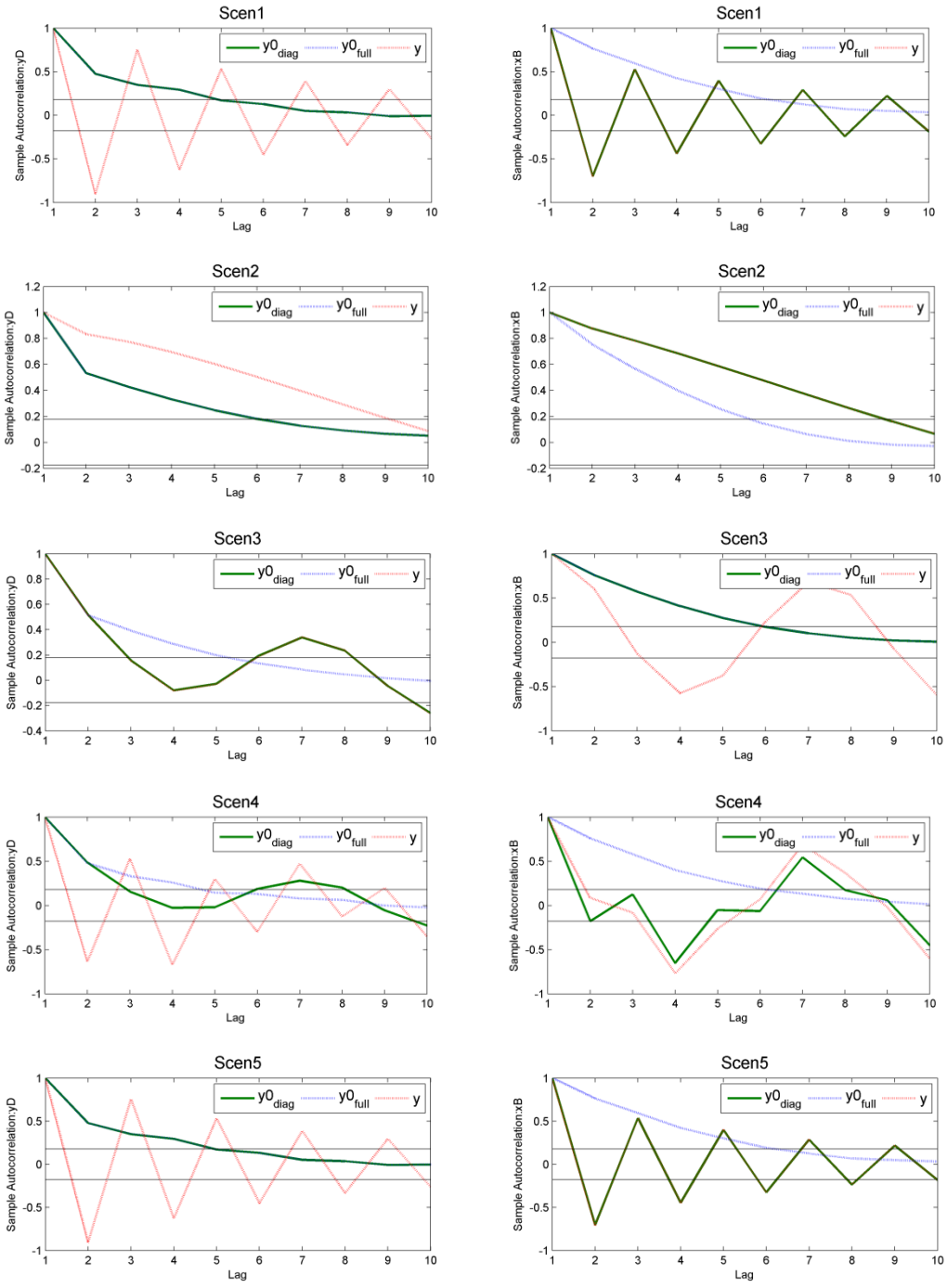

Figure 4.9: High purity distillation column case: ACF of the scenarios

Table 4.3: High purity distillation column case: Results of the model assessment

		yD	xB
	SSE	27.33	0.96
Scen1	$Ivar$	23.81	2.12
(MQI=8e-5)	$Ivar_{diag}$	23.81	1.00
	$iMQI$	0.007	0.94
	SSE	19.12	1.17
Scen2	$Ivar$	2.80	2.00
(MQI 3e-3)	$Ivar_{diag}$	2.80	1.00
	$iMQI$	0.04	0.91
	SSE	0.98	14.77
Scen3	$Ivar$	1.42	3.46
(MQI=2e-3)	$Ivar_{diag}$	1.00	3.46
	$iMQI$	1.00	0.04
	SSE	28.77	14.77
Scen4	$Ivar$	26.35	5.88
(MQI=1e-3)	$Ivar_{diag}$	20.55	1.62
	$iMQI$	0.03	0.07
	SSE	28.27	13.75
Scen5	$Ivar$	23.65	2.22
(MQI=1e-4)	$Ivar_{diag}$	23.68	0.99
	$iMQI$	0.01	0.81

Table 4.3 shows that the proposed method captures the variable affected by the modeling problems and its effect in the other output. In all cases the $Ivar$ of yD and xB is far from one, which means that the variables are affected by a modeling problem. The $Ivar_{diag}$ of xB in Scen1 and Scen2 as well as yD in Scen3 are equal to one, showing that the models of these variables do not have problems. In both cases, the SSE is near to zero, also denoting the inexistence of modeling problem in the corresponding variables.

In Scen5 the SSE is high for both variables even the $Ivar_{diag}$ of xB being near to one. It means that there is a modeling error in xB model, but it is not impacting the MPC performance. It could be confirmed by the similarity between the outputs of this scenario with Scen1. The Scen2 makes evident that the method is paring independent, since the result obtained was in accordance with the added MPM. These results corroborate the fact that the evaluate de modeling error is not appropriated for the assessment of MPC models.

The Scen4 show that both variables have modeling problems (high $Ivar_{diag}$) and the modeling of each is impacting in the other, since $Ivar_{diag} \neq Ivar$ for yD and xB.

The Sun *et al.* (2013) method provided results similar to the proposed method. The existence of MPM in the system was captured by the small values of MQI in all scenarios. The $iMQI$ interpretation is compatible with the $Ivar_{diag}$, such that are always higher than 0.8 in the controlled variables without modeling errors.

The ACF (Figure 4.9) also capture the existence of a oscillatory behavior in outputs due to modeling problems since, for all scenarios, ACF(y) have oscillatory behavior and ACF($y_{0_{diag}}$) do not have. The similarity between ACF(y_0) and ACF($y_{0_{diag}}$) indicates the existence of modeling problem in the corresponding variable (i.e, yD in Scen1 and Scen4 and xD in Scen2). For Scen4 the ACF make evident that both variables have modeling problems, since ACF(y_0)≠ ACF($y_{0_{diag}}$)≠ ACF(y) for yD and xB.

4.3.2 Shell Heavy Oil Fractionator

The Shell Heavy Oil Fractionator is a problem originally presented by Prett e Morari (1987). This system is characterized by high interaction among the variables as well large time delays. Figure 4.10 illustrate the system.

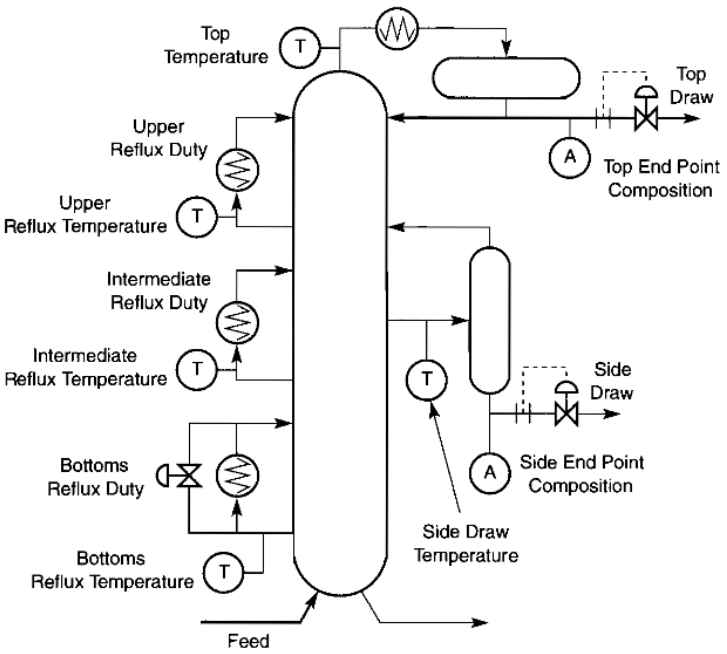

Figure 4.10: Schematic representation of Shell Heavy Oil Fractionator (Maciejowski ,2002).

This system was implemented in *Matlab/Simulink* and a MPC was configured, based on Farenzena (2008). The main objective is to control the top composition ($y1$), the side composition ($y2$) and the bottom reflux temperature ($y3$) in the respective setpoint by the manipulation of the top draw ($u1$), side draw ($u2$) and bottom reflux duty ($u3$). The process model (G_0) is presented in equation 4.18 and the controller tuning parameters in Table 4.4.

$$G_0 = \begin{bmatrix} \frac{4.05}{50s+1}e^{-27} & \frac{1.77}{60s+1}e^{-28} & \frac{5.88}{50s+1}e^{-27} \\ \frac{5.39}{50s+1}e^{-18} & \frac{5.72}{60s+1}e^{-14} & \frac{6.9}{40s+1}e^{-15} \\ \frac{4.38}{33s+1}e^{-20} & \frac{4.42}{44s+1}e^{-22} & \frac{7.2}{19s+1}e^{-19} \end{bmatrix} \quad (4.18)$$

Table 4.4: The Shell heavy oil fractionator case: MPC Tuning Parameters

Sample Time	2 min
Prediction Horizon	20
Control Horizon	4
Controlled Variable Weight	$Q_{y1} = 1, Q_{y2} = 6, Q_{y3} = 2$
Move Suppression	$Q_{\Delta u1} = Q_{\Delta u2} = Q_{\Delta u2} = 0.2$
MVs upper limits	$u1_{hard}^{max} = u2_{hard}^{max} = u3_{hard}^{max} = 3$
MVs lower limits	$u1_{hard}^{min} = u2_{hard}^{min} = u3_{hard}^{min} = -3$

The estimation of the output sensitivity function (S_0) was performed from a simulation of the system considering a perfect model ($G = G_0$). From the results, the S_0 model was identified considering a Box-Jenkins model. Several model orders were evaluated and the best result (5th order) was considered.

For the process model (equation 4.18), the diagonal elements of dynamic RGA are presented in Figure 4.11. The RPN weight functions are shown in Figure 4.12.

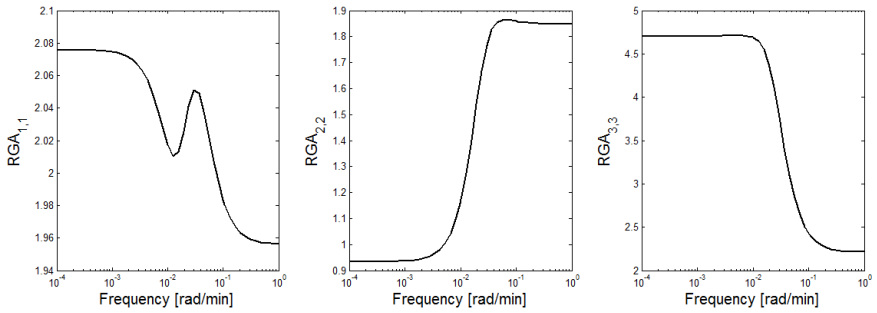

Figure 4.11: The Shell heavy oil fractionator case: dynamic RGA

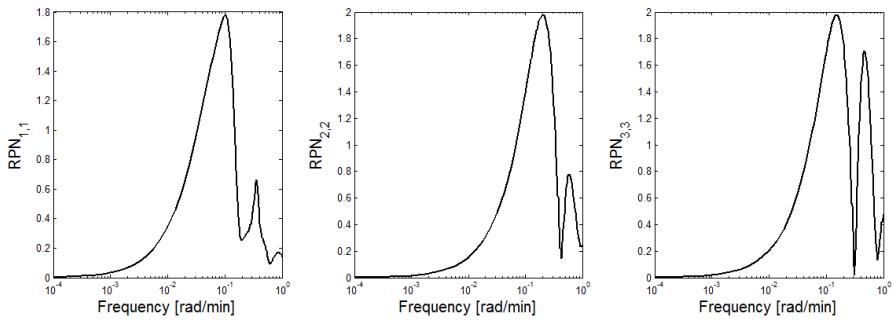

Figure 4.12: The Shell heavy oil fractionator case: RPN weight function

Figures 4.11 and 4.12 make evident that in the frequency of the controller actuation ($\cong 10^{-1}\, rad/s$) all diagonal elements of the RGA are approximately equal to 2, which means that there is a coupling between the variables.

Scenarios were generated considering step changes in the setpoints (y_{set}) and the addition of model-plant mismatches (MPM), unmeasured disturbances (UD) and variations in the controller tuning. A white noise with zero mean and standard deviation of 0.02 was added to the measured outputs. Figure 4.13 shows the generated data for the nominal case (i.e., in absence of MPM and UD), where u_{lim} are the constraints of the manipulated variables.

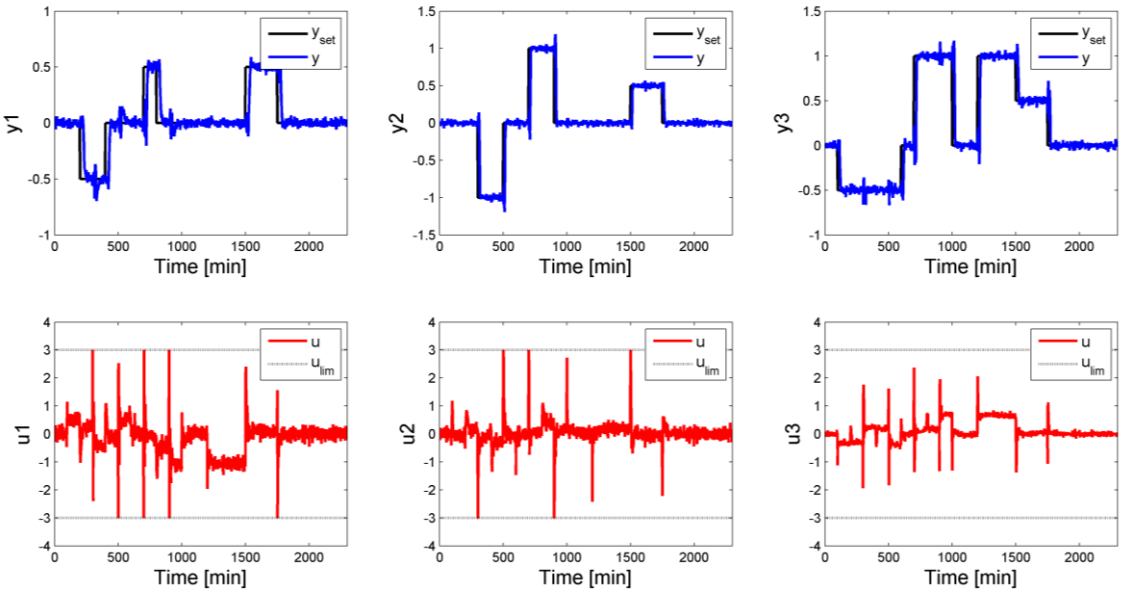

Figure 4.13: The Shell heavy oil fractionator case: Inputs and outputs of the nominal case

Each scenario was evaluated according the indicators presented in sections 4.2.1 and 4.2.2 as well as by the Sun *et al.* (2013) method. The square sum of simulation errors (SSE) were also evaluated, according to equation (4.17). The results are discussed below.

Scenario 1: Moderate MPM

This scenario considers a model-plant mismatch in the time constant of pair $y1\ X\ u1$, according to equation 4.19. Figure 4.14 present the inputs (u) and outputs (y) when steps in the setpoints (y_{set}) were performed, showing that $y1$ is not adequately controlled. The

model assessment methods were in this data and results are presented in Figure 4.15 and Table 4.5.

$$G(1,1) = \frac{4.05}{65s + 1} e^{-27} \tag{4.19}$$

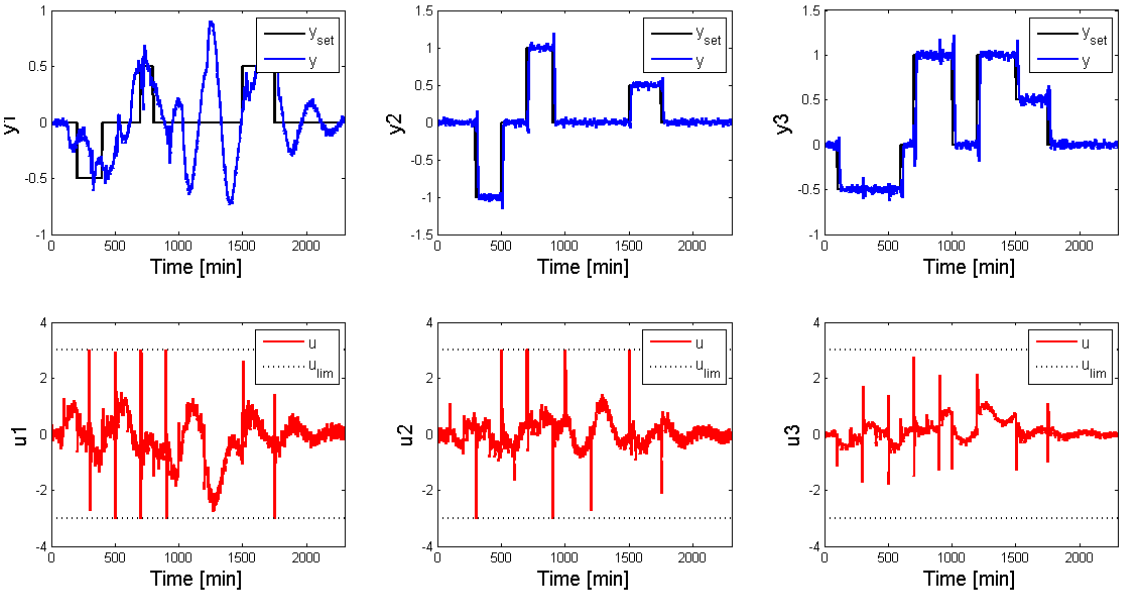

Figure 4.14: The Shell heavy oil fractionator case: Inputs and Outputs for Scenario 1

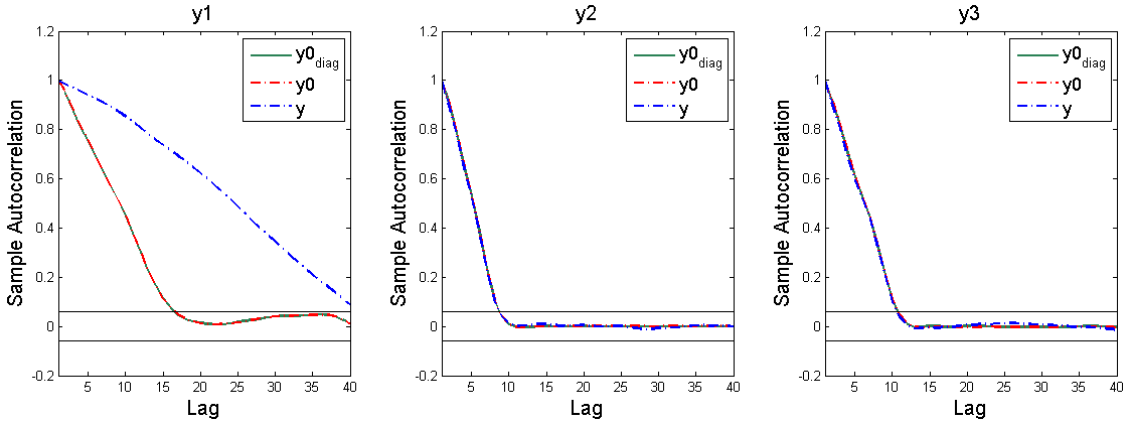

Figure 4.15: The Shell heavy oil fractionator case: ACF for Scenario 1

Table 4.5: : The Shell heavy oil fractionator case: Indicators Results for Scenario 1

		$y1$	$y2$	$y3$
MQI=0.64	SSE	439.9	18.7	17.9
	$Ivar$	4.54	1.02	0.99
	$Ivar_{diag}$	4.54	1.02	1.00
	$iMQI$	0.58	0.84	0.85

From Table 4.5, it is possible to observe that the proposed method captures the expected behavior, indicating the existence of an impactful modeling problem in $y1$, because SSE_{y1} is large and $Ivar_{y1} > 1$. This modeling problem only affects $y1, since$ variance indexes ($Ivar$) of $y3$ and $y2$ are near to one. The values of SSE_{y2} and SSE_{y2} could be attributed to the white noise effect. The difference between the ACF decay ratio of $y1_0$ and $y1$ (Figure 4.15) indicates that the modeling problem make the system response slower than the nominal case.

The Sun *et al.* (2013) captures the existence of MPM by the MQI. The $iMQI$ interpretation is compatible with the $Ivar_{diag}$, such that are higher than 0.8 in the controlled variables without modeling errors ($y2$ and $y3$) and 0.58 for $y1$.

Scenario 2: MPM make the system oscillatory

This scenario considers model-plant mismatch in the steady-state gain and time delay of pair $y2\ X\ u1$, according to equation 4.20. Figure 4.16 presents the inputs (u) and outputs (y) when steps in the setpoints (y_{set}) were performed, showing that all the outputs are oscillating. The oscillating behavior makes the inputs track around their constraints. The results of the model assessment are presented in Figure 4.17 and Table 4.6.

$$G(2,1) = \frac{9.45}{50s + 1} e^{-20} \tag{4.20}$$

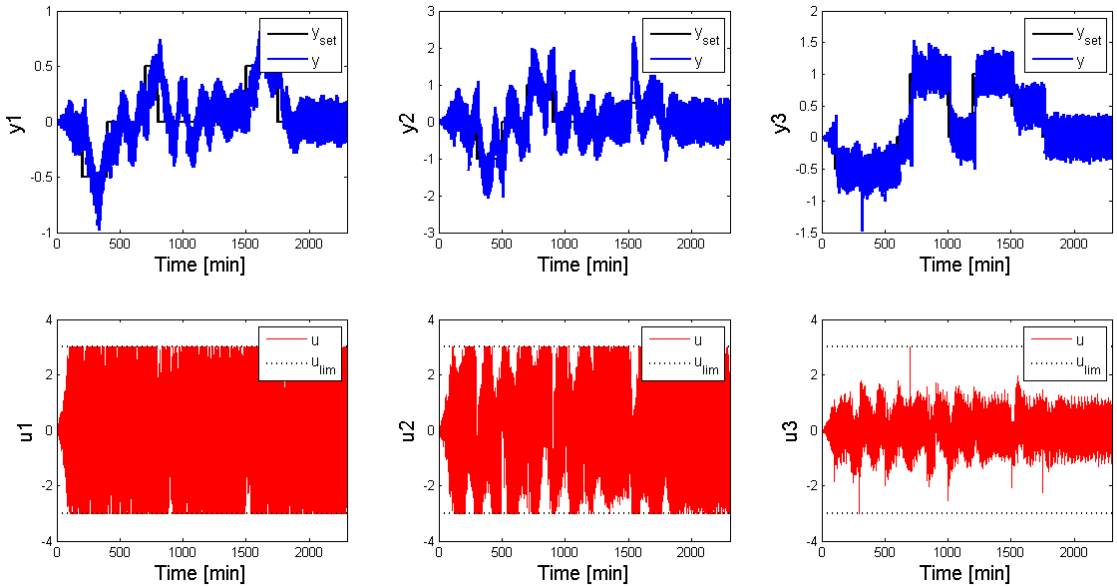

Figure 4.16: The Shell heavy oil fractionator case: Inputs and Outputs for Scenario 2

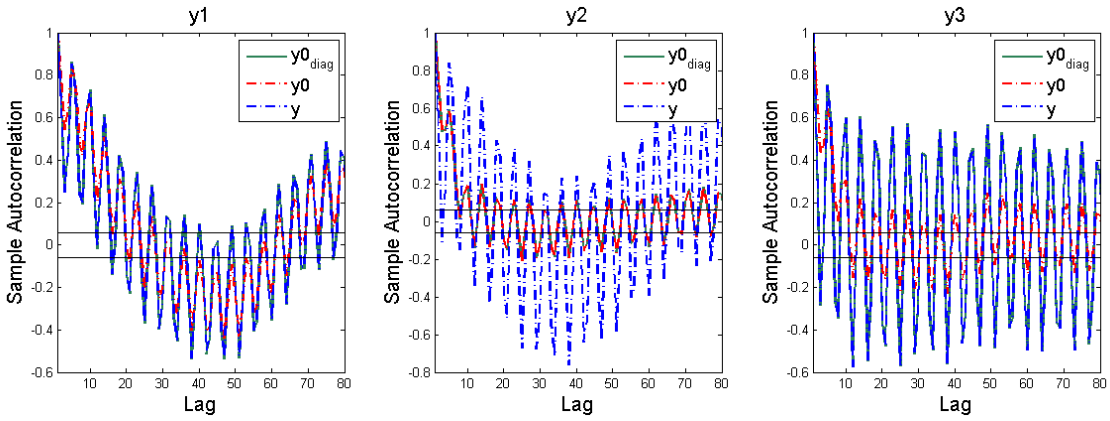

Figure 4.17: The Shell heavy oil fractionator case: ACF for Scenario 2

Table 4.6: The Shell heavy oil fractionator case: Indicators for Scenario 2

		$y1$	$y2$	$y3$
MQI=0.02	SSE	18.3	655.4	18.8
	$Ivar$	1.30	8.01	2.1
	$Ivar_{diag}$	1.00	8.01	1.00
	$iMQI$	0.89	0.12	0.96

Results of Table 4.6 indicates that a modeling problem is impacting in all system variables, because the $Ivar$ of all outputs are higher than 1. The modeling problem is only in $y2$ since this is the only variable with $Ivar_{diag}$ far from one. The ACF (Figure 4.17) makes evident that the oscillatory behavior of outputs come from a modeling problem, since ACF(y) has oscillatory behavior and ACF($y_{0_{diag}}$) does not oscillate significantly in all outputs. The modeling problem is in $y2$ because $y2_{0_{diag}} \cong y2_0 \neq y2$.

The Sun *et al.* (2013) captures the existence of MPM by the small value of MQI. The $iMQI$ interpretation is compatible with the $Ivar_{diag}$, such that are higher than 0.8 in the controlled variables without modeling errors ($y1$ and $y3$) and 0.12 for $y2$.

Scenario 3: Non-impactful MPM

This scenario considers model-plant mismatch in the pair $y3\ X\ u3$, according to equation 4.21. Figure 4.18 present the inputs (u) and outputs (y) when steps in the setpoints (y_{set}) were performed, showing that the MPM does not have effect in the system behavior (see Figure 4.13). Table 4.7 and Figure 4.19 present the results of the model assessment for this scenario.

$$G(3,3) = \frac{5495s + 12.2}{14250s^2 + 769s + 1} e^{-19} \tag{4.21}$$

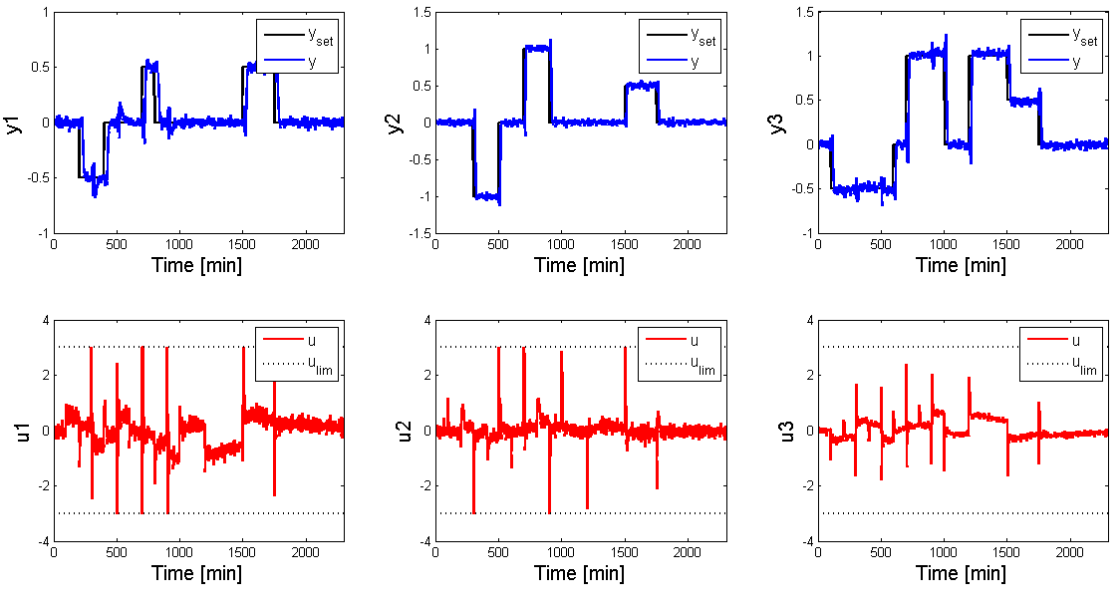

Figure 4.18: The Shell heavy oil fractionator case: Inputs and Outputs for Scenario 3

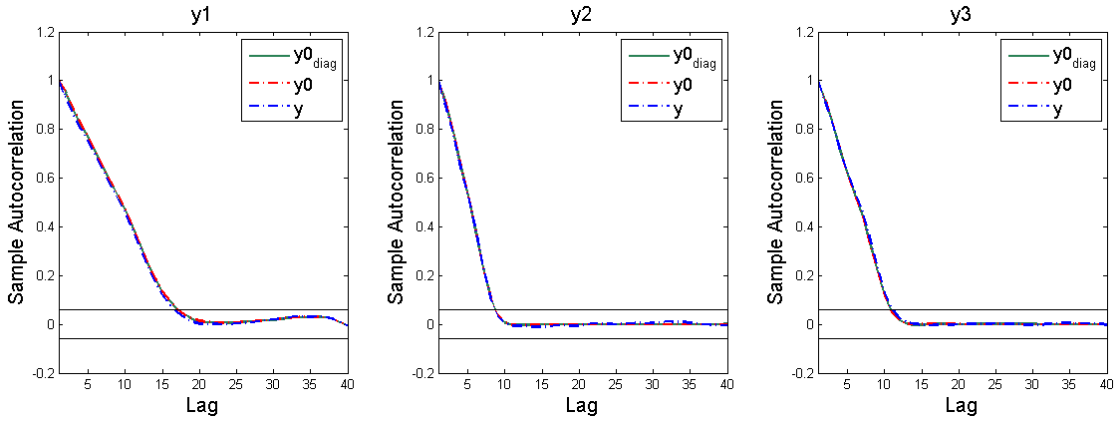

Figure 4.19: The Shell heavy oil fractionator case: ACF for Scenario 3

Table 4.7: Shell heavy oil fractionator case: Indicators Results for Scenario 3

		$y1$	$y2$	$y3$
MQI=0.82	SSE	17.58	18.16	196.04
	$Ivar$	1.02	1.02	1.04
	$Ivar_{diag}$	1.03	1.02	1.05
	$iMQI$	0.87	0.87	0.89

From Table 4.7 and Figure 4.19, it is possible to confirm that there is a modeling problem in $y3$, because SSE_{y3} has a high value, but it does not have significant effect in the controller performance since all $Ivar$ are near to one and the ACF of , y_0 and $y_{0_{diag}}$

are similar. The Sun *et al.* (2013) provides similar results, since MQI and all $iMQIs$ are higher than 0.8, indicating the inexistence of significant modeling problems.

Scenario 4: Non-impactful MPM and Bad Tuning

This scenario combines a model-plant mismatch in the pair $y3\ X\ u3$ (equation 4.21) with the following change in MPC tuning parameters: $Q_{\Delta u1} = Q_{\Delta u2} = Q_{\Delta u3} = 10$ and $Q_{y1} = 60$. Figure 4.20 presents the inputs (u) and outputs (y) of this scenario, showing that $y1$ has a performance problem. Table 4.8 and Figure 4.21 present the results of the model assessment. It is important to emphasizes that, for this case, a new estimation of S_0 was performed, considering the current tuning.

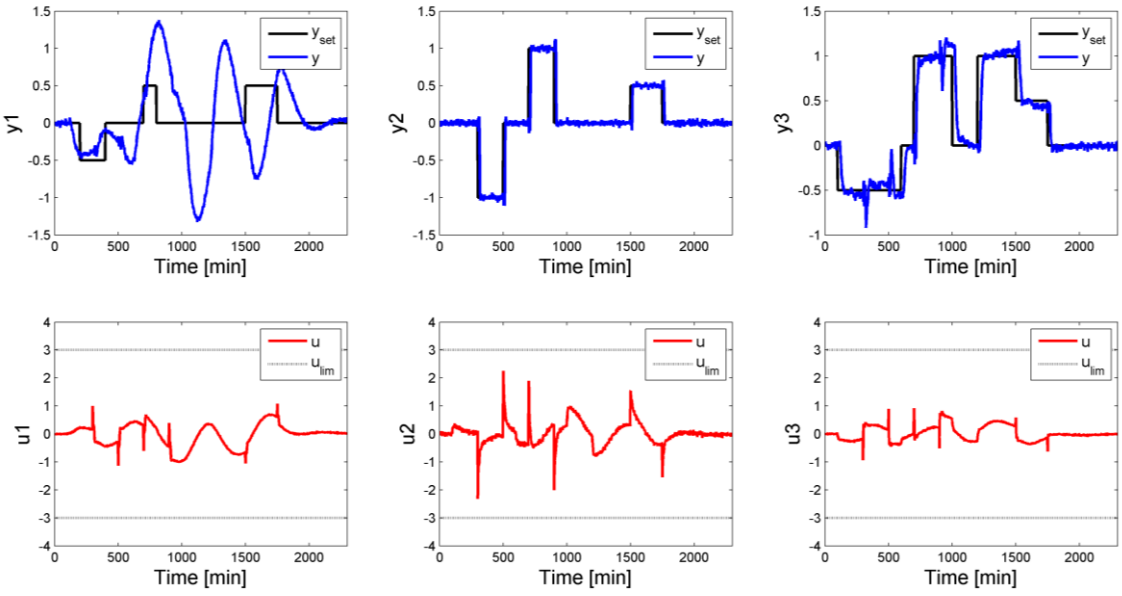

Figure 4.20: The Shell heavy oil fractionator case: Inputs and outputs for Scenario 4

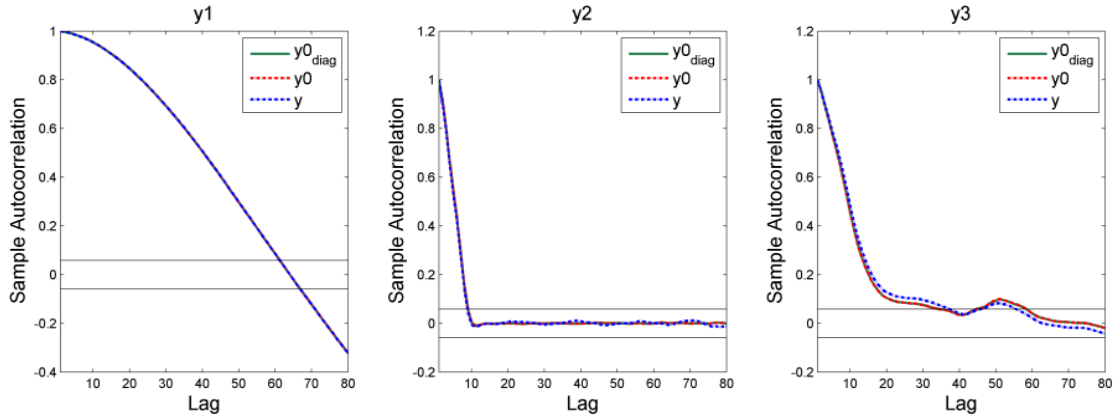

Figure 4.21: The Shell heavy oil fractionator case: ACF for Scenario 4

Table 4.8: The Shell heavy oil fractionator case: Indicators for Scenario 4

		$y1$	$y2$	$y3$
MQI=0.81	SSE	18.18	17.77	221.92
	$Ivar$	1.00	1.00	1.05
	$Ivar_{diag}$	1.00	1.01	1.05
	$iMQI$	0.86	0.86	0.82

Table 4.8 shows that there is a modeling error (high value of SSE_{y3}) but the bad performance of $y1$ is not due to a modeling problem, since all the variances indexes are near to one. Similarly to scenario 3, the modeling problem in $y3$ does not have significant effect in the controller performance. The similar behavior of y, y_0 and $y_{0_{diag}}$ ACFs (Figure 4.21) also show that there is no significant modeling problem in this scenario. The Sun *et al.* (2013) provides similar results, since MQI and all $iMQIs$ are higher than 0.8, indicating the inexistence of significant modeling problems.

Scenario 5: Moderate unmeasured disturbance in $y3$

This scenario considers unmeasured disturbance added in $y3$. Figure 4.22 show the disturbance signal. Figure 4.23 show the inputs (y) and outputs (u) of this scenario. It is evident that only $y3$ has a performance problem. Table 4.9 and Figure 4.24 present the model assessment results for the scenario.

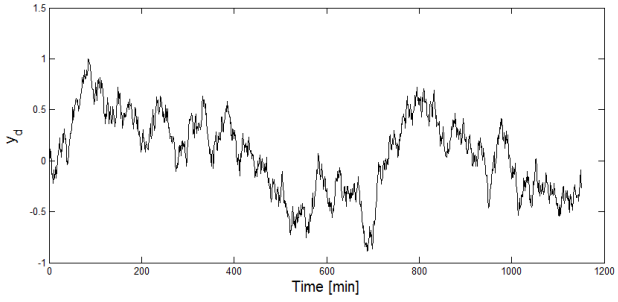

Figure 4.22 The Shell heavy oil fractionator case: Unmeasured Disturbance Added in $y3$ for Scenario 5

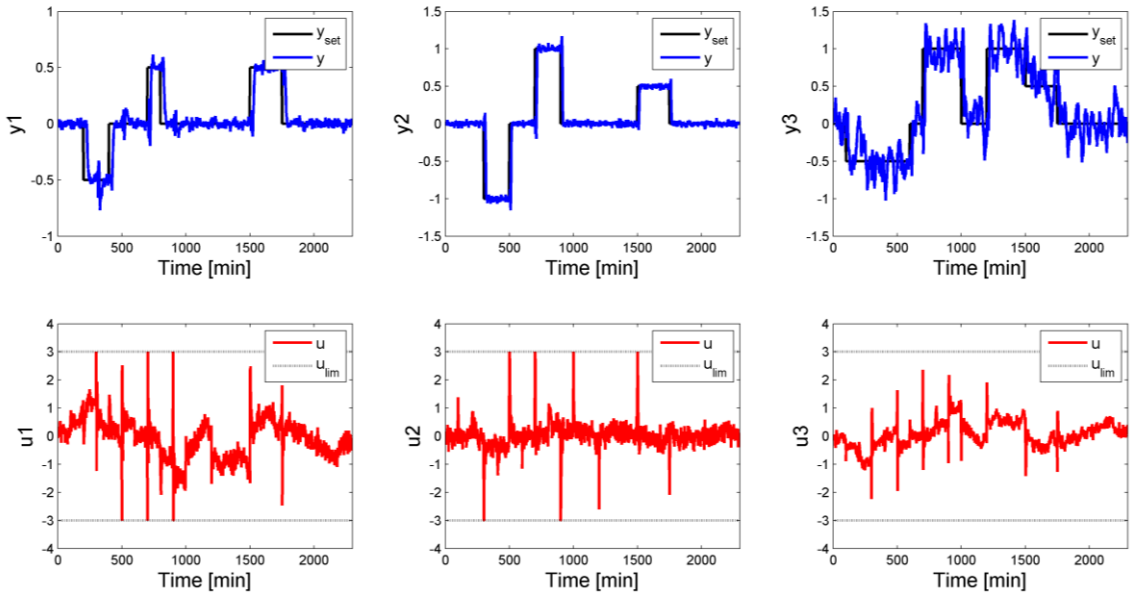

Figure 4.23: The Shell heavy oil fractionator case: Inputs and outputs for Scenario 5

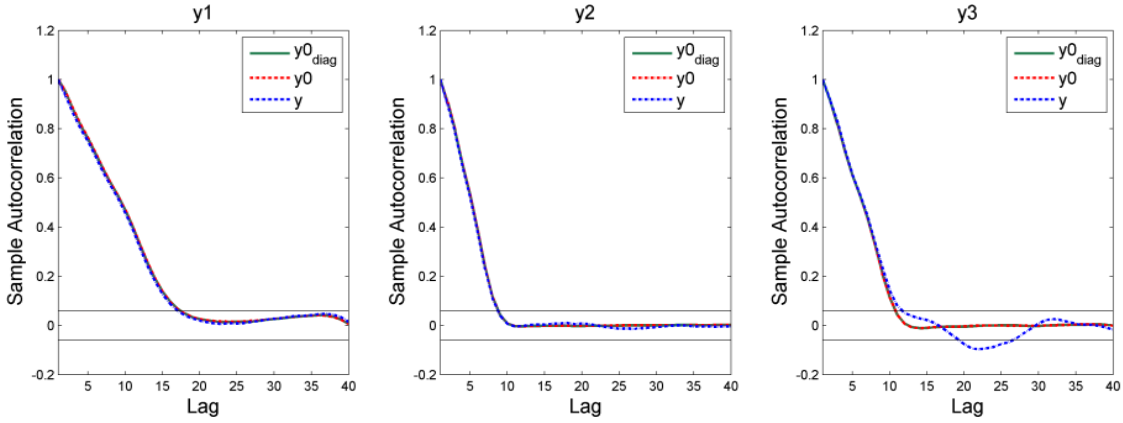

Figure 4.24: The Shell heavy oil fractionator case: ACF for Scenario 5

Table 4.9: The Shell heavy oil fractionator case: Indicators Results for Scenario 5

		$y1$	$y2$	$y3$
MQI=0.54	SSE	18.00	18.11	378.6
	$Ivar$	1.01	1.04	2.16
	$Ivar_{diag}$	1.01	1.04	2.16
	$iMQI$	0.87	0.88	0.70

Table 4.9 shows that the method indicates the existence of an impactful modeling problem in $y3$, because SSE_{y3} is large and $Ivar_{y3} > 1$. This modeling problem only

affects $y3$, since variance indexes ($Ivar$) of $y1$ and $y2$ are near to one. The difference between the ACF of $y3_0$ and $y3$ (Figure 4.24) indicates that the modeling problem causes oscillation in this variable.

The Sun *et al.* (2013) captures the existence of MPM by the small value of MQI. The $iMQI$ interpretation is compatible with the $Ivar_{diag}$, such that are higher than 0.8 in the controlled variables without modeling errors ($y1$ and $y2$) and 0.70 for $y3$.

Scenario 6: Unmeasured disturbance in $y2$ make the system oscillatory

In this scenario an unmeasured disturbance added in the signal $y2$. Figure 4.25 presents the disturbance and Figure 4.26 the inputs and outputs of this scenario, showing that all the output variables have performance problem. Table 4.10 and Figure 4.27 present the model assessment results.

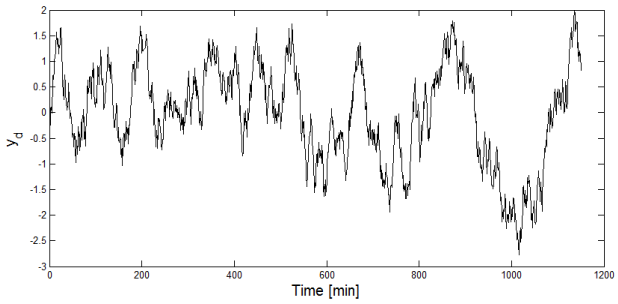

Figure 4.25: The Shell heavy oil fractionator case: Unmeasured Disturbance Added in $y2$ for Scenario 6

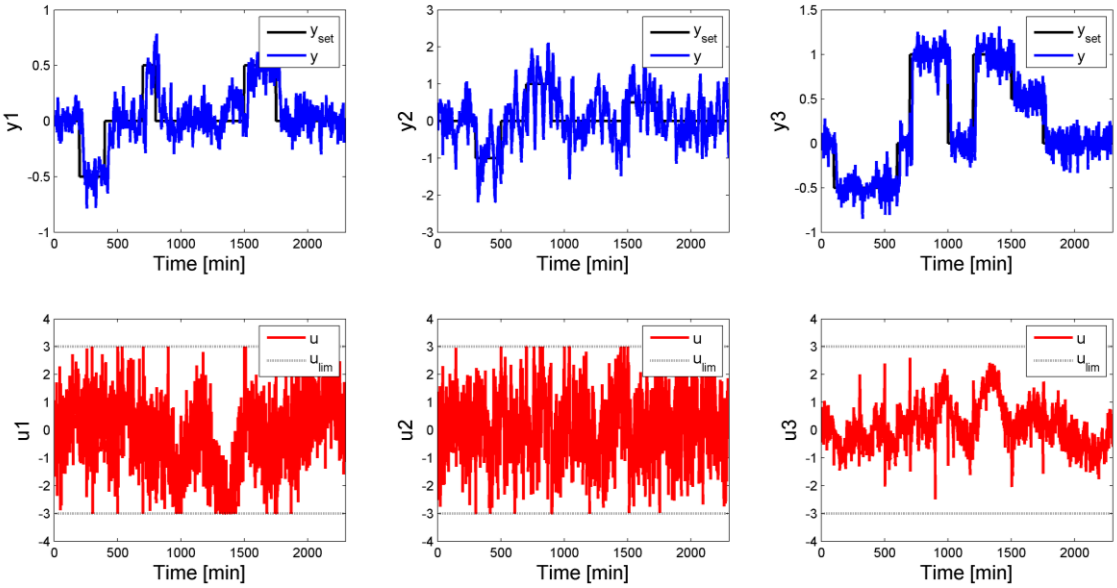

Figure 4.26: The Shell heavy oil fractionator case: Inputs and outputs of Scenario 6

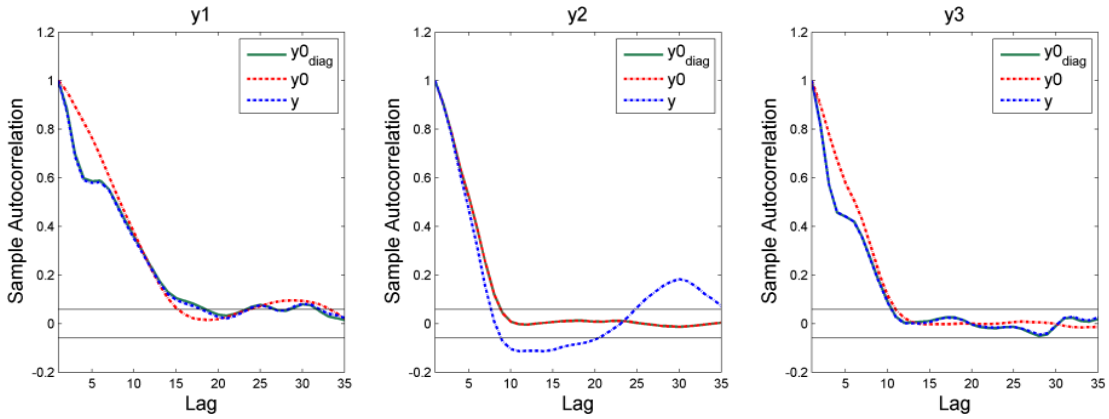

Figure 4.27: The Shell heavy oil fractionator case: ACF for Scenario 6

Table 4.10: The Shell heavy oil fractionator case: Indicators Results for Scenario 6

		$y1$	$y2$	$y3$
MQI=0.49	SSE	18.39	1063	18.93
	$Ivar$	1.30	10.1	1.28
	$Ivar_{diag}$	1.02	10.07	1.02
	$iMQI$	0.98	0.69	0.98

Results of Table 4.10 indicate that a modeling problem is impacting in all system variables, because the $Ivar$ of all outputs are different from 1. The modeling problem is only in $y2$ since this is the only variable with $Ivar_{diag}$ far from one. The ACF (Figure 4.27) makes evident that the oscillatory behavior of outputs come from a modeling problem, since ACF(y) have oscillatory behavior and ACF($y_{0_{diag}}$) do not oscillate significantly in all outputs. The modeling problem is in $y2$ because $y2_{0_{diag}} \cong y2_0 \neq y2$.

The Sun *et al.* (2013) captures the existence of MPM by the small value of MQI. The $iMQI$ interpretation is compatible with the $Ivar_{diag}$, such that are higher than 0.8 in the controlled variables without modeling errors ($y1$ and $y3$) and 0.69 for $y2$.

Scenario 7: Scenario 2 + Scenario 5

This scenario combines a model-plant mismatch in the pair $y2\ X\ u1$ (equation 4.20) with an unmeasured disturbance added in $y3$ (Figure 4.22). Figure 4.28 presents the inputs and outputs of this scenario, showing that all outputs have strong performance problems. Table 4.11 and Figure 4.29 present the model assessment results for the scenario.

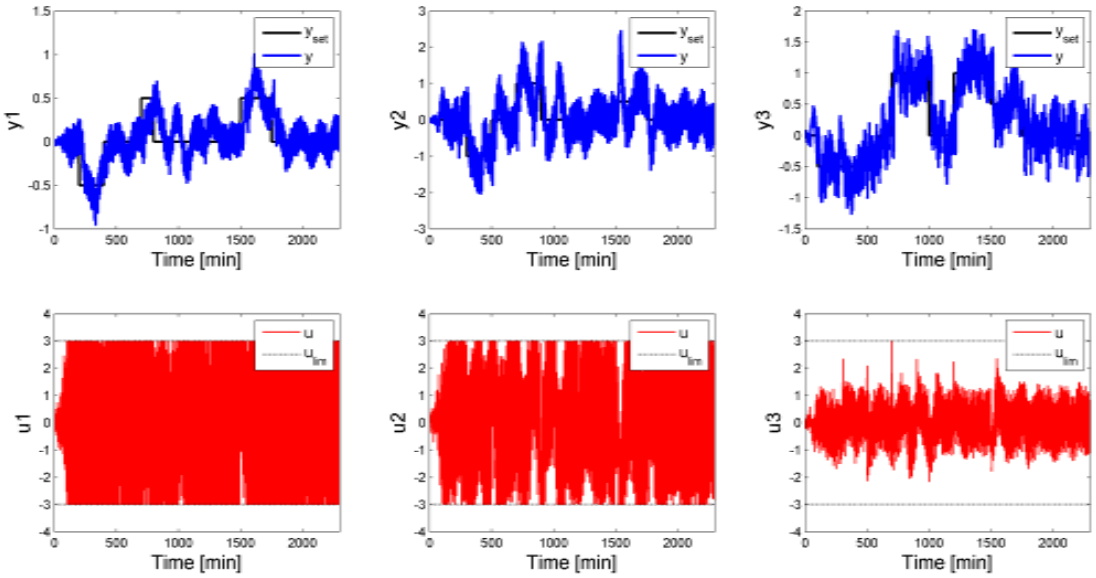

Figure 4.28: The Shell heavy oil fractionator case: Inputs and outputs of Scenario 7

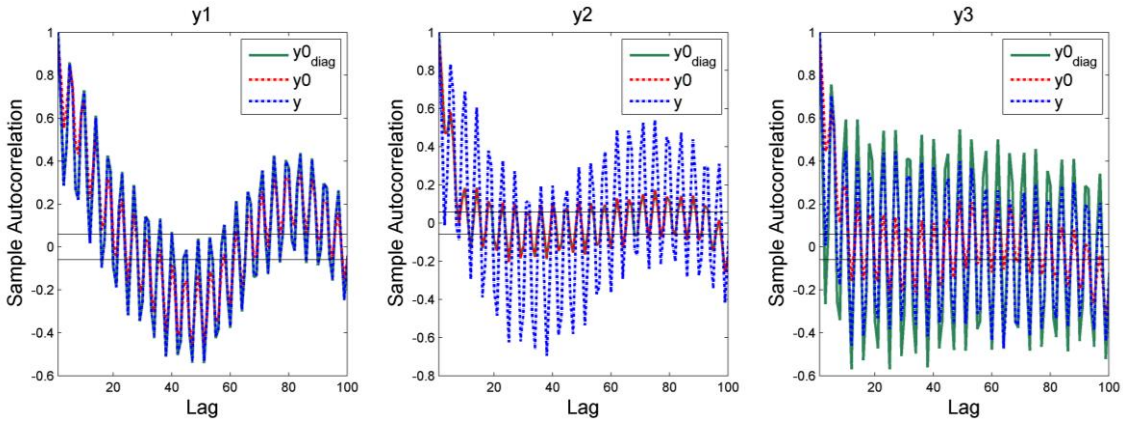

Figure 4.29: The Shell heavy oil fractionator case: ACF of Scenario 7

Table 4.11: The Shell heavy oil fractionator case: Indicators Results for Scenario 7

		$y1$	$y2$	$y3$
MQI=0.04	SSE	18.68	929.3	397.4
	$Ivar$	1.26	12.96	2.94
	$Ivar_{diag}$	1.01	12.96	1.68
	$iMQI$	0.95	0.16	0.84

Table 4.11 shows that all variables are affected by modeling problems, since all $Ivar$ are different from 1. The model of $y1$ do not have problems, because $Ivar_{diag}$ of $y1$ is near to one. The $y2$ has modeling problems and its performance deterioration is exclusively due to a problem in its own model, since $Ivar_{diag} \cong Ivar$. $y3$ also has modeling problems, but part of its performance deterioration come from the problem in $y2$, because $Ivar_{diag} < Ivar$. The similar behavior between ACF($y1$) and ACF($y1_{0_{diag}}$)

as well as ACF($y2_{0_{diag}}$) and ACF($y2_0$) confirm the described conclusions, as illustrated by Figure 4.29.

The Sun *et al.* (2013) captures the existence of MPM by the small value of MQI. However, the method was incapable to detect the modeling problem in $y3$, showing a $iMQI$ smaller than 0.8 only for $y2$. The constraint activation of the inputs in some instants (see Figure 4.28) make the outputs loss the setpoint dependency (due to the loss of one degree of freedom). Since the estimation of the HORX model (equation 4.1) is setpoint dependent, the estimation of e^d is bad and make the method fail.

Scenario 8: Scenario 1 + Scenario 6

This scenario combines a model-plant mismatch in the pair $y1\ X\ u1$ (equation 4.19) with an unmeasured disturbance added in $y2$ (Figure 4.25). Figure 4.30 presents the inputs and outputs of this scenario, showing that all outputs have performance problems. Table 4.12 and Figure 4.31 present the model assessment results for the scenario.

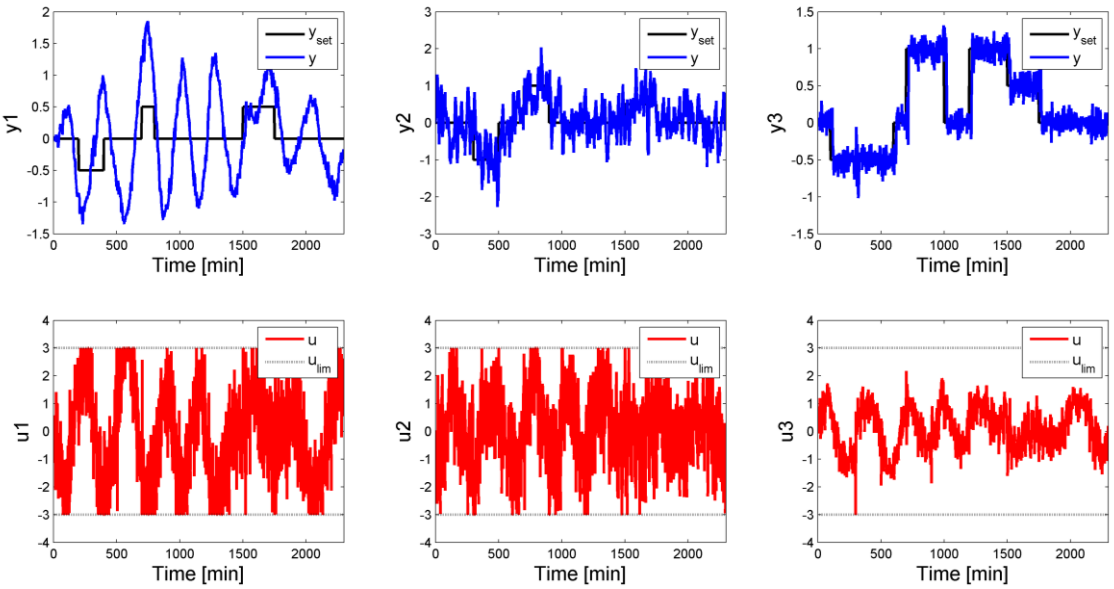

Figure 4.30: The Shell heavy oil fractionator case: Inputs and output for Scenario 8

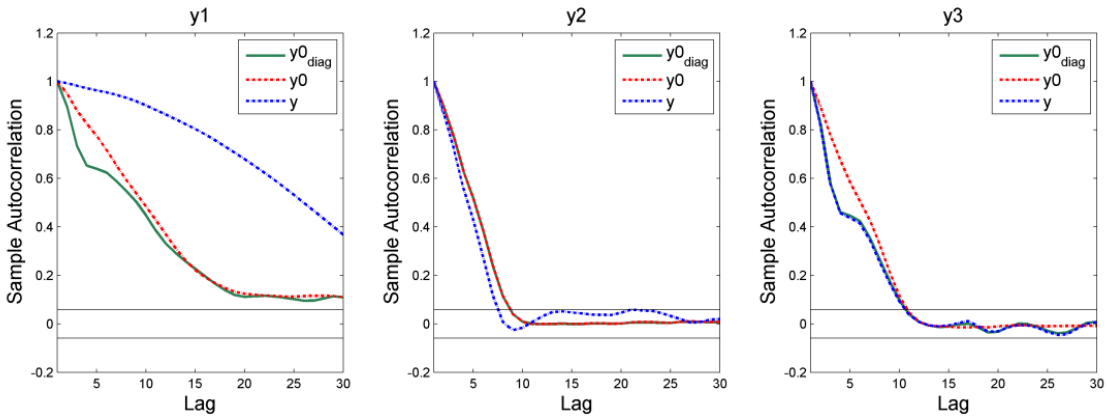

Figure 4.31: The Shell heavy oil fractionator case: ACF for Scenario 8

Table 4.12: The Shell heavy oil fractionator case: Indicators Results for Scenario 8

		$y1$	$y2$	$y3$
MQI=0.49	SSE	734.8	778,7	17.99
	$Ivar$	10.41	8.85	1.32
	$Ivar_{diag}$	8.83	8.85	1.00
	$iMQI$	0.86	0.69	0.98

Table 4.12 shows that all variables are affected by modeling problems, since all $Ivar$ are different from 1. The model of $y3$ does not have problems, because $Ivar_{diag}$ of $y3$ is near to one. The $y2$ have modeling problems and it performance deterioration is exclusively due to a problem in its own model, since $Ivar_{diag} \cong Ivar$. $y1$ also has modeling problems, but part of its performance deterioration comes from the problem in $y2$, because $Ivar_{diag} < Ivar$. The similar behavior between ACF($y3$) and ACF($y3_{0_{diag}}$) as well ACF($y2_{0_{diag}}$) and ACF($y2_0$) confirm the described conclusions, as illustrated by Figure 4.31.

Similarly to the previous scenario, the Sun *et al.* (2013) captures the existence of MPM by the small value of MQI. However, the method was incapable to detect the modeling problem in $y1$, showing a $iMQI$ smaller than 0.8 only for $y2$.

4.4 Conclusions

In this paper, an extension of the methodology proposed by Botelho et *al.* (2015a/cap. 3) is introduced, whose main contribution is to detect the location and the source of modeling problems and investigate how it impacts in all the process, for highly coupled systems. We propose the estimation of the nominal outputs and residuals considering only the diagonal elements of sensitivity matrix and the comparative evaluation with the conventional approach.

The method was compared with Sun *et al.* (2013) through two case studies: a high purity distillation column and The Shell heavy oil fractionator. Several scenarios were performed, containing MPM and/or unmeasured disturbances and bad tuning. The results show that the method is capable to precisely detect the presence of modeling problems in all considered cases, indicating the interaction effect caused by this problems and diagnosis the root. The results are superior of Sun *et al.* (2013), since this method fail when more than one modeling problem is present and input constraint activation occurs.

Capítulo 5 – **Diagnosis of poor performance in model predictive controllers: Unmeasured Disturbance versus Model-Plant Mismatch**

Abstract[7]**:** Poor model quality in model predictive controller (MPC) is often an important source of performance degradation. A key issue in MPC model assessment is to identify whether the bad performance comes from model-plant mismatches (MPM) or unmeasured disturbances (UD). This paper proposes a method for distinguishing between such degradation sources, where the main idea is to compare the statistical distribution of the estimated nominal outputs with the actual modeling error. The proposed approach relies on the assessment of three case studies: a simple SISO Linear MPC and two multivariable cases, where the linear controller is subject to a linear and nonlinear plant, respectively. Results show that the proposed method provides a good indicator of the model degradation source, even when both effects are present but one of them is dominant.

Keywords: model predictive control, model-plant mismatch, unmeasured disturbance, model quality assessment

---

[7] *Submetido para publicação no periódico "Industrial & Engineering Chemistry Research".*

5.1 Introduction

Model predictive controllers (MPCs) are the standard solution of the supervisory control layer, since they can work with multivariable complex dynamic systems. The MPC uses a dynamic process model to predict the behavior of controlled variables (CVs) along the future horizon, based on past control actions and disturbances. From this result, an optimization algorithm calculates the control actions that lead the process toward its optimal trajectory, respecting the constraints. The maintenance of MPC is an important and challenging problem, since performance degradation may stem from many different sources, such as: bad tuning (control and prediction horizon, weighting matrices, sampling time, etc.), poor model quality, poor disturbance rejection, and inappropriate constraint setup (Sun *et al.,* 2013). Among all these sources, poor model quality is the most frequent and impactful. Considering that a model is an abstraction of the real system behavior, modeling inconsistences will always be present. However, sometimes these inconsistences are so strong that the closed loop cannot achieve good performance. Therefore, it is necessary to quantify the modeling error, which cannot be compensated by feedback controller and, therefore, will deteriorate the corresponding closed loop behavior (Wang *et al.*, 2012).

Several methods are focused on model quality investigation. Some of them are based on model validation metrics and investigate the need for a model re-identification (e.g., Huang *et al.*,2003; Conner & Seborg,2005; Jiang *et al.*,2012). Other approaches (e.g., Badwe *et al.,*2009; Kano *et al.*, 2010; Ji *et al.*, 2012) are focused on identifying which portion of the model (i.e. controlled variable or pair-controlled versus manipulated variable) is degraded.

A key issue of MPC model assessment is to identify the source of a modeling inconsistency, which could be a model-plant mismatch (MPM) or an unmeasured disturbance (UD). The first occurs when the model cannot adequately describe the relations between its input and output variables and a re-identification is required. An UD is characterized by the absence of an input variable in the process model. Both cause similar effects in the process and isolating each effect is not trivial.

Several methods for disturbance detection were proposed. Tornhill & Horch (2007) provide an overview of the most important. According to their work, different approaches are needed depending on whether the disturbance is oscillating or non-oscillating. For the first case, the methods fall into three main classes, namely those which use the time domain, those using auto-covariance functions, and spectral peak detection. Most of the methods are off-line and exploit these advantages, such as the use of the entire data history. In the case of non-oscillatory, spectral decomposition methods as principal component analysis (PCA), independent component analysis (ICA), and non-negative matrix factorization (NNMF) have been used to find significant spectral features.

This paper proposed a new data-based approach for MPC model assessment. The method complements an extensive class and techniques available in literature (e.g., Schafer & Cinar, 2004; Badwe *et al.*, 2010; Sun *et al.*,2013; Botelho *et al.*, 2015/cap.3; Botelho *et al.*, 2015/cap.4), which detect lack of quality in the prediction model. Once an unconformity between the model prediction and the actual outputs is detected, it is necessary to diagnosis its causes, which can be related to MPM and/or UD. Here, we

propose a statistical approach to identify whether the performance degradation is related to MPM or UD.

5.2 Proposed method

The proposed method is based on the statistical comparison between the system outputs in the absence of MPM and UD (called nominal output) and the error between this value and actual outputs. The next sections describe the fundamental concepts of the proposed approach.

5.2.1 Estimation of nominal outputs

The first step in our approach consists of the nominal output estimation following the method proposed by Botelho *et al.* (2015*a*/cap. 3*)* and Botelho *et al.* (2015b/cap. 4*)*. We assume the control loops illustrated in Figure 5.1, with a MPC controller C and nominal model G_0, which is used in the MPC to describe the real plant G. The model-plant mismatch (MPM) magnitude is ΔG. The theoretical system without mismatch is shown in Figure 5.1a, for which nominal closed-loop outputs are y_0. T_0 is the nominal complementary sensitivity function. The real system, in a scenario subject to MPM, is shown in Figure 5.1b, where y_{set} corresponds to the setpoints, u are the manipulated variables, y are the measured outputs, y_{sim} are the simulated outputs of the nominal model perturbed by the actual control actions u, and T is the actual complementary sensitivity function. Figure 5.1c illustrates the case with an unmeasured disturbance (UD), where v is a sequence of independent random variables, G_d is the unknown disturbance model, and y_d are the disturbance signals.

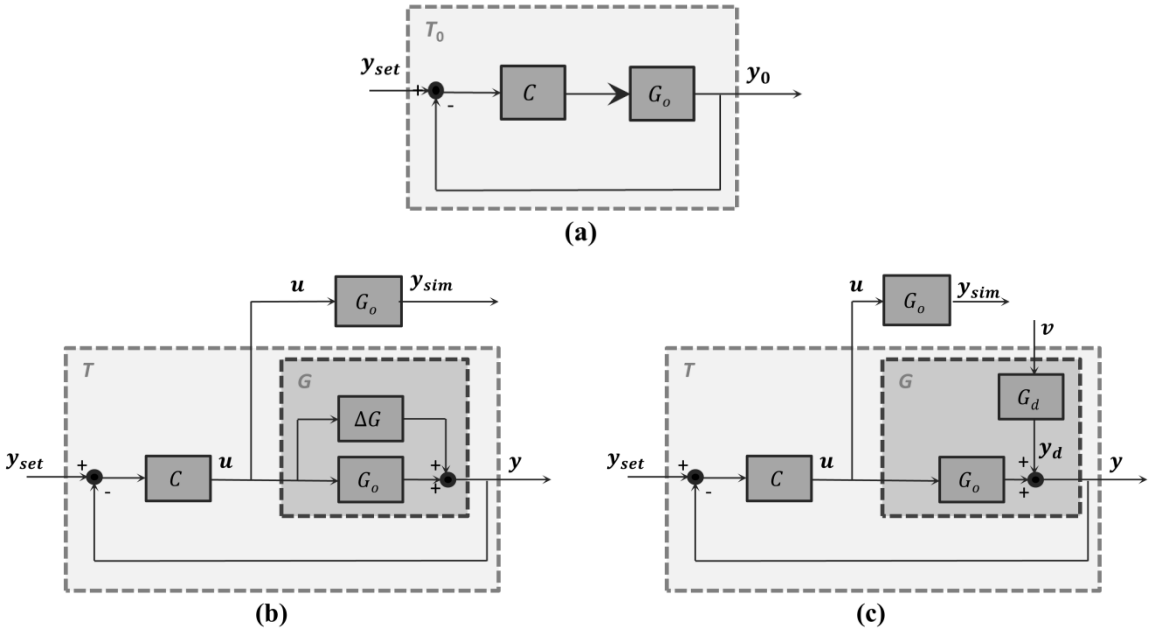

Figure 5.1: Schematic diagram of closed-loop (a) nominal case, (b) system with model-plant mismatch (MPM), and (c) system with unmeasured disturbance (UD)

Botelho et al. (2015a/cap. 3) define the nominal output (y_0) as the output of the system in the absence of MPM or UD. This can be estimated according to:

$$y_0 = S_0\,(y_{sim} - y) + y \tag{5.1}$$

S_0 is the nominal sensitivity funcion, given by:

$$S_0 + T_0 = I \tag{5.2}$$

The nominal sensitivity function (S_0) is a square transfer matrix that characterizes the system response in closed loop. Its dimensions are equal to the number of outputs. The diagonal elements ($S_{0_{diag}}$) give the closed-loop behavior of the outputs when their references (setpoints or soft constraints) are changed. The remaining elements provide the impact of these reference variations on the other outputs. Thus, Botelho et al. (2015b/cap. 4) suggest the estimation of the nominal output considering only the diagonal sensitivity function ($y_{0_{diag}}$) to locate the controlled variable (CV) with model errors. For this case, equation (5.1) can be rewritten as:

$$y_{0_{diag}} = S_{0_{diag}} (y_{sim} - y) + y \tag{5.3}$$

$S_{0_{diag}}$ produces a softening effect on the simulation residuals ($y_{sim} - y$) and retains only the part not removed by the controller feedback that is impacting the performance of the corresponding output. Thus, CVs without significant MPM or UD will have $y_{0_{diag}} \cong y$, because their simulation errors are close to zero. S_0 provides the complete diagnosis of the model, showing the effect of the MPMs or UDs in the corresponding output as well as how it is propagating onto the others. Thus $y_0 \neq y$ even for variables without significant MPM or UD, considering the existence of MPM or UD in another CV model. The stronger the coupling between the channels, the larger the difference between y_0 e y.

5.2.2 Relation between nominal outputs and modeling errors

According to Botelho *et al.* (2015a/cap. 3), y_0 is the estimated output free from modeling errors, which includes model-plant mismatches and unmeasured disturbances. Defining the nominal error e_0 as the effect of the modeling problems in the loop, we have:

$$e_0 = y_0 - y \tag{5.4}$$

The outputs of a system with MPM and UD are (Skogestad & Postlethwaite, 1996):

$$y = Ty_{set} + Sy_d \tag{5.5}$$

were y_d is the disturbance signal entering in the loop. First, let us consider a system under a model-plant mismatch only (Figure 5.1b). In this case, $y_d = 0$ and equation 5.5 is reduced to:

$$y = Ty_{set} \tag{5.6}$$

Analogously, the nominal output is (see Figure 5.1a):

$$y_0 = T_0 y_{set} \tag{5.7}$$

and equation 5.4 becomes:

$$e_0 = (T_0 - T)\, y_{set} = \Delta T y_{set} \tag{5.8}$$

From (5.7) and (5.8) we can observe that the relation between the nominal error (e_0) and nominal output (y_0) in the presence of model-plant mismatch are a function of the same input signal (i.e., y_{set}) passing through two different functions (ΔT and T_0). Although these functions are different, T and T_0 are functions of C, making them dependent. Therefore, the statistical behavior of e_0 and y_0 are correlated.

Now, let us consider a system under unmeasured disturbance only (Figure 5.1c). In this case, $G = G_0$, so $T = T_0$ and $S = S_0$. Then the measured output could be written as:

$$y = T_0 y_{set} + S_0 y_d \tag{5.9}$$

And the nominal error is:

$$e_0 = T_0 y_{set} - (T_0 y_{set} + S_0 y_d) = - S_0 y_d \tag{5.10}$$

From (5.7) and (5.10) we can observe that the relation between the nominal error (e_0) and nominal output (y_0) in the presence of unmeasured disturbance is given by two independent signals (y_{set} and y_d) passing through a "single function" (and its complementary, i.e., T_0 and $-S_0$), which means that the variations of e_0 and y_0 will also be independent.

In sum, when a process output is under a MPM, the control objectives (y_{set}) are the only signals showing that e_0 and y_0 are dependent, which explains why their variation have similarities. However, when a process output is under UD, e_0 will be dependent solely on the external signal y_d, while y_0 is dependent solely on the control objectives. This means that the variation of y_0 and e_0 do not bear resemblance. Therefore, considering that the process is sufficient excited, the similarity between the variations of y_0 and e_0 are indicative of MPM presence.

Remark 1:

Although the premise of the method is the evaluation of similarity between e_0 and y_0, the direct application of Person correlation is not ideal to compare them because both signals are estimated through T_0 (see equations 5.7, 5.8, and 5.10). This means that the correlation tends to be high in the presence of any MPM, even when its impact is negligible compared to an UD present in the same output. Since most real processes have MPM, its influence will mask the effect of UD, even when the importance is high. Then, we proposed the comparison of the statistical distribution along a moving window, which will be described below.

Remark 2:

Taking into account that the objective is to know the MPMs and UDs contained in each output, it is more appropriate to compare $y_{0_{diag}}$ (equation 5.3) and $e_{0_{diag}}$, since they capture the isolated effect of each de modeling error, disregarding the effects of interaction between the CVs (see Botelho *et al.*, 2015b/cap. 4). The $e_{0_{diag}}$ is defined by:

$$e_{0_{diag}} = y_{0_{diag}} - y \tag{5.11}$$

Thus, using $y_{0_{diag}}$ and $e_{0_{diag}}$, it is possible to locate the modeling problem in each output.

5.2.3 *Statistical Distribution in a Moving Window*

Our proposed diagnosis procedure to distinguish between model-plant mismatches and unmeasured disturbances consists in a comparative analysis of the statistical distributions. A moving window (MW) is defined and the statistical distribution of $e_{0_{diag}}$ and $y_{0_{diag}}$ is determined for each subset. Figure 5.2 illustrates the procedure, where Ts is the sampling time.

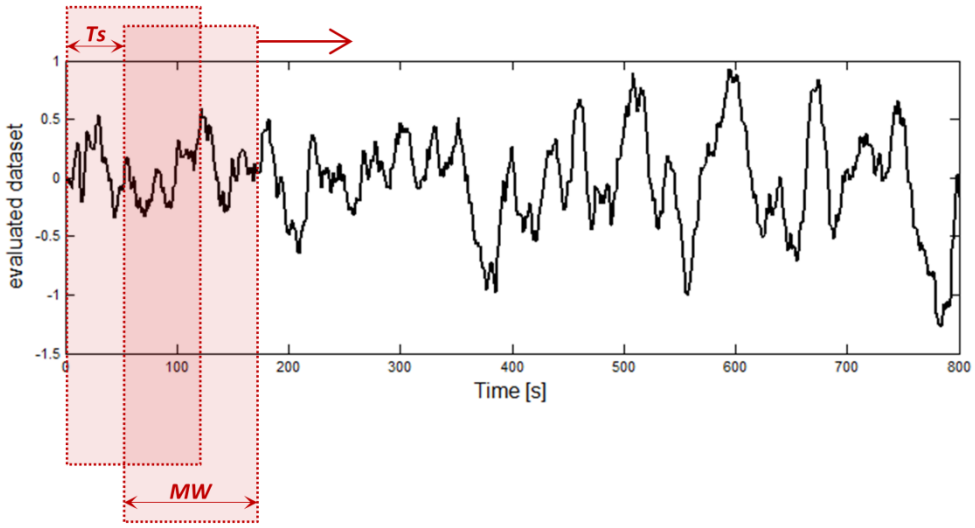

Figure 5.2: Illustration of a moving window evaluation procedure

The statistical distribution is evaluated by the skewness (skn) and kurtosis (kts) coefficients. These indexes show how far the signal is from a normal distribution. It is important to note that the data is seldom normally distributed, so we consider these indicators merely as a reference.

The kurtosis coefficient (kts) provides the shape of the probability density function. A high value of kurtosis means that the data has a large number of observations far from the mean, when compared with a normal distribution. The sample skewness (skn) provides an indicator of how asymmetric the dataset is. A positive value of skewness means that there is a higher concentration of values smaller than the mean (Adams & Lawrence, 2015). These coefficients are calculated as follows:

$$kts_{Xi}^{MW} = \frac{m_3}{\left(\sqrt{m_3}\right)^3} \tag{5.12}$$

$$skn_{Xi}^{MW} = \frac{m_4}{\left(\sqrt{m_2}\right)^4} \tag{5.13}$$

where m_2, m_3, and m_4 are the second, third, and fourth order central moment, defined as:

$$m_l = \frac{\sum_{i=1}^{MW}(X_i - \bar{X})^l}{MW}, l = 2,3,4 \tag{5.14}$$

Where X_i is the evaluated dataset ($y_{0_{diag}}$ or $e_{0_{diag}}$) and $\bar{X}$ is its corresponding mean value. Figures 5.3 and 5.4 illustrate the expected result for a hypothetical case. When a MPM is present, the variation of statistical distributions of $e_{0_{diag}}$ and $y_{0_{diag}}$ shows the major variation at the same time (see the peaks), which does not occur when a UD is present.

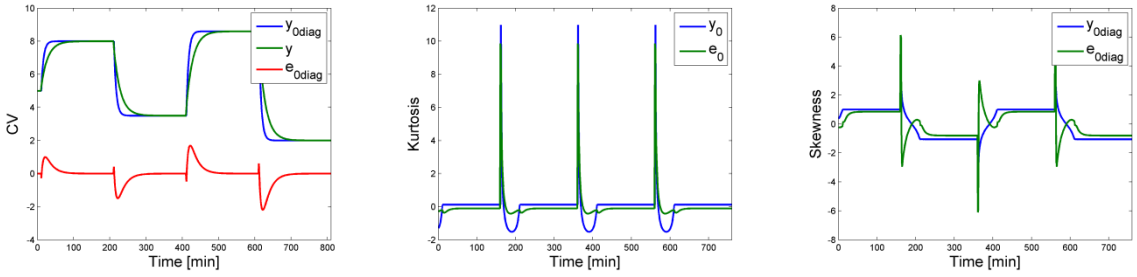

(a) **(b)** **(c)**

Figure 5.3: Hypothetical case with MPM: (a) measured y, estimated $y_{0_{diag}}$, and $e_{0_{diag}}$; (b) kurtosis coefficients along a moving window; and (c) skewness coefficients along a moving window

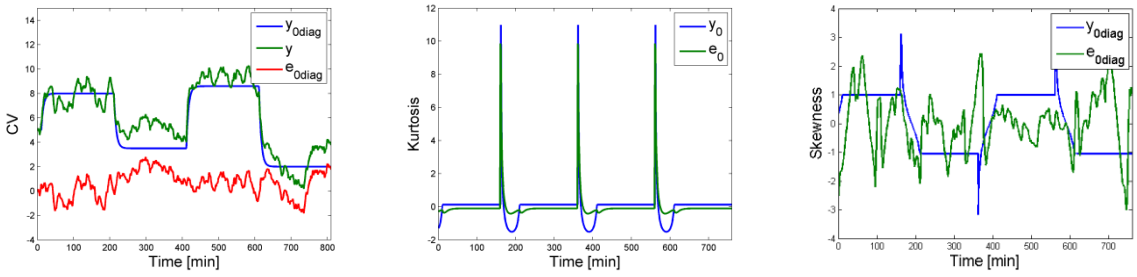

(a) **(b)** **(c)**

Figure 5.4: Hypothetical case with UD: (a) measured y, estimated $y_{0_{diag}}$ and $e_{0_{diag}}$; (b) kurtosis coefficients along a moving window; and (c) skewness coefficients along a moving window

5.2.4 Diagnosis Procedure

As described in section 5.2.2, the diagnosis of MPM and UD is grounded on the comparison of the nominal output and corresponding nominal error. Two approaches based on the data scatter are considered for quantifying the relation between the variations of the statistical distributions. The first one is based on the Pearson correlation coefficients of skewness and kurtosis of $e_{0_{diag}}$ and $y_{0_{diag}}$ signals. A scan is performed varying MW size in the neighborhood of the prediction horizon (we suggest from $0.5ph$ to $2ph$, where ph is the MPC's prediction horizon). This scan is necessary to ensure that all the inconsistencies in the work frequency of MPC will be considered. The correlation indicator (co_Z) is based on the mean of absolute correlation between the statistical distributions:

$$co_Z = \frac{\sum_{MW=0.5ph}^{2ph} \left| corr\left(Z_{e_{0_{diag}}}^{MW}, Z_{y_{0_{diag}}}^{MW}\right) \right|}{n_{MW}} \tag{5.15}$$

where n_{MW} is the number of scanned MW, $corr$ is the Pearson correlation coefficient, and Z is the evaluated coefficient (kts or skn). With the increase in the co_Z, higher is the probability of a model-plant mismatch dominance.

Another similar procedure is based on confidence ellipse scatter. A scan is performed varying MW size in the neighborhood of the prediction horizon and for each evaluated MW the ellipses are constructed considering the covariance matrix of $\left(Z_{e_{0_{diag}}}^{MW}\right) x \left(Z_{y_{0_{diag}}}^{MW}\right)$, where Z is the evaluated coefficient (kts or skn). The angle of the largest eigenvalue corresponds to the ellipse inclination (α_z^{MW}). The ellipse's major axis (a_z^{MW}) and minor axis (b_z^{MW}) are given, respectively, by the square root of the largest and the lowest eigenvalues multiplied by the critical chi-square value ($\chi_{\text{crit}}{}^2$) associated with a given probability level (Santos-Fernadéz, 2012). Figure 5.5 illustrates the expected behavior for each scenario: the confidence ellipse is less circular (i.e., the greater is a_z^{MW}/b_z^{MW}) and more diagonal (the nearest to $\pi/4$ is a_z^{MW}) when the similarity between statistical distributions is more significant, indicating the presence of a model-plant mismatch.

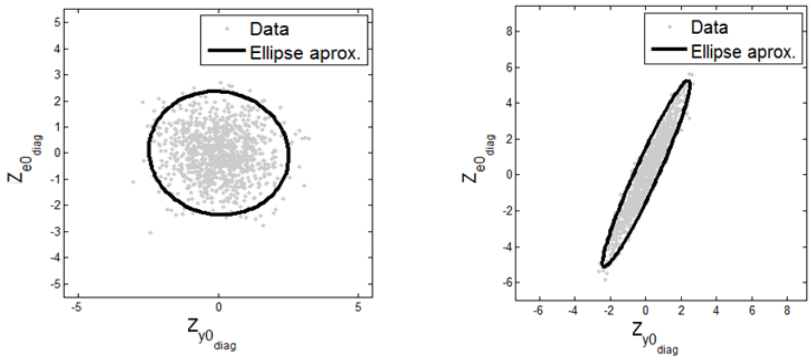

(a) **(b)**

Figure 5.5: Expected response of linear and elliptical approximation (a) under UD and (b) under MPM

The indicators based on the ellipse angle ($\bar{\alpha}_Z$) and ellipse dimensions ratio ($\overline{DR}_Z$) are based on the mean of the resulting ellipses:

$$\bar{\alpha}_Z = \sum_{MW=0.5ph}^{2ph} (\alpha_z^{MW}) \tag{5.16}$$

$$\overline{DR}_Z = \sum_{MW=0.5ph}^{2ph} \left(\frac{a_z^{MW}}{b_z^{MW}}\right) \tag{5.17}$$

The confidence ellipse indicator (ce_Z), which considers simultaneously the shape and the inclination of the ellipse is defined below:

$$ce_Z = \frac{\sum_{MW=0.5ph}^{2ph} \left(\frac{4\alpha_z^{MW}}{\pi} \sqrt{1 - \frac{b_z^{MW}}{a_z^{MW}}} \right)}{n_{MW}} \tag{5.18}$$

where n_{MW} are the numbers of scanned MW. The α_z^{MW} must be reduced to half of the first quadrant (i.e., 0 <$\alpha_z^{MW} < \pi/4$) to calculate the indicator. Increasing values of ce_Z means a higher probability of a model-plant mismatch dominance.

To emphasize the differences between MPM and UD we also suggest quantifying the differentiated statistical distributions, since the derivatives are capable to better capture the tendency of the signals (Trierweiler & Machado, 2004). The indicators based on the derivative ellipse angle ($\bar{\alpha}_{dZ}$) and dimensions ratio ($\overline{DR}_{dZ}$), as well the correlation derivative indicator (co_{dZ}), and confidence ellipse derivative indicator (ce_{dZ}) are defined by:

$$\bar{\alpha}_{dZ}=\sum_{MW=0.5ph}^{2ph}(\alpha_{dz}^{MW}) \tag{5.19}$$

$$\overline{DR}_{dZ}=\sum_{MW=0.5ph}^{2ph}\left(\frac{a_{dz}^{MW}}{b_{dz}^{MW}}\right) \tag{5.20}$$

$$co_{dZ} = \frac{\sum_{MW=0.5ph}^{2ph}\left|corr\left(\frac{d}{dt}Z_{e_{0_{diag}}}^{MW},\frac{d}{dt}Z_{y_{0_{diag}}}^{MW}\right)\right|}{n_{MW}} \tag{5.21}$$

$$ce_{dZ} = \frac{\sum_{MW=0.5ph}^{2ph}\left(\frac{4\alpha_z^{MW}}{\pi}\sqrt{1-\frac{b_{dz}^{MW}}{a_{dz}^{MW}}}\right)}{n_{MW}} \tag{5.22}$$

where α_{dz}^{MW}, a_{dz}^{MW}, and b_{dZ}^{MW} are, respectively, the inclination, the major axis and the minor axis of the ellipses constructed considering the covariance matrix of $\left(\frac{d}{dt}Z_{e_{0_{diag}}}^{MW}\right)x\left(\frac{d}{dt}Z_{y_{0_{diag}}}^{MW}\right)$. According to our experience, after several tests considering the proposed method, if at least one of the indicators (kurtosis or skewness) is higher than 0.1, is indicative of MPM dominance.

5.3 Case Studies

5.3.1 Simple MPC SISO

This case study illustrates the method applied to a simple case study. A SISO MPC was configured in MATLAB™, whose tuning parameters of the controlled variable (CV) and manipulated variable (MV) are shown in Table 5.1. Three scenarios are evaluated. In the first (Scenario 1), there is a model-plant mismatch (MPM) and no unmeasured disturbance was considered. In the second (Scenario 2), the measured output is corrupted by an unmeasured disturbance (UD) and the plant model is perfect (i.e., the process behavior is equal to controller prediction model). The last scenario (Scenario 3), contains both MPM and UD. Table 5.2 shows the disturbance model Gd and the plant model, whose behaviors are shown in Figure 5.6.

Table 5.1: MPC SISO case: Tuning parameters of MPC

Sample Time	10s
Prediction Horizon	11
Control Horizon	3
CV weight	5500
Move suppression weight	3000
Controller Model	$G_0(s) = \frac{-100s + 3.04}{305s^2 + 40s + 1}$
MV lower variable limit	-10
MV upper variable limit	10

Table 5.2: MPC SISO case: Scenarios definitions

Unmeasured disturbance	$\frac{0.3s + 2}{100s^2 + 30s}$
Model-plant mismatch	$G(s) = \frac{-100s + 18.25}{305s^2 + 40s + 1}$

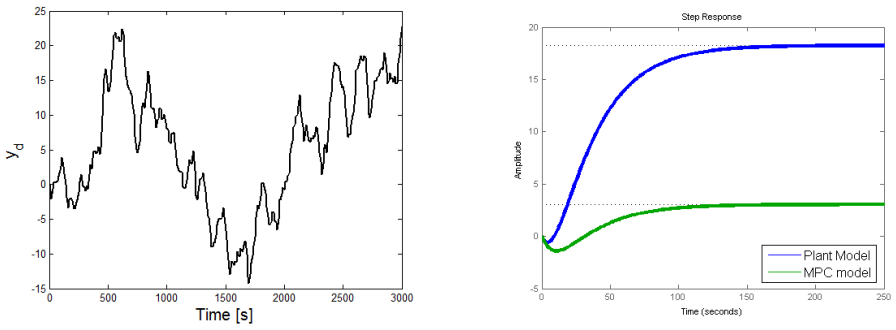

(a) **(b)**

Figure 5.6: MPC SISO case: (a) UD signal and (b) step response of plant model versus controller model

The scenarios described were simulated under perturbation of controlled variable setpoint (y_{set}), where two frequencies of excitation were considered in order to evaluate the dependency of method with the perturbation pattern. Figure 5.7 illustrates the performed perturbation and respective nominal signal (y_0), i.e., the output obtained without model-plant mismatch.

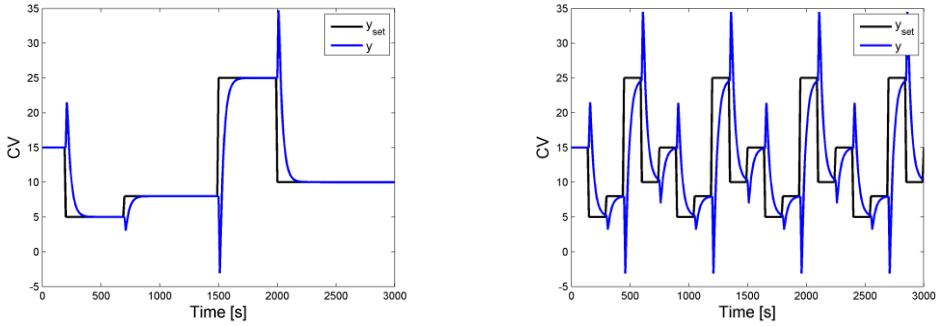

(a) less frequent setpoint changes **(b) more frequent setpoint changes**

Figure 5.7: MPC SISO case: Perturbations in the setpoint and respective nominal response

A white noise with mean 0 and standard deviation 2% of the variable range was added to the measured output. Data were generated for three considered scenarios and the proposed method was applied. The results of Scenarios 1, 2, and 3 with less frequent setpoint changes are presented in Figures 5.8, 5.9, and 5.10, respectively. To illustrate the method, the kurtosis derivative confidence ellipses were constructed for these scenarios considering the $MW = 11$ ($MW = ph$), as shown in Figure 5.11.

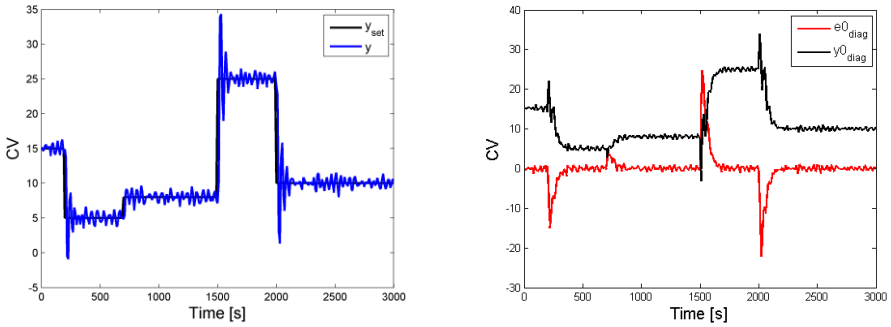

(a) **(b)**

Figure 5.8: MPC SISO case: (a) measured output (y) and (b) estimated $y_{0_{diag}}$ and $e_{0_{diag}}$ for Scenario 1 with less frequent setpoint changes

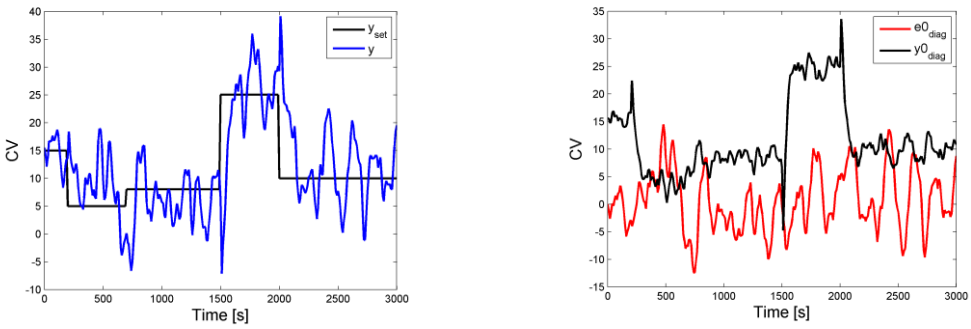

(a) **(b)**

Figure 5.9: MPC SISO case: (a) measured output (y) and (b) estimated $y_{0_{diag}}$ and $e_{0_{diag}}$ for Scenario 2 with less frequent setpoint changes

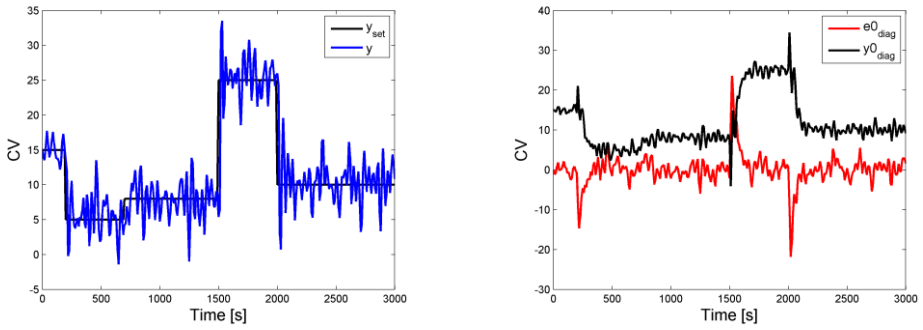

(a) **(b)**

Figure 5.10: MPC SISO case: (a) measured output (y) and (b) estimated $y_{0_{diag}}$ and $e_{0_{diag}}$ for Scenario 3 with less frequent setpoint changes

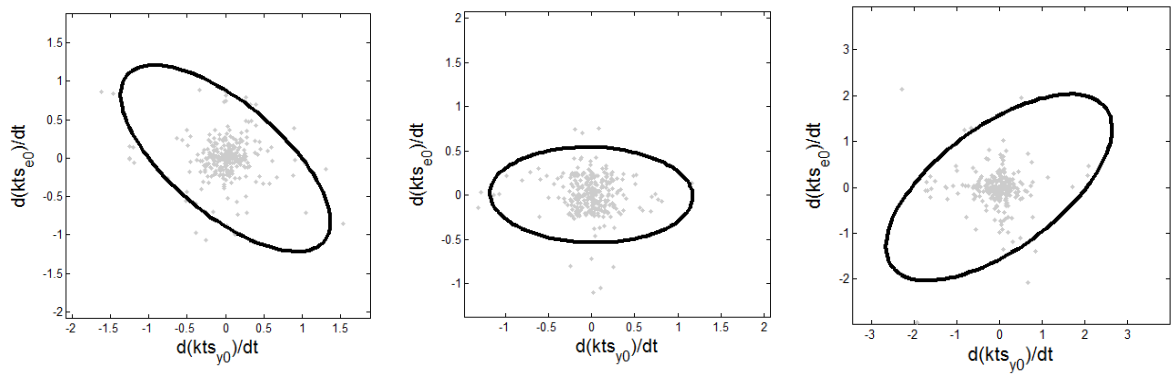

(a) **(b)** **(c)**

Figure 5.11: MPC SISO case: Kurtosis derivative confidence ellipses for (a) Scenario 1, (b) Scenario 2, and (c) Scenario 3 with less frequent setpoint changes

The comparison of Figures 5.8a and 5.9a with Figure 5.7 demonstrates that both scenarios cause changes in MPC performance. Figure 5.8b illustrates the dependence relation of $y0_{diag}$ and $e0_{diag}$ in case of MPM, since the peaks in the data occur at the same instant and have similar magnitudes. However, this behavior does not occur in presence of unmeasured disturbance (Figures 5.9b). For the scenario with MPM and UD (Figure 5.10), the effect of the model-plant mismatch is most significant. The ellipse shape (Figure 5.11) captures the dominant effect, since the shape tends to be more inclined with MPM dominance and to have a horizontal orientation when an UD is dominant.

We calculated the indices presented in section 5.2.4 considering a moving window size (MW) varying from 6 to 22 ($0.5ph$ to $2ph$). Tables 5.3 and 5.4 summarize the results.

Table 5.3: MPC SISO case: Indices calculated for scenarios with less frequent setpoint changes

		$\vartheta = Z$		$\vartheta = dZ$	
Scenario	***Indicator***	$Z = kts$	$Z = skn$	$Z = kts$	$Z = skn$
MPM (Scenario 1)	$\overline{\alpha}_{\vartheta}$	28.8	37.5	41.3	37.7
	$\overline{DR}_{\vartheta}$	0.50	0.52	0.52	0.56
	ce_{ϑ}	0.45	0.59	0.60	0.55
	co_{ϑ}	0.53	0.55	0.52	0.53
UD (Scenario 2)	$\overline{\alpha}_{\vartheta}$	9.1	20.9	3.40	7.19
	$\overline{DR}_{\vartheta}$	0.60	0.75	0.58	0.66
	ce_{ϑ}	0.08	0.20	0.03	0.07
	co_{ϑ}	0.06	0.12	0.03	0.05
MPM+UD (Scenario 3)	$\overline{\alpha}_{\vartheta}$	23.1	42.6	32.7	33.7
	$\overline{DR}_{\vartheta}$	0.52	0.53	0.56	0.53
	ce_{ϑ}	0.36	0.63	0.48	0.46
	co_{ϑ}	0.47	0.55	0.47	0.41

Table 5.4: MPC SISO case: Indices calculated for scenarios with more frequent setpoint changes

		$\vartheta = Z$		$\vartheta = dZ$	
Scenario	***Indicator***	$Z = kts$	$Z = skn$	$Z = kts$	$Z = skn$
MPM (Scenario 1)	$\bar{\alpha}_\vartheta$	29.4	36.2	40.7	36.8
	$\overline{DR}_\vartheta$	0.51	0.41	0.52	0.54
	ce_ϑ	0.46	0.63	0.60	0.57
	co_ϑ	0.51	0.70	0.56	0.54
UD (Scenario 2)	$\bar{\alpha}_\vartheta$	7.16	8.01	2.81	3.58
	$\overline{DR}_\vartheta$	0.53	0.65	0.51	0.57
	ce_ϑ	0.11	0.10	0.06	0.04
	co_ϑ	0.18	0.12	0.08	0.06
MPM+UD (Scenario 3)	$\bar{\alpha}_\vartheta$	23.6	34.1	40.9	36.0
	$\overline{DR}_\vartheta$	0.56	0.52	0.62	0.65
	ce_ϑ	0.55	0.56	0.56	0.49
	co_ϑ	0.43	0.38	0.45	0.40

Considering the kutosis and skewness evaluation, when the system is under a single model inconsistency (i.e., unmeaseured disturbance or model-plant mismatch) the use of the raw signal or its derivatives are capable to detect the source of the modeling problem. However, as expected, the indices based on derivatives can better capture the tendency of the modeling problem, showing sharper and clearer decision values and threshold for the cases with MPM or UD. For example, using the derived signals, the mean angles ($\bar{\alpha}_{dZ}$) do not exced 7.5° in Scenario 2 and are higher than 35° in Scenario 1. When the raw signals are considered, these limits ($\bar{\alpha}_Z$) are 21° and 28.5°. Similarly, ce_{dZ} and co_{dZ} are smaller than 0.08 in the presence of UD and higher than 0.53 in the presence of MPM, while the ce_Z and co_Z limits are 0.20 and 0.45.

When the system is under unmeasured disturbance and model-plant mismatch at the same time (Scenario 3), the method indicates the dominant effect of the MPM, because the indicators (co_ϑ and ce_ϑ) are higher than 0.35 and the angles ($\bar{\alpha}_\vartheta$) are higher than 23°. The results are analoguos in both cases of setpoint changes, which means that the method does not depend on a steady state condition in the dataset. In all cases, the ellipse dimension ($\overline{DR}_\vartheta$) does not provide any useful information when evaluated alone.

To illustrate a case with the dominanect of an UD, a new scenario was generated (Scenario 4), using the gain from the disturbance model (Table 5.2) five times higher. Figure 5.12 illustrates the results for the measurements and kurtosis confidence ellipses with $MW = 11$.

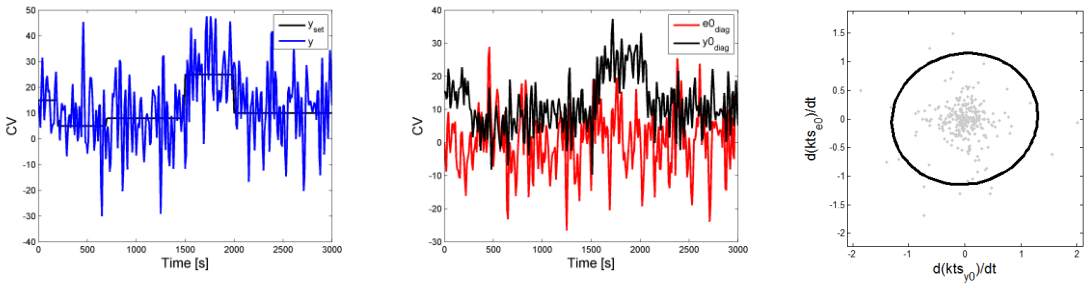

(a) **(b)** **(c)**

Figure 5.12: MPC SISO case: (a) measured output (y), (b) estimated $y0_{diag}$ and $e0_{diag}$, (c) kurtosis confidence ellipse for Scenario 4 with less frequent setpoint changes

The comparison of Figure 5.12a with Figure 5.7 highlights the fact that Scenario 4 cause changes in MPC performance. Figure 5.12b illustrates a small dependence relation between $y0_{diag}$ and $e0_{diag}$ and highlights the dominance of an UD. The circular tendency of the ellipses (Figure 5.12c) captures the dominant UD effect. Table 5.5 show the indexes described in section 5.2.4 for a moving window size (MW) varying between 6 and 22.

Table 5.5: MPC SISO case: Indices calculated for Scenario 4

		$\vartheta = Z$		$\vartheta = dZ$	
setpoint change	***Indicator***	$Z = kts$	$Z = skn$	$Z = kts$	$Z = skn$
Less frequent	$\overline{\alpha}_\vartheta$	37.4	27.9	17.7	13.4
	$\overline{DR}_\vartheta$	0.71	0.65	0.85	0.92
	ce_ϑ	0.44	0.35	0.12	0.08
	co_ϑ	0.32	0.34	0.06	0.03
More frequent	$\overline{\alpha}_\vartheta$	16.36	13.06	16.36	13.06
	$\overline{DR}_\vartheta$	0.76	0.80	0.83	0.88
	ce_ϑ	0.36	0.21	0.14	0.09
	co_ϑ	0.24	0.11	0.10	0.04

Table 5.5 shows that, for Scenario 4, the use of the derived signals generates superior results when compared with the use of the raw signals, since ce_{dZ} and co_{dZ} do not exceed 0.15 while ce_Z and co_Z reach values greater than 0.4, even with a dominant effect of UD (see Figure 5.12). Results also show that, although $\bar{\alpha}_{dZ}$ are high, the ellipses dimension rate $\overline{DR}_{dZ}$ is also high, denoting its circular trend. Therefore, it is necessary to evalute both dimensions for a correct diagnosis. Consequently, the analysis based on ce_{dZ} or co_{dZ} is simpler, conclusive, and relies on a direct comparison with the recommended threshold.

5.3.2 The Shell Heavy Oil Fractionator

The Shell Heavy Oil Fractionator is a problem originally presented by Prett & Morari (1987). The main feature of this process is the high coupling among all channels as well as large time delays. The fractionator is characterized by three product draws and three side pumparounds. The heat requirement of the column enters with the feed, which is a gaseous stream. Product specifications for the top and side draw streams are determined by economics and operating requirements. There is no product specification for the bottom draw, but there is an operating constraint on the temperature in the lower part of the column. The three circulating loops remove heat to achieve the desired product separation. Figure 5.13 illustrates the process.

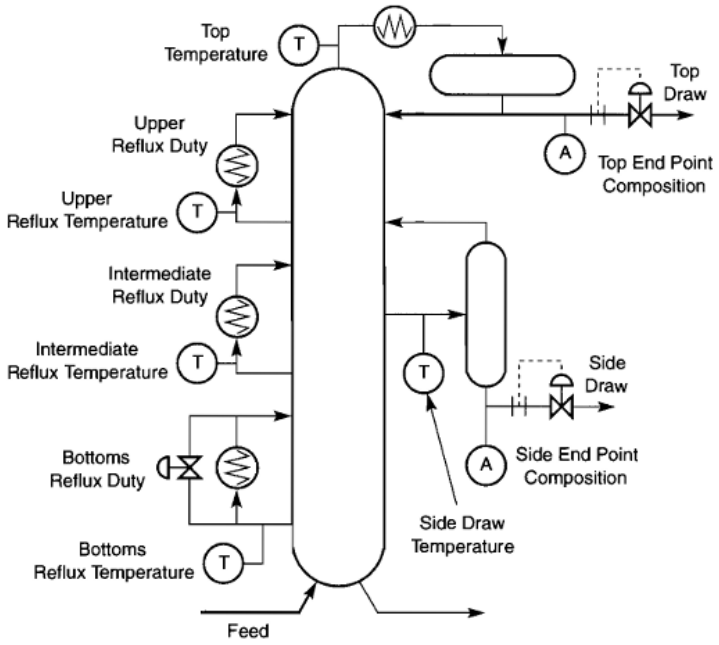

Figure 5.13: Schematic representation of Shell Heavy Oil Fractionator. (Maciejowski, 2002)

This system was implemented in *Matlab/Simulink* and a MPC was configured. The main objective was to control the top composition ($y1$), the side composition ($y2$), and the bottom reflux temperature ($y3$) in the respective setpoint by the manipulation of the top draw ($u1$), side draw ($u2$), and bottom reflux duty ($u3$). The process model (G_0) is given by:

$$G_0 = \begin{bmatrix} \frac{4.05}{50s+1}e^{-27} & \frac{1.77}{60s+1}e^{-28} & \frac{5.88}{50s+1}e^{-27} \\ \frac{5.39}{50s+1}e^{-18} & \frac{5.72}{60s+1}e^{-14} & \frac{6.9}{40s+1}e^{-15} \\ \frac{4.38}{33s+1}e^{-20} & \frac{4.42}{44s+1}e^{-22} & \frac{7.2}{19s+1}e^{-19} \end{bmatrix} \quad (5.23)$$

The tuning was set based on Farenzena (2008), whose parameters are presented in Table 5.6. Four MPMs are defined for $G_{0_{y1,u2}}$, which are shown in Figure 5.14. Four UD signals are also defined (Figure 5.15) and added in $y1$.

Table 5.6: Shell heavy oil fractionator case: Tuning Parameters of MPC

Sample Time	2 min
Prediction Horizon	20
Control Horizon	4
Controlled Variable Weight	$Q_{y1} = 1, Q_{y2} = 6, Q_{y3} = 2$
Move Suppression	$Q_{\Delta u1} = Q_{\Delta u2} = Q_{\Delta u3} = 0.2$

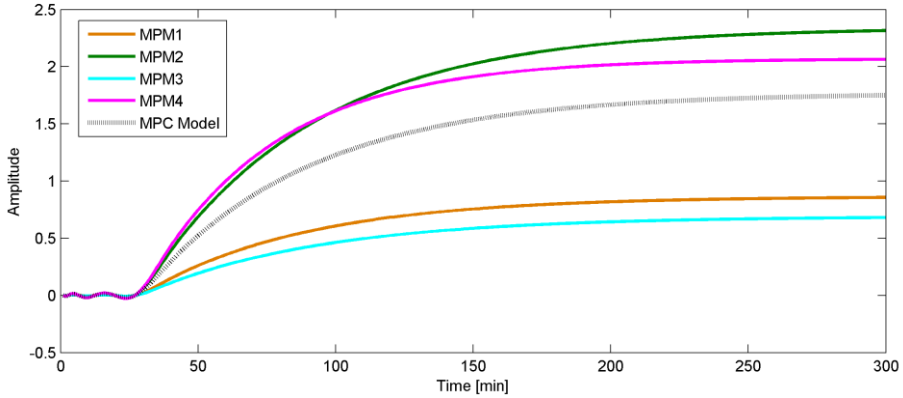

Figure 5.14: Shell heavy oil fractionator case: Step response of MPMs in $G_{0_{y1,u2}}$

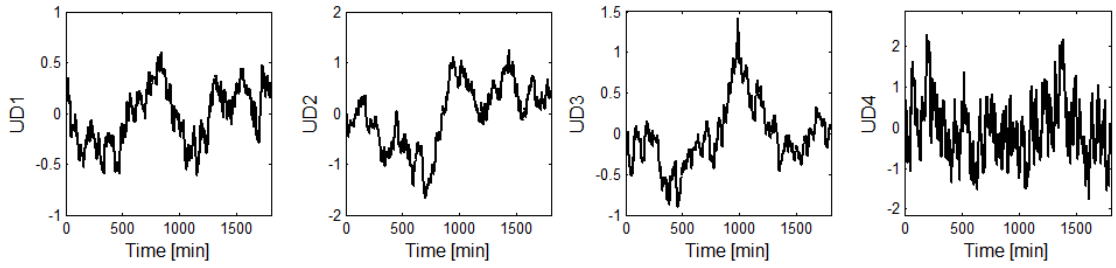

Figure 5.15: Shell heavy oil fractionator case: UD signals added in $y1$.

Figure 5.16 shows the setpoint perturbations used in the diagnosis procedure applied to the different scenarios containing MPMs and UDs. For the generated data, the indices

ce_{dZ} and co_{dZ} were calculated with moving windows (MW) varying from 10 to 40. Here, only the indices based on the derivatives were used, once they have shown a better result, as presented in section 5.3.1. Table 5.7 summarizes this analysis. The evaluation was performed only for $y1$ since the MPMs and UDs were only added in this CV.

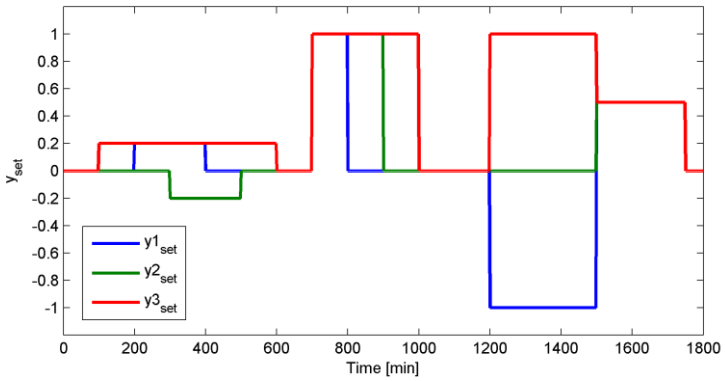

Figure 5.16: Shell heavy oil fractionator case: Perturbations in the setpoints.

Table 5.7: Shell heavy oil fractionator case: Indicators for Scenario containing MPM or UD in $y1$

	ce_{dkts}	ce_{dskn}	co_{dkts}	co_{dskn}
MPM1	0.03	0.10	0.11	0.22
MPM2	0.05	0.13	0.08	0.21
MPM3	0.21	0.43	0.36	0.52
MPM4	0.02	0.11	0.03	0.18
UD1	0.016	0.024	0.031	0.036
UD2	0.018	0.044	0.025	0.036
UD3	0.015	0.031	0.021	0.039
UD4	0.10	0.11	0.038	0.039

Results in Table 5.7 show that, for all evaluated cases, at least one of the statistical distributions indicates MPM when it was present. The highest ce_{dZ} for each scenario is superior to 0.1 when a MPM is present and does not exceed 0.05 when an unmeasured disturbance occurs, except for UD4, where $ce_{dskn} = 0.11$. The co_{dZ} works in all scenarios, indicating at least one co_{dZ} higher than 0.18 when a MPM is present and not exceeding 0.04 in cases with UD. Based on this evaluation, we can conclude that the co_{dZ} is more reliable than ce_{dZ}. Furthermore, the difference in the co_{dZ} between the cases with MPM and UD is higher, allowing an easier and more conclusive the interpretation. Moreover, for the success of the method, it is fundamental to evaluate both kurtosis and skewness. As the method is a statistical approach, it is not always possible to detect the similarities

between the statistical distributions for both coefficients. Thus, when more coefficients are evaluated, the greater the likelihood of finding the MPM effects.

We also simulated and applied the method to scenarios containing MPM and UD at the same time. To evaluate the method efficiency, we estimate the real dominant effect (MPM or UD) and compare the results with the corresponding co_{dZ} and ce_{dZ}. The real dominant effect is determined by comparison of the Variance Index (Botelho *et al.*, 2015a/cap. 3) of the data generated only with MPM, only with UD and with both. The Variance Index is defined as:

$$Ivar = \frac{var(y - y_{set})}{var(y_0 - y_{set})} \tag{5.24}$$

Thus, the $Ivar$ was calculated for the data generated only with MPM ($Ivar_{MPM}$) and only with UD ($Ivar_{UD}$). The results were compared with the Variance Index for the case with MPM+UD ($Ivar_{MPM+UD}$). The closer the $Ivar_{MPM}$ or $Ivar_{UD}$ of $Ivar_{MPM+UD}$, the higher the dominance of the corresponding effect. Table 5.8 shows the results. The evaluation was performed only for $y1$ since the MPMs and UDs were added in this CV.

Table 5.8: Shell heavy oil fractionator case: Indices for the scenarios containing MPM and UD in $y1$

	MPM1+UD1	**MPM2+UD2**	**MPM3+UD3**	**MPM4+UD4**
$\boldsymbol{Ivar_{MPM}}$	3.21	1.24	9.72	1.48
$\boldsymbol{Ivar_{UD}}$	1.19	2.67	1.25	3.02
$\boldsymbol{Ivar_{MPM+UD}}$	3.07	3.46	9.78	3.09
$\boldsymbol{ce_{dkts}}$	0.09	0.03	0.46	0.06
$\boldsymbol{ce_{dskn}}$	0.31	0.04	0.35	0.08
$\boldsymbol{co_{dkts}}$	0.16	0.04	0.58	0.03
$\boldsymbol{co_{dskn}}$	0.35	0.03	0.43	0.04

The results in Table 5.8 show that the method is capable to detect the dominant effect when both model-plant mismatches and unmeasured disturbances are occurring at the same time. For the case MPM1+UD1, the $Ivar_{MPM+UD}$ is nearest of $Ivar_{MPM}$, indicating that the MPM is dominant. The ce_{dskn} and co_{dskn} are equal to 0.31 and 0.35, respectively. For the case MPM4+UD4, the $Ivar_{MPM+UD}$ is nearest to $Ivar_{UD}$, indicating that the UD is dominant. The ce_{dskn} and co_{dskn} are equal to 0.08 and 0.04, respectively.

5.3.3 The Quadruple-Tank Process

This case study aims to illustrate the application of the method in a nonlinear plant. The system is composed of four cylindrical tanks connected according to Figure 5.17. Water is pumped into the tanks through the pumps with voltages $v1$ and $v2$. The flow of

each pump is split up using the valves, with openings equal to $x1$ and $x2$, respectively. More details can be found in Johanson (2002).

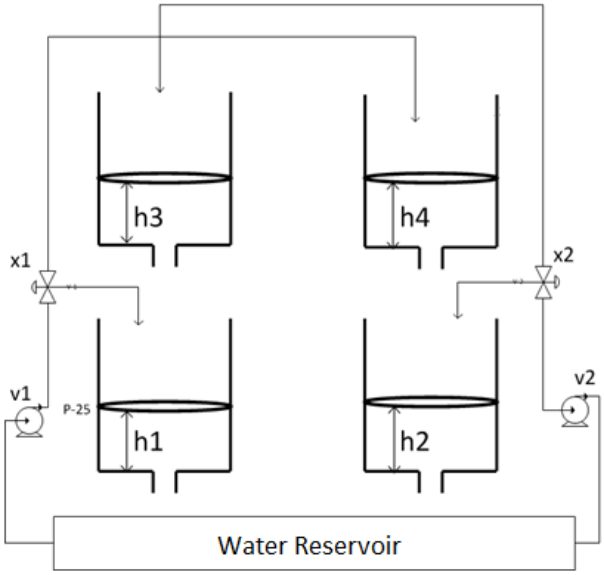

Figure 5.17: Diagram of the Quadruple-Tank Process case study.

The Mass balances around each tank are:

$$\frac{dh_1}{dt} = -\frac{cd_1}{A_1}(h_1)^{exp1} + \frac{cd_3}{A_1}(h_3)^{exp3} \tag{5.25}$$

$$\frac{dh_2}{dt} = -\frac{cd_2}{A_2}(h_2)^{exp2} + \frac{cd_4}{A_2}(h_4)^{exp4} \tag{5.26}$$

$$\frac{dh_3}{dt} = -\frac{cd_3}{A_3}(h_3)^{exp3} + \frac{(1-x_2)k_2}{A_3}v_2 \tag{5.27}$$

$$\frac{dh_4}{dt} = -\frac{cd_4}{A_4}(h_4)^{exp4} + \frac{(1-x_1)k_1}{A_4}v_1 \tag{5.28}$$

Where h_i is the level of each tank, k_1v_1 and k_2v_2 are the pump output flows, A_i is the cross-section area of each tank, cd_i is the discharge coefficient of each tank, and $expi$ is the discharge exponent. Table 5.9 provides the model parameters.

Table 5.9: The Quadruple-Tank Process case: model parameter values

$\boldsymbol{A_1}$	$28\ cm^2$	$\boldsymbol{cd_4}$	$2.525\ cm^{2.5}/s$
$\boldsymbol{A_2}$	$28\ cm^2$	$\boldsymbol{k_1}$	$3.33\ cm^3/s$
$\boldsymbol{A_3}$	$32\ cm^2$	$\boldsymbol{k_2}$	$3.35\ cm^3/s$
$\boldsymbol{A_4}$	$32\ cm^2$	$\boldsymbol{exp1}$	0.5
$\boldsymbol{cd_1}$	$3.145\ cm^{2.5}/s$	$\boldsymbol{exp2}$	0.5
$\boldsymbol{cd_2}$	$2.525\ cm^{2.5}/s$	$\boldsymbol{exp3}$	0.5
$\boldsymbol{cd_3}$	$3.145\ cm^{2.5}/s$	$\boldsymbol{exp4}$	0.5

To illustrate the proposed approach, a MPC controller was simulated in *Matlab/Simulink*, whose controlled variables are the four levels (h_1, h_2, h_3 and h_4) and the manipulated variables are pump voltages (v_1 and v_2) and valve openings (x_1 and x_2).

The linear model, used by the MPC, was obtained from the linearization of the nonlinear model at the operating point defined by the manipulated variables $v1 = 3.2$, $v2 = 3.15, x1 = 0.43$, and $x2 = 0.34$, given by:

$$G_0(s) = \begin{bmatrix} \frac{0.048}{s+0.016} & \frac{0.0025}{s^2+0.028s+0.0002} & \frac{0.35}{s+0.015} & \frac{-0.0096}{s^2+0.41s+0.0004} \\ \frac{0.0009}{s+0.016} & \frac{0.035}{s+0.011} & \frac{-0.0055}{s^2+0.024s+0.0002} & \frac{0.323}{s+0.011} \\ 0 & \frac{0.078}{0.028s+0.25} & 0 & \frac{-0.37}{s+0.026} \\ \frac{0.045}{s+0.018} & 0 & \frac{-0.31}{s+0.018} & 0 \end{bmatrix} \quad (5.29)$$

The controller was tuned using RPN methodology (Trierweiler & Farina, 2003), whose values are shown in Table 5.10.

Table 5.11 shows the different scenarios evaluated in this case study. Case 0 is the nominal case, without MPM and unmeasured disturbances. Cases 1 to 4 and 7 to 10 show a MPM whereas the others have unmeasured disturbances. The data used in this study was simulated using a sequence of step setpoint changes (Figure 5.18) and including a white noise with magnitude 2% of the variables range was added on the output measurements. The plant is simulated considering the nonlinear model of equations 5.25 to 5.28.

Table 5.10: The Quadruple-Tank Process case: MPC tuning parameters

Sample Time	10s
Prediction Horizon	48
Control Horizon	12
CVs Weights	$Q_{h1} = Q_{h2} = Q_{h3} = Q_{h4} = 10$
Move Suppression	$Q_{v1} = Q_{v2} = Q_{x1} = Q_{x2} = 50$
MVs lower limits	$v1_{hard}^{min} = v2_{hard}^{min} = 0.1,\ x1_{hard}^{min} = x2_{hard}^{min} = 0.05$
MVs upper limits	$v1_{hard}^{max} = v2_{hard}^{max} = 10,\ x1_{hard}^{max} = x2_{hard}^{max} = 0.95$
CVs lowe limits	$h1_{hard}^{min} = h2_{hard}^{min} = h3_{hard}^{min} = h4_{hard}^{min} = 0$
CVs upper limits	$h1_{hard}^{max} = h2_{hard}^{max} = h3_{hard}^{max} = h4_{hard}^{max} = 20$

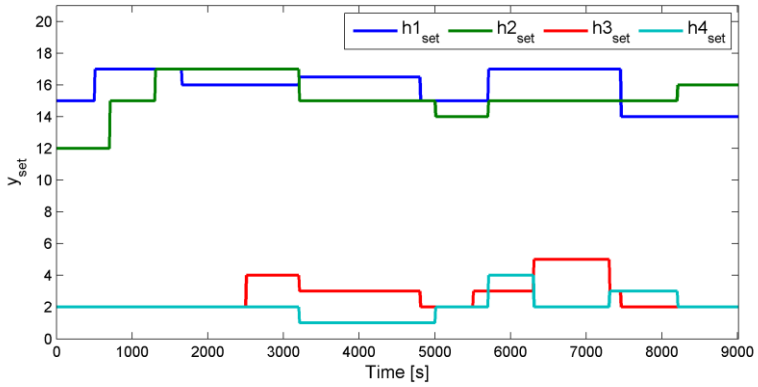

Figure 5.18: The Quadruple-Tank Process Case Study: Perturbations in the Setpoints

Table 5.11: The Quadruple-Tank Process case: Scenarios Configuration

MI	Parameter	Value
0	--	--
1	cd_1	$7.86\ cm^{2.5}/s$
2	cd_3	$1.05\ cm^{2.5}/s$
3	A_2	$256\ cm^2$
4	A_4	$4\ cm^2$
5	Unmeasured disturbance in $h4$	$\frac{8}{70s+1}$
6	Unmeasured disturbance in $h2$	$\frac{5}{5s+1}$
7	$exp3$	0.1
8	$exp2$	0.75
9	cd_2	*2.5
10	cd_1	*1/3
11	Unmeasured disturbance in $h1$	$\frac{-0.2s+0.15}{10s}$
12	Unmeasured disturbance in $h2$	$\frac{50}{50s+1}$
13	Unmeasured disturbance: Extra flow to tank 1	$\frac{-0.2s+0.15}{10s}$
14	Unmeasured disturbance: Extra flow to tank 2	$\frac{50}{50s+1}$

The method was applied in the most affected controlled variable for each scenario. This selection was made considering the corresponding CV with the highest variance of $Ivar$ (equation 5.24). For each selected CV, the confidence ellipses considering $MW = 20$ are presented in Figures 5.19 and 5.20. Table 5.12 shows the ce_{dZ} and co_{dZ} for a moving windows size (MW) varying from 10 to 40

Table 5.12: The Quadruple-Tank Process case: co_{dZ} and ce_{dZ} for each scenario

MI	Evaluated CV	ce_{dskn}	ce_{dkts}	co_{dskn}	co_{dkts}
1	$h1$	0.44	0.79	0.30	0.83
2	$h1$	0.28	0.63	0.23	0.70
3	$h2$	0.17	0.14	0.34	0.30
4	$h4$	0.33	0.68	0.20	0.64
5	$h4$	0.01	0.00	0.03	0.01
6	$h2$	0.01	0.00	0.02	0.02
7	$h1$	0.27	0.57	0.23	0.67
8	$h2$	0.27	0.60	0.31	0.78
9	$h2$	0.34	0.72	0.36	0.88
10	$h1$	0.52	0.59	0.52	0.62
11	$h1$	0.01	0.00	0.03	0.01
12	$h2$	0.04	0.01	0.11	0.08
13	$h1$	0.01	0.01	0.03	0.02
14	$h2$	0.01	0.01	0.05	0.04

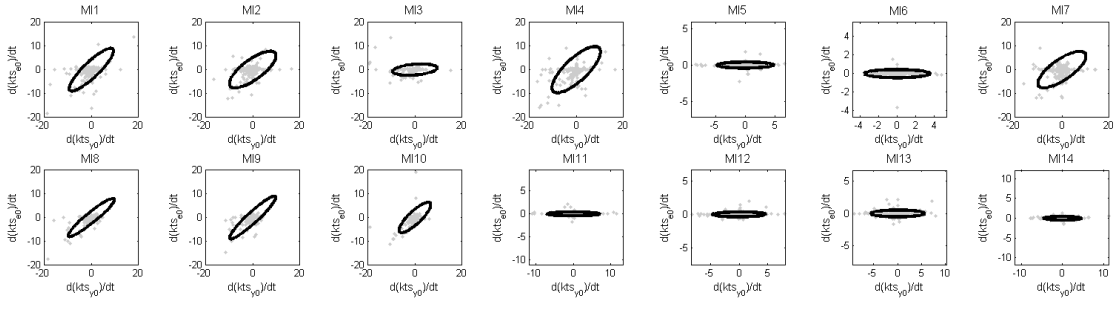

Figure 5.19: The Quadruple-Tank Process Case Study: Kurtosis derivative confidence ellipse for $MW = 20$

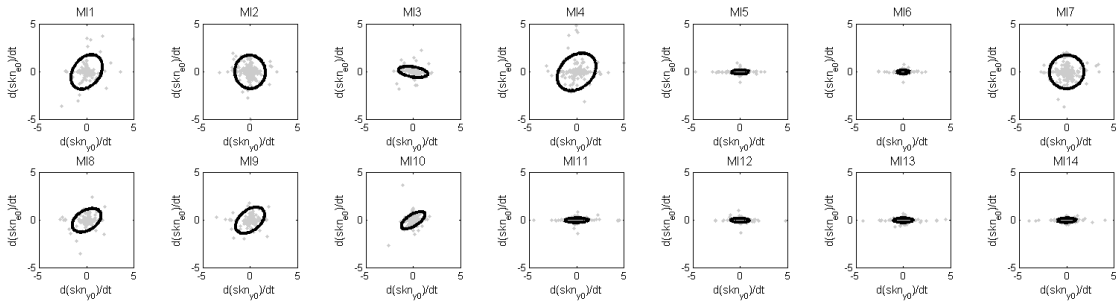

Figure 5.20: The Quadruple-Tank Process Case Study: Skewness derivative confidence ellipse for $MW = 20$

The results show that the indices based on skewness and kurtosis evaluation allows us to distinguish the root cause of the problem and points to the channel with mismatch, in all scenarios. The ellipses (Figure 5.19 and 5.20) tend to be more sloped when a MPM is present. Table 5.12 shows the highest ce_{dz} superior to 0.17 when a MPM is present and not exceeding 0.04 when a UD occurs. The highest co_{dz} is superior to 0.23 when a MPM is present and does not exceed 0.04 when a UD occurs. In the simulated scenarios, the nonlinearity of the plant does not impact the system behavior, since the diagnosis was compatible with the added MPM/UD. However, when the nonlinearity is significant, the diagnosis will indicate a MPM.

5.4 Conclusions

This paper proposed an approach to distinguish between model-plant mismatch or unmeasured disturbance impacting in the performance of model predictive controllers. The idea behind the method is to compare the nominal system outputs with the nominal error. When a MPM is responsible for the performance degradation, these signals have similarities because both are dependent on the control actions. However, when a UD is present, the nominal error depends on the disturbance signal, which comes from an external source. Thus, the nominal error does not have relation with the nominal output.

The comparison between the nominal error and nominal output was performed considering the statistical distribution of the signals along moving windows. The statistical distribution is defined from the kurtosis and skewness coefficients. Four indicators were proposed: one was based on the Person's correlation coefficient (co), another based in the confidence ellipse of the statistical distributions (ce), beyond the average ellipses angles ($\bar{\alpha}$) and average size of the generated ellipses ($\overline{DR}$). Besides, we also proposed the evaluation of the indicators using the derivative of statistical distributions.

Firstly, a SISO Linear MPC case study was presented to illustrate the method and verify the best approach among the suggested indices. The results show that, although both alternatives provide similar results in most cases, the use of statistical distribution derivatives is more conclusive than the use of the raw signals, since it is superior in capturing dataset tendency. Among the indices, the co_{dz} and ce_{dz} are the most recommended, since the angle ($\bar{\alpha}_{dz}$) and the dimensions ($\overline{DR}_{dz}$) must be analyzed in combination, once the MPM or UD indicator depends on the shape and inclination of the confidence ellipses. When the system contains MPM and UD at the same time, the method is capable of detecting the dominant effect, indicating higher values of co_{dz} and ce_{dz}, as the effect of the MPM is more evident.

Two MIMO case studies are also discussed: the Shell heavy oil fractionator and the Quadruple-tanks process. Various scenarios were generated for both cases, considering only model-plant mismatches, only unmeasured disturbances, and both at the same time. The results show that the proposed method is capable of distinguishing between MPM or UD in all simulated experiments. The co_{dz} was more reliable than ce_{dz}, not failing in any case. Its value does not exceed 0.1 when a UD is present and is always superior to this amount when a MPM is present. Results also show that, when a MPM occurs, kurtosis and skewness do not necessarily both have indicator values higher than 0.1. Thus, the analysis of kurtosis and skewness are complementary, and just one of them indicating MPM is necessary for this diagnosis be true.

Capítulo 6 – **Performance Assessment and Diagnosis of MPCs with Control Ranges**

Abstract[8]**:** Many industrial model predictive control applications use as reference a range where the variable should be kept inside, instead of a specific value (setpoint). Although assess the model quality of these controllers is fundamental, most available MPC assessment techniques require setpoints as reference, providing misleading results when they are unavailable. The methods proposed by Botelho *et al.* (2015a/cap. 3), Botelho *et al.* (2015b/cap. 4) and Botelho *et al.* (2015c/cap. 5) allows the MPC model assessment and diagnosis for both setpoint and control range MPC configurations. This paper shows the application of these methods in a MPC where the variables are controlled by control range. The Shell Heavy Oil Process is used as case study, showing that the method was capable to estimate the effect of modeling problems and indicate the controlled variable associated as well as if the problem is due to a model-plant mismatch or unmeasured disturbance.

Keywords: model predictive control, model assessment, model-plant mismatch, unmeasured disturbance, soft constraints.

[8] *Submetido para publicação no periódico "Control Engineering Practice".*

6.1 Introduction

Model predictive controllers (MPCs) have been widely used in the process industry over the last decades. They uses a dynamic process model to predict the behavior of controlled variables (CVs) along the future horizon, based on past control actions. From this result, an optimization algorithm calculates the control actions that lead the process to the optimal trajectory. The maintenance of MPC is an important and challenging problem, since the performance degradation can come from many different sources, such as: wrong tuning parameters (i.e., control and prediction horizon, weighting matrices, sampling time, etc.), poor model quality, poor disturbance rejection, and inappropriate constraint setup (Sun *et al.*, 2013).

Although predictive controllers rely on a solid theoretical foundation, the industrial and commercial MPCs have their own control policy (see Holkar & Waghmare, Qin & Badgwell, 2003) This means that they use different combinations of operational pratices, algorithms and variable considerations. Among these policies, the MPCs with variables controlled by range is a needed pratice in the most real process. Usually, these controllers have the number of monitored variables larger than the manipulated ones. Therefore, the MPC do not have degrees of freedom enough to maintain all the monitored variables in the setpoints and the control objective is to keep them inside a range instead of setpoints. The range limits (soft-constraints) can be violated but a penalization term is included in the MPC cost function when it occurs. In some cases, the same controller has separate strategies for different variables (setpoints and soft-constraints).

Regardless the applied control strategy, monitoring and evaluating the quality of the MPC's model is fundamental, since this is one of the most important and critical points for the controller operation. Several techniques are available in literature (e.g. Huang *et al.*, 2003; Conner & Seborg, 2005; Jiang et *al.*, 2012; Badwe *et al*., 2009*;* Badwe *et al.* 2010; Sun *et al.* 2013; Kano *et al., 2010,* Ji *et al.,* 2012*)*. Although most of them are efficient for the case with setpoints, they cannot working with control range variables and when they are applied on these cases, they produce misleading and inconclusive results.

Botelho *et al.* (2015a/cap. 3), Botelho *et al.* (2015b/cap. 4) and Botelho *et al.* (2015c/cap. 5) proposed a series of methods for MPC model assessment for detecting the controlled variable (CV) with performance problems and, in the case of bad performance, diagnose if it come from a model-plant mismatch (MPM) or unmeasured disturbance (UD). The main advantage of these methods is the setpoint independence. Moreover, the methods are simple to apply and interpret. These characteristics make the methodologies flexible to several controller formulations, including MPCs by range, facilitating their industrial application for controllers assessment.

"Real" MPC applications have available models with all channels corrupted in different levels, demanding, thus, methods for assessment that are able to deal with this diversity, and point the variables that really impact the final performance. Therefore, this paper aims to make an exhaustive test for the methods and verify their efficiency under a diversity of modeling errors. Hundreds of random scenarios were generated considering a MPC by range applied in the Shell Heavy Oil Fractionator process. The paper also presents an evaluation of the amount of uncertainties allowed in the nominal sensitivity function without diagnosis quality loss.

6.2 Methods for MPC model assessment

This section summarizes the method proposed by Botelho *et al.* (2015a/cap. 3, b/cap. 4 and c/cap. 5), which considers a control loop as shown in Figure 6.1, where C is the MPC controller, G_0 the nominal model, and G the real plant. The model-plant mismatch (MPM) magnitude is ΔG. The theoretical system without mismatch is shown in Figure 6.1a, for which nominal closed loop outputs are y_0. T_0 is the nominal complementary sensitivity function. The real system, in a scenario subject to MPM, is shown in Figure 6.1b, where y_{set} corresponds to the setpoints, u are the manipulated variables, y are the measured outputs, y_{sim} are the simulated outputs of the nominal model perturbed by the actual control actions u, and T is the complementary sensitivity function. Figure 6.1c shows the real system subject to an unmeasured disturbance (UD), where v is the sequence of independent random variables, G_d is the unknown disturbance model and y_d are the disturbance signals.

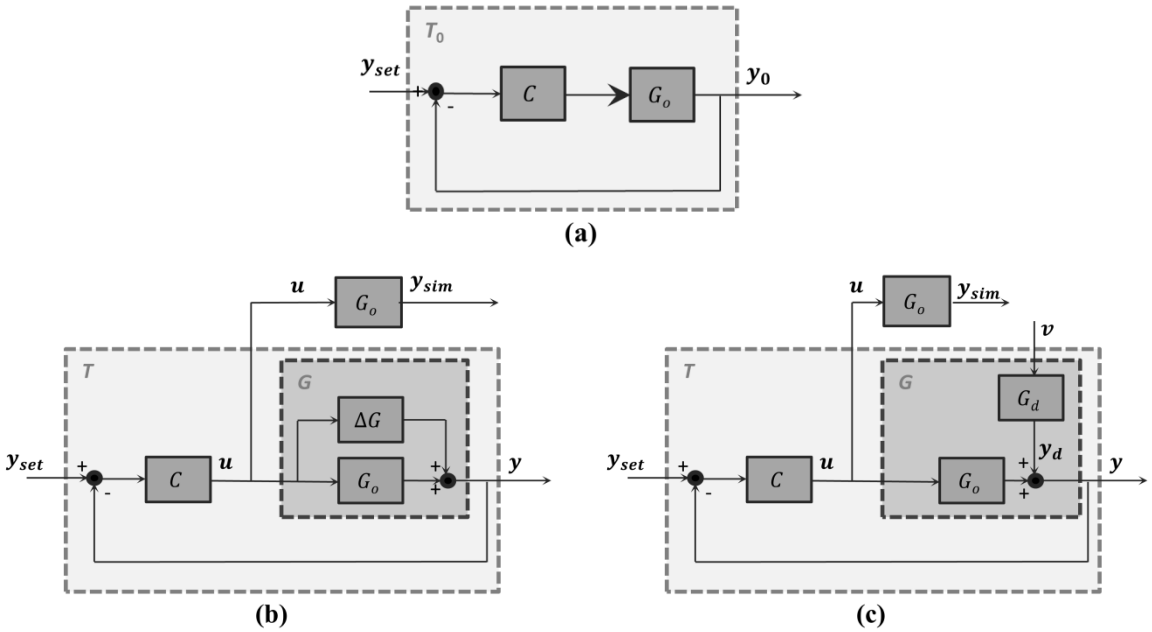

Figure 6.1: Schematic diagram of closed-loop (a) nominal system, (b) with model-plant mismatch (MPM) and (c) with unmeasured disturbance (UD)

The method is based on the premise that an effective model should represent the real system at the frequency where the MPC works. Thus, to assess the real influence of the model-plant mismatch, the closed-loop performance must be considered. The following definitions can be found in many classical control books (e.g., Skogestad & Postlethwaite, 1996):

$$y_0 = T_0 y_{set} \tag{6.1}$$

$$T_0 = G_0 C (I + G_0 C)^{-1} = (I + G_0 C)^{-1} G_0 C \tag{6.2}$$

$$S_0 + T_0 = I \tag{6.3}$$

$$y_{sim} = G_0 u \tag{6.4}$$

where S_0 is the nominal sensitivity funcion and I is the identity matrix. Botelho *et al.* (2015a/cap. 3) show that the nominal output y_0 (i.e., the output of the system in the absence of MPM or UD) could be estimated according to:

$$y_0 = y + S_0\,(y_{sim} - y) \tag{6.5}$$

The nominal sensitivity function (S_0) is a square transfer matrix that characterizes the system response in closed loop (see equations 6.1, 6.2 and 6.3). Its dimensions are equal to the number of outputs. The diagonal elements ($S_{0_{diag}}$) give the closed loop behavior of the outputs when their references (setpoints or soft constraints) are changed. The remaining elements provide the impact of these references variation in the others outputs. Thus, Botelho *et al.* (2015b/cap. 4) suggest an extension of equation 6.5, as follow:

$$y_{0_{diag}} = y + S_{0_{diag}}\,(y_{sim} - y) \tag{6.6}$$

The $S_{0_{diag}}$ works as a softening for the simulation residuals ($y_{sim} - y$), and retains only the part that is not removed by the controller feedback and is impacting in the performance of corresponding output. Variables without significant MPM or UD will have $y_{0_{diag}} \cong y$, because their simulation errors are near to zero. Applying S_0 instead of $S_{0_{diag}}$ can be used to verify how the outputs affect each other. In this case, $y_0 \neq y$ can occur even for variables without any significant MPM or UD. This difference is produced by a MPM and/or UD in another output variable and is transmitted to the other channels by coupling in S_0. The stronger is the coupling among the variable, the larger is the difference $y_0 \neq y$, considering the existence of MPMs or UDs in the system.

Since y_0 and $y_{0_{diag}}$ are estimations of the process outputs in the absence of a model-plant mismatch or unmeasured disturbance, they could be considered benchmarks for controller-model output response, indicating how the modeling errors are being propagated and were they are located, respectively. A useful index is the comparison of output variances in nominal and real case:

$$Ivar = \frac{var(y - \bar{y})}{var(y_0 - \bar{y}_0)} \tag{6.7}$$

$$Ivar_{diag} = \frac{var(y - \bar{y})}{var(y_{0_{diag}} - \bar{y}_{0_{diag}})} \tag{6.8}$$

If $Ivar \cong 1$ means that there is no modeling problem and unmeasured disturbances affecting the corresponding output, on the other hand, when $Ivar \neq 1$ and $Ivar_{diag} \neq 1$, the corresponding output has a MPM or UD. Otherwise, when $Ivar \neq 1$ and $Ivar_{diag} \cong 1$ the corresponding output does not have trouble in their models, but its variance is being affected by MPM or UD that originates at other outputs.

Another possibility is to analyze the autocorrelation function (ACF) of $y - \bar{y}$, $y_0 - \bar{y}_0$, and $y_{0_{diag}} - \bar{y}_{0_{diag}}$. A high value of ACF means that the current signal value is strongly correlated with the past values. The ACF curves are useful to analyze the effect of MPMs and UDs in MPC speed of response or to detect oscillatory behavior (Huang & Shah, 1999).

Once the outputs with modeling problem were detected, it is desirable to identify the cause. A key issue is to determine whether the decline in performance is due to MPM or UD. The former occurs when the process model cannot adequately describe the relations

between model input and output variables and a re-identification is required. On the other hand, an unmeasured disturbance occurs when there is a deterministic unknown signal influencing the output behavior. The effects of a MPM and UD in the process outputs are very similar (see Figures 6.1b and 6.1c), thus, they are not easily distinguished. To overcome this problem, Botelho *et al*. (2015c/cap. 5) proposed a systematic for identifying if the dominant effect is related to MPM or UD. The main idea is quantify the correlation distribution between the nominal diagonal outputs $y_{0_{diag}}$ with the nominal error $e_{0_{diag}}$ defined by:

$$e_{0_{diag}} = y_{0_{diag}} - y \tag{6.9}$$

Considering that $y_{0_{diag}}$ is the estimated output free from model-plant mismatch and unmeasured disturbances, $e_{0_{diag}}$ can be interpreted as the effect of the modeling problems in the output. When an output is under a MPM, the error come from the model, then $e_{0_{diag}}$ will be dependent of the inputs (u), as well as $y_{0_{diag}}$, causing a similar frequency pattern. When an output is under an unmeasured disturbance, $e_{0_{diag}}$ is independent of u because the disturbances come from an external source. Nonetheless, $y_{0_{diag}}$ continues to be dependent on the input variables movements. This means that the frequency of variation of $y_{0_{diag}}$ and $e_{0_{diag}}$ are uncorrelated. Therefore, the comparison between $y_{0_{diag}}$ and $e_{0_{diag}}$ patterns can be used to discriminate between model-plant mismatch and unmeasured disturbances. According to the author, the method uses the $y_{0_{diag}}$ instead y_0 because the diagonal terms allow the location of the modeling problem in each output.

The diagnosis procedure to distinguish between MPM and UD consists of the analysis of the statistical distribution of $y_{0_{diag}}$ and $e_{0_{diag}}$ along a moving window (MW). The statistical distribution is evaluated by the skewness (skn) and kurtosis (kts) coefficients:

$$kts_{Xi}^{MW} = \frac{m_3}{\left(\sqrt{m_3}\right)^3} \tag{6.10}$$

$$skn_{Xi}^{MW} = \frac{m_4}{(\sqrt{m_2})^4} \tag{6.11}$$

where m_2, m_3 and m_4 are the second, third and fourth order central moment, defined as:

$$m_l = \frac{\sum_{i=1}^{MW}(X_i - \bar{X})^l}{MW}, l = 2,3,4 \tag{6.12}$$

Where X_i is the evaluated dataset ($y_{0_{diag}}$ or $e_{0_{diag}}$) and $\bar{X}$ is it corresponding mean. A high value of kurtosis means that the data present a large number of recordings away from the mean, when compared with a normal distribution. The sample skewness provides an indicator of how asymmetric is the dataset. Figures 6.2 and 6.3 illustrate the expected result for a hypothetical case. When a MPM is present, the variation of statistical distributions of $e_{0_{diag}}$ and $y_{0_{diag}}$ shows the major variation at the same time (see the peaks), which does not occur when a UD is present.

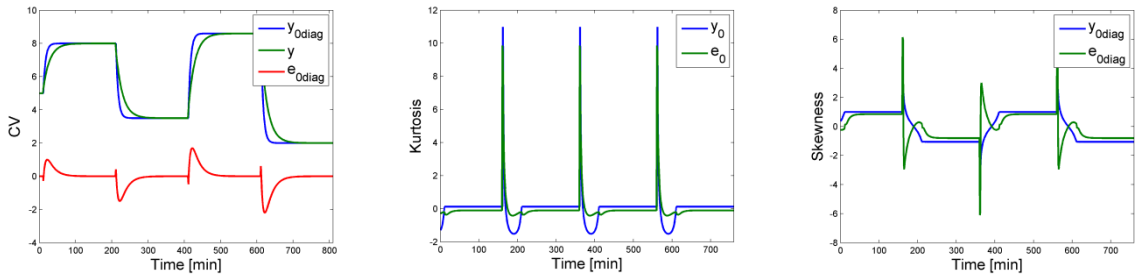

(a) **(b)** **(c)**

Figure 6.2: Illustrative situation with MPM: (a) measured y, estimated $y_{0_{diag}}$, and $e_{0_{diag}}$; (b) kurtosis coefficients along a moving window; and (c) skewness coefficients along a moving window

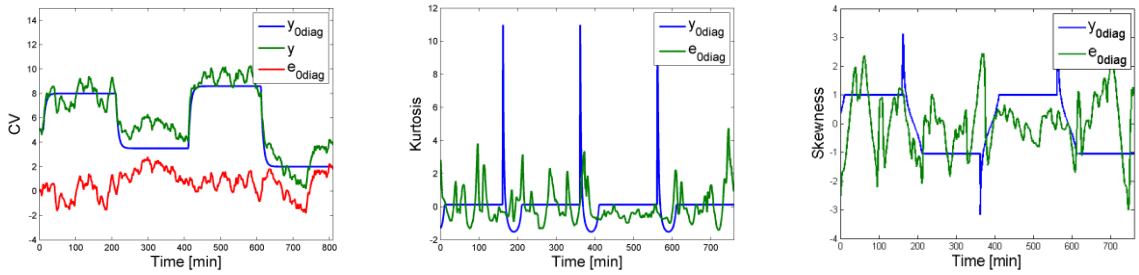

(a) **(b)** **(c)**

Figure 6.3: Illustrative situation with UD: (a) measured y, estimated $y_{0_{diag}}$ and $e_{0_{diag}}$; (b) kurtosis coefficients along a moving window; and (c) skewness coefficients along a moving window

Botelho *et al.* (2015c/cap. 5) analyze different approaches to compare $y_{0_{diag}}$ and $e_{0_{diag}}$. The most reliable alternative is based on the Pearson's correlation coefficients of skewness and kurtosis derivatives. A scan is performed varying MW size in the neighborhood of the prediction horizon ($0.5ph$ to $2ph$, where ph is the MPC's prediction horizon). The indicators (co_{dkts} and co_{dskn}) are based in the mean of absolute correlation between the derivatives of statistical distributions:

$$co_{dkts} = \frac{\sum_{MW=0.5ph}^{2p} \left| corr\left(\frac{d}{dt} kts_{e_{0_{diag}}}^{MW}, \frac{d}{dt} kts_{y_{0_{diag}}}^{MW}\right)\right|}{n_{MW}} \tag{6.13}$$

$$co_{dskn} = \frac{\sum_{MW=0.5ph}^{2p} \left| corr\left(\frac{d}{dt} skn_{e_{0_{diag}}}^{MW}, \frac{d}{dt} skn_{y_{0_{diag}}}^{MW}\right)\right|}{n_{MW}} \tag{6.14}$$

where n_{MW} are the number of scanned MW, $corr$ is the Pearson's correlation coefficient. The larger the values of co_{dkts} and co_{dskn}, the higher is the probability of a model-plant mismatch dominance. It enough one of these indices be high for classifying the performance issue caused by MPM. Thus, I_{MPM} is defined by:

$$I_{MPM} = \max(c_{dkts}, c_{dskn}) \tag{6.15}$$

6.3 MPC by Control Range

The square controllers are characterized by a system with the same number of manipulated variables (MVs) as controlled variables (CVs), leading to a control problem with a unique solution (Qin, 2003). Thus, the controller has enough degrees of freedom to keep each CV in the corresponding setpoints. Although this ideal case is the most studied in the literature, it is an uncommon industrial MPC implementation.

There are two kinds of rectangular systems. The best situation corresponds to the fat plant cases, where the number of MVs is higher than CVs. In this case, the extra degrees of freedom available are used to optimize the operation and targets for the manipulated variables are usually applied to achieve the economic performance (Qin, 2003). Unfortunately, the usual case for a nonsquare configuration is with more CVs than MVs (thin plant case). Here, it is not possible to meet all of the control objectives, so that, the most common strategy consists of defining operational bands for CVs instead of a fixed setpoint (Campos *et al.*, 2013; Qin, 2003). We can also call these control bands as fatpoints and the MPC with control range. It is possible to operate the MPC purely by range or maintain some CVs with fix setpoint and the others with range, depending on the process objectives.

Soft constraints are commonly used to replace setpoints in control algorithms. Rather than maintain all CVs to a specific value, upper and lower limits are specified. The control algorithm tries to maintain the control variable within these limits unless necessity forces it to relax the constraints (Yuan & Lennox, 2006). A straightforward way for softening the constraints is to introduce slack variables which are defined such that they are non-zero only if the corresponding constraint is violated (Kerrigan & Maciejowski, 2000). The term of the soft constraint in the MPC cost function is defined as:

$$\begin{aligned} &\min_{\delta} \sum_{i=0}^{ph-1} \tau\, \delta^{2} \\ &st: \quad y_{soft}^{max} + \delta \;\geq y\; \geq y_{soft}^{min} - \delta \\ &\qquad\qquad\quad \delta \geq 0 \end{aligned} \tag{6.16}$$

where ph is the prediction horizon, y_{soft}^{max} and y_{soft}^{min} are the upper and upper lower of soft constraint, τ is the penalization of soft constraint violation and δ is the slack variable. When $\delta = 0$, the constraint is satisfied and no penalization is inserted in the cost function.

Usually, MPC by control range is combined with a simple real time optimization layer, which set the optimal steady state value for MVs (targets) according to economic objectives. Figure 6.4 shows the typical architecture of these systems.

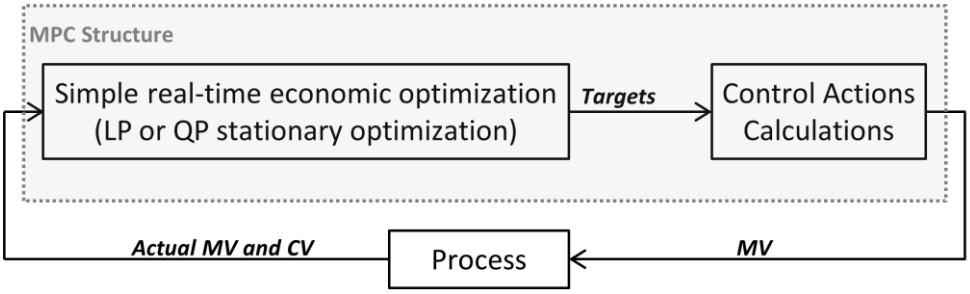

Figure 6.4: Architecture of MPC controller with optimizer (adapted from Campos *et al., 2013)*

Thus, when some CV violates its soft constraints, the MPC will use its degrees of freedom (MVs available) to take the CV back to its control range. In a normal situation, the controller will work to lead the process to the optimal cost. In the most cases, it means maintain some CVs with a soft constraint active, whose maximum number must equal to the number of available MVs. In this situation, the plant is reduced to a square sub-system and the active soft constraints works as "pseudo-setpoints".

The method presented in section 6.2 has the benefit to be independent of control policy (setpoint or soft-constraints), allowing its utilization, for example, in MPCs whose variables are controlled by control range. The core of the method is the analysis of the nominal sensitivity function (S_0) and the corresponding complementary sensitivity function (T_0), i.e. the nominal closed loop response (equation 6.3). By definition, these functions are related with the setpoints (see equation 6.1). Thus, some considerations need to be defined when the controller is setpoint independent, which are described below.

Firstly, considering a system where all the CVs have fixed setpoint, it is expected that the diagonal of complementary nominal sensitivity function ($T_{0_{diag}}$) be a model with static gain equal to one and the remaining models with a zero at the origin (i.e., null static gain). Now let us consider a MPC whose variables are controlled by range, where the following situations may occur:

- The evaluated CV have an active soft constraint: in this case, its behavior is very similar to a fixed setpoint case. Thus, the static gains of the corresponding $T_{0_{diag}}$ will be 1. The effect of this CV in another variable with active soft constraint will generate an off-diagonal T_0 with a zero at the origin (i.e., null static gain). The effect of this CV in a variable inside the range will generate an off-diagonal T_0 with static gain different from zero, because this variable will assume a new steady state value.

- The evaluated CV is inside the range: in this case, the variable does not have any influence in the control actions. It means that the effect of the controller feedback in this variable is null. Thus, $T_0 = 0$ (diagonal and off-diagonal models) and equation 6.6 is reduced to:

$$y_{0_{diag}} = y_{sim} \tag{6.17}$$

Figure 6.5 summarizes the previous discussion illustrating the complementary nominal sensitivity function of a hypothetical MPC by range.

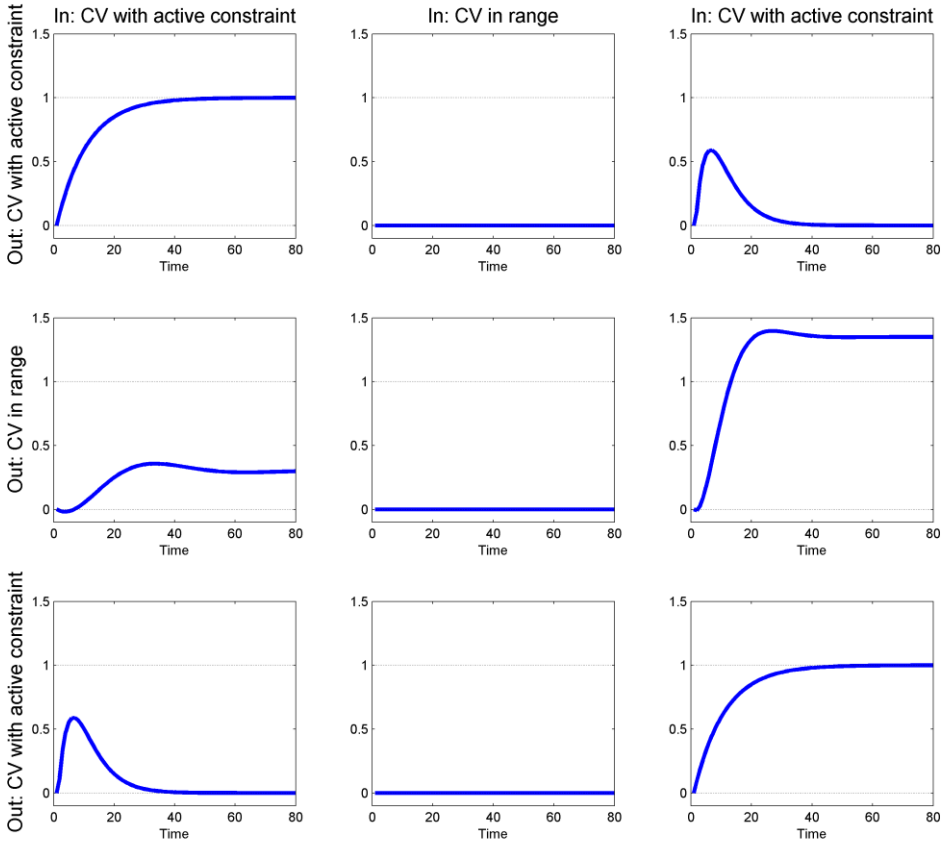

Figure 6.5: Complementary nominal sensitivity function (T_0) of a hypothetical MPC by range

6.4 Case Study

The Shell Benchmark Process was proposed by Prett & Morari (1987) and is composed by a heavy oil fractionator, as represented in Figure 6.6. The main feature of this process is the high interaction among the variables as well as large time delays. The fractionator is characterized by three product draws and three side circulating loops. The heat requirement of the column enters with the feed, which is a gaseous stream. Product specifications for the top and side draw streams are determined by economics and operating requirements. There is no product specification for the bottom draw, but there is an operating constraint on the temperature in the lower part of the column. The three circulating loops remove heat to achieve the desired product separation.

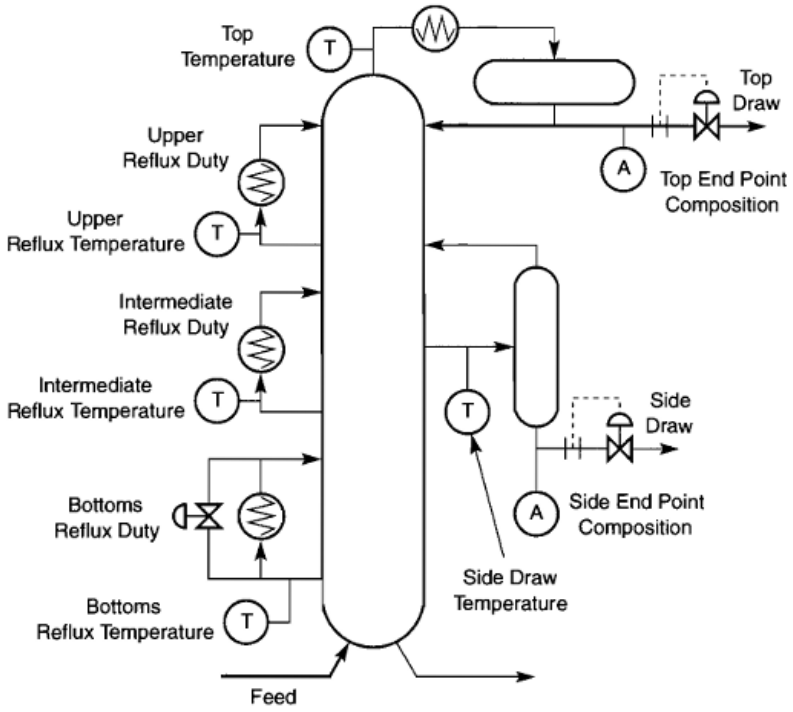

Figure 6.6: Schematic representation of Shell Heavy Oil Fractionator (Maciejowski, 2002)

A linear MPC was configured based on Maciejowski (2002). The controller is composed by 7 controlled variables (CVs), 3 manipulated variables (MVs) and 2 measured disturbances (MDs), which are presented in Table 6.1.

The linear model for this process is given by:

$$G_0 = \begin{bmatrix} 4.05e^{-27s}\frac{1}{50s+1} & 1.77e^{-28s}\frac{1}{60s+1} & 5.88e^{-27s}\frac{1}{50s+1} & 1.20e^{-27s}\frac{1}{45s+1} & 1.44e^{-27s}\frac{1}{40s+1} \\ 5.39e^{-18s}\frac{1}{50s+1} & 5.72e^{-14s}\frac{1}{60s+1} & 6.90e^{-15s}\frac{1}{40s+1} & 1.52e^{-15s}\frac{1}{25s+1} & 1.83e^{-15s}\frac{1}{20s+1} \\ 3.66e^{-2s}\frac{1}{9s+1} & 1.65e^{-20s}\frac{1}{30s+1} & 5.53e^{-2s}\frac{1}{40s+1} & 1.16\frac{1}{11s+1} & 1.27\frac{1}{6s+1} \\ 5.92e^{-11s}\frac{1}{12s+1} & 2.54e^{-12}\frac{1}{27s+1} & 8.10e^{-2s}\frac{1}{20s+1} & 1.73\frac{1}{5s+1} & 1.79\frac{1}{19s+1} \\ 4.13e^{-5s}\frac{1}{8s+1} & 2.38e^{-7s}\frac{1}{19s+1} & 6.23e^{-2s}\frac{1}{10s+1} & 1.31\frac{1}{2s+1} & 1.26\frac{1}{22s+1} \\ 4.06e^{-8s}\frac{1}{13s+1} & 4.18e^{-4s}\frac{1}{33s+1} & 6.53e^{-1s}\frac{1}{9s+1} & 1.19\frac{1}{19s+1} & 1.17\frac{1}{24s+1} \\ 4.38e^{-20s}\frac{1}{33s+1} & 4.42e^{-22s}\frac{1}{44s+1} & 7.20\frac{1}{19s+1} & 1.14\frac{1}{27s+1} & 1.26\frac{1}{32s+1} \end{bmatrix} \quad (6.18)$$

where each row represents a CV ($y1$ to $y7$), the first three columns are the MVs ($u1$ to $u3$) and the others are the MDs ($d1$ and $d2$).

Table 6.1: MPC Variables

Role	Name	Description
Manipulated Variables (MVs)	$u1$	Top Draw
	$u2$	Side Draw
	$u3$	Bottoms Reflux Duty
Measured Disturbances (MDs)	$d1$	Intermediate Reflux Duty
	$d2$	Upper Reflux Duty
Controlled Variables (CVs)	$y1$	Top End Point
	$y2$	Side End Point
	$y3$	Top Temperature
	$y4$	Upper Reflux Temperature
	$y5$	Side Draw Temperature
	$y6$	Intermediate Reflux Temperature
	$y7$	Bottoms Reflux Temperature

The linear MPC controller was configured in *Matlab™/Simulink™*. The MPC used has a simple real-time optimization layer, which set the optimal operating point according to economic objectives. The scheme presented by Figure 6.4 illustrates its architecture. The cost function of the simple real-time optimization is defined by:

$$\begin{aligned} &\min_{u_{tgt}} \sum_{i=1}^{nu} (\varphi_u u_{tgt})_i \\ &s.t. \quad \begin{aligned} y_{soft}^{max} &\geq y_{set} \geq y_{soft}^{min} \\ u_{hard}^{max} &\geq u_{tgt} \geq u_{hard}^{min} \end{aligned} \end{aligned} \tag{6.19}$$

where φ_u are the manipulated variables costs, y_{set} are the corresponding to the closed-loop steady-state prediction of CVs, y_{soft}^{max} and y_{soft}^{min} are the soft constraints of controlled variables, u_{hard}^{max} and u_{hard}^{min} are the constraints of MVs and u_{tgt} are the MVs targets.

The optimal values calculated from the optimizer (u_{tgt}) are transferred to the MPC optimization problem. Since the system contains more CVs than MVs, all the CVs of the

controller was configured by range. In this case, the MPC works to maintain all the controlled variables inside the soft constraint. The MPC cost function is formulated as follows:

$$\min_{\Delta u(k|k)\ldots\Delta u(mh-1+k|k),\delta} \sum_{i=0}^{ph-1}\left\{\sum_{j=1}^{nu}\left[|Q_{\Delta u}\Delta u(k+i|k)|^2_{i,j} + |Q_u(u(k+i|k)-u_{target}(k+i|k)|^2_{i,j}\right] + \tau_y{\delta_y}^2\right\}$$

$$s.t. \quad \begin{matrix} u_{hard}^{max} \geq u \geq u_{hard}^{min} \\ y_{hard}^{max} \geq y \geq y_{hard}^{min} \\ y_{soft}^{max} + \delta_y \geq y \geq y_{soft}^{min} - \delta_y \\ \delta_y \geq 0 \end{matrix} \tag{6.20}$$

where mh is the control horizon, ph is the prediction horizon, nu is the number of available MVs, Q_u is the target weighting of MVs, $Q_{\Delta u}$ is the move suppression, δ_y is the slack variable for soft the constraints, τ_y is the penalization weight of soft constraint violation, y_{hard}^{max} and y_{hard}^{min} are the hard constraints of CVs. Table 6.2 summarizes the controller tuning and constraints used in this case study.

The described system was simulated considering step changes in the measured disturbances (MDs) according to Figure 6.7. The generated inputs and outputs (in absence of MPM and UD) are presented in Figures 6.8 and 6.9, respectively. The Basis Case corresponds to these results, which are the references for comparison along of this study.

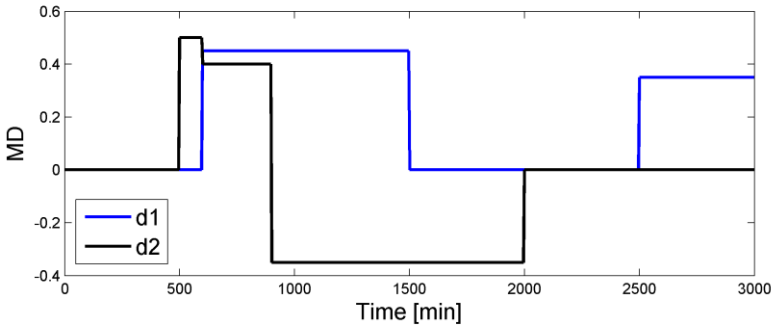

Figure 6.7: Step changes in the measured disturbances.

Table 6.2: Tuning parameters and constraints of the MPC

Sample Time	4min
Prediction Horizon (ph)	75
Control Horizon (mh)	15
MV Cost (φ_u)	$\varphi_{u1} = 8, \varphi_{u2} = 3, \varphi_{u3} = 4$
MV Target Weight (Q_u)	$Q_{u1} = Q_{u2} = Q_{u3} = 1$
Move Suppression ($Q_{\Delta u}$)	$Q_{\Delta u1} = Q_{\Delta u2} = Q_{\Delta u3} = 25$
Weight of soft the constraints violation (τ_y)	$\tau_{y1} = \tau_{y2} = \tau_{y3} = \tau_{y4} = \tau_{y5} = \tau_{y6} = \tau_{y7} = 100$
MV hard constraints (u_{hard}^{max} and u_{hard}^{max})	$u1_{hard}^{max} = u2_{hard}^{max} = u3_{hard}^{max} = 0.5$ $u1_{hard}^{min} = u2_{hard}^{min} = u3_{hard}^{min} = -0.5$
CV hard constraints (y_{hard}^{max} and y_{hard}^{max})	$y1_{hard}^{max} = y2_{hard}^{max} = y3_{hard}^{max} = y4_{hard}^{max} = y5_{hard}^{max} = y6_{hard}^{max} = y7_{hard}^{max} = 1$ $y1_{hard}^{min} = y2_{hard}^{min} = y3_{hard}^{min} = y4_{hard}^{min} = y5_{hard}^{min} = y6_{hard}^{min} = y7_{hard}^{min} = -1$
CV soft constraints (y_{hard}^{max} and y_{hard}^{max})	$y1_{soft}^{max} = y2_{soft}^{max} = y3_{soft}^{max} = y4_{soft}^{max} = y5_{soft}^{max} = y6_{soft}^{max} = 0.5, y7_{soft}^{max} = 0$ $y1_{soft}^{min} = y2_{soft}^{min} = 0, y3_{soft}^{min} = y4_{soft}^{min} = y5_{soft}^{min} = y6_{soft}^{min} = y7_{soft}^{min} = -0.5$

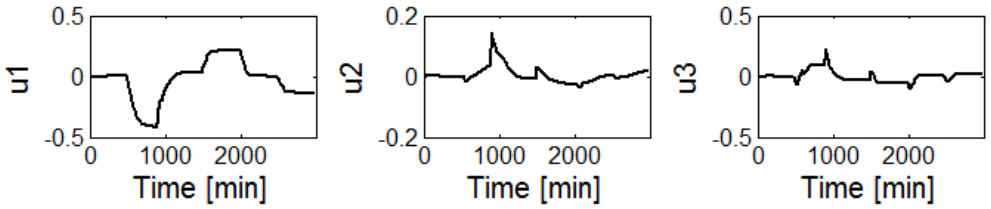

Figure 6.8: Manipulated Variables for the Basis Case.

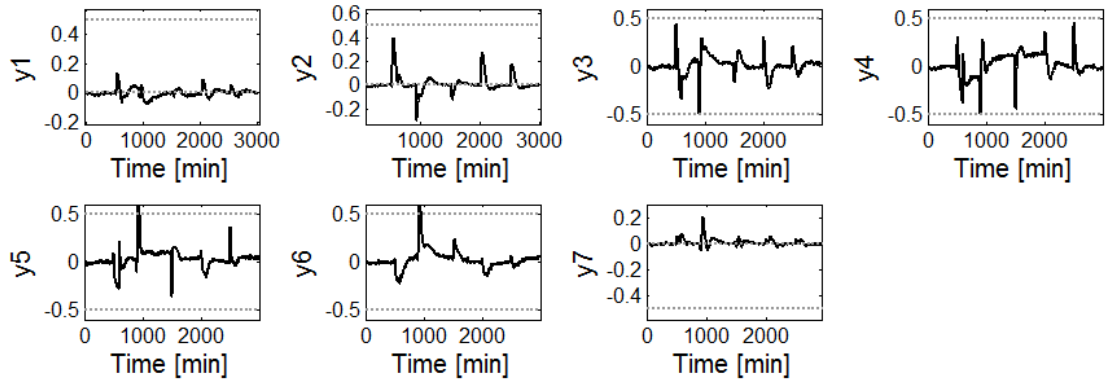

Figure 6.9: Controlled Variables for the Basis Case

Figures 6.8 e 6.9 show that, for the considered perturbations, all the MVs are available (i.e., not saturated). Thus, the MPC works to keep $y1$ and $y2$ in their lower limits (y_{soft}^{min}) and $y7$ in its upper limit (y_{soft}^{max}). The others CVs remain between y_{soft}^{min} and y_{soft}^{max}. As discussed in section 6.3, variables whose predictions not have influence in the controller feedback and the modeling errors are preserved ($T_0 = 0$). When a soft constraint is active, the controller feedback eliminates part of the modeling error. Based on this, the output sensitivity function (S_0) consistent with the Basis Case was identified, and is illustrated in Figure 6.10.

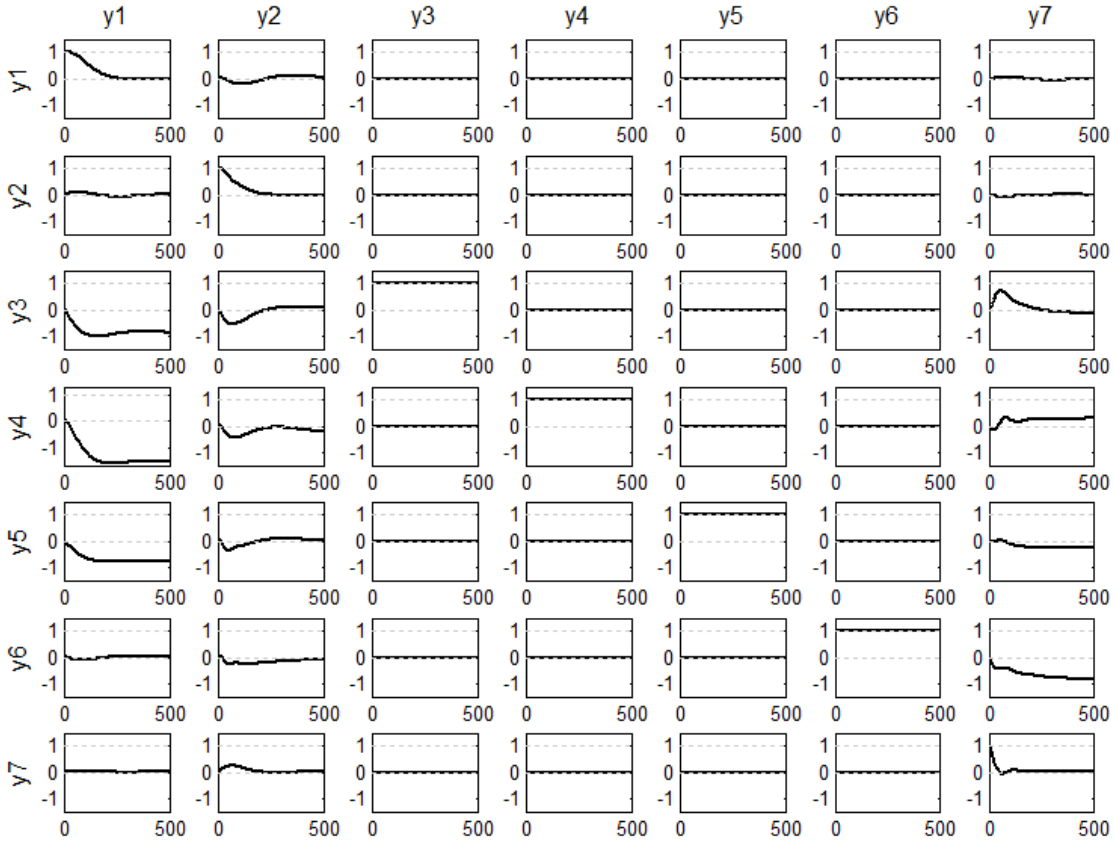

Figure 6.10: Output sensitivity function (S_0)

6.5 Results and discussions

6.5.1 Scenarios pre-defined

Table 6.3 shows ten different scenarios containing model-plant mismatches and unmeasured disturbances that are analyzed in this section for the Shell fractionator case study. The scenarios are composed by model-plant mismatches added in the models MV x CV (type MPM), unmeasured disturbances added in the CVs signals (type UD) and model-plant mismatches added in the feed-forward models, i.e., models MD x CV (type MPM-FF).

Table 6.3: Scenarios Configuration

Name	Type	Affected Output	Affected Input	Description
Scen0	***	**	**	Basis Case
Scen1	MPM	$y7$	$u2$	Do not impact the closed-loop behavior
Scen2	MPM	$y1$	$u3$	Impact in $y1$ only (optimized CV)
Scen3	MPM	$y3$	$u1$,$u2$ and $u3$	Impact in $y3$ only (CV in range)
Scen4	MPM	$y2$	$u1$	Impact all over the system
Scen5	UD	$y1$	**	Impact in $y1$ only (optimized CV)
Scen6	UD	$y7$	**	Do not impact in the system
Scen7	UD	$y4$	**	Impact in $y4$ only (CV in range)
Scen8	UD	$y2$	**	Impact all over the system
Scen9	MPM + UD	$y2$ and $y3$	$u1$,$u2$ and $u3$	Scen8 + Scen 3
Scen10	MPM +UD	$y2$ and $y1$	$u1$	Scen4 + Scen 5
Scen11	MPM –FF	$y1$	$d2$	Impact all over the system
Scen12	MPM – FF	$y3$	$d1$	Impact in $y3$ only (CV in range)

Each scenario was simulated considering the step changes in MDs presented in Figure 6.7. A noise with magnitude 1% was added in the measurements. The methods described in section 6.2 were applied in the generated data. The model fit is captured by the modeling error $e_{sim} = y_{sim} - y$, which can be totalized by the $TSSE$ (total sum of squared simulation errors) defined by:

$$TSSE = \sum_{i=i}^{ny} \sqrt{\sum_{j=1}^{nsample} (y_{sim} - y)^2} \tag{6.21}$$

where ny is the number of outputs and $nsample$ is the number of sampled data. Figure 6.11 shows the $TSSE$ for all scenarios. The $Ivar$ (equation 6.7) quantifies the influence of MPMs or UDs in the output variances, which cannot be compensated by MPC. The results of this index are presented in Figure 6.12.

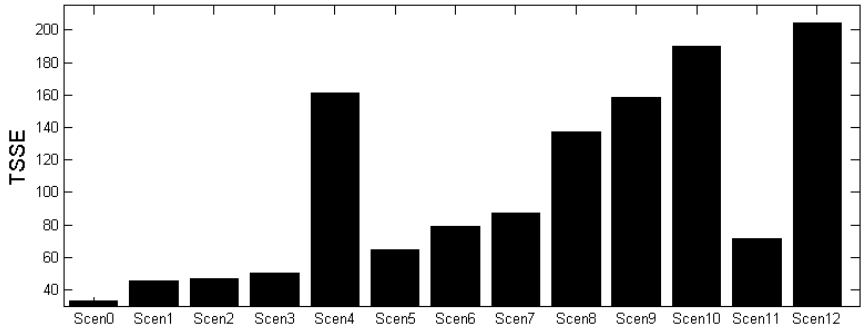

Figure 6.11: Results of $TSSE$

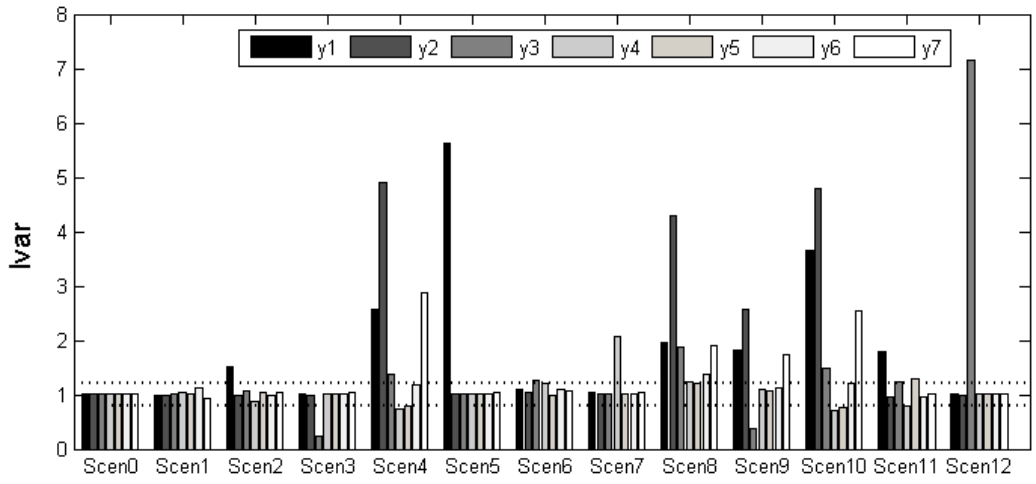

Figure 6.12: Results of $Ivar$. The values outside the threshold lines (dot lines) indicate that the MPC performances were different than the expected behavior

Figure 6.11 makes evident that all scenarios contain modeling errors, since $TSSE$ is higher than the Basis Case. However, not always these errors affect the controller performance, as shown in Scen1 and Scen6, where $Ivar$ is near to one although of $TSSE$ is high. The interpretation of $Ivar$ is coherent with the reality of each scenario (see Table 6.3), showing that the problems in Scen4, Scen8, Scen9 and Scen10 affects all the CVs and in Scen2, Scen3 and Scen7 affect manly one CV. The main conclusion of this indicator is that all scenarios, (except Scen1 and Scen6) have modeling problems impacting in the outputs variances.

To detect in which variables the modeling problem is concentrated, the $Ivar_{diag}$ is used. Figure 6.13 shows the results for $Ivar_{diag}$.

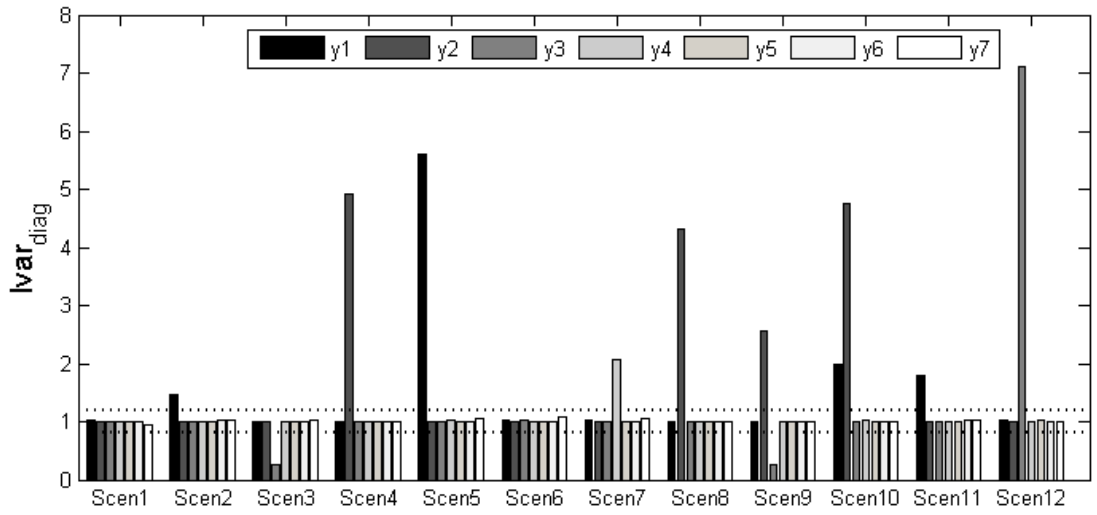

Figure 6.13: Results of $Ivar_{diag}$. The values outside the threshold lines (dot lines) indicate that the MPC performances were different than the expected behavior.

Results from Figure 6.13 show that $Ivar_{diag}$ can detect the variables with model inconsistences responsible for the increase/decrease of the system variance pointed by $Ivar$. In Scen4 and Scen8, a modeling problem in $y2$ affect all others CVs. When a single variable is affected (e.g., Scen2, Scen3, Scen5 and Scen7) the diagnosis of $Ivar_{diag}$ and $Ivar$ are analogous. When more than one CV suffers a performance degradation as shown in Scen9 and 10, $Ivar_{diag}$ is capable to point correctly all the variables responsible for the bad performance.

Figures 6.13 and 6.14 make evident that the method is also capable to detect the modeling inconsistences when they are present in the measured disturbance models (feed-forward models), since the of $Ivar$ for Scen11 and Scen12 are coherent with the reality of each scenario (see Table 6.3) and the $Ivar_{diag}$ can detect the variables with model inconsistences responsible for the increase/decrease of the system variance pointed by $Ivar$.

The comparison of ACF functions of y, yo and yo_{diag} are shown in Figure 6.14. This analysis is less sensitive than the $Ivar$. However it allows a more complete diagnosis, because can detect oscillatory behaviors or changes in the speed of response. For example, in Scen5 the ACF make evident that $y1$ has an oscillatory behavior due to a modeling problem, since $y \neq y0$ and this error is in the own variable ($y1$), because $y0_{diag}$ is similar to $y0$.

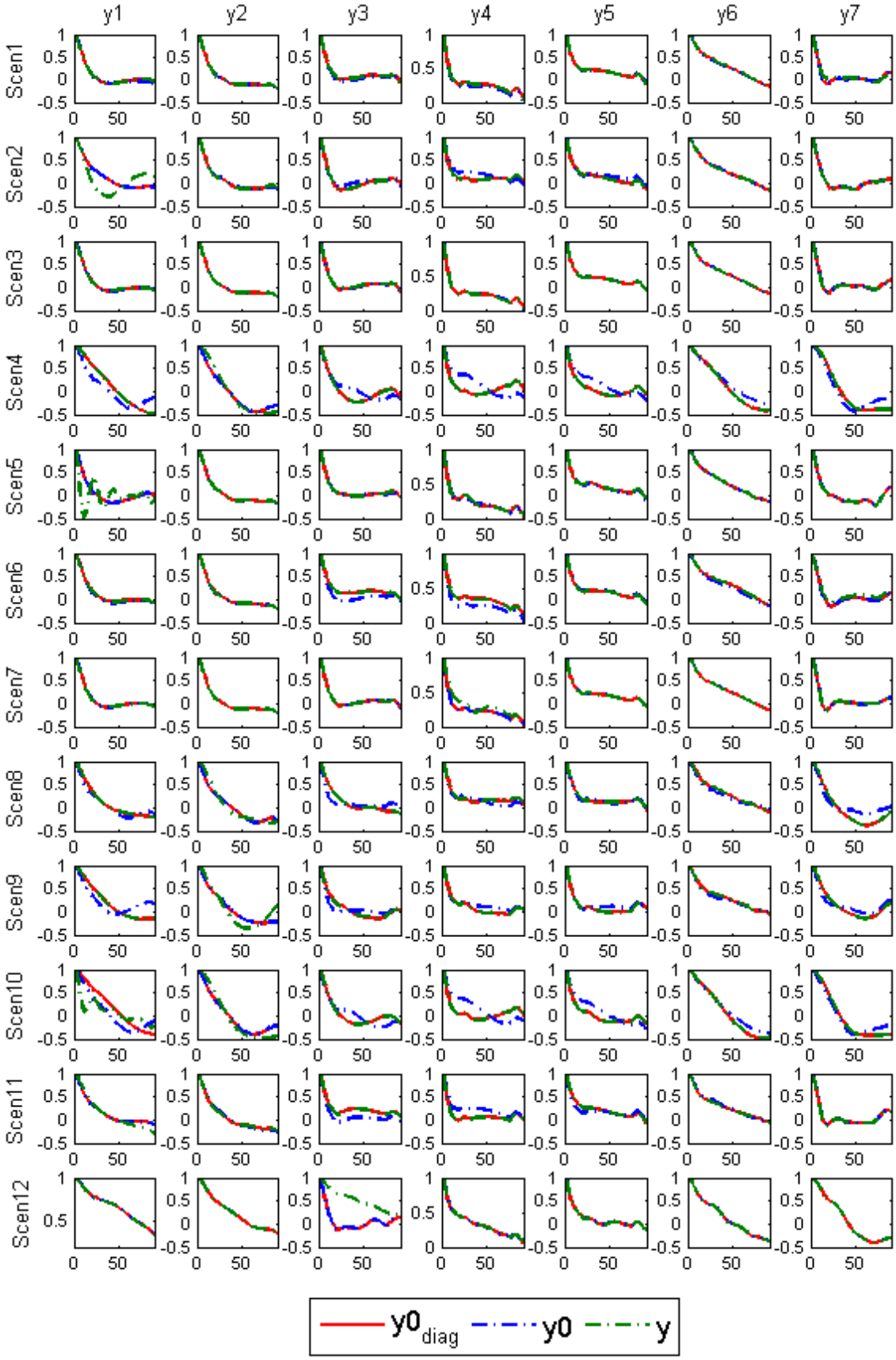

Figure 6.14: Results of ACF functions

After the identification of the variables with modeling inconsistences the next step is to detect their source. The method described in section 6.2 is applied and the results for kurtosis(co_{dkts}) and skewness (co_{dskn}) are shown in Figure 6.15.

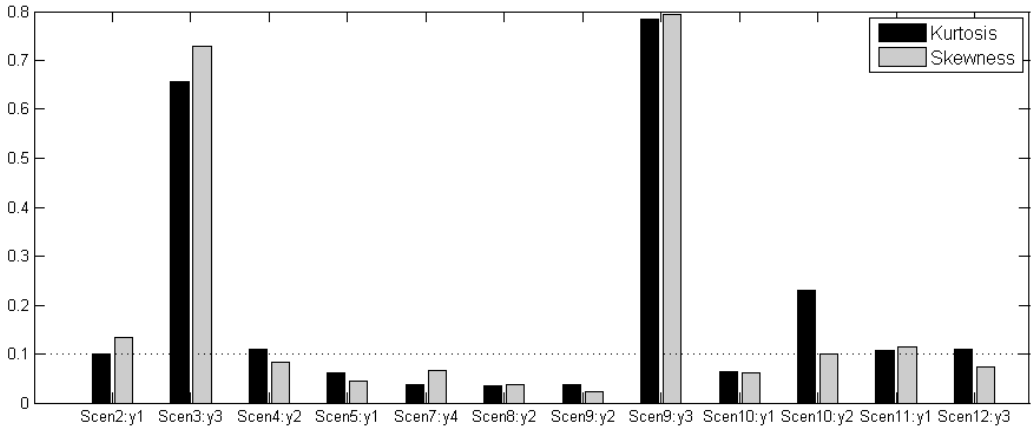

Figure 6.15: Correlation indicator of Skewness (co_{dskn}) and Kurtosis (co_{dkts})

Figure 6.15 shows the accuracy of the proposed indices to find the cause of the problem. In presence of MPM, at least one of indicators (kurtosis or skewness) tends to indicate higher values (Scen2 to Scen4, Scen9 for $y3$ and Scen10 for $y2$). In presence of UD both indicators are low (Scen5 to Scen8, Scen9 for $y2$ and Scen10 for $y1$). The method can also detect the presence of model-plant mismatches in the measured disturbance models (Scen11 and Scen12).

6.5.2 Exhaustive tests

CV affected by a MPM or UD

The method was exhaustively tested to evaluate its effectivity, where 300 experiments were performed, in which 150 contain only model-plant mismatches. The channels (i.e., pair CV *versus* MV) affected for the MPM in each experiment as well as the corrupted parameter of the model (static gain, time delay or time constant) and it value were randomly selected. The remaining 150 experiments were generated considering only unmeasured disturbances. The CV affect for each disturbance as well the disturbance model Gd (Figure 6.1) are also randomly selected. Table 6.4 summarizes the possible range of each random parameter. The random selection generates MPM and disturbance of different frequencies and magnitudes, where some examples are shown in Figure 6.16.

Table 6.4: Range of random parameters

G	Static Gain	Multiplied by 0.3 to 1.5
	Time Constant	Multiplied by 0.3 to 3
	Time Delay	Added to -2 to 2
Gd (first order model)	Static Gain	Equal to 0.1 to 3
	Time Constant	Equal to 30 to 300

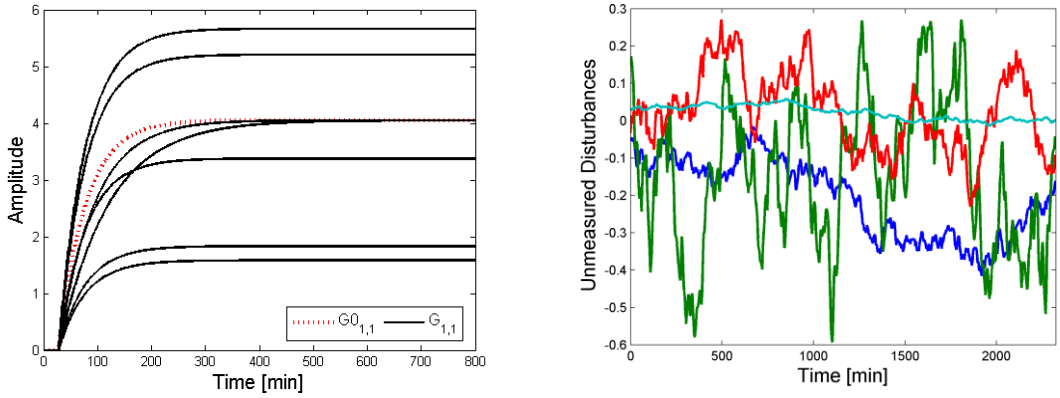

(a) **(b)**

Figure 6.16: Examples of (a) four different MPM in $G_{1,1}$ (dot line is the nominal model) and (b) four different UD randomly generated for $y1$

Simulations were performed considering step changes in the MD variables ($d1$ and $d2$), according to Figure 6.17. Firstly, the nominal system (i.e., without MPM or unmeasured disturbance) was simulated and designated as Basis Case. Each random experiment was also simulated and the methods of model assessment applied in the generated data. A noise of magnitude 1% was added in the measurements. Considering that the simulations are randomly generated, some experiments resulted in infeasible conditions. These cases corresponded to 4% of the total of experiments and were excluded of the evaluation procedure.

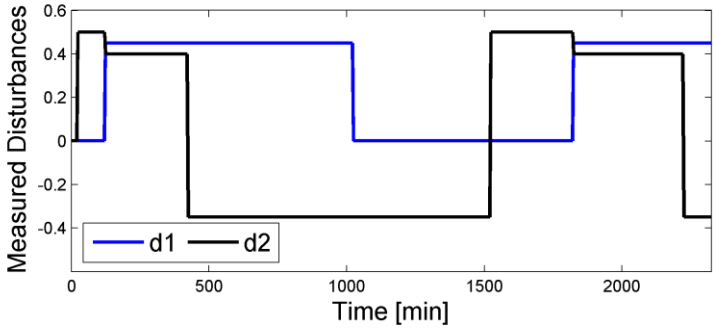

Figure 6.17: Measured disturbances step changes for the exhaustive tests

The full variance indexes $Ivar$ (equation 6.7) are compared with the Basis Case, considering the $Ivar_{basis}$:

$$Ivar_{basis} = \frac{var(y - \bar{y})}{var(y_{basis} - \bar{y}_{basis})} \tag{6.22}$$

The results are summarized in Figure 6.18. The points in the plot represent $Ivar_{basis}$ *versus* $Ivar$ for each CV in each experiment.

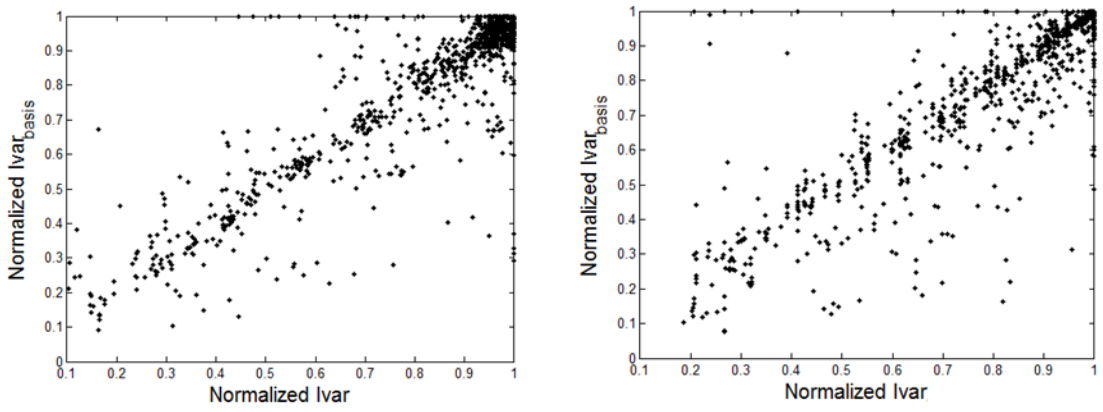

(a) MPM **(b) UD**

Figure 6.18: $Ivar_{basis}$ *versus* $Ivar$ for all CVs in each random experiment with (a) MPM and (b) with UD

Figure 6.18 show a linear tendency between the $Ivar_{basis}$ and $Ivar$. The determination coefficients (R^2) were 0.80 and 0.78 for the MPM and UD cases, respectively. It means that the method provide an estimative of MPM or UD effects in the system variance compatible with the reality.

The next steps consist in the detection of the variables and the sources responsible for the MPC degradation. In this study we consider non-impactful MPMs or UDs when $0.8 < Ivar < 1.2$. Values inside these limits represent small effects in the variables due the noise or to small numerical error. Figure 6.19 shows two experiments affecting $y1$ were $Ivar$ are 1.09 and 1.23, respectively. In the first case, y and $y0$ are very similar and do not make sense search for modeling problems. In the second, there is some detachment between y and $y0$.

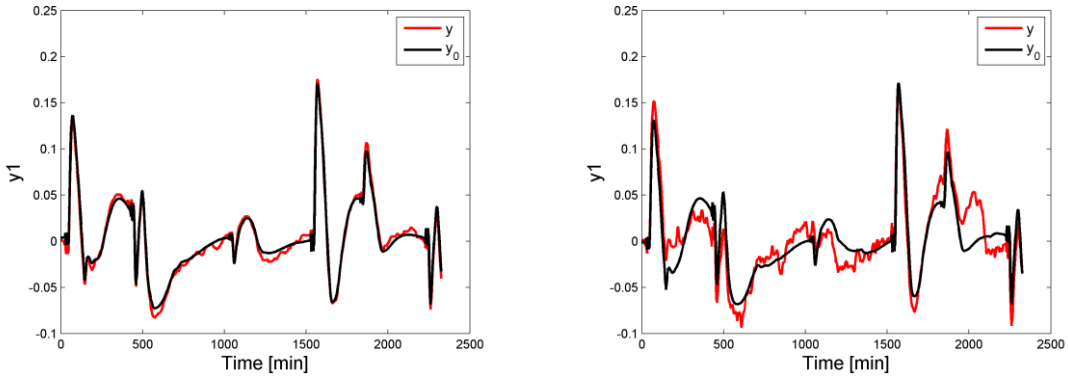

(a) **(b)**

Figure 6.19: Behavior of $y1$ in an random experiment with (a) $Ivar$=1.09 and (b) $Ivar = 1.23$

Considering cases with impactful modeling problems ($Ivar < 0.8$ and $Ivar > 1.2$) we use the $Ivar_{diag}$ (equation 6.8) to detect the variable affect by the MPM or UD. The selected variable in each case was the one with the $Ivar_{diag}$ farthest from 1. The indicated CV were confronted with the CV that, in fact, we add the MPM or UD during the data generation. This comparison was performed using the confusion matrix, presented in

Figure 6.20. A confusion matrix illustrates the number of correct classifications (at this case, the CV truly affected) *versus* the predicted classifications (at this case, the CV indicated by the $Ivar_{diag}$). The numbers of hit for each variable are located in the diagonal of the matrix while the off-diagonal elements represent the errors (except the last row and column, which are the summarization of the results). The results show that the $Ivar_{diag}$ was capable to correctly indicate the variable affected by the modeling problem in 100% of the evaluated cases.

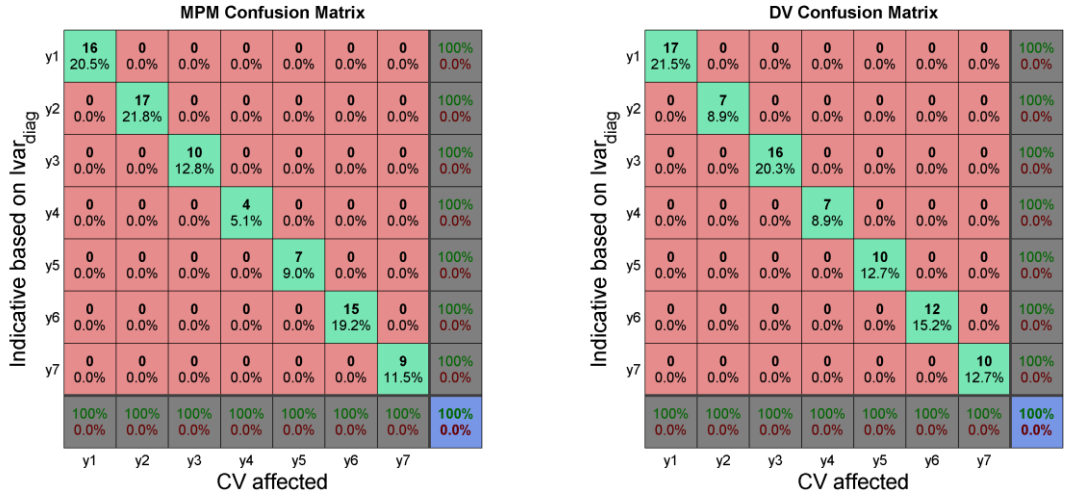

(a) MPM **(b) UD**

Figure 6.20: Confusion matrix of random experiments with impactful (a) MPM and (b) UD: Indicator based in $Ivar_{diag}$ *versus* truly CV affected

The last step of the method is to verify if the CVs indicated by $Ivar_{diag}$ are corrupted by a MPM or UD. The results considering the I_{MPM} indicator (equations 6.10 to 6.15) are presented in Figure 6.21.

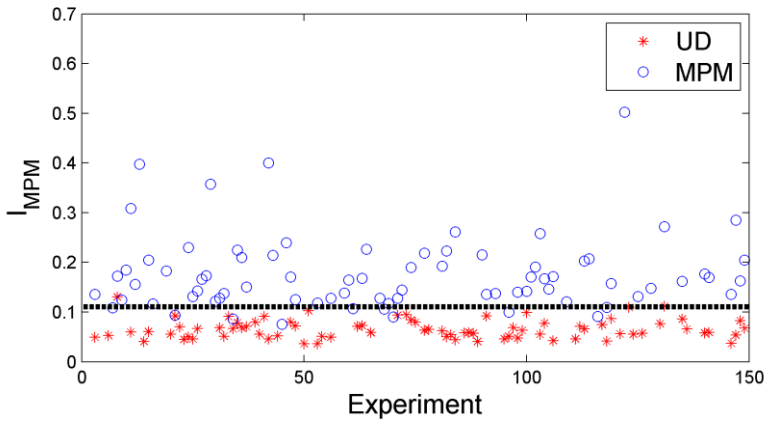

Figure 6.21: I_{MPM} indicator for the valid random experiments with MPM or UD. Threshold value corresponds to the dashed line ($I_{MPM} = 0.1$)

Figure 6.21 shows that the method was capable to discern between MPM and UD in the most cases. In 97.5% of experiments with UD the I_{MPM} was smaller than 0.1. The highest value was 0.13, the lowest was 0.035 and the mean was 0.065. For the

experiments with MPM, in 92.3% of cases the I_{MPM} was larger than 0.1. The lowest value was 0.075, the highest was 0.5 and the mean was 0.18.

CV affected by a MPM and UD

In most real process, it is common that the variables are affected by MPMs and UDs at the same time. Thus, the method of model assessment must to be capable to capture the dominant effect. To illustrate, 100 random experiments containing MPM and UD were performed, considering the ranges of Table 6.4. Simulations were performed considering step changes in the MD variables ($d1$ and $d2$), according to Figure 6.17. Each experiment was simulated three times: Firstly only with MPM, next only with UD and finally with both. Noise with magnitude of 1% was added in the measurements. The experiments that resulted in infeasible conditions are excluded of the evaluation procedure. The $Ivar$ for each scenario (i.e., with MPM and UD) is compared with the $Ivar_{basis}$, as shown in Figure 6.22.

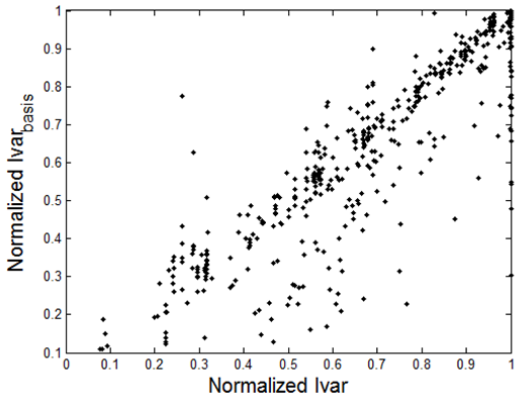

Figure 6.22: $Ivar_{basis}$ *versus* $Ivar$ for all CVs in each random experiment with MPM and UD

Figure 6.22 shows a linear relation between the $Ivar_{basis}$ and $Ivar$, with determination coefficients (R^2) of 0.78, showing that the method provide an estimative of modeling inconsistences effects in the system variance compatible with the reality. Considering cases with impactful modeling problems ($Ivar < 0.8$ and $Ivar > 1.2$) we use the $Ivar_{diag}$ (equation 6.8) to detect the variable affect. The selected variable in each case was the one with the $Ivar_{diag}$ farthest to 1. The indicated CV were confronted with the CV that, in fact, we add the MPM and UD during the data generation. This comparison was performed using a confusion matrix, presented in Figure 6.23. The results show that the $Ivar_{diag}$ was capable to correctly indicate the variable affected by the modeling problem in 100% of the evaluated cases.

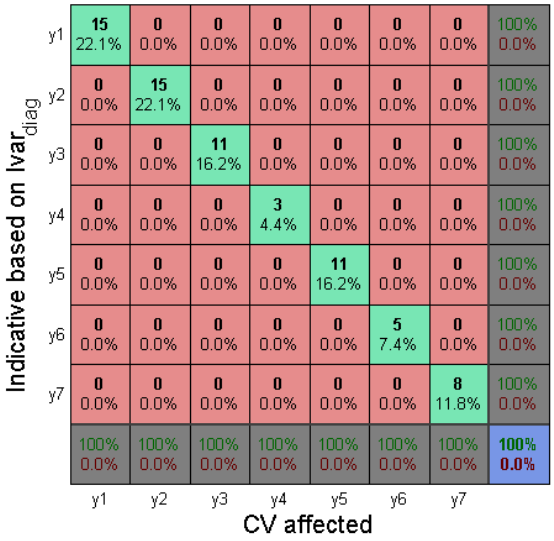

Figure 6.23: Confusion matrix of random experiments with MPM and UD: Indicator based in $Ivar_{diag}$ *versus* truly CV affected

The last step of the method is to verify if the CVs indicated by $Ivar_{diag}$ are dominantly corrupted by a MPM or UD. The dominant effect was determinate according to:

$$dominance_{MPM}(i) = \frac{Ivar_{diag}^{MPM}(i)}{Ivar_{diag}^{MPM}(i) + Ivar_{diag}^{UD}} \tag{6.23}$$

were $Ivar_{diag}^{MPM}$ and $Ivar_{diag}^{UD}$ are the $Ivar_{diag}$ for the experiments generated only with MPM and UD respectively and *i* is the affected CV. These results are confronted with the I_{MPM} in Figure 6.24.

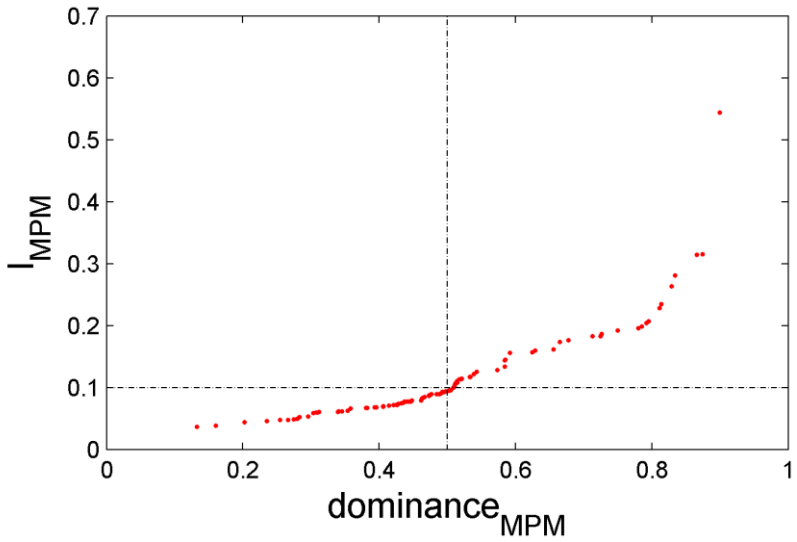

Figure 6.24: Dominance of MPM *versus* I_{MPM} of random experiments with MPM and UD

Figure 6.24 shows that the I_{MPM} becomes higher as more dominant is the MPM. When both effects are similar ($dominance_{MPM} \cong 0.5$) the I_{MPM} is near to 0.1. Cases where the UD is much more evident ($dominance_{MPM} < 0.3$) the I_{MPM} tends to be

smaller than 0.05. Similarly, when a MPM is much more evident ($dominance_{MPM} > 0.7$) the I_{MPM} tends to be higher than 0.2. These results prove that the method is capable to assess the MPC model even when more than one modeling inconsistence is present.

Sensitivity of S_0

The heart of proposed method is the sensitivity function (S_0), which provides the system closed loop response. Considering that the studied MPC is based in the optimization problem presented equation 6.19 and 6.20, it has a varying control structure. It means that the closed loop response of the system will not depend solely of the tuning, but also of the active soft constraints as well of the manipulated variables that are available. Therefore, there is not a single S_0 that characterizes the proposed MPC.

Although the estimation of the sensitivity function is a simple procedure, it is desirable to evaluate the impact of uncertainty in S_0 , which is the scope of this section. The evaluation is restricted to the diagonal S_0.

Considering the diagonal elements S_0 of $y1$, $y2$ and $y7$ (Figure 6.10), which are the CVs that have active constraints in the basis case. Each diagonal model was approximated by the following second order model:

$$S_0^{aprox} = 1 - \frac{1}{{\tau_{S0}}^2 s^2 + 2\tau_{S0}\xi_{S0}s + 1} \tag{6.24}$$

Modifications are performed in the S_0^{aprox} by multiplication of τ_{S0} and ξ_{S0} for a constant varying from 0.2 to 2. Figures 6.25 and 6.26 compared the real model ($S_{0_{true}}$) with the modified ($S_{0_{modified}}$).

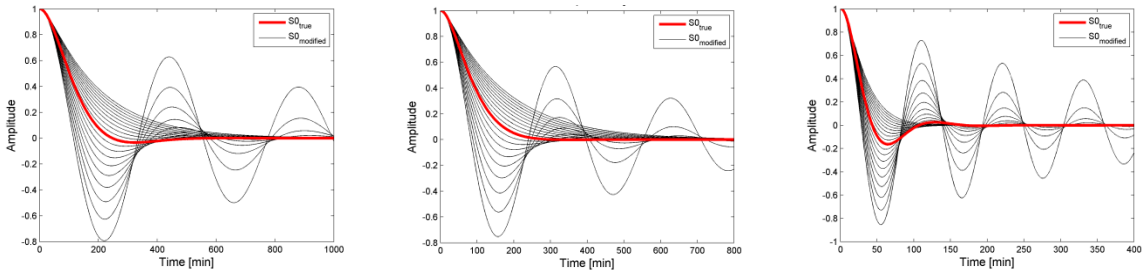

(a) **(b)** **(c)**

Figure 6.25: $S_{0_{modified}}$ by ξ_{S0} variation in the diagonal of sensitivity $y1$(a), $y2$(b) and $y7$(c)

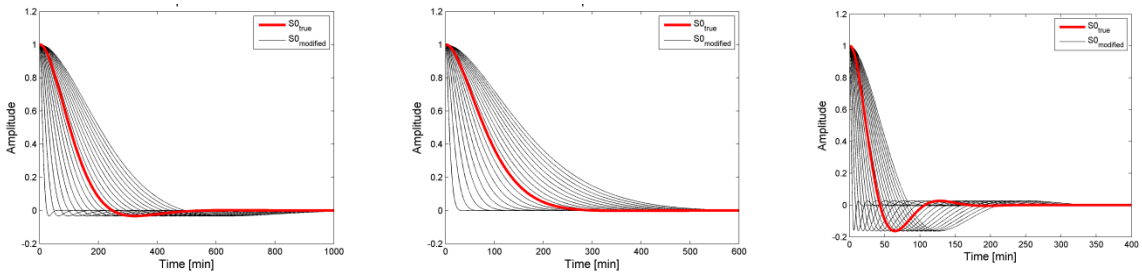

(a) **(b)** **(c)**

Figure 6.26: $S_{0_{modified}}$ by τ_{S0} variation in the diagonal sensitivity of $y1$(a), $y2$(b) and $y7$(c)

Considering all the 400 random experiments described in section 6.5.2, the ones were the affected CV are $y1$, $y2$ and $y7$ were selected. For each experiment, equation 6.8 was applied considering all modified models. The obtained relation of $Ivar_{diag}$ of modified and true models ($Ivar_{modified}$ and $Ivar_{true}$) are presented in Figures 6.27, 6.28 and 6.29, where each line is associated with a different experiment.

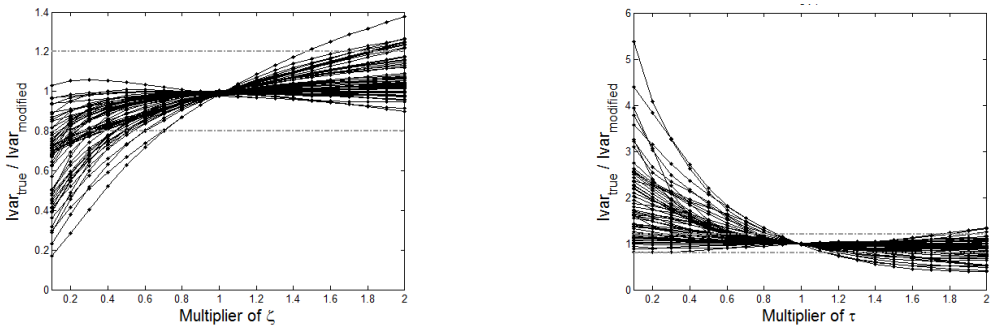

(a) **(b)**

Figure 6.27: Relation between the $Ivar_{diag}$ of true and modified S_0 for $y1$

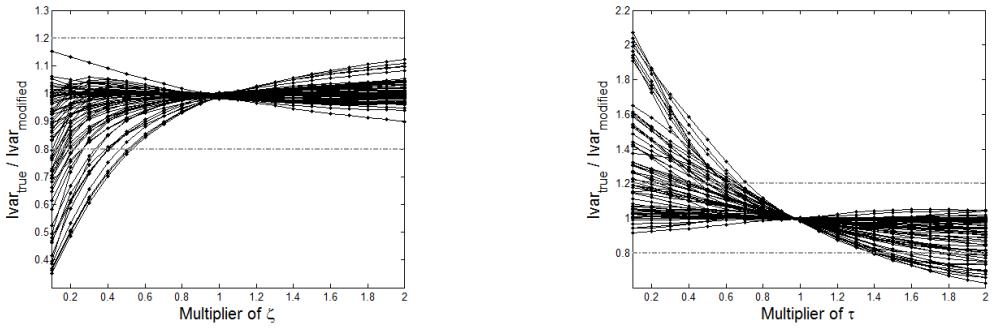

(a) **(b)**

Figure 6.28: Relation between the $Ivar_{diag}$ of true and modified S_0 for $y2$

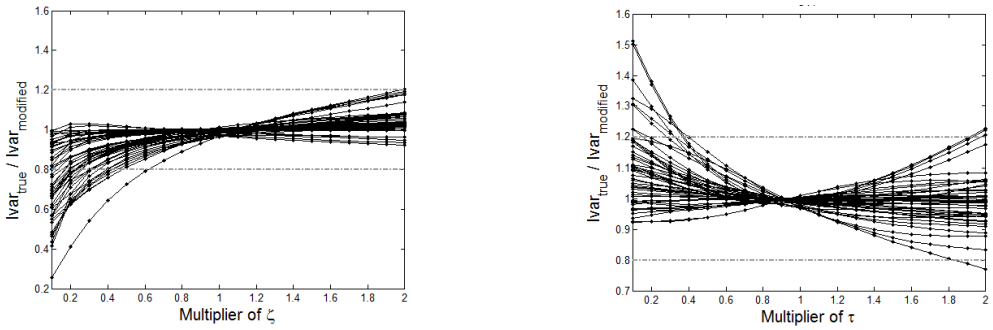

(a) **(b)**

Figure 6.29: Relation between the $Ivar_{diag}$ of true and modified S_0 for $y7$

Figures 6.27, 6.28 and 6.29 show that an uncertainty of 25% in S_0 (i.e., multipliers between 0.75 and 1.25) causes an increment of ±0.2 in the $Ivar_{diag}$, when compared with the true result, which is the acceptable tolerance in the variance of this system (see Figure 6.19). Multipliers far from these limits cause an increment in the $Ivar_{diag}$ which could affect the result of the methodology. The question now is, how much a change in the MPC control structure impact in S_0?

Suppose a hypothetical case where $u1$ is unavailable (i.e., it is fixed). In this condition one degree of freedom is lost, and now 2 CVs ($y1$ and $y2$) are optimized while $y7$ remains inside the soft constraints. Figures 6.30 and 6.31 illustrate the expected behavior when a step disturbance is added in $y1$. The diagonal S_0 for $y1$ was estimated considering the described scenario. Figure 6.32 illustrate the result.

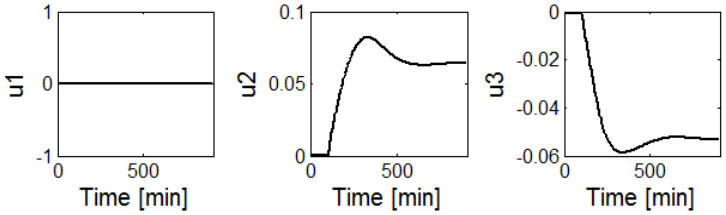

Figure 6.30: Expected behavior of MVs when $u1$ is fixed

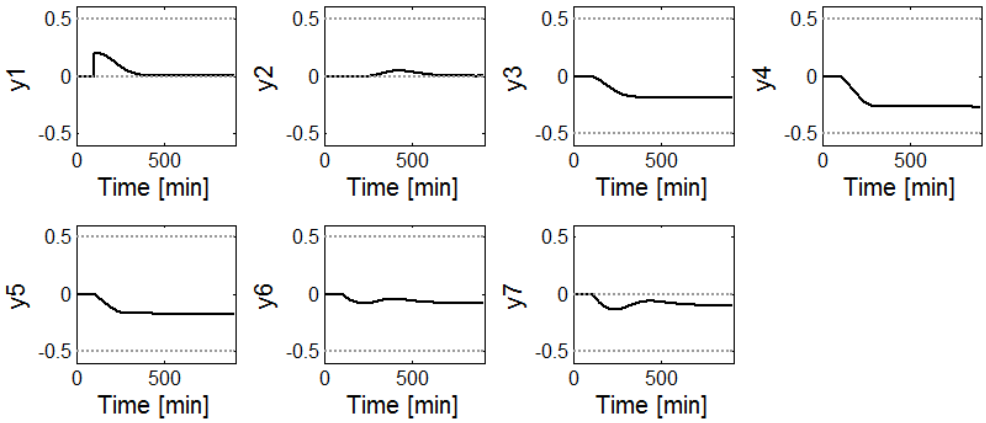

Figure 6.31: Expected behavior of CVs when $u1$ is fixed

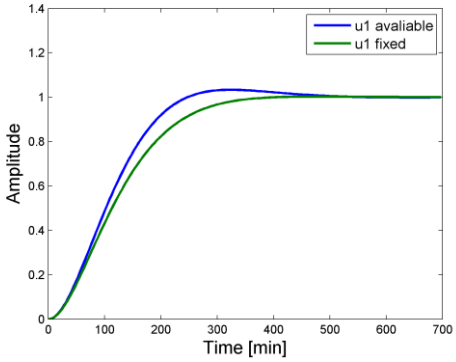

Figure 6.32: Estimated diagonal S_0 for $y1$ considering $u1$ fixed and $u1$ avaliable

Figure 6.32 show that, although a significant change in the control structure has occurred, the sensitivity of the system has a small change. The multiplayer of τ_{S0} and ξ_{S0} are 1.03 and 1.18, respectively. This result illustrates that the method allow a certain degree of uncertainty in S_0 which is compatible with a change in the control structure of the MPC.

6.6 Conclusions

This paper aims to evaluate the effectiveness of the methods proposed by Botelho *et al.* (2015a/cap. 3, b/cap. 4 and c/ cap. 5) for MPC model assessment in controllers where range variables (i.e. soft constraints) are used. This control policy is a common practice in industry due to the absence of degrees of freedom in the most real plants and because of optimization layer. The independence of setpoint is one the advantages of the method that allow its application in these systems.

The methods have been applied in the Shell Heavy Oil Fractionator case study. The configured controller contains 7 controlled variables, 3 manipulated variables and two measured disturbance. The objective of the MPC is to operate the system in the best profit and keep the CVs inside of the soft constraints.

Twelve scenarios containing MPMs and UDs were selected to represent some common effects of modeling problems in MPCs. The results show that, in all cases, the proposed method was capable to providing the diagnosis compatible with the corresponding scenario, indicating the effect of the modeling problems in all variables, pointing the affected variable and if the problem come from a MPM or UD. The method also works for evaluating modeling problems in feed-forward models.

The method was also exhaustively tested performing 400 experiments were, in which 150 only contained MPM and 150 only contained UD and 100 contained both. Firstly, the variance index of estimated nominal output was compared with the basis case (i.e., data generated without MPM or UD). The results show a linear relation between them ($R^2 \cong 0.8$), indicating that the method is capable to estimate the effect of a MPM in the variance of the system. For the cases where the variance of the system suffered significant variance increase, the method indicates in 100% what is the CV were the modeling problem is contained. The method was capable of indicating if the modeling problem is a MPM or DV, indicating in 95% of experiments that contain MPM or DV the correct problem. When both effects are available, the method shows a coherent result, showing a higher indicative of MPM as the effect of this problem is more dominant.

The sensitivity of $S_{0_{diag}}$ was evaluated considering the 400 random experiments previously generated. The results shows that the method allow an uncertainty of 25% in the $S_{0_{diag}}$ and that this value was compatible with the change in control structure tested.

Capítulo 7 – **Model Assessment of an Industrial MPC**

Abstract[9]**:** The poor model quality is one of the most frequent causes of performance deterioration in Model Predictive Controllers. So, a frequent model evaluation and correction is a fundamental. Several methods of model assessment are available in literature, but most of them are not able to deal with Model Predictive Controllers (MPCs) without fixed setpoints for the controlled variables. Botelho *et al.* (2015a/cap.3, b/cap.4 and c/cap.5) proposed a series of methods for assessment of MPC models, which consider the controller tuning in the assessment procedure. Their main advantage is the setpoint independence. This paper presents the application of these methods in an industrial MPC that operate by range. The system is a MPC of a fractionating column from a delayed coke unit of a refinery locate in Brazil. The results illustrate that the method can correctly quantify the effect of modeling problems and identify it come from a model-plant mismatch or unmeasured disturbance.

Keywords: model predictive control, model assessment, model-plant mismatch, unmeasured disturbance.

[9] *Submetido para publicação no periódico "Control Engineering Practice".*

7.1 Introduction

The operation of industrial chemical plants is dependent of strategies to control the process variables. A few decades ago the unique existent control structures were grounded in classical policies, as PID. However, the technological advances promoted the rise of the complexity of the processes, and required the development of more elaborated control systems, emerging the Advanced Process Control. Among the advanced techniques, the model predictive controllers (MPCs) are the most used in the industry (Holkar e Waghmare, 2010).

The frequent maintenance of a MPC is fundamental so that it operate properly. However, this task still is a challenge due to the multi-causal nature of these controllers. The high number of tuning parameters, the strong dependency of the process model and the high diversity of commercial MPC algorithms are the major difficulties. Several works are available in literature (Huang *et al.*, 2003; Conner & Seborg*,* 2005; Badwe *et al.*, 2009; Jiang *et al.,* 2009; Kano *et al.,* 2010; Ji *et al.*, 2012; Jiang *et al.*, 2012, among others) which proposes methods for MPC monitoring and diagnosis. However, most of them are based in the classical MPC structures (i.e., with fixed setpoint). Industrial processes often do not have degrees of freedom enough to keep all the controlled variables (CVs) in a unique setpoint, and the MPCs must be configured with CVs by range. At these cases the control objective is to keep the CVs inside a limit. Therefore, the setpoints dependent techniques for MPC assessment are inadequate.

Among the sources of MPC deterioration, the presence of model-plant mismatch (MPM) and/or unmeasured disturbances (UD) are the most impactful. Bad or incomplete models could generate control actions very far from the optimal ones. Sun *et al.* (2013) estimate that more than 80% of the time of a MPC project is spent in the identification of the models, due to its importance. Hence, assess and maintaining the model quality is fundamental.

Botelho *et al.* (2015a/cap. 3), Botelho *et al.* (2015b/cap. 4) and Botelho *et al.* (2015c/cap. 5) proposed a series of methods for MPC model assessment for detecting the controlled variable (CV) with performance problems and, in the case of bad performance, diagnose if it come from a model-plant mismatch (MPM) or unmeasured disturbance (UD). The main advantage of these methods is the setpoint independence. Moreover, the methods are simple to apply and interpret. These characteristics make the methodologies flexible to several controller formulations, including MPCs with CVs by range, facilitating their industrial application for controller's assessment.

This paper presents the application of these methods in an industrial MPC where the CVs are controlled by range. The system is a fractionating column from a delayed coke unit of a refinery, located in Brazil. A description of the methods is presented in section 7.2. Section 7.3 presents the evaluated process. The results of the methods application are presented in section 7.4.

7.1 Methods for MPC model assessment

This section summarizes the method proposed by Botelho *et al.* (2015a/cap. 3, b/cap. 4 and c/cap. 5), which considers a control loop as shown in Figure 7.1, where C is the MPC controller, G_0 the nominal model, and G the real plant. The model-plant mismatch (MPM) magnitude is ΔG. The theoretical system without mismatch is shown in Figure 7.1a, for

which nominal closed loop outputs are y_0. T_0 is the nominal complementary sensitivity function. The real system, in a scenario subject to MPM, is shown in Figure 7.1b, where y_{set} corresponds to the setpoints, u are the manipulated variables, y are the measured outputs, y_{sim} are the simulated outputs of the nominal model perturbed by the actual control actions u, and T is the complementary sensitivity function. Figure 7.1c shows the real system subject to an unmeasured disturbance (UD), where v is the sequence of independent random variables, G_d is the unknown disturbance model and y_d are the disturbance signals.

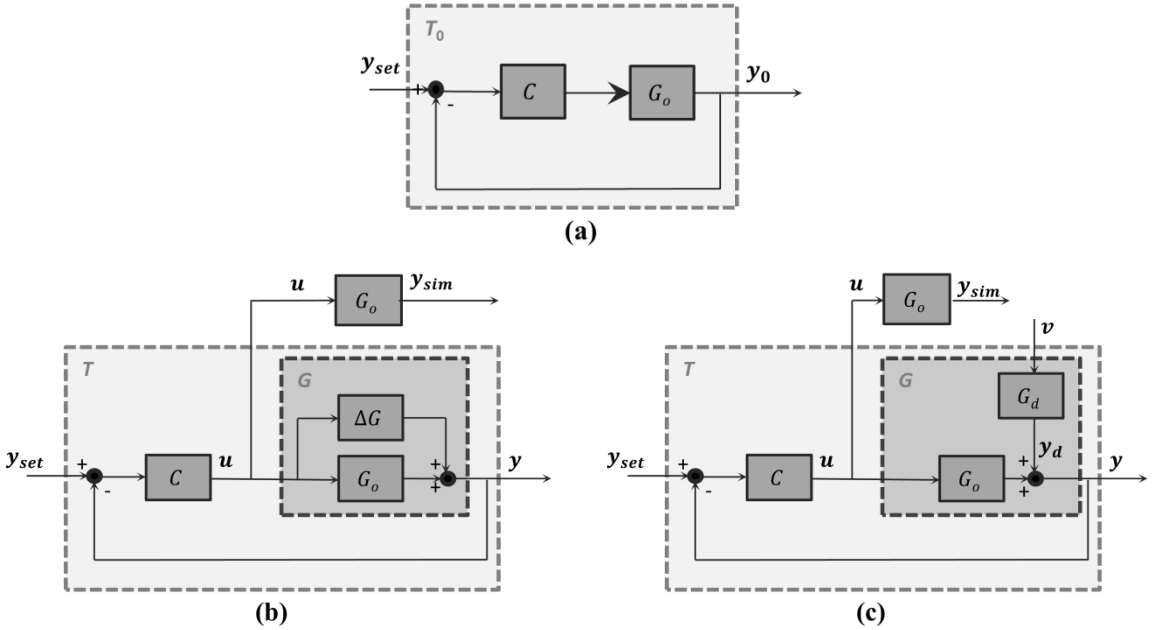

Figure 7.1: Schematic diagram of closed-loop (a) nominal system, (b) with model-plant mismatch (MPM) and (c) with unmeasured disturbance (UD)

The method is based on the premise that an effective model should represent the real system at the frequency where the MPC works. Thus, to assess the real influence of the model-plant mismatch, the closed-loop performance must be considered. The following definitions can be found in many classical control books (e.g., Skogestad & Postlethwaite, 1996):

$$y_0 = T_0 y_{set} \tag{7.1}$$

$$T_0 = G_0 C (I + G_0 C)^{-1} = (I + G_0 C)^{-1} G_0 C \tag{7.2}$$

$$S_0 + T_0 = I \tag{7.3}$$

$$y_{sim} = G_0 u \tag{7.4}$$

where S_0 is the nominal sensitivity funcion and I is the identity matrix. Botelho *et al.* (2015a/cap. 3) show that the nominal output y_0 (i.e., the output of the system in the absence of MPM or UD) could be estimated according to:

$$y_0 = y + S_0 \, (y_{sim} - y) \tag{7.5}$$

The nominal sensitivity function (S_0) is a square transfer matrix that characterizes the system response in closed loop (see equations 7.1, 7.2 and 7.3). Its dimensions are equal to the number of outputs. The diagonal elements ($S_{0_{diag}}$) give the closed loop behavior

of the outputs when their references (setpoints or soft constraints) are changed. The remaining elements provide the impact of these references variation in the others outputs. Thus, Botelho *et al.* (2015b/cap. 4) suggest an extension of equation 7.5, as follow:

$$y_{0_{diag}} = y + S_{0_{diag}} (y_{sim} - y) \tag{7.6}$$

The $S_{0_{diag}}$ works as a softening for the simulation residuals ($y_{sim} - y$), and retains only the part that is not removed by the controller feedback and is impacting in the performance of corresponding output. Variables without significant MPM or UD will have $y_{0_{diag}} \cong y$, because their simulation errors are near to zero. Applying S_0 instead of $S_{0_{diag}}$ can be used to verify how the outputs affect each other. In this case, $y_0 \neq y$ can occur even for variables without any significant MPM or UD. This difference is produced by a MPM and/or UD in another output variable and is transmitted to the other channels by coupling in S_0. The stronger is the coupling among the variable, the larger is the difference between y_0 and y, considering the existence of MPMs or UDs in the system.

Since y_0 and $y_{0_{diag}}$ are estimations of the process outputs in the absence of a model-plant mismatch or unmeasured disturbance, they could be considered benchmarks for controller-model output response, indicating how the modeling errors are being propagated and were they are located, respectively. A useful index is the comparison of output variances in nominal and real case:

$$Ivar = \frac{var(y - \bar{y})}{var(y_0 - \bar{y}_0)} \tag{7.7}$$

$$Ivar_{diag} = \frac{var(y - \bar{y})}{var(y_{0_{diag}} - \bar{y}_{0_{diag}})} \tag{7.8}$$

If $Ivar \cong 1$ means that there is no modeling problem and unmeasured disturbances affecting the corresponding output, on the other hand, when $Ivar \neq 1$ and $Ivar_{diag} \neq 1$, the corresponding output has a MPM or UD. Otherwise, when $Ivar \neq 1$ and $Ivar_{diag} \cong 1$ the corresponding output does not have trouble in their models, but its variance is being affected by MPM or UD that originates at other outputs.

Another possibility is to analyze the autocorrelation function (ACF) of $y - \bar{y}$, $y_0 - \bar{y}_0$, and $y_{0_{diag}} - \bar{y}_{0_{diag}}$. A high value of ACF means that the current signal value is strongly correlated with the past values. The ACF curves are useful to analyze the effect of MPMs and UDs in MPC speed of response or to detect oscillatory behavior (Huang & Shah, 1999).

Once the outputs with modeling problem were detected, it is desirable to identify the cause. A key issue is to determine whether the decline in performance is due to MPM or UD. The former occurs when the process model cannot adequately describe the relations between model input and output variables and a re-identification is required. On the other hand, an unmeasured disturbance occurs when there is a deterministic unknown signal influencing the output behavior. The effects of a MPM and UD in the process outputs are very similar (see Figures 7.1b and 7.1c), thus, they are not easily distinguished. To overcome this problem, Botelho *et al*. (2015c/cap. 5) proposed a systematic for identifying if the dominant effect is related to MPM or UD. The main idea

is quantify the correlation distribution between the nominal diagonal outputs $y_{0_{diag}}$ with the nominal error $e_{0_{diag}}$ defined by:

$$e_{0_{diag}} = y_{0_{diag}} - y \tag{7.9}$$

Considering that $y_{0_{diag}}$ is the estimated output free from model-plant mismatch and unmeasured disturbances, $e_{0_{diag}}$ can be interpreted as the effect of the modeling problems in the output. When an output is under a MPM, the error come from the model, then $e_{0_{diag}}$ will be dependent of the inputs (u), as well as $y_{0_{diag}}$, causing a similar frequency pattern. When an output is under an unmeasured disturbance, $e_{0_{diag}}$ is independent of u because the disturbances come from an external source. Nonetheless, $y_{0_{diag}}$ continues to be dependent on the input variables movements. This means that the frequency of variation of $y_{0_{diag}}$ and $e_{0_{diag}}$ are uncorrelated. Therefore, the comparison between $y_{0_{diag}}$ and $e_{0_{diag}}$ patterns can be used to discriminate between model-plant mismatch and unmeasured disturbances. According to the author, the method uses the $y_{0_{diag}}$ instead y_0 because the diagonal terms allow the location of the modeling problem in each output.

The diagnosis procedure to distinguish between MPM and UD consists of the analysis of the statistical distribution of $y_{0_{diag}}$ and $e_{0_{diag}}$ along a moving window (MW). The statistical distribution is evaluated by the skewness (skn) and kurtosis (kts) coefficients:

$$kts_{Xi}^{MW} = \frac{m_3}{\left(\sqrt{m_3}\right)^3} \tag{7.10}$$

$$skn_{Xi}^{MW} = \frac{m_4}{(\sqrt{m_2})^4} \tag{7.11}$$

where m_2, m_3 and m_4 are the second, third and fourth order central moment, defined as:

$$m_l = \frac{\sum_{i=1}^{MW}(X_i - \bar{X})^l}{MW}, l = 2,3,4 \tag{7.12}$$

Where X_i is the evaluated dataset ($y_{0_{diag}}$ or $e_{0_{diag}}$) and $\bar{X}$ is it corresponding mean. A high value of kurtosis means that the data present a large number of recordings away from the mean, when compared with a normal distribution. The sample skewness provides an indicator of how asymmetric is the dataset.

Botelho *et al.* (2015c/cap. 5) analyze different approaches to compare $y_{0_{diag}}$ and $e_{0_{diag}}$. The most reliable alternative is based on the Pearson's correlation coefficients of skewness and kurtosis derivatives. A scan is performed varying MW size in the neighborhood of the prediction horizon ($0.5ph$ to $2ph$, where ph is the MPC's prediction horizon). The indicators (co_{dkts} and co_{dskn}) are based in the mean of absolute correlation between the derivatives of statistical distributions:

$$co_{dkts} = \frac{\sum_{MW=0.5ph}^{2p}\left|corr\left(\frac{d}{dt}kts_{e_{0_{diag}}}^{MW}, \frac{d}{dt}kts_{y_{0_{diag}}}^{MW}\right)\right|}{n_{MW}} \tag{7.13}$$

$$co_{dskn} = \frac{\sum_{MW=0.5ph}^{2p} \left| corr\left(\frac{d}{dt} skn_{e_{0diag}}^{MW}, \frac{d}{dt} skn_{y_{0diag}}^{MW}\right) \right|}{n_{MW}} \tag{7.14}$$

where n_{MW} are the number of scanned MW, $corr$ is the Pearson's correlation coefficient. The larger the values of co_{dkts} and co_{dskn}, the higher is the probability of a model-plant mismatch dominance. It enough one of these indices be high for classifying the performance issue caused by MPM. Botelho *et al.* (2015c/cap. 5) suggests that values higher than 0.1 characterize MPM dominance.

7.2 Case Study

7.2.1 Process description

The evaluated system is a delayed coke unit of a petroleum refinery located in Brazil. The process has the objective to convert heavy fractions of petroleum in light fractions with higher added-value through a thermal cracking. In parallel to the reactions of cracking occurs the reaction of coking, which produces a solid by-product with high molecular weight and high content of carbon (called coke) that have low commercial value (Mattos & Longhi, 2013). Figure 7.2 illustrates the system.

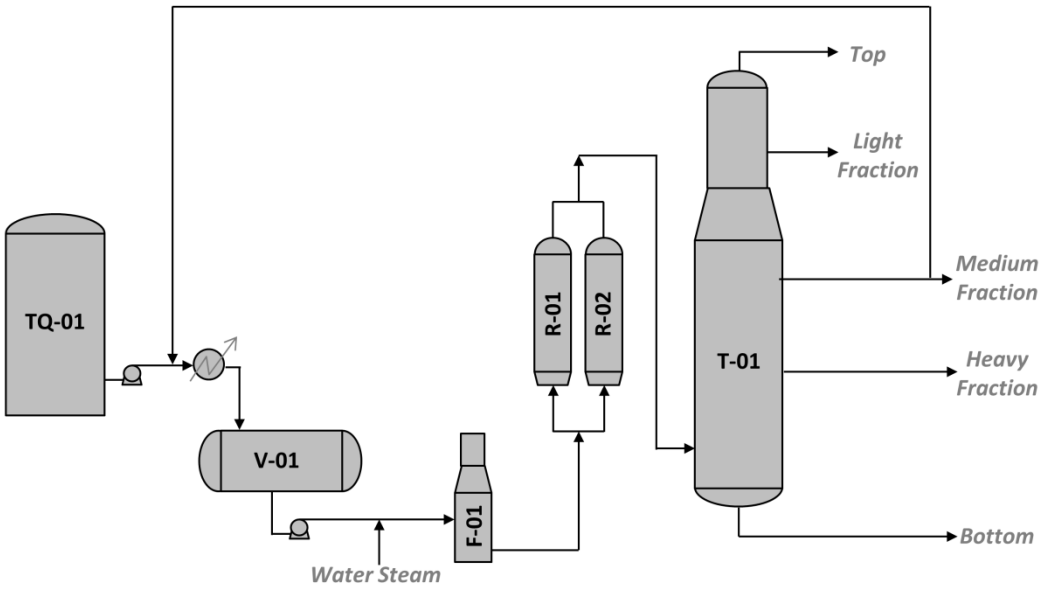

Figure 7.2: Schematic representation of the delayed coke process (Adapted from Mattos & Longhi, 2013)

The system's inlet (V-01) is composed by heavy fractions of petroleum coming from the residuals of vacuum distillation unit, stored in the TQ-01 and a recycle stream. It is sent to a preheating furnace (F-01), where its temperature reaches 500°C. Water steam is injected, increasing the flow speed to retard the reaction of coking and avoid the generation of coke inside the furnace. The outlet of F-01 feeds the coke drums (R-01 and R-02). These reactors operate alternately in batch, each one with execution cycles of 24 hours. It is necessary to remove de coke accrued inside the drums. Thus, after each execution cycle the reactors are exchanged (i.e., the flow is deviated from the drum in operation to the other drum) and the reactor out of operation is cleaned (i.e., the coke is removed) and prepared for another cycle. A fractionating column (T-01) separate the products of the cracking (Mattos & Longhi, 2013; Longhi *et al.*, 2008).

The assessed control structure is the MPC of the fractionating column (T-01). This MPC has a simple real-time optimization layer, which established the optimal operating point according to economic objectives. The scheme presented by Figure 7.3 illustrates its architecture.

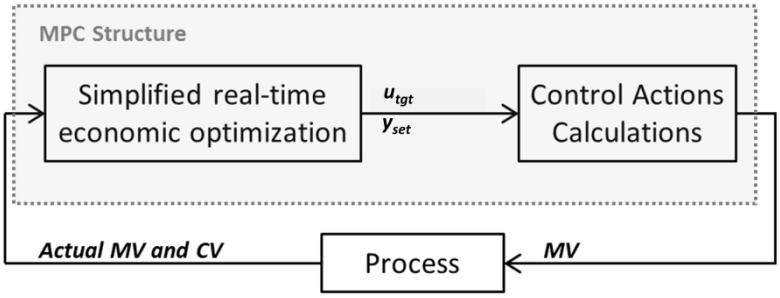

Figure 7.3: Architecture of MPC controller with optimizer (adapted from Campos *et al.,*2013)

The optimizer determines best values of MVs (u_{tgt}) and corresponding steady state solution of the CVs (y_{set}) based in the operational costs and process limits. The optimal values from the optimizer (u_{tgt} and y_{set}) are the base for the control actions calculations. This MPC operates fully by range, which means that the controller cost function is configured in terms of manipulated variables. The CVs are penalized only in cases of soft constraint violation (y_{soft}).

The MPC is composed by 12 controlled variables (CVs) operating by range and 7 manipulated variables (MVs). Besides there are two measured disturbances (DVs) which come from the operation of exchange and preparation of the coke drums.

7.2.2 Data characterization

For the described system, two datasets were selected, which are called Period 1 and Period 2. These periods are approximately 40 days apart from each other and either have about 3 days of operational plant data. Figures 7.4 illustrates the measured values of CVs (y) and its respective optimal values (y_{set}) and soft constraints (y_{soft}). Figure 7.5 presents de measured MVs (u) and respective optimal values (u_{tgt}) and constraints (u_{hard}). Figure 7.6 shows the measured disturbances.

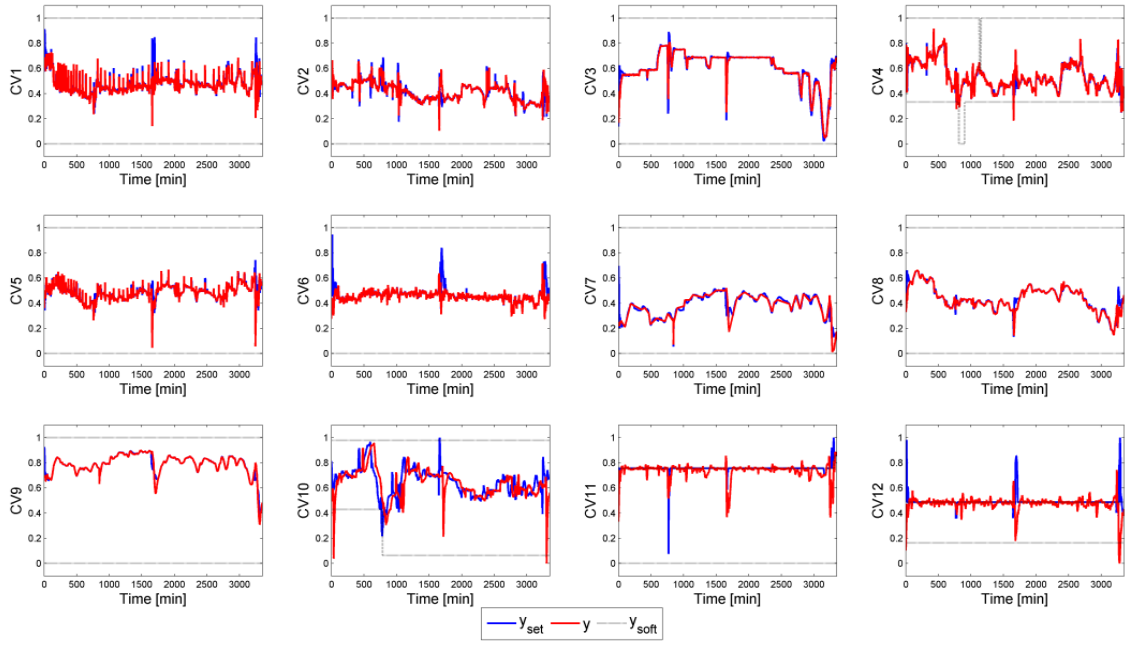

(a)

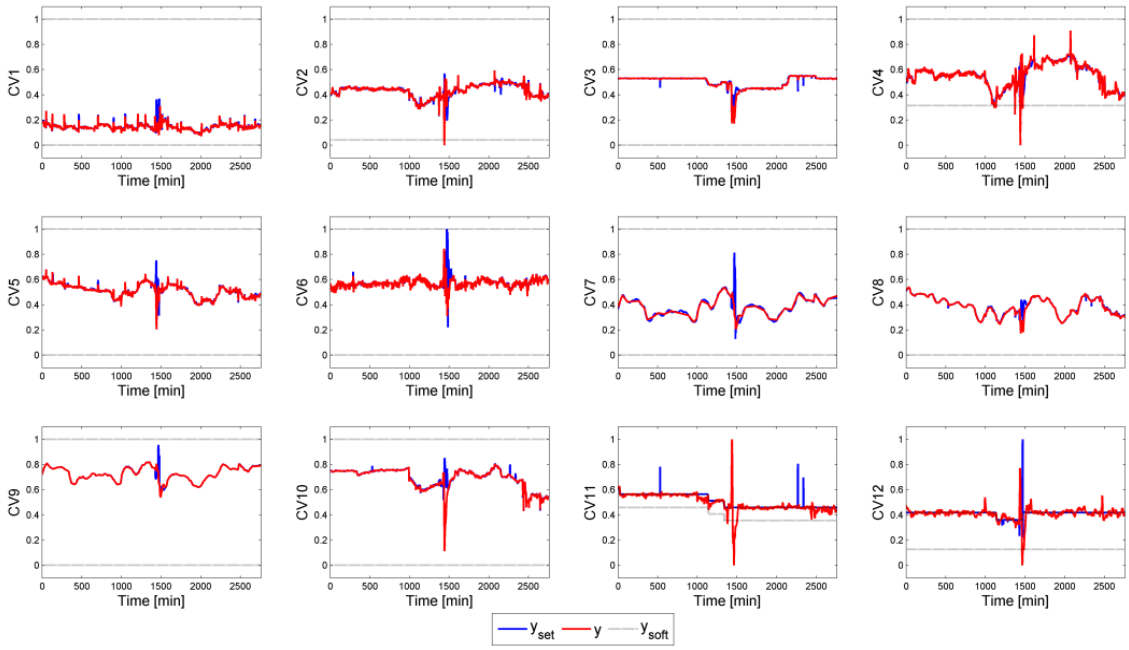

(b)

Figure 7.4: Controlled Variables of (a) Period 1 and (b) Period 2.

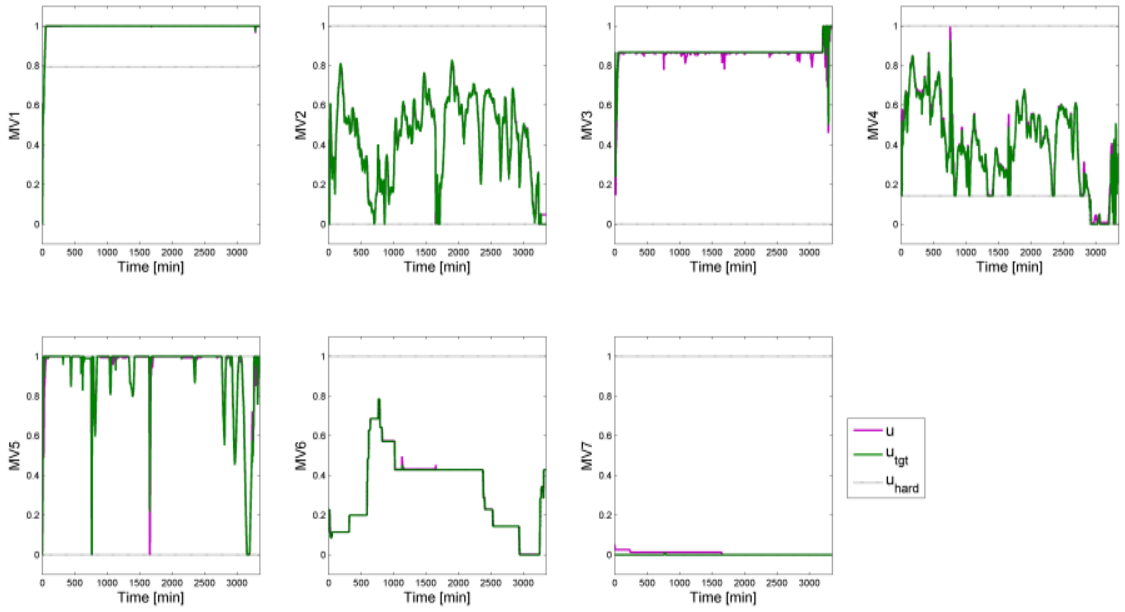

(a)

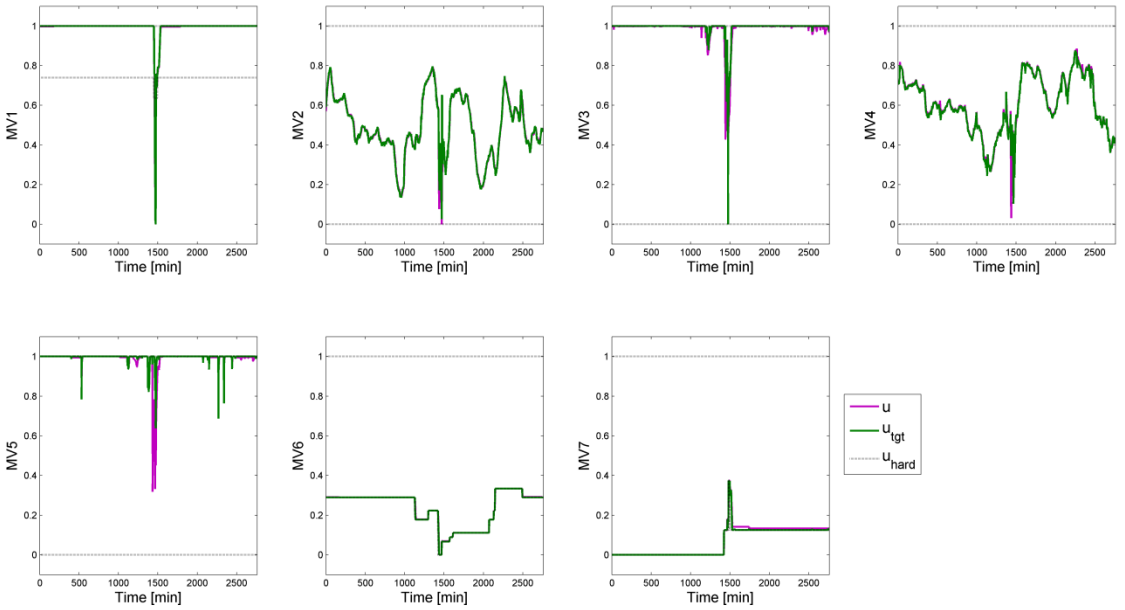

(b)

Figure 7.5: Manipulated Variables of (a) Period 1 and (b) Period 2.

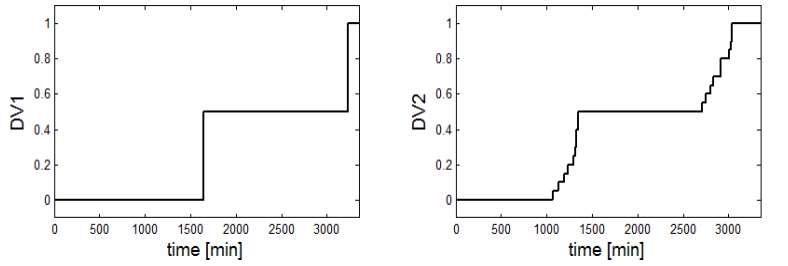

(a)

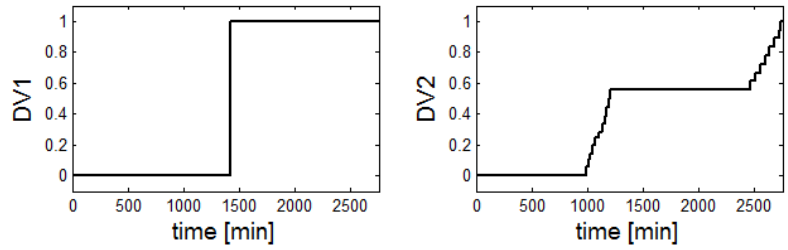

(b)

Figure 7.6: Measured Disturbances of (a) Period 1 and (b) Period 2.

Figure 7.6 shows that the selected periods include at least one complete execution cycle. Besides, according to Figure 7.5, the controller works with two degrees of freedom ($MV2$ and $MV4$) at most of time. It allows that $CV11$ and $CV12$ to have their upper soft constraints actives (Figure 7.4). The other CVs remain inside the range. Thus, we assume this scenario to estimate the closed loop response. The complementary sensitivity function (T_0) of each controlled variable (CV) of an MPC by range is defined as follows:

- The evaluated CV have an active soft constraint: in this case, its behavior is very similar to a fixed setpoint case. Thus, the static gains of the corresponding $\mathrm{T}_{0_{\mathrm{diag}}}$ will be 1. The effect of this CV in another variable with active soft constraint will generate an off-diagonal T_0 with a zero in the origin (i.e., null static gain). The effect of this CV in a variable inside the range will generate an off-diagonal T_0 with static gain different from zero, because this variable will assume a new steady state value.

- The evaluated CV is inside the range: in this case, the variable does not have any influence in the control actions. It means that the effect of the controller feedback in this variable is null. Thus, $T_0 = 0$ (diagonal and off-diagonal models) and all the simulation error is preserved.

Based on the considerations described above, the $CV1$ to $CV10$ have $T_0 = 0$, since they are inside the range. The complementary sensitivity function of $CV11$ and $CV12$ are presented in Figure 7.7. They are obtained from a simulation of the controller (see appendix A3).

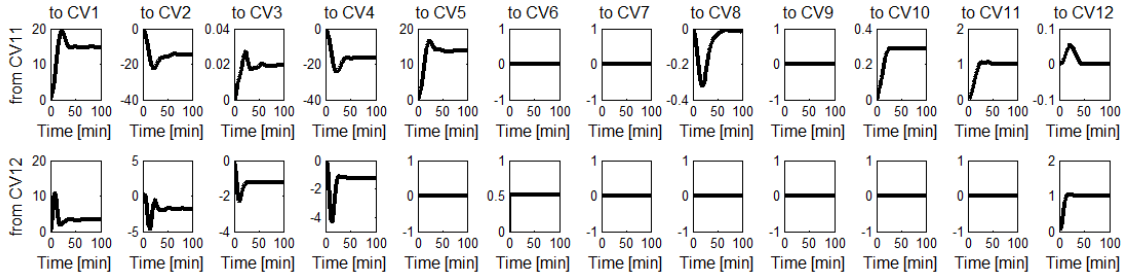

Figure 7.7: Step response of T_0 for $CV11$ and $CV12$ as input.

Figure 7.7 shows that, for the considered scenario, $CV11$ is the variable with greater interaction, since it impacts in the most CVs (except $CV6$, $CV7$ and $CV9$). The $CV12$ impacts in the behavior of $CV1$ to $CV4$ and $CV6$. All others CVs do not interact because they are inside the range. Therefore, they have none influence in the controller feedback.

7.3 Results and discussions

The methods presented in section 7.1 were applied in the selected datasets. Firstly the Variance Indexes (equations 7.7 and 7.8) were calculated. The results are presented in Table 7.1. According to this table, and considering the premise presented by Botelho *et al.* (2015d/cap. 6), that an important modeling problem occurs when $Ivar < 0.8$ or $Ivar > 1.2$, in both periods $CV3$ is the single variable that do not suffer effect of modeling problems. $CV6$, $CV7$, $CV9$, $CV11$ and $CV12$ are affected by modeling problems and they are in its own models, since $Ivar \cong Ivar_{diag}$. $CV2$ and $CV10$ have problem in their models, but they are even more affected by modeling problems coming from other CVs, because the $Ivar$ is farther to one than $Ivar_{diag}$. Some disparity was founded in the results of $CV1$, $CV4$, $CV5$ and $CV7$ between the datasets. In these cases the $Ivar_{diag}$ of one period is near to one while the other period it is significant. It means that the modeling problem not always is evident for these variables.

Table 7.1: Variances Indexes

	Period 1		Period 2	
	$Ivar$	$Ivar_{diag}$	$Ivar$	$Ivar_{diag}$
$CV1$	0.24	1.15	0.13	0.37
$CV2$	0.18	0.73	0.30	0.78
$CV3$	1.04	1.07	0.99	1.07
$CV4$	0.21	0.53	0.42	1.00
$CV5$	0.22	0.97	0.47	2.03
$CV6$	0.48	0.53	0.26	0.28
$CV7$	0.89	0.89	1.70	1.70
$CV8$	1.89	2.07	1.88	1.97
$CV9$	1.87	1.88	2.41	2.41
$CV10$	0.52	0.77	0.41	0.51
$CV11$	0.53	0.56	0.76	0.77
$CV12$	0.69	0.78	0.64	0.62

The ACFs were estimated and the results are presented in Figure 7.8. In some cases, the ACF shows the effect of modeling errors in the CVs decay ratio through the difference between y and y_0 (for example$CV9$, $CV11$ and$CV12$). Besides, this indicator also shows that the modeling problems affecting $CV6$, $CV7$, $CV9$, $CV11$ and $CV12$ are in the own variables, since $ACF(y_{0_{diag}}) \cong ACF(y_0)$

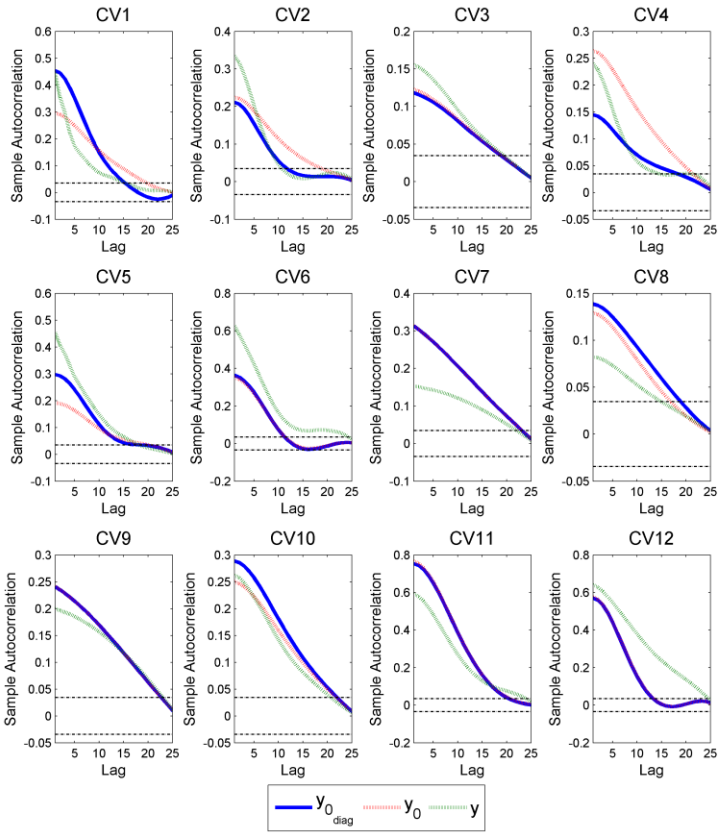

(a)

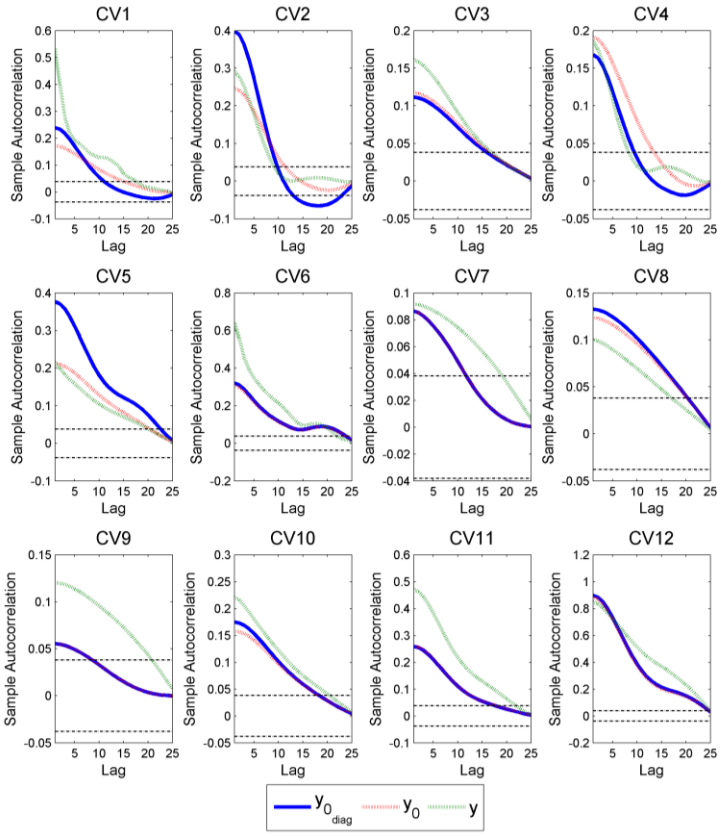

(b)

Figure 7.8: ACF for (a) Period 1 and (b) Period 2.

For the variables with significant $Ivar_{diag}$, the sources of the dominant modeling problems were evaluated. The kurtosis and skewness indicators (equations 7.13 and 14) as well as the corresponding diagnosis are presented in Table 7.2.

Table 7.2: Kurtosis and skewness indicators

	Period 1			Period 2		
	co_{dkts}	co_{dskn}	Diagnosis	co_{dkts}	co_{dskn}	Diagnosis
$CV1$	--	--	--	0.33	0.45	MPM
$CV2$	0.07	0.12	MPM	0.21	0.31	MPM
$CV3$	--	--	--	--	--	--
$CV4$	0.05	0.09	UD	--	--	--
$CV5$	--	--	--	0.07	0.14	MPM
$CV6$	0.06	0.25	MPM	0.2	0.42	MPM
$CV7$	--	--	--	0.05	0.06	UD
$CV8$	0.03	0.03	UD	0.09	0.08	UD
$CV9$	0.01	0.02	UD	0.01	0.01	UD
$CV10$	0.45	0.48	MPM	0.25	0.06	MPM
$CV11$	0.23	0.25	MPM	0.13	0.19	MPM
$CV12$	0.17	0.05	MPM	0.20	0.14	MPM

Results of Table 7.2 show that $CV8$ and $CV9$ are clearly been affected by a UD while $CV6$, $CV10$, $CV11$ and $CV12$ have MPM. The $CV4$ in Period 1 and $CV7$ in Period 2 are being affected by a UD, denoting that some punctual disturbance may have occurred in this dataset. The $CV1$ and $CV5$ in Period 2 have a MPM. Comparing Figure 7.5a and 7.5b is observed that the behavior of MVs is different between the periods. Hence the MPM diagnoses are evident only in Period 2. This fact highlights the importance of a good data selection as well as the execution of several tests, to have a reliable diagnosis of the model.

Considering that Table 7.2 indicated a significant MPM in $CV11$ and this is the variable with highest impact in the rest of the system (see Figure 7.7), the re-identification of its model was performed. As example, only a channel (i.e., a pair MV *versus* CV) $MV5\ vs. CV11$ was re-identified. Table 7.3 compare the indicators ($Ivar, Ivar_{diag}, co_{dkts}$ and co_{dskn}) for $CV11$ before and after the model re-identification.

Table 7.3: Indicators for $CV11$ before and after $CV11\ vs.\ MV5$ model re-identification

	Period 1		Period 2	
	Before	After	Before	After
$Ivar$	0.53	0.73	0.76	1.11
$Ivar_{diag}$	0.56	0.73	0.77	1.11
co_{dkts}	0.23	0.17	0.13	0.06
co_{dskn}	0.25	0.20	0.19	0.12

Results of Table 7.3 show that the re-identification of $CV11\ vs.\ MV5$ model improves the performance of $CV11$, since its $Ivar$ and $Ivar_{diag}$ are nearest to one in both datasets when the new model is considered. Besides, a reduction in values of co_{dkts} and co_{dskn} occurs. It means that the new model contributes to reduce the incidence of MPM in $CV11$.

To evaluate the effect of the new model in the remains CVs we compare the $Ivar$ after and before the model update with the corresponding $Ivar_{diag}$. The diagonal indicator of these CVs has not changed with the new model because the new model is only of $CV11$. Thus, when closer are $Ivar_{diag}$ and $Ivar$, smaller is the interaction due to the modeling errors. Figure 7.9 illustrate the results.

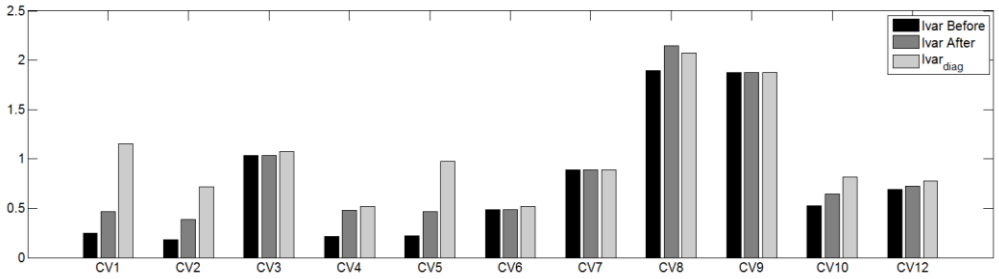

(a)

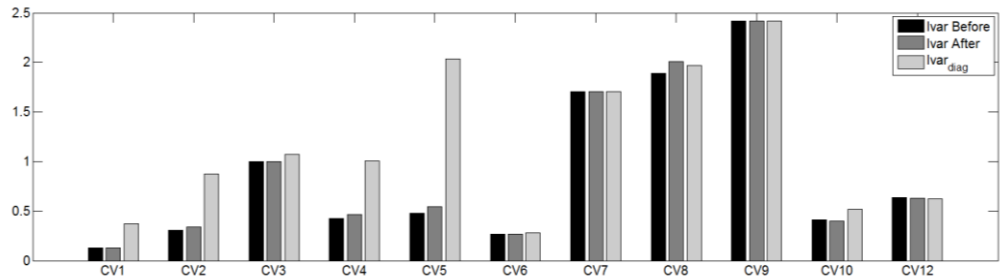

(b)

Figure 7.9: $Ivar_{diag}$ and $Ivar$ of the remain CVs before and after $CV11\ vs.\ MV5$ model re-identification for (a) Period 1 and (b) Period 2.

Results of Figure 7.9 show that the $Ivar$ of the variables after the $CV11\ vs.\ MV5$ model re-identification tends to be closer to $Ivar_{diag}$ than $Ivar$ before the re-identification. Thus, the improvement of $CV11$ had a beneficial effect in all system. This result is more evident in Period 1 than in Period 2 because the $MV5$ varies less in the second dataset.

7.4 Conclusions

This paper presented the application of the methods proposed by Botelho *et al.* (2015 a/cap.3, b/cap.4 and c/cap.5) for the assessment of MPC models of a fractionating column from a delayed coke unit of a refinery located in Brazil.

Results show that the methods are capable of indicating the model errors impacting in the controller performance based only in process data and in the response in closed loop. The methods indicate the effect of the modeling problems in the own controlled variable as well as how each CV are being affected by problems coming from other models. The methods also allow the diagnosis the root of the modeling problem, discerning between model-plant mismatches or unmeasured disturbances. It must be emphasized that the method has the advantage to work with MPCs by range, which make it flexible to the most of industrial applications.

Additionally, the methods allow to verify the benefits achieved after a model re-identification. This approach opens another field for the methods, which complements the model identification procedure, so that the identified models can be assessed before they are implanted in the controller.

Capítulo 8 – **Considerações Finais**

8.1 Conclusões

Este trabalho teve como objetivo principal o desenvolvimento de uma ferramenta para avaliação de modelos de controladores preditivos. Tal ferramenta é capaz de fornecer diagnósticos compatíveis com as características dos controladores industriais reais, destacando-se os sistemas de controle não quadrados, onde o número de variáveis controladas é maior que o número de manipuladas e, consequentemente, a operação por faixas é necessária.

Uma revisão dos principais métodos disponíveis na literatura foi realizada. Constatou-se que, embora exista uma vasta gama de metodologias, a maioria delas possui pouca aplicabilidade prática, principalmente por serem baseadas em referências incompatíveis com os MPCs reais (como LQG, MVC, etc.) ou por necessitarem de testes intrusivos na planta. As técnicas de maior potencial foram testadas em dois controladores hipotéticos: um deles com a configuração clássica de um MPC e o outro com as CVs operando por faixas. Os resultados obtidos indicaram que as mesmas não são capazes de promover um diagnóstico confiável dos modelos quando o sistema de controle não possui setpoints fixos para as variáveis controladas.

Esta tese de doutorado desenvolveu uma metodologia que leva em conta a sintonia do controlador na investigação dos problemas operacionais de MPCs. Os resultados mostraram que o emprego da sensibilidade nominal da malha, que é a base da metodologia proposta, é capaz de detectar corretamente o impacto dos problemas de modelagem no desempenho do MPC. Os resultados foram comparados com o método de Badwe *et al.* (2010) e se mostraram superiores, já que, ao contrário do método de Badwe *et al.* (2010), a metodologia proposta independe dos setpoints e de identificações de modelos baseada em dados de processo.

Uma extensão da metodologia anteriormente descrita foi desenvolvida, cujo objetivo consiste na localização das variáveis controladas com os erros de modelagem responsáveis pela degradação do desempenho. Esta técnica é especialmente útil para

sistemas com elevado grau de acoplamento, de modo que pequenos erros de modelagem podem levar todo o sistema muito próximo a sua instabilidade. A técnica proposta foi comparada com o método de Sun *et al.* (2013) através de dois estudos de caso, a qual mostrou resultados superiores, especialmente nos casos onde as variáveis manipuladas oscilam nas suas restrições e existe mais de um problema de modelagem ocorrendo ao mesmo tempo.

Para complementar a ferramenta, mais uma metodologia foi desenvolvida. Seu objetivo consiste na detecção da causa da degradação do modelo, indicando se a mesma é proveniente de uma discrepância no modelo ou de um distúrbio não modelado ou medido. A metodologia se baseia na comparação entre a distribuição estatística do comportamento nominal do sistema com os erros de modelagem. Diversos indicadores foram sugeridos. Os resultados mostraram que a técnica é capaz de discernir entre o problema dominante (MPM ou UD) de forma adequada e que a avaliação da derivada dos coeficientes de assimetria e curtose é o indicador mais eficiente.

A ferramenta completa (i.e, as técnicas de detecção do impacto dos erros de modelagem, localização das CVs responsáveis e identificação da fonte de degradação) foi aplicada a um sistema simulado, no qual contou com um MPC configurado por faixas e camada de otimização dinâmica. A ferramenta foi testada exaustivamente a partir de centenas de experimentos aleatórios que geraram dados contendo discrepâncias de modelos e distúrbios não medidos. Concluiu-se que a taxa de acertos no diagnóstico dos modelos é superior a 90%. Neste mesmo estudo de caso, testes foram realizados a fim de se quantificar o grau de incerteza admitido na função de sensibilidade. Constatou-se que erros da ordem de 20% são admitidos, o que indica que a mesma é flexível a pequenas mudanças na estrutura de controle (devido à saturação das MVs, ou mudança de restrição ativa das CVs, por exemplo) sem que S_0 precise ser atualizado.

A ferramenta também foi aplicada ao controlador preditivo da Unidade de Coqueamento Retardado da REFAP. A qualidade dos resultados obtidos foi similar aos estudos de casos testados até então. As metodologias propostas foram capazes de detectar discrepâncias de modelos e distúrbios não medidos. Adicionalmente, elas permitiram que se analisasse a qualidade da solução proposta, o que permite a sua utilização na solução dos problemas, indo além das etapas de auditoria e diagnóstico.

Pode-se concluir que o presente trabalho levou a resultados coerentes e conclusivos em todas as aplicações estudadas. Ainda há muito a ser desenvolvido, dada à complexidade do assunto, porém espera-se que este seja a base de uma ferramenta funcional, que possa fornecer um diagnóstico efetivo dos MPCs reais, desenvolvida com enfoque em controle preditivos normalmente empregados na indústria.

8.2 Sugestões para trabalhos futuros.

Um grande esforço está sendo realizado para que esta metodologia vire um padrão viável de aplicação industrial. Isso significa que, além de ser flexível às diversas estruturas de controle existentes na indústria, ela deve exigir pouca carga computacional e gerar resultados de fácil interpretação. Resultados preliminares já indicaram que os métodos desenvolvidos possuem potencial de serem aplicados na prática, contudo, ainda existem alguns aspectos a serem aperfeiçoados.

Dentre os aspectos a serem estudados está à obtenção da função de sensibilidade nominal. Alguns estudos indicaram que as técnicas propostas admitem certo grau de incerteza nesta propriedade. Entretanto, é necessário se avaliar o quão realista é esse grau de incerteza e se o mesmo é semelhante para a maioria dos processos. Deve-se também estudar qual é a hipótese de se utilizar um identificador online para S_0, o qual deve detectar a condição atual do processo (i.e., quais variáveis estão com suas restrições ativas) e identificar os modelos nestas condições. Como S_0 é obtido a partir de dados simulados, os parâmetros do modelo bem como as perturbações que favorecem sua obtenção podem ser configurados previamente, o que torna a identificação destes modelos um processo relativamente simples.

Também é desejável que a ferramenta indique, não só a variável controlada, mas também o par $CV\ vs.\ MV$ cujo modelo está com problemas. Indo além, almeja-se que sejam sugeridas variáveis candidatas a serem incluídas na matriz de modelos do MPC. Ressalta-se que estudos desta natureza estão em desenvolvimento no grupo de pesquisa e resultados promissores vêm sendo obtidos.

Referências

Adams, K., Lawrence, E. (2015). *Research Methods, Statistics, and Applications*. Sage Publications, California

Agarwal, N., Huang, B. (2007a). Assessing Model Prediction Control (MPC) Performance. 1. Probabilistic Approach for Constraint Analysis. *Industrial & Engineering Chemistry Research*, v. 46, p., 8101-8111.

Agarwal, N., Huang, B. (2007b). Assessing Model Prediction Control (MPC) Performance 2. Bayesian Approach for Constraint Tuning. *Industrial & Engineering Chemistry Research*, v. 46, p., 8112-8119.

Alcala,C., Qin, S. (2009). Reconstruction-based contribution for process monitoring. *Automatica*, v. 45, p. 1593-1600.

Alcala,C., Qin, S. (2011). Analysis and generalization of fault diagnosis methods for process monitoring. *Journal of Process Control*, v. 21, p. 322–330.

Alghazzawi A., Lennox, B. (2009). Model predictive control monitoring using multivariate statistics. *Journal of Process Control*, v. 19, p. 314–327.

Badwe, A., Gudi, R., Patwarhan, R., Shah, S., Patwarhan, S. (2009). Detection of model-plant mismatch in MPC applications. *Journal of Process Control*, v. 19, p. 1305–1313.

Badwe, A., Patwarhan, R., Shah, S., Patwarhan, S., Gudi, R. (2010). Quantifying the impact of model-plant mismatch on controller performance. *Journal of Process Control*, v. 20, p. 408–425.

Basseville, M. (1998). On-board component fault detection and isolation using the statistical local approach. *Automatica*. v. 34, p. 1391-1415.

Botelho, V., Trierweiler, J., Farenzena, M., Duraiski, R. (2015a/cap. 3). A methodology for detecting model-plant mismatches affecting MPC performance. *Industrial & Engineering Chemistry Research* (accepted).

Botelho, V., Trierweiler, J., Farenzena, M., Duraiski, R. (2015b/cap. 4). MPC model assessment of highly coupled systems. *Industrial & Engineering Chemistry Research* (submitted).

Botelho, V., Trierweiler, J., Farenzena, M., Duraiski, R. (2015c/cap. 5). Diagnosis of poor performance in model predictive controllers: Unmeasured Disturbance versus Model-Plant Mismatch. *Industrial & Engineering Chemistry Research* (submitted).

Botelho, V., Trierweiler, J., Farenzena, M., Duraiski, R. (2015d/cap. 6). Performance Assessment and Diagnosis of MPCs with Control Ranges. *Control Engineering Pratice* (submitted).

Camacho, E., Bordons, C. (2004). *Model Predictive Control, 2nd Edition*. Springer-Verlag, London.

Campos, M., Gomes, M., Perez, J. (2013). *Controle Avançado e Otimização na Indústria do Petróleo*. Interciência, Rio de Janeiro.

Carlsson, R., 2010. *A practical approach to detection of plant model mismatch for MPC*. Ph.D. Thesis, Linkoping University, Sweden.

Conner, J., Seborg, D. (2005). Assessing the Need for Process Re-identification. *Ind. Eng. Chem. Res.*, v. 44, p. 2767–2775.

Desborough, L., Harris, T. (1992). Performance assessment measures for univariate feedback control. *The Canadian Journal of Chemical Engineering*. v. 70 , p. 1186-1197.

Farenzena, M. (2008). *Novel methodologies for assessment and diagnostics in control loop management*. Ph.D. Thesis, Federal University of Rio Grande do Sul, Brazil.

Hägglund, T. (1995). A control-loop performance monitor. *Control Engineering and Practice*, v. 3, p. 1543–1551.

Harrison, C., Qin, S. (2009). Discriminating between disturbance and process model mismatch in model predictive control. *Journal of Process Control.* v.19, p-1610-1616.

He, D., Shao, S. Yang, P., Zhang, S. (2012). Research on Diagnosis Method of Predictive Control Performance Model Based on Data. *Advances in Neural Networks: Lecture Notes in Computer Science*, v. 7368, p. 468-477.

Holkar, S., Waghmare, L. (2010). An Overview of Model Predictive Control. *International Journal of Control and Automation.* v.3, p. 47-64.

Huang, B., Shah, S. (1999). *Performance assessment of control loops*. Springer, Berlin.

Huang, B., Malhotra, A., Tamayo, E. (2003). Model Predictive Control Relevant Identification and Validation. *Chemical Engineering Science*, v. 58, p. 2389-2401.

Huang, B., Thornhill, N. (2006). Alternative solutions to multi-variate control performance assessment problems. *Journal of Process Control.* v.16, p. 457- 471.

Hugo, A. (2002). Process Controller Performance Monitoring and Assessment. *Control Arts Inc. (www.controlartsinc.com*).

Jelali, M. (2006). An overview of control performance assessment technology and industrial applications. *Control Engineering Practice.* v. 14, p. 441–466.

Jelali, M. (2013). *Control Performance Management in Industrial Automation: Assessment, Diagnosis and Improvement of Control Loop Performance.* Springer-Verlag, London.

Ji, G.; Zhang, K.; Zhu, Y. (2012). A method of MPC model error detection. *Journal of Process Control*, v.22, p.635-642.

Jiang, H., Huang, B., Shah, S. (2009). Closed-loop model validation based on the two-model divergence method. *Journal of Process Control*, v.19, p.644-655.

Jiang, H., Shah, S., Huang, B., Wilson, B., Patwardhan, R., Szeto, F., (2012) Model analysis and performance analysis of two industrial MPCs. *Control Engineering Practice*. v. 20, p. 219–235.

Johanson, K. (2000). The Quadruple-Tank Process: A Multivariable Laboratory Process with an Adjustable Zero. *IEEE Transactions on Control Systems Technology*. v. 8, p. 456-465.

Kano, M., Shigi, Y., Hasebe, S., Ooyama, S. (2010). Detection of Significant Model-Plant-Mismath from Routine Operation Data of Model Predictive Control System. *Proceedings of the 9th International Symposium on Dynamics and Control of Process Systems – DYCOPS*.

Kerrigan, E., Maciejowski, J. (2000). Soft Constraints and Exact Penalty Functions in Model Predictive Control. *Proceeding of the UKACC International control conference*.

Lee, K., Huang, B., Tamayo, E. (2008). Sensitivity analysis for selective constraint and variability tuning in performance assessment of industrial MPC. *Control Engineering Practice*. v. 16, p. 1195–1215.

Ljung, L. (1999). *System Identification: Theory for the User*. Prentice Hall, New Jersey.

Longhi, L., Kempf, A., Lusa, L., Caumo, L., Fleck, T., Teixeira, H., Cortez, C., Trierweiler, J. (2008). Solução em tempo real para o gerenciamento de malhas de controle aplicada a uma Unidade de Coqueamento Retardado. *Petro e Química*. v. 305, p. 110-117.

Loquasto, F., Seborg, D. (2003). Model Predictive Controller Monitoring Based on Pattern Classification and PCA. *Proceedings of American Control Conference.*

Luyben, M., Luyben, W. (1997). *Essentials of process control*, McGrawHill, New York.

Maciejowski, J. (2002). *Predictive Control with Constraints*. Prentice Hall, New Jersey.

Matos, A., Longhi, L. (2013). Comparação entre técnicas ARC e APC aplicadas a um vaso pulmão integrador de uma unidade industrial de Coqueamento retardado. *Proceedings of VII Rio Automação.*

Morari , M., Lee, J. (1999). Model predictive control: past, present and future. Computers & Chemical Engineering. v. 23, p. 667-682.

Pannocchia, G., Luca, A. (2012). Performance degradation diagnosis and remedies in offset-free MPC. *Proceedings of American Control Conference.*

Prett, D., Morari, M. (1987). *The Shell Process Control Workshop*. Butterworths, Boston.

Qi, F., Huang, B.(2011). Bayesian methods for control loop diagnosis in the presence of temporal dependent evidences. *Automatica* v. 47, p. 1349–1356.

Qin , S., Badgwell, T. (2003). A survey of industrial model predictive control technology. *Control Engineering Practice.* v. 11, p. 733–764.

Rawlings, J.; Mayne, *D. Model Predictive Control: Theory and Design: 1st Edition*; Nob-Hill Publishing: London, 2009.

Santos-Fernández, E. (2013). *Multivariate Statistical Quality Control Using R*. Springer, New York.

Schäfer, J., Cinar, A. (2004). Multivariable MPC system performance assessment, monitoring, and diagnosis. *Journal of Process Control*, v. 14, p. 113-129.

Skogestad, S., Postlethwaite, I (1996). *Multivariable Feedback Control: Analysis and Design.* John Wiley & Sons, New York.

Sun, Z., Qin, J., Singhal, A., Megan, L. (2013). Performance monitoring of model-predictive controllers via model residual assessment. *Journal of Process Control*, v. 23, p. 473–482.

Tian, X., Chen, G., Chen, S. (2011). A data-based approach for multivariate model predictive control performance monitoring . *Neurocomputing*. v.74, p. 588–597.

Tornhill, N., Horch, A. (2007). Advances and new directions in plant-wide disturbance detection and diagnosis. *Control Engineering Practice*. v. 15, p. 1196-1206.

Trierweiler, J., Engell, S., Marquardt, W. (1997). *A Systematic Approach to Control Structure Design*. PhD Thesis. Technical University of Dortmund, Dortmund.

Trierweiler, J., Farina, L. (2003). RPN tuning strategy for model predictive control. *Journal of Process Control*. v. 13, p. 591–598.

Trierweiler, J., Machado, V. (2004). Which is the best criterion for identification of dynamic models? *Proceedings of 7th IFAC Symposium on Dynamics and Control of Process Systems.*

Whang, H., Song, Z., Xie, L. (2012). Parametric Mismatch Detection and Isolation in Model Predictive Control System. *Proceedings of the 8th IFAC Symposium on Advanced Control of Chemical Processe.*

Yu, J., Qin, S.(2008a). Statistical MIMO controller performance monitoring. Part I: Data-driven covariance benchmark. *Journal of Process Control*, v. 18, p. 277–296.

Yu, J., Qin, S.(2008b). Statistical MIMO controller performance monitoring. Part II: Performance diagnosis. *Journal of Process Control*, v. 18, p. 297–319.

Yuang, Q., Lennox, B. (2006). Improved model predictive control using PCA. *Proceedings of* 6th IFAC Symposium on Fault Detection, Supervision and Safety of Technical Processes.

Zanin, A., Moro, L., Gomes, A., Santos, E., Carvalho, F., Junior, H. (2014). Monitoração on-line do desempenho do controle avançado. *Proceedings of 20th Congresso Brasileiro de Automática.*

Zhang, Q., Shaoyuan, L. (2006). Performance Monitoring and Diagnosis of Multivariable Model Predictive Control Using Statistical Analysis. *Chinese Journal of Chemical Engineering.* v. 14, p. 207-215.

Zhang,D., Bing-Rui, Bao-chun, L., Zhi-quan, W. (2013). Improved LQG Benchmark Based Control Performance Monitoring for Multivariable Systems. *Proceedings of the 25th Chinese Control and Decision Conference.*

Zhao, C., Hongye, S., Yong, G., Jian, C. (2009). A Pragmatic Approach for Assessing the Economic Performance of Model Predictive Control Systems and Its Industrial Application. *Chinese Journal of Chemical Engineering.* v. 17, p. 241-250.

Zhao, Y., Jiang, C., Hongye, S., Huang, B. (2010). Multi-step prediction error approach for controller performance monitoring. *Control Engineering Practice.* v.18, p. 1–12.

Apêndice A1: Diretrizes para a implementação das metodologias da literatura

Neste apêndice são detalhados os procedimentos empregados para implementar as metodologias disponíveis na literatura que foram estudas na seção 2 deste trabalho.

A1.1 Método de Sun

1) Estimar os distúrbios estocásticos (e^d) contidos nas CVs através da identificação de um modelo ARX de elevada ordem entre as saídas (y) e os setpoints (y_{set}):

$$y(k) = \sum_{i=1}^{MO1} AO_i y(k-i) + \sum_{i=1}^{MO2} BO_i y_{set}(k-i) + e^d(k) \quad \text{(A1.1)}$$

onde M01 e MO2 são as ordens (parâmetro de ajuste do método) e AO e BO são os parâmetros do modelo ARX.

2) Determinar a predição um passo a frente para as CVs ($\hat{y}$) a partir das entradas (u) e saídas (y) medidas:

$$\hat{y}(k) = {G_{d0}}^{-1} G_0 u(k-1) + \left[1 - {G_{d0}}^{-1}\right] y(k-1) \quad \text{(A1.2)}$$

onde G_0 é o modelo do processo e G_{d0} é o modelo de distúrbio. Caso G_{d0} seja desconhecido, deve-se projetar um filtro (predictor) capaz de capturar o efeito do distúrbio (Ljung, 1999).

3) Determinar o erro de predição:

$$e^p(k) = \hat{y}(k) - y(k) \quad \text{(A1.3)}$$

4) Calcular o indicador de qualidade do modelo (MQI), o qual relaciona o erro proveniente dos distúrbios estocásticos com o erro de predição.

$$MQI = \frac{\sum_{i=1}^{ns} e^d(k)^T Q_y e^d(k)}{\sum_{i=1}^{ns} e^p\,(k)^T Q_y e^p\,(k)} \tag{A1.4}$$

onde Q é o peso de cada CV configurado no MPC.

MQI pode variar entre 0 e 1, de modo que quando maior for o seu valor, melhor é o modelo, já que a maior parte do erro de predição é decorrente dos distúrbios estocásticos.

A1.2 Método de Badwe *et al.* (2009)

1) Remover o ruído das entradas (u) e saídas (y).

2) Calcular a predição das saídas ($\hat{y}$) e respectivo erro de predição ($e^p = \hat{y} - y$)

3) Descorrelacionar cada MV das demais MVs: Obter o efeito isolado de cada entrada ($\varepsilon 1_i$) através da identificação de um modelo OE (Output-Error) entre cada entrada i (u_i) em relação às entradas restantes (U^i).

$$u_i(k) = V1_i U^i(k) + \varepsilon 1_i \tag{A1.5}$$

onde $V1_i$ é o vetor de parâmetros do modelo OE.

4) Similarmente, descorrelacionar o efeito de cada MV nos erros de predição: Obter o efeito isolado de cada entrada no erro de predição ($\varepsilon 2_{i,j}$) através da identificação de um modelo OE (Output-Error) entre o erro de predição da saída j (e_j^p) e as entradas restantes (U^i), isto é, todas as entradas, exceto u_i.

$$e_j^p(k) = V2_{i,j} U^i(k) + \varepsilon 2_{i,j} \tag{A1.6}$$

5) Calcular a correlação cruzada entre $\varepsilon 1_i$ e $\varepsilon 2_{i,j}$. Valores de correlação elevados indicam a presença de erro no modelo do canal $u_i\ X\ y_j$.

A1.3 Método de Yu & Qin (2008 a e b)

Passo 1: Análise da variabilidade global

1) Selecionar um conjunto de dados históricos de referência (y_I e y_{set_I}), onde o desempenho do controlador seja o desejável.

2) Determinar o índice de variabilidade global:

$$I_{v=}\frac{\det\{cov[y_{II}-y_{set_{II}}]\}}{\det\{cov[y_I-y_{set_I}]\}} \tag{A1.7}$$

onde y_{II} e $y_{set_{II}}$referem-se aos dados avaliados.

Quanto mais distante de 1 for o valor de I_v, maior a diferença entre a variabilidade dos dados de referência e dos dados avaliados.

Passo 2: Avaliar direções de melhora e piora de desempenho

1) Determinar os autovalores (μ) e autovetores (p) do seguinte problema de autovalor generalizado (GEVP):

$$cov(y_{II}-y_{set_{II}})p=\mu cov(y_I-y_{set_I})p \tag{A1.8}$$

2) Calcular as projeções ($z_{I,p}$ *e* $z_{II,p}$) dos erros de controle ($y-y_{set}$) na direção de cada autovetor (p).

3) Calcular a autocorrelação das projeções $z_{I,p}$ *e* $z_{II,p}$ ($\rho_{I,p}$ *e* $\rho_{II,p}$);

4) Construir uma inferência estatística para os dados (f_I *e* f_{II}):

$$f_d^{(i)}=1+2\sum_{j=1}^{ns_d}\left(1-\frac{j}{ns_d}\right)\rho_{d(i),j}^2 \tag{A1.9}$$

onde o sub-índice '*d*' se refere ao conjunto de dados (I ou II), ns é o número de amostras e i representa cada um dos autovetores e j cada lag da autocorrelação.

5) Determinar o intervalo de confiança de cada autovalor:

$$UL(\mu_i)=\mu_i\left[1-z_{\propto/2}\sqrt{2\left(\frac{f_I^{(i)}}{ns_I-1}+\frac{f_{II}^{(i)}}{ns_{II}-1}\right)}\right]^{-1} \tag{A1.10}$$

$$LL(\mu_i)=\mu_i\left[1+z_{\propto/2}\sqrt{2\left(\frac{f_I^{(i)}}{ns_I-1}+\frac{f_{II}^{(i)}}{ns_{II}-1}\right)}\right]^{-1} \tag{A1.11}$$

onde UL e LL são os limites inferiores e superiores de confiança, $z_{\propto/2}$ é o valor crítico de uma distribuição normal com nível de confiança $(1-\propto)100\%$.

Caso UL e LL sejam maiores que 1, o desempenho dos dados avaliados é pior na direção do autovetor correspondente, se UL e LL sejam menores que 1, o desempenho dos dados avaliados é melhor.

Passo 3: Localizando as variáveis responsáveis pela mudança de desempenho

1) Construir um subespaço agrupando todos os autovetores que indicarem piora (UL e LL maiores que 1) e melhora (UL e LL menores que 1), denominados P_w e P_b, respectivamente.

2) Calcular o ângulo entre cada saída e os subespaços (${\theta_y}^w$ e ${\theta_k}^b$).

$$cos({\theta_y}^w) = \left\|P_w({P_w}^T P_w)^{-1}{P_w}^T ev_y\right\|\text{E} \quad \text{(A1.12)}$$

$$cos({\theta_y}^b) = \left\|P_b({P_b}^T P_b)^{-1}{P_b}^T ev_y\right\|\text{E} \quad \text{(A1.13)}$$

onde ev_y é o vetor unitário representativo de cada saída

3) Determinar o limite de confiança dos ângulos:

$$\beta = \sqrt{\frac{1}{2} + \frac{z_{\propto/2}}{\sqrt{2n_g}}} \quad \text{(A1.14)}$$

onde n_g é a média geométrica entre o número de amostras dos dados de referência e dos dados avaliados.

Quando os valores de $cos({\theta_y}^w)$ ou $cos({\theta_y}^b)$ foram maiores que β ,a saída correspondente é a responsável pela alteração no desempenho do controlador.

Apêndice A2: Diretrizes para a implementação da metodologia proposta

A metodologia proposta tem o objetivo de avaliar a existência de erros de modelagem que impactem no desempenho do MPC. Ela pode ser dividia em três etapas sequenciais. Na primeira, o objetivo é verificar o efeito global dos erros de modelagem. Na segunda, as variáveis controladas nas quais os erros de modelagem estão contidos são localizadas. A última etapa consiste em caracterizar os erros, determinando se os mesmos provêm de uma discrepância de modelo ou de um distúrbio não medido. A seguir, as diretrizes para a aplicação de cada uma das etapas será apresentada. Ressalta-se que ao longo do trabalho diversos indicadores foram sugeridos. Neste apêndice serão apresentados apenas os melhores indicadores de cada etapa.

Etapa 1: Determinação do impacto global dos erros de modelagem

A partir do modelo do processo (G_0), dos valores medidos das variáveis de entrada (u) e saída (y), da função de sensibilidade nominal (S_0) e com base no desenvolvimento apresentado na seção 3, a primeira etapa da metodologia pode ser aplicada da seguinte forma:

1) Simular o modelo do processo:

$$y_{sim} = G_0 u \tag{A2.1}$$

2) Estimar a saída nominal:

$$y_0 = y - S_0(y - y_{sim}) \tag{A2.2}$$

3) Calcular os indicadores de qualidade do modelo para cada uma das CVs.

Os indicadores de qualidade do modelo devem relacionar a saída medida (y) com a saída nominal estimada (y_0), já que y_0 representa as saídas do sistema na ausência de

erros de modelagem. Neste trabalho foram sugeridos dois indicadores. Um deles é o índice de variância ($Ivar$), o qual consiste na razão entre as variâncias de y e y_0:

$$Ivar = \frac{var(y - y_{set})}{var(y_0 - y_{set})} \tag{A2.3}$$

Onde y_{set}representa o setpoint da variável controlada correspondente. Para casos onde as CVs não possuem setpoints fixos (controladores por faixas), o $Ivar$ pode ser definido como:

$$Ivar = \frac{var(y - \bar{y})}{var(y_0 - \bar{y}_0)} \tag{A2.4}$$

Onde $\bar{y}$ e $\bar{y}_0$ representam os valores médios dos vetores correspondentes. Quando o $Ivar$ de uma CV for diferente de 1, significa que a variância da mesma está sendo impactada por problemas de modelagem.

Outro indicador sugerido é a comparação das funções de autocorrelação de y e y_0. A ideia consiste em avaliar graficamente as ACF obtidas para ambos os conjuntos de dados. A partir da disparidade entre as curvas é possível detectar oscilações ou diferenças nas velocidades de respostas causadas por problemas de modelagem, conforme ilustrado na Figura A2.1.

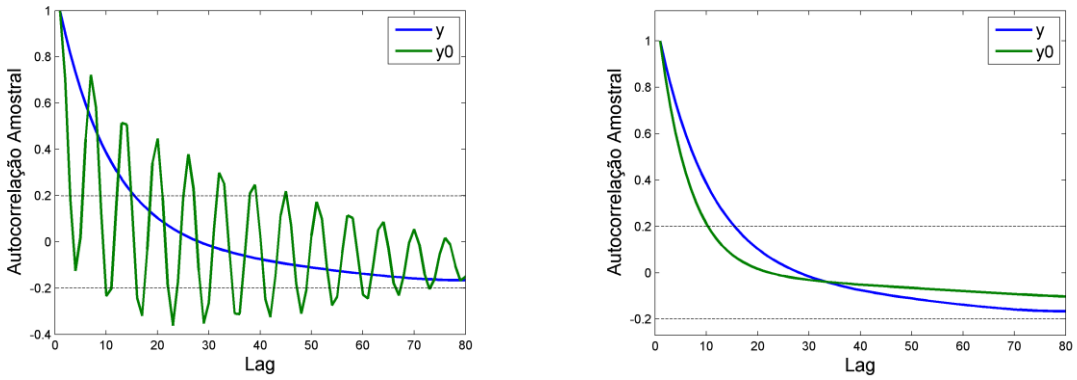

Figura A2.1: Avaliação baseada na função de autocorrelação

A Figura A2.1 apresenta o comportamento típico da função de autocorrelação quando há problemas de modelagem. No primeiro caso (Figura A2.1a) é possível detectar que a CV avaliada possui comportamento oscilatório decorrente de um problema no modelo, já que ACF(y) oscila mas ACF(y_0) não oscila. Já no segundo caso (Figura A2.1b) há um erro de modelagem tornando a resposta da CV avaliada mais lenta, já que ACF(y) decai mais lentamente que ACF(y_0).

É importante mencionar que, especialmente quando o acoplamento entre as variáveis do sistema é elevado, o erro no modelo de uma única variável pode ser capaz de degradar o desempenho de todas as outras CVs. Dessa forma, após a determinação do

impacto global dos erros de modelagem fornecido pela etapa 1, é necessário localizar em quais variáveis estes erros estão contidos, sendo esta a próxima etapa do método.

Etapa 2: Localização dos erros de modelagem

Esta etapa é realizada logo após a etapa 1, quando a mesma indica a presença de erros de modelagem significativos. Seu objetivo consiste em localizar quais as CVs possuem erros em seus modelos. A partir do modelo do processo (G_0), dos valores medidos das variáveis de entrada (u) e saída (y), da função de sensibilidade nominal (S_0) e com base no desenvolvimento apresentado na seção 4, a segunda etapa da metodologia pode ser aplicada da seguinte forma:

1) Simular o modelo do processo (equação A2.1)

2) Obter a matriz de sensibilidade nominal diagonal ($S_{0_{diag}}$), a qual consiste em uma matriz contendo apenas os elementos da diagonal principal de S_0.

3) Estimar a saída nominal diagonal:

$$y_{0_{diag}} = y - S_{0_{diag}}(y - y_{sim}) \tag{A2.5}$$

4) Calcular os indicadores de qualidade do modelo para cada uma das CVs

Os indicadores desta etapa são análogos aos apresentados na etapa 1 ($Ivar$ e ACF), porém calculados em relação a $y_{0_{diag}}$:

$$Ivar_{diag} = \frac{var(y - y_{set})}{var(y_{0_{diag}} - y_{set})} \tag{A2.6}$$

ou:

$$Ivar_{diag} = \frac{var(y - \bar{y})}{var(y_{0_{diag}} - \bar{y}_{0_{diag}})} \tag{A2.7}$$

Quando o $Ivar_{diag}$ de uma CV for diferente de 1, significa que existem erros em seu modelo. Quanto maior a similaridade entre $Ivar_{diag}$ e $Ivar$, menor é a influência dos erros de modelagem das demais CVs impactando na CV analisada.

De forma similar, quando houver disparidade entre as curvas de autocorrelação (y e $y_{0_{diag}}$) de uma CV, significa que existem erros em seu modelo. Quanto maior a similaridade entre ACF($y_{0_{diag}}$) e ACF(y_0), menor é a influência dos erros de modelagem das demais CVs impactando na CV analisada.

Etapa 3: Caracterização dos erros de modelagem

Após a localização da variável controlada contendo erro de modelagem através da etapa 2, a última etapa da metodologia consiste em caracterizar os erros, informando se os mesmo provém de uma discrepância de modelo ou de um distúrbio não medido. A partir das saídas medidas (y), das saídas nominais diagonais ($y_{0_{diag}}$, equação A2.5) e com

base no desenvolvimento apresentado na seção 5, a terceira etapa da metodologia pode ser aplicada da seguinte forma:

1) Calcular o erro nominal diagonal:

$$e_{0_{diag}} = y_{0_{diag}} - y \tag{A2.8}$$

2) Definir um vetor contendo diferentes tamanhos de janelas móveis a serem avaliadas. O primeiro elemento do vetor (menor janela móvel) deve ser em torno da metade do horizonte de predição e o último elemento (maior janela móvel) deve ser aproximadamente o dobro do horizonte de predição.

3) Definir o tamanho da janela móvel (MW) igual ao primeiro elemento do vetor de janelas móveis.

4) Calcular os coeficientes de assimetria e curtose para cada subconjunto de $e_{0_{diag}}$, considerando um horizonte deslizante de tamanho MW ($skn_{e_{0_{diag}}}^{MW}$ e $kts_{e_{0_{diag}}}^{MW}$).

5) Calcular os coeficientes de assimetria e curtose para cada subconjunto de $y_{0_{diag}}$, considerando um horizonte deslizante de tamanho MW ($skn_{y_{0_{diag}}}^{MW}$ e $kts_{y_{0_{diag}}}^{MW}$).

6) Calcular a derivada dos vetores contendo coeficientes de assimetria e curtose originados nos itens 4 e 5.

7) Calcular o coeficiente de correlação entre a derivada dos coeficientes de assimetria de $e_{0_{diag}}$ e $y_{0_{diag}}$:

$$co_{dskn_{MW}} = corr\left(\frac{d}{dt} skn_{e_{0_{diag}}}^{MW}, \frac{d}{dt} skn_{y_{0_{diag}}}^{MW}\right) \tag{A2.9}$$

8) Calcular o coeficiente de correlação entre a derivada dos coeficientes de curtose de $e_{0_{diag}}$ e $y_{0_{diag}}$:

$$co_{dkts_{MW}} = corr\left(\frac{d}{dt} kts_{e_{0_{diag}}}^{MW}, \frac{d}{dt} kts_{y_{0_{diag}}}^{MW}\right) \tag{A2.10}$$

9) Repetir os itens de 4 à 8 considerando todos os tamanhos de janela móvel definidos no item 2.

10) Calcular a média aritmética de $co_{dkts_{MW}}$ e $co_{dskn_{MW}}$, considerando todos os tamanhos de janela móvel avaliados (co_{dkts} e co_{dskn}).

Se pelo menos um dos indicadores (co_{dkts} ou co_{dskn}) for elevado (maior que 0.1), significa que há a dominância de uma discrepância de modelo. Caso contrário, o erro de modelagem é proveniente de um distúrbio não medido.

Apêndice A3: Determinação experimental da função de sensibilidade nominal

Teoricamente, a função de sensibilidade nominal pode ser obtida analiticamente a partir do modelo do controlador, conforme discutido na seção 3. Entretanto, no caso dos controladores preditivos, a obtenção do modelo do controlador não é trivial, já que o mesmo é configurado a partir de um problema de otimização. Neste caso, a alternativa é se obter uma estimativa da função de sensibilidade nominal experimentalmente, a partir de uma simulação do controlador considerando o modelo do processo utilizado pelo MPC no lugar do planta real. O procedimento empregado será discutido a seguir.

Passo 1 - Configurando a simulação

O controlador deve ser configurado de acordo com o comportamento típico do processo nos dados de planta a serem avaliados, conforme as seguintes etapas:

a. Definir quais variáveis manipuladas (MVs) estão disponíveis e quais estão saturadas ou em modo manual.

b. Configurar o simulador mantendo constante o valor das MVs indisponíveis. Relaxar as restrições das MVs disponíveis para garantir que as mesmas não irão saturar ao longo da simulação.

c. Definir quais variáveis controladas (CVs) possuem setpoints fixos, quais operam dentro de uma faixa e quais possuem uma restrição ativa.

d. Configurar o simulador relaxando os limites das CVs que estão dentro da faixa. Isso irá garantir que as mesmas irão permanecer dentro da faixa durante a simulação.

e. Configurar uma condição inicial para a simulação de acordo com as definições dos itens a e c.

Passo 2 - Determinando T_0 para CVs com setpoints fixos

Caso existam CVs com setpoints fixos, o seguinte procedimento deve ser realizado para cada uma delas. Caso elas não existam, avançar para o item j.

f. Partir a simulação.

g. Depois de transcorrido um pequeno tempo de simulação, garantindo que o sistema esteja em estado estacionário e respeitando as definições dos itens a e c, realizar uma perturbação do setpoint da CV avaliada (y_{set}^{i}).

h. Simular até que o sistema esteja em estado estacionário.

i. Utilizando um modelo *Box-Jenkins*, realizar uma identificação SIMO (*single input multiple output*) do seguinte modelo:

$$y_{sim} = T_0^i y_{set}^i \tag{A3.1}$$

onde y_{sim} é a matriz contendo todos as saídas da simulação e T_0^i representa a linha da matriz complementar de sensibilidade (T_0) referente a perturbações no setpoint da variável i.

Passo 3 - Determinando T_0 para CVs por faixa com restrições ativas

Caso existam CVs operando por faixas e com restrições ativas, o seguinte procedimento deve ser realizado para cada uma delas. Caso elas não existam, avançar para o item n.

j. Partir a simulação

k. Depois de transcorrido um pequeno tempo de simulação, garantindo que o sistema esteja em estado estacionário e respeitando as definições dos itens a e c, realizar uma perturbação do na restrição ativa da CV avaliada ($y_{soft_{act}}^{i}$).

l. Simular até que o sistema esteja em estado estacionário.

m. Utilizando um modelo *Box-Jenkins*, realizar uma identificação SIMO (*single input multiple output*) do seguinte modelo:

$$y_{sim} = T_0^i y_{soft_{act}}^i \tag{A3.2}$$

onde y_{sim} é a matriz contendo todos as saídas da simulação e T_0^i representa a linha da matriz complementar de sensibilidade referente a perturbações na restrição ativa da variável i.

Passo 4 - Determinando T_0 para CVs por faixa com restrições ativas

Caso existam CVs operando dentro das faixas, o seguinte procedimento deve ser realizado para cada uma delas. Caso elas não existam, avançar para o item o.

n. Definir T_0^i como um vetor nulo de dimensões igual ao número de CVs, já que variáveis dentro da faixa não influenciam nas ações de controle do MPC.

Passo 5: Gerando a matriz de sensibilidade nominal S_0

A partir dos modelos T_0^i identificados, S_0 pode ser determinado da seguinte forma:

o. Gerar a matriz de modelos MIMO T_0 a partir da combinação de todos os vetores de modelos SIMO T_0^i gerados através dos itens i, m e n.

p. Obter S_0 a partir de T_0:

$$S_0 + T_0 = I \tag{A3.3}$$

onde I é a Matriz Identidade.